MRI White Matter Lesion Central Veins in Multiple Sclerosis

Amal Prasanna Rohan Samaraweera
BMedSci (Hons), BMBS, MRCP
Division of Clinical Neuroscience
School of Medicine
University of Nottingham

February 2017

Thesis submitted to the University of Nottingham for the degree of Doctor of Philosophy

Contents

Declaration

I, Amal Samaraweera confirm that this work is my own. Where work and help has been contributed from other sources and by my colleagues, I indicate this in the specific chapter and acknowledgments sections.

Acknowledgements

I would like to thank all those who have encouraged and supported me during the last few years.

I am indebted to my supervisors, Dr Nikos Evangelou and Professor Paul Morgan for their advice and guidance during the ups and downs of the research process. I could not have asked for more helpful supervisors. I must also thank Dr Rob Dineen who helped with understanding the clinical applications of the thesis and Dr Martin Duddy, Royal Victoria Infirmary, Newcastle, for his support during my period of research. I would like to thank Dr Chris Tench for his patience and helpful guidance with some of the statistical concepts, and Dr Andrea Venn, whose excellent Statistics drop-in clinics helped me understand which statistical tests to use. I received advice on image analysis and experimental design from Dr Alain Pitiot and Dr Olivier Mougin who in addition helped with image fusion and scanning patients. I would also like to thank Dr Molly Bright who provided impromptu sessions on the basics of MRI.

The projects in this thesis would not have been possible without the help of the Sir Peter Mansfield Imaging Centre, University of Nottingham and the clinical MS team at the Queen's Medical Centre who helped identify patients for various projects. Thanks to Jan Alappadan Paul, Carolyn Costigan, Chris Bradley and Kath Shaw for all their help and time with MRI scanning.

Thank you to Megi Clarke, Dr Yasser Falah, Matt South and Amy Whitehead who acted as blinded raters for various chapters, and Dr Rasha Abdel-Fahim, Dr Radu Tanasescu and Elena Morandi for their practical guidance. Thank you to my family and in particular, my wife Ela, who has supported me through the highs and lows of research.

None of the projects would have been possible without funding from the MRC Confidence in Concept Award given to my supervisors which helped kick start early projects, and the Nottingham University Hospitals Charity which funded more recent projects.

Finally, my thanks to all the patients who volunteered to have MRI scans and who returned for further scans purely to help with research.

List of Tables

List of Figures

Abstract

This thesis focuses on the use of the Magnetic Resonance Imaging (MRI) white matter lesion (WML) central vein as a biomarker for multiple sclerosis (MS). MS remains a clinical diagnosis, with reliance on MRI to support the diagnosis. Misinterpretation of the MRI can lead to misdiagnoses of diseases that mimic MS. With the increase in disease modifying treatments, accurate and timely diagnosis is needed now more than ever.

Using T2* weighted imaging at 3 Tesla (T) MRI, I explored different aspects of WML central veins in patients with relapsing-remitting (RRMS), primary progressive MS (PPMS), and ischaemic small vessel disease (SVD) including: (1) the effect of using different T2* weighted sequences; (2) how T2* and susceptibility weighted imaging (SWI) and fused imaging techniques such as fluid attenuated inversion recovery (FLAIR)-SWI affected the proportion of WML central veins and; (3) determining if WML central veins were as prevalent in patients with PPMS. Further objectives included: (4) attempting to determine if vascular risk factors altered the proportion of WML central veins in patients with MS and; (5) using statistical modelling to calculate a simple diagnostic rule using WML central veins to differentiate MS from SVD.

The proportion of WMLs with central veins differed significantly between patients with MS and SVD. Variations of the T2* sequence altered the proportion of WMLs with central veins, but the difference between MS and SVD remained statistically significant. T2* and SWI allowed a higher proportion of WMLs with central veins to be detected, with T2* being just as accurate as FLAIR-SWI in allowing the diagnosis of MS or SVD. Patients with PPMS and RRMS have a similarly high proportion of WMLs with central veins. High sensitivity and specificity for the diagnosis of MS versus SVD can be achieved by identifying a subset of WMLs with central veins.

WML central veins could be used as an MRI biomarker using T2* imaging at 3T to differentiate cases of diagnostic uncertainty with RRMS, PPMS and SVD. Application of this imaging technique to patients with diagnostic uncertainty in prospective studies needs to be studied along with refining a clinical diagnostic rule.

List of Abbreviations

ADEM	Acute Disseminated Encephalomyelitis
AIDS	Acquired Immunodeficiency Syndrome
ANA	Anti-nuclear antibody
ANOVA	Analysis of variance
APS	Anti-phospholipid syndrome
BENEFIT	Betaferon in Newly Emerging Multiple Sclerosis for Initial Treatment study
BMI	Body mass index
CADASIL	Cerebral Autosomal Dominant Arteriopathy with Subcortical Infarcts and Leukoencephalopathy
CHAMPIONS	Controlled High Risk Avonex Multiple Sclerosis Prevention Study In Ongoing Neurological Surveillance
CHAMPS	Controlled High-Risk Subjects Avonex Multiple Sclerosis Prevention Study
CI	Confidence interval
CIS	Clinically isolated syndrome
CMV	Cytomegalovirus
CNS	Central nervous system
CSF	Cerebrospinal fluid
CT	Computerised tomography
DAWM	Dirty appearing white matter
DICOM	Digital Imaging and Communications in Medicine
DIS	Dissemination in space
DIT	Dissemination in time
DMT	Disease modifying treatment
DTI	Diffusion Tensor Imaging
DWM	Deep white matter
EBV	Epstein-Barr virus
EDSS	Expanded Disability Status Scale
ENA	Extractable nuclear antigen
EPI	Echo Planar Imaging
ETOMS	Early Treatment of MS study
FLAIR	Fluid attenuated inversion recovery
FLAIR-SWI	Fluid attenuated inversion recovery susceptibility weighted imaging
FLASH	Fast low-angle shot
GE	General Electric
GFAP	Glial fibrillary acidic protein
GM	Grey matter
GRE	Gradient recalled echo
HIV	Human Immunodeficiency Virus
HLA	Human Leukocyte Antigen
ICC	Intraclass correlation coefficient
IFNβ	Interferon Beta
IgG	Immunoglobulin G
IM	Infectious mononucleosis
IQR	Interquartile range

IT	Infratentorial
JC	Juxtacortical
KIR4.1	Inwardly rectifying potassium channel
LoA	Limits of Agreement
LLA	Lower limit of agreement
MRI	Magnetic Resonance Imaging
MS	Multiple Sclerosis
NAGM	Normal appearing grey matter
NAWM	Normal appearing white matter
NBD	Neuro-Behçet's disease
Nf	Neurofilaments
NfL	Neurofilament light chains
NIfTI	Neuroimaging Informatics Technology Initiative file format
NMO	Neuromyelitis Optica
NMOSD	Neuromyelitis Optica Spectrum Disorder
NPV	Negative predictive value
OCBs	Oligoclonal bands
OR	Odds ratio
PD	Proton density
PML	Progressive Multifocal Leucoencephalopathy
PPMS	Primary Progressive multiple sclerosis
PPV	Positive predictive value
PreCISe	Evaluate Early Glatiramer Acetate Treatment in Delaying Conversion to Clinically Definite Multiple Sclerosis of Subjects Presenting With Clinically Isolated Syndrome
PV	Periventricular
RF	Radiofrequency
RIS	Radiologically isolated syndrome
RRMS	Relapsing Remitting multiple sclerosis
SD	Standard deviation
SLE	Systemic lupus erythematosus
SPMS	Secondary Progressive multiple sclerosis
SPSS	Statistical Package for the Social Sciences
STAR MS	Single Test to ARrive at MS diagnosis study
SVD	Small Vessel Disease
SWAN	Susceptibility weighted angiography
SWI	Susceptibility weighted imaging
T	Tesla
T2*	T2* weighted imaging
TE	Time to echo
TR	Time to repeat
ULA	Upper limit of agreement
UVR	Ultraviolet radiation
VEP	Visual Evoked Potentials
WM	White matter
WMLs	White matter lesions

Publications and Prizes associated with this thesis

Samaraweera AP, Clarke MA, Whitehead A, Falah Y, Driver ID, Dineen RA, Morgan PS, Evangelou N. The Central Vein Sign in Multiple Sclerosis Lesions Is Present Irrespective of the T2* Sequence at 3T. J Neuroimaging. 2017 Jan;17;27(1):114-121

Mistry N, Abdel-Fahim R, **Samaraweera A**, Mougin O, Tallantyre E, Tench C, Jaspan T, Morris P, Morgan PS, Evangelou N. Imaging central veins in brain lesions with 3T T2*-weighted magnetic resonance imaging differentiates multiple sclerosis from microangiopathic brain lesions. Mult Scler. 2016 Sep;22(10):1289-96

Sati P, Oh J, Constable RT, Evangelou N, Guttmann CR, Henry RG, Klawiter EC, Mainero C, Massacesi L, McFarland H, Nelson F, Ontaneda D, Rauscher A, Rooney WD, **Samaraweera AP**, Shinohara RT, Sobel RA, Solomon AJ, Treaba CA, Wuerfel J, Zivadinov R, Sicotte NL, Pelletier D, Reich DS; NAIMS Cooperative. The central vein sign and its clinical evaluation for the diagnosis of multiple sclerosis: a consensus statement from the North American Imaging in Multiple Sclerosis Cooperative. Nat Rev Neurol. 2016 Dec;12(12):714-722

Sue Watson Postgraduate Presentation prize (1st prize) for oral presentation of PhD work. Reducing misdiagnosis in multiple sclerosis; Validation of the central vein sign as a Magnetic Resonance Imaging biomarker, 23rd February 2016, University of Nottingham.

Chapter 1. MS, its diagnosis and MRI tools to reduce misdiagnosis

1.1 A brief overview of Multiple Sclerosis

1.1.1 Epidemiology

Multiple sclerosis (MS) is a chronic, disabling condition of the central nervous system (CNS). In the developed world it is the second most common cause of neurological disability in young adults, after neurological trauma (Koch-Henriksen and Sorensen, 2010; Josey *et al.*, 2012), and has a predilection to affect young adults in their working life. Current prevalence in the UK is approximately 126,000; 289 per 100,000 women and 115 per 100,000 men, with one study indicating just over 6000 new cases diagnosed during 2010 (Mackenzie *et al.*, 2014). The incidence is higher in North America and Europe and lowest in South East Asia and sub-Saharan Africa with a few exceptions. The estimated worldwide prevalence is approximately 2.5 million with the incidence rising in many regions, especially amongst women (Koch-Henriksen and Sorensen, 2010).

John Kurtzke highlighted the geographical pattern of MS and defined MS prevalence as high (more than 30 per 100,000), medium (5-25 per 100,000) and low (less than 5 per 100,000) (Kurtzke, 1975). Some differences in incidence and prevalence rates may be accounted for by different diagnostic methods, how criteria are applied in clinical practice and variances in the ethnicity of the populations studied. Additionally, completeness of the data in cases where there is magnetic resonance imaging (MRI) availability or awareness of MS by the public and clinicians, may also be different (Marrie, 2004).

There exists an interesting difference in susceptibility to MS, dependent on ethnicity, with MS being uncommon in Samis (from the northernmost parts of Norway), native north Americans living in Canada (with the few people who do have MS having a Caucasian ancestor), native south Americans, black Africans (with a higher prevalence in English speaking white South Africans), New Zealand Maoris and Chinese. In contrast the Sardinian population has one of the highest prevalence rates in the world (144-152 per 100,000), thought possibly to be due to a founder effect (when a new population is founded by a few members of the original population, which may lead to reduced genetic variation and non-random selection of genes from the original population, therefore leading to increased risk of disease) (O'Gorman *et al.*, 2012).

An environmental role in the pathogenesis of MS has been suggested due to various migration and latitudinal studies (Marrie, 2004). Immigrants from a low risk country who emigrate to a high risk country e.g. UK, keep their original low risk. However the children of these immigrants have a risk equivalent to the population risk in the destination country i.e. higher than their parents (Elian and Dean, 1987; Elian *et al.*, 1990). On the other hand, migrants from an area of high risk, emigrating to a low risk region experience a reduction in risk to an intermediate level.

The latitudinal pattern of MS has been recognised for a long time with higher latitudes linked to higher incidence and prevalence (again with a few exceptions) (Simpson *et al.*, 2011). For example, a study in New Zealand demonstrated that prevalence increased by threefold from the north to the south of the country. This did not change when the population studies were stratified for age, sex and ethnicity, although the gradient was strongest with those of European descent

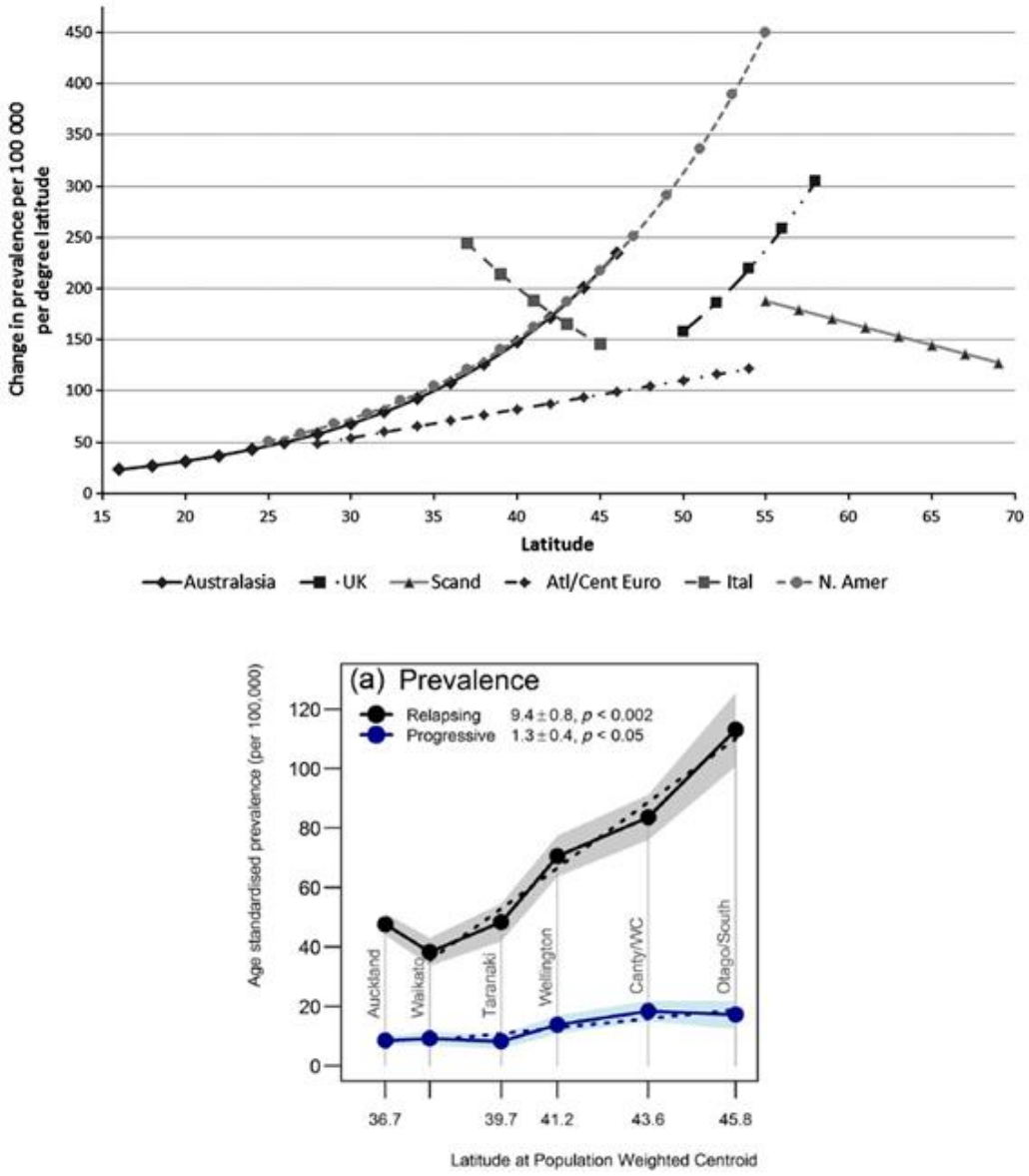

Figure 1. Latitudinal gradient of MS.

Positive and negative latitudinal gradients and association with the prevalence of MS (Top) (Simpson *et al.*, 2011), and prevalence of MS phenotypes according to latitudinal gradients in New Zealand (Bottom) (Taylor *et al.*, 2010)

(Taylor *et al.*, 2010). The latitudinal gradient was also seven times higher with cases of relapsing remitting MS (RRMS) and secondary progressive MS (SPMS) compared to primary progressive MS (PPMS), and three times higher if females were compared to males with MS (Figure 1).

1.1.2 Proposed risk factors for MS

The exact aetiology of MS has yet to be fully determined, but is most likely multifactorial with a genetic susceptibility and environmental factors both combining, leading to a final common pathway for disease onset. The higher prevalence of MS as one travels towards the poles of the northern and southern hemispheres, has implicated the lack of ultraviolet radiation (UVR) which inversely correlates with latitude (Orton *et al.*, 2011). Certain wavelengths of UV light (UV-A and UV-B) are said to be immunosuppressive and have direct effects on the immune system (such as influencing regulatory T cell function and increasing levels of immunosuppressive cytokines such as interleukin-4 and 10) and also have a major influence on the production of vitamin D (Hayes, 2000; Ascherio and Munger, 2007). In fact vitamin D or 1,25-dihydroxycholecalciferol in humans is produced mainly from sunlight (rather than from diet), converting precholecalciferol in the skin, which itself is synthesized to cholecalciferol. Cholecalciferol undergoes hydroxylation to the inactive form of vitamin D (25-hydroxycholecalciferol) which is finally converted to the active form of vitamin D in the kidneys (Hayes, 2000). The biological mechanisms as to how vitamin D may affect the immune system and when this influences risk, is beyond the scope of this thesis. However various studies have shown that low levels play a role in developing MS after a clinically isolated syndrome (CIS) (Martinelli *et al.*, 2014), may influence relapse rates (Smolders *et al.*, 2008) and may affect a developing foetus via maternal vitamin D levels causing the so called month of birth effect on MS risk (Dobson *et al.*, 2013).

A further risk factor involves the Epstein-Barr virus (EBV). Although most of the adult population is seropositive, MS continues to be a relatively uncommon

disorder, suggesting that EBV is not the final common pathway for developing the disease. However it is uncommon to find MS patients who are seronegative for EBV (Disanto *et al.*, 2013). EBV can be asymptomatic or present clinically, when it is then defined as infectious mononucleosis (IM). Patients with a history of confirmed IM subsequently have an increased risk of MS (Handel *et al.*, 2010), usually many years after the infection with one such study in Oxford demonstrating a fourfold increase in MS risk (Goldacre *et al.*, 2004). However some data suggest that EBV may not be an absolute requirement for the disease, with one study demonstrating that 14% of 126 children studied with MS were seronegative for the virus (Banwell *et al.*, 2007). Furthermore, the association between EBV infection and the Human Leukocyte Antigen (HLA) gene, HLA-DRB1*15 has been studied, with some indicating an increased risk in patients with this allele and previous IM infection (Nielsen *et al.*, 2009). Others demonstrate that individuals with the antibody to EBV nuclear antigen have an increased risk of MS with the presence of the HLA-DRB1*15 gene being additive to the risk (De Jager *et al.*, 2008). Whether EBV is definitively a causative agent is yet to be confirmed.

Smoking tobacco appears to be another (and more likely modifiable) risk factor for MS onset, as well as progression (Ascherio and Munger, 2007). The risk appears to be dose and duration dependent, and also includes an increased risk for passive smokers, with one study indicating an odds ratio of 2.7 for developing MS (Hedstrom *et al.*, 2016). Previous prospective studies have indicated between 1.4-1.8 times greater chance of developing MS than people who have never smoked (Hernan *et al.*, 2005). Additionally smoking appears to affect the MS course independent of the age of exposure to smoking (Hedstrom *et al.*, 2013), unlike other risk factors such as EBV and vitamin D deficiency which may have more impact

earlier in life. Interestingly smoking can also influence the risk of switching to secondary progressive disease, with smokers 3-5 times more likely to develop this subtype of MS compared to non-smokers (Hernan *et al.*, 2005). Possible mechanisms for smoking induced CNS damage include nitric oxide causing axonal degeneration or negative effects on oligodendrocytes.

1.1.3 The perivenous pathology of MS lesions

Pathophysiological causes of MS are still being investigated and debated. In general terms, MS has often been described as a disease of the cerebral white matter (WM), with demarcated inflammatory plaques of demyelination, axonal loss and gliosis being the hallmark of MS (Kuhlmann *et al.*, 2017). However, grey matter (GM) pathology, both cortical and deep GM have also been demonstrated over the decades (Brownell and Hughes, 1962; Bø *et al.*, 2003), as well as abnormalities in the normal appearing white matter (NAWM) (Allen and McKeown, 1979; Evangelou *et al.*, 2000) and normal appearing grey matter (NAGM) (Ciccarelli *et al.*, 2001).

A recent review by Rae-Grant and colleagues summarises how the role of blood vessels in MS has been postulated since the mid-19th century, sometimes described as integral to the pathogenesis of MS, at other times referred to as a vehicle for the agents (immune or viral) responsible for MS, and at times observed as being simply innocent bystanders. In 1863, George Eduard von Rindfleisch, demonstrated that a blood vessel was usually seen in the centre of MS plaques after brain autopsy. He also described changes within the walls of the vessels suggesting chronic inflammation (Rae-Grant *et al.*, 2014).

Jean-Martin Charcot at the Salpêtrière Hospital in Paris, provided the early descriptive account of 'sclérose en plaques' in the latter half of the 19th century, with the English translation of some of his labels for the disease being 'disseminated sclerosis'. He however felt that any involvement of the blood vessel was as a consequence of other pathological processes affecting neuroglia (Compston *et al.*, 2005).

In 1916 James Dawson published, 'The Histology of Disseminated Sclerosis'. This aimed to highlight the pathological aspects of MS from the histology of nine cases. He noted the presence of sclerosis originating from the side of the lateral ventricles and projecting into the WM, and showed areas of MS plaques near or surrounding blood vessels, although he found it difficult to attribute these to the causation of MS (Dawson, 1916). His micro-photographs taken post mortem from these nine patients, depict a number of lesions with veins within them (Figure 2). Subsequent pathological studies have demonstrated the relationship of veins to MS lesions. Robert Dow and George Berglund in 1942, concluded that the presence of a 'central vein' within a lesion is not by chance, but could not provide a definitive role in the pathogenesis of MS. Histological examination from 60 lesions from 5 post mortem examinations demonstrated that 66% had a visible central vein (Dow and Berglund, 1942). Six of the 20 lesions that were classed as 'central vein absent' in fact had multiple veins through the lesion, but were excluded from the final numbers due to the lack of a single vein. Furthermore they confirmed that a central artery could not be found. Lesions that were described as 'elongated' had veins that followed their long axis (Figure 2). This feature can often be seen on MRI. In the mid-60s Fog histologically examined 51 lesions from two patients with MS to find that 28 (55%) were perivenous (Fog, 1964). He concluded that the path of the periventricular

veins followed the course of the veins from the subependymal plexus. In the 1980s, Adams demonstrated damage to the vein wall within MS lesions, including fibrin deposition and haemorrhage within the walls and haemosiderin deposition (Adams, 1988)

More recently at the beginning of the 21st century, Claudia Lucchinetti demonstrated the immunopathological differences within MS WM lesions (WMLs) (Lucchinetti *et al.*, 2000). After examining lesions from a total of 83 autopsies or biopsies, four distinct patterns of demyelinating lesions were revealed. All WMLs had T lymphocyte infiltrates and macrophages, but they could be separated into four distinct lesional patterns based, amongst other features, the appearance of oligodendrocyte destruction or immunoglobulin and complement deposition. In addition, three of the four patterns (I, II and IV) showed perivenous demyelination.

The WML central vein is the pathological feature of the MS lesion that I will seek to study using 3T MRI and T2* weighted sequences (described later) to determine if it is an accurate biomarker for the disease.

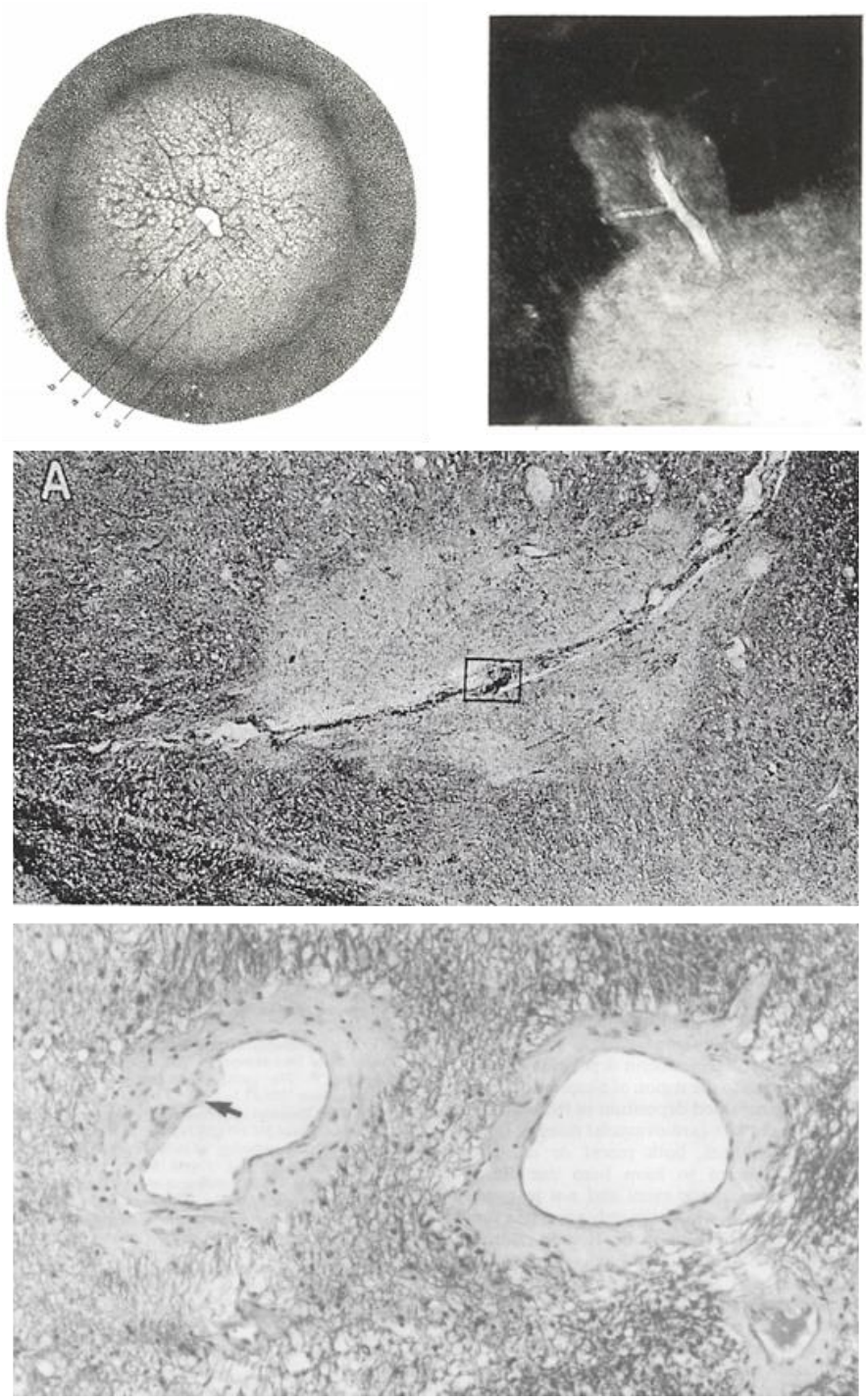

Figure 2. Perivenous MS lesions.

Top figure (left): An 'early' pale sclerotic area with a central blood vessel; Top figure (right): Small capillary within an area of sclerosis (Dawson, 1916). Middle figure: A lesion with a thrombosed central vein (Dow, 1942). Bottom figure: Veins with thickened walls of collagen within a MS lesion (Adams, 1988).

1.1.4 Clinical phenotypes and natural history

Following an international survey in 1996, which questioned physicians and researchers of their preferences and understanding of the subtypes of MS, definitions of RRMS, SPMS and PPMS were produced (Confavreux and Vukusic, 2006b). This allowed more consistency in the phenotype of patients recruited to clinical trials, enabled more consistent documentation of the subtypes seen in day to day clinical practice and has allowed guidance for licensing of treatments for particular subgroups.

However, these definitions relied on the original clinical descriptions of the majority of those surveyed at the time. In 2012 these definitions were reviewed with the aim of incorporating MRI into these phenotypes. The original terms provided a framework for the new definitions. Alongside these, CIS was introduced as part of the MS spectrum. The level of disease activity (assessed by ongoing clinical relapses, gadolinium enhancing lesions or new T2 or enlarging T2 lesions) and a sense of disability progression (assessed by clinical examination), both add to the overall picture of the disease and imply ongoing inflammation or neurodegeneration (Figure 3) (Lublin *et al.*, 2014). Nevertheless, as yet there is no biomarker that can distinguish between the phenotypes of MS, and none that can identify the change from RRMS to SPMS.

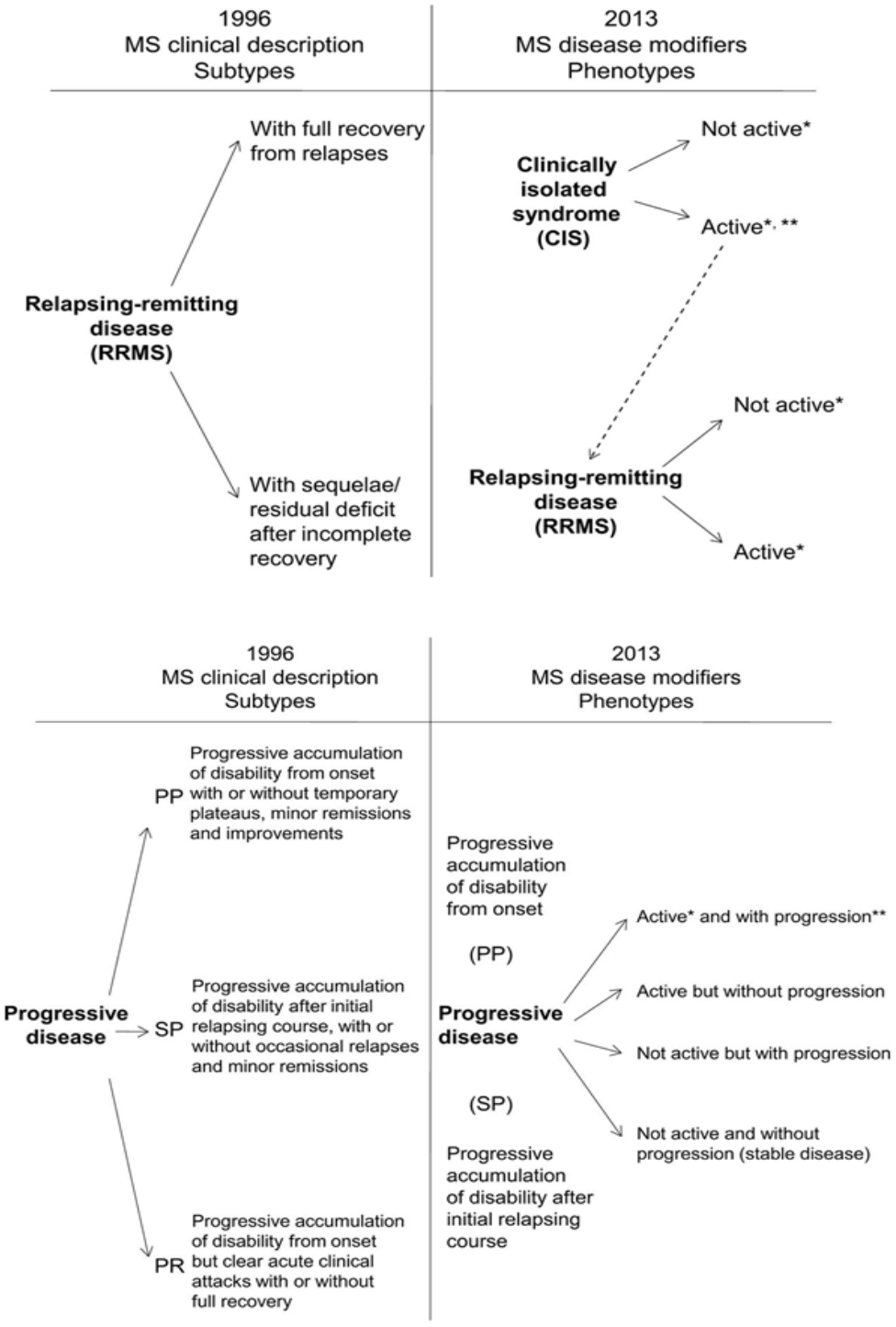

Figure 3. Clinical descriptions of CIS, RRMS, SPMS and PPMS.

Disease activity and presence of progression describe ongoing disease pathology and further refine the MS subtypes (Lublin *et al.*, 2014).

A CIS has been defined as the possible presentation of MS, with characteristics of demyelination that has not however demonstrated dissemination in time (DIT)

(Lublin *et al.*, 2014). The baseline MRI in these patients has been shown to be abnormal with WMLs present in approximately 60% at presentation (Morrissey *et al.*, 1993). The most recent, large observational study in Barcelona has shown that the higher the T2 lesion number on MRI at baseline, the faster the rate of reaching clinically definite MS. Patients with CIS and 10 or more lesions had a hazard ratio of 12.7. The presence of cerebrospinal fluid (CSF) oligoclonal bands (OCBs) and the higher the number of T2 lesions on MRI resulted in increasingly higher hazard ratios for developing MS (Canto *et al.*, 2015). Lesion number at baseline also had some influence on the risk of developing a certain level of disability. A recent prospective study from Barcelona demonstrated that 11% of patients with 10 or more lesions on their baseline MRI attained an Expanded Disability Status Scale (EDSS) of 3 at 5 years, but 30% attained this score after 10 years (Tintoré *et al.*, 2015). Fisniku et al. showed results of a similar theme with patients who have more than 10 lesions at baseline, being more likely to reach EDSS 3 and 6 after 20 years (Fisniku *et al.*, 2008). MRI therefore appears to be the best predictor of developing MS in the CIS group and these latest results reproduce the results of other cohorts studied (O'Riordan *et al.*, 1998; Fisniku *et al.*, 2008).

RRMS is defined as acute deteriorations in neurological function with complete or incomplete recovery, with no evidence of progression in between relapses. Updates to the clinical course now include the level of clinical activity (the number of relapses) or MRI activity (new T2 lesions or gadolinium enhancing lesions) (Lublin *et al.*, 2014). The 20 year longitudinal study by Fisniku showed that patients with higher lesion volumes on MRI during the first 5 years of disease were more likely to develop SPMS (Fisniku *et al.*, 2008).

Patients with SPMS initially follow a relapsing and remitting course, followed by steady progression with occasional fluctuations in disability but maintaining a deteriorating trend. The progressive phenotype has also been refined lately with the addition of clinical or MRI activity and whether the patient has clinical progression (Lublin *et al.*, 2014).

I describe the PPMS phenotype in detail in chapter 4 so will not repeat it here.

1.2 Diagnostic criteria for MS for patients with a typical clinical onset

The fundamental framework in order to diagnose a patient with MS has not changed over the last 50 years since the concept of dissemination in space (DIS) and time (DIT) was introduced by Schumacher in 1965 (Schumacher *et al.*, 1965). DIS, indicating pathological involvement of one or more CNS areas and DIT, indicating two or more attacks of demyelination lasting more than 24 hours, separated by 30 days or more has remained crucial for the diagnosis. In addition to these criteria, a final important point is that there should be no other better explanation for the patient's symptoms and signs. The diagnosis can be made on purely clinical grounds although there is no single clinical symptom, sign or biomarker to confirm the diagnosis. Like many neurological diseases the diagnosis has always been a clinical one. The use of supporting neurological tests has evolved over the last 30 years, with MRI becoming increasingly important both in day-to-day practice and clinical trials (Evans *et al.*, 1997).

In 1983, Poser and colleagues, in an effort to ensure patients recruited into research had definite MS, further refined the diagnostic criteria. They included the presence of unmatched CSF OCBs , evoked potentials and introduced computed tomography

(CT) and nuclear magnetic resonance as paraclinical evidence of disease, in addition to clinical criteria (Poser *et al.*, 1983). This introduced the terms 'clinically definite', 'laboratory supported definite' 'clinically probable' and 'laboratory supported probable' MS. This was in contrast to the previous Schumacher criteria which were used purely to distinguish clinically definite MS from non-MS.

In 2001, for the first time, the firm inclusion of MRI into diagnostic criteria was proposed by McDonald and colleagues (McDonald *et al.*, 2001). These criteria, developed by an international panel on the diagnosis of MS, introduced MRI criteria put forward by Barkhof and colleagues (Barkhof et al., 1997) and was supported by a study by Tintoré et al. which compared the criteria of Poser, Fazekas and Barkhof (Tintoré *et al.*, 2000). These criteria applied to patients between the ages of 10-59 with typical symptoms suggestive of MS. It was emphasised that patients with an unusual or atypical presentation should be investigated with additional tests. They also aimed to allow a patient with CIS to be diagnosed with MS based on paraclinical tests such as MRI, CSF or visual evoked potentials (VEP). The Barkhof DIS MRI criteria included three of the four following imaging conditions: (1) one gadolinium enhancing lesion or nine T2 hyperintense WMLs if enhancing lesions were not present; (2) at least one infratentorial lesion; (3) at least one juxtacortical lesion and; (4) at least three periventricular lesions. DIT was determined by the presence of a new gadolinium enhancing lesion on MRI, if performed 3 months or more after a clinical event and if excluding the anatomical site to explain the clinical event. If there was no enhancing lesion at this time, a further scan was needed at least 3 months later showing an enhancing or new T2 lesion. Lesions had to be larger than 3mm in diameter (Barkhof *et al.*, 1997; McDonald *et al.*, 2001). The manner in which patients presented and whether there

were objective signs, determined the use of the MRI criteria. Overall the criteria had a high specificity and sensitivity of 83% each, a positive predictive value (PPV) of 75% and negative predictive value (NPV) of 89% (Milo and Miller, 2014).

In 2005, the McDonald criteria were revised and it was suggested that DIT was changed to include a new T2 lesion compared to a baseline scan performed at 30 days (rather than 90 days). Spinal cord lesions were more accurately defined. Furthermore, a spinal cord lesion could be considered equal to an infratentorial lesion or, substituted as one brain lesion to reach the total number of 9 T2 lesions. In addition an enhancing spinal cord lesion could be regarded as equal to an enhancing brain lesion (Polman *et al.*, 2005).

In 2010 a further revision was introduced with simplification of MRI criteria for DIS (Polman *et al.*, 2011). A study by Swanton et al. showed that although this could be simplified, overall sensitivity improved with very little reduction in specificity of the McDonald criteria (87% compared to 91.1% specificity with the McDonald 2001 criteria (Swanton *et al.*, 2007). DIS was revised to include 1 or more lesions in 2 or more characteristic CNS locations; juxtacortical, periventricular, infratentorial or spinal cord (with a symptomatic brainstem or spinal cord syndrome being excluded from the DIS count). DIT was simplified to include a new T2 or gadolinium enhancing lesion on a repeat MRI compared to baseline, regardless of the timing of the baseline scan or, the simultaneous presence of non-enhancing and enhancing, asymptomatic lesions on a single MRI scan.

The McDonald criteria informs a clinician more about the prognosis of a patient with typical symptoms of CIS developing MS, rather than being able to discriminate between atypical cases of MS and common MS mimics (Nielsen *et al.*, 2005). The

exclusion of MS mimics is therefore intended to occur *before* application of the McDonald criteria. Hence there is no single test to help differentiate between the many conditions that present in a clinically and radiologically similar manner to MS.

1.3 The misdiagnosis of MS

In 1916 Dr James Dawson commented in his work on the histology of disseminated sclerosis (Dawson., 1916, p.634):

> *The great variation in the nervous symptoms has resulted in a tendency, on the one hand, for any disease of nervous origin of which the symptoms are unusual or difficult to interpret to be classified as "disseminated sclerosis"; while, on the other hand, the way in which the symptoms of a case of true disseminated sclerosis may simulate other nervous diseases has often led to errors in diagnosis.*

One hundred years later, in 2016, misdiagnosing MS and misinterpretation of neurological symptoms can at times still be problematic. Misdiagnosing a patient with MS remains a significant, unaddressed problem, which has the potential to be increasingly troublesome over the coming years due to the rapid increase and use of potent disease modifying treatments (DMTs) (Solomon *et al.*, 2012). The proportion of patients misdiagnosed is difficult to accurately ascertain, but estimates are between 5-10% (Solomon and Weinshenker, 2013).

Diagnosing MS can, at times, be difficult due to the lack of availability of a single test to differentiate MS from mimics, and the sometimes non-specific nature of the illness. The difficulty arises due to the variety of conditions that mimic the

symptoms, neurological signs, CSF and MRI seen in MS. Many other conditions, both systemic and neurological can have a fluctuating course, with distinct episodes of neurological disability affecting different regions of the CNS (Kelly *et al.*, 2012). Diagnostic uncertainty can therefore arise and patients frequently wait months and occasionally years before diagnostic confirmation. This in turn delays potential treatment of MS or treatment for an alternate condition. Being incorrectly diagnosed with MS poses its own physical risks of being started on potent immunomodulatory therapies. Additionally, there is a psychological impact of being diagnosed with, and becoming accustomed to, a chronic disabling condition, only to be informed that one may not actually have the condition and an alternate disease may have been overlooked (Solomon *et al*., 2012). Misinterpretation of MRI has been suggested as a common cause of misdiagnosis (Solomon *et al*., 2012). As such the development of an imaging or serological biomarker is an unmet need. The use of WML central veins on MRI as an imaging biomarker has grown in interest in the last 16 years, but needs further validation using clinical MRI scanners.

The McDonald criteria apply to 'typical' cases of MS with typical objective signs and apply to a specific age group. Additionally the studies involved in developing the MRI criteria studied groups of patients in western research institutions and may not always apply to paediatric populations or cohorts of patients from other ethnic backgrounds. Therefore patients with an atypical clinical presentation need careful deliberation before a diagnosis of MS is made. The McDonald criteria stress that there should be no better explanation than MS for the clinical picture (McDonald *et al.*, 2001; Polman *et al.*, 2011). These patients with 'diagnostic doubt' need further investigations which may be helpful or sometimes complicate the clinical picture

further. Conversely there are a considerable number of patients who have MRI brain scans for reasons other than investigating for MS, in whom WM abnormalities are seen. The thought of MS may not have even been considered by the patient or physician. Yet, incidental WM abnormalities, which can also be found in healthy individuals, can look similar to MS WMLs, raising the suspicion of MS based solely on an MRI scan. In a study by Kelly et al., 41 of 244 (17%) referrals for suspected MS were due to abnormal MRI brain or spinal scans. The most common reason for performing the MRI was headache (24%) followed by tinnitus, hearing loss/vertigo, transient paraesthesia and general malaise and symptoms suggestive of transient ischaemic attacks. Of the 41 only 8 (20%) were eventually given the diagnosis of MS (Kelly *et al*., 2012).

Charles Poser studied the number of patients who had been misdiagnosed in a cohort of patients who had been referred for a second opinion. Being one of the leading authorities on MS at the time, he may have received more referrals than others for a second opinion, and the fact they were referred indicates there may have been diagnostic doubt. With this in mind, of 366 patients, 130 (35%) were incorrectly diagnosed with MS by the referring neurologist. These patients had disseminated encephalomyelitis (48/130), chronic fatigue syndrome (28/130), complicated migraine (5/130), psychiatric disorders (3/130), myelopathy (27/130), post traumatic syndrome (5/130) and unknown disorders in 14/130. It is unclear if some of these patients may have had CIS. In addition, fourteen of those misdiagnosed were receiving a form of β-interferon and a further ten patients indicated that their neurologist had recommended this medication (Poser, 1997). A retrospective case note review by Carmosino and colleagues found that out of 281 patients referred to their MS clinic to confirm if they had MS, only 93/281 (33%)

patients were eventually diagnosed with it and of these only 66% had typical signs. A further 103/281 (37%) of patients were referred due to an abnormal MRI brain scan which suggested MS, but only 11% (12/103) of this group eventually received the diagnosis. Similar to previous studies this showed that many alternative conditions were diagnosed rather than MS, the most common being migraine and stroke, and a significant number having possible psychiatric disease (22.5%) (Carmosino *et al.*, 2005).

A study by Levin et al. demonstrated the rate of misdiagnosis especially among patients who initially presented with non-specific or sensory symptoms, with 58% given an alternate diagnosis to MS when they were originally seen. More than half of these were given a psychiatric diagnosis or told they had medically unexplained symptoms at presentation. In addition this demonstrated that on average patients were diagnosed 3.5 years after their initial symptoms (Levin *et al.*, 2003).

The financial cost of misdiagnosing MS has been recently highlighted (Solomon and Weinshenker, 2013). It has been estimated that if approximately 5% of the 400,000 patients with MS in the United States were misdiagnosed, with the assumption that 50% of these patients were on DMTs, then the cost of this group would be nearly 500 million US dollars for DMTs alone. This is, of course a broad estimate but shows the potential high costings that could be saved. Additionally the risk of enrolling such patients in experimental drug trials, causing risk to themselves, risk of litigation and compromising the results was also highlighted.

A recent survey by the same author unveiled the high number of mistaken cases of MS seen by neurologists in the US and Canada (Solomon *et al*., 2012). The study was completed by 122 of 242 neurologists. This revealed that 39.7% had seen

between 3-5 patients in the last year who they strongly felt did not have MS (although previously being diagnosed with MS by another physician). Surprisingly, 17% of respondents declared they had seen more than 10 patients with a mistaken diagnosis of MS in the preceding year. Nearly 65% of respondents thought that more than 25% of all misdiagnosed patients were on DMTs. The survey revealed that within the preceding year, all neurologists surveyed had seen 279 patients misdiagnosed with MS who were taking DMTs. Many cases were attributed to misinterpretation of the MRI scan, with the majority of respondents citing non-specific WM abnormalities, migraine, psychiatric disease, small vessel ischaemia and Neuromyelitis Optica (NMO) as being the alternate diagnoses. The 279 estimated cases would have cost approximately 11 million US dollars in medical expenses.

1.4 MS in elderly patients and risk of misdiagnosis

The onset of MS after the age of 50 has been reported in many studies (Martinelli *et al.*, 2004; Kis *et al.*, 2008) and although not uncommon, can cause some hesitation in diagnosing it early. Noseworthy demonstrated the difficulty of diagnosing MS in this age group even amongst experienced neurologists (Noseworthy *et al.*, 1983). Of 838 patients with MS at the University Hospital, Western Ontario, 79 presented after the age of 50. Of these only 34% were diagnosed with MS after the first neurological assessment by their neurologist. Alternate diseases that were initially considered included spondylitic myelopathy, vascular disease, motor neuron disease, hereditary and spinocerebellar degeneration and familial progressive paraplegia. Younger patients more commonly presented with sensory symptoms and signs indicating spinal cord damage and older patients presented with a slow deterioration in motor function. They concluded that MS

maybe underdiagnosed in the elderly and due to the co-existence of other neurological disorders that may produce similar neurological signs, the diagnostic approach was more difficult.

De Seze et al. studied 20 patients who had interpretable MRI scans out of 46 patients who developed MS after age 50, with age matched controls. This showed that the Barkhof MRI criteria (Barkhof et al., 1997) had a sensitivity of 85% and specificity of 65% when used to diagnose MS in an older age group (de Seze *et al.*, 2005). They also demonstrated that juxtacortical lesions were more numerous than in lesions in the infratentorial region. De Leeuw et al. demonstrated the high number of WMLs in predominantly asymptomatic, elderly women within the frontal and parietal subcortical regions and periventricular area. Of all 1077 subjects, only 5% were free of WMLs. Subjects within the age group of 60-70 showed that 13% and 32% were completely free of subcortical and periventricular WMLs respectively (de Leeuw *et al.*, 2001).

There is no gold standard for the identification of lesion size or shape therefore small, incidental WMLs could be misinterpreted (Wang *et al.*, 1997). Wang et al. studied lesion size in MS patients using MRI at 1.5 Tesla (T). Eighty percent of the total number of WMLs were smaller than 8 mm in diameter, with a mean WML size of 36 mm^2 and 20% of the total WML load being less than 3.5 mm in diameter. Therefore incidental small WMLs can easily be misinterpreted.

1.5 Performance of McDonald 2010 MRI criteria in differentiating MS from mimics

Current diagnostic criteria are used to predict the conversion of patients with CIS to MS. However if the appearance of the MRI strays from the defined criteria then

the suspicion of alternate diseases should be raised. Revisions to the McDonald criteria published in 2010 simplify the DIS requirements, and inappropriately applying the simplified DIS criteria could lead to a higher rate of false positive cases (Selchen *et al.*, 2012).

A recent study in 2013 by Liu et al. highlights this (Liu *et al.*, 2013). They retrospectively reviewed the MRI brain scans of patients who had presented to their clinic with headache, including scans with gadolinium. Fluid attenuated Inversion Recovery (FLAIR) and T2 weighted imaging were used to analyse the images and classify WMLs according to the original Barkhof DIS criteria and the Swanton DIS MRI criteria published in 2010. Periventricular and juxtacortical lesions were defined as 'WM hyperintensities having an edge within 3mm of the surfaces'. Between 2.4% and 7.1% of headache patients had WMLs fulfilling the original Barkhof criteria and the authors' own lesion perimeter definitions respectively. Furthermore between 24.4% and 34.5% of patients met the criteria for a diagnosis of MS when using the McDonald 2010 MRI criteria. Liu also concluded that inclusion of DIT criteria and spinal cord imaging would increase the number of headache patients who meet the 2010 criteria further. However abnormal spinal cord imaging is not usually found in asymptomatic patients or patients with headache, so inclusion of this specific criterion may not actually alter the number.

Nielsen and colleagues studied the specificity of the Swanton DIS MRI criteria (Nielsen *et al.*, 2010). Their work highlights that the McDonald criteria and subsequent revisions allow conversion of patients with typical episodes of CIS to MS based on MRI findings, but do not help differentiate MS from similar conditions. They comment that patients included into these original studies were based at tertiary centres with other diagnoses first excluded. This group studied the

specificity of the McDonald 2005 and 2010 criteria in differentiating MS from other conditions in clinical practice. Of 377 patients referred by a neurologist for a second opinion, 28 were eventually diagnosed with 'other neurological diseases' including cerebrovascular disease, primary vasculitis, multiple system atrophy and other single diagnoses. They did however find similar specificity with the McDonald 2010 DIS criteria compared to the original report by Swanton et al. in 2007.

1.6 MRI mimics of MS

1.6.1 Migraine

Numerous studies have shown the frequency of WM hyperintensities in patients with migraine. Kruit et al. demonstrated infratentorial WMLs in 13/295 migraineurs and one healthy control. Three of these patients had one or more WMLs between 2 – 5mm in size located in the deep cerebral WM. These patients also had more lesions in the periventricular and deep WM regions, with 86% of this group having pontine hyperintensities (Kruit *et al.*, 2006). The same group also showed that female patients with migraine with or without aura had an increased chance of deep WMLs (Kruit *et al.*, 2004).

The MRI of patients with migraine can also fulfil radiological criteria for MS. This was recently demonstrated by Seneviratne et al. who found that of 44 patients with migraine with MRI brain imaging, 4 had WMLs in locations that met the McDonald 2005 MRI criteria for DIS (Seneviratne *et al.*, 2013). Although the number meeting the McDonald criteria is low (possibly explained by the small sample size), this study shows how the results of such MRI scans could subsequently reinforce the diagnosis (or rather misdiagnosis) of MS. Their study also highlights that since the

revision of the McDonald criteria in 2010, new simplified MRI criteria for DIS may reduce the specificity.

1.6.2 Neuromyelitis optica

NMO, is a relapsing remitting inflammatory, demyelinating condition, or more specifically an autoimmune astrocytopathy (Lucchinetti *et al.*, 2014) affecting the optic nerves, brainstem and spinal cord. A potentially severe form of inflammatory CNS disease, relapses can lead to sustained disability and as such the disease is treated more aggressively than in MS, hence the need for accurate diagnosis. It predominantly affects women with some studies reporting a ratio of 9:1 (Flanagan and Weinshenker, 2014) and a median age of onset of approximately 39; 10 years later than the onset of MS (Wingerchuk *et al.*, 2007). Incidence rates have varied between less than 1/100,000 to 4.4/100,000 (Jarius *et al.*, 2014). Once thought to be a variant of MS, it is now known to be a separate entity with antibodies to aquaporin-4, one of the main channels that controls water movement in the CNS, mainly found on astrocytic foot processes, near the blood-brain barrier (Wingerchuk et al., 2007). Presence of this is said to be 91% specific and 73% sensitive for the diagnosis (Pittock *et al.*, 2006).

Recent consensus diagnostic criteria suggest using the term NMO spectrum disorder (NMOSD) was more appropriate for this group of patients because the immunopathology and treatment of NMOSD is not different to patients with the historical description of NMO. This would also encompass patients with incomplete forms of NMO, who will later match NMO criteria, patients with less common cerebral hemisphere, brainstem or diencephalic lesions and those with negative aquaporin-4 serology (Wingerchuk *et al.*, 2015). Diagnosis is guided by the presence or absence of aquaporin-4 antibodies, with more strict criteria that

needs to be fulfilled for patients with negative serology. Patients with positive serology also require one of six 'core' clinical syndromes needing to be present. Patients without aquaporin-4 antibodies need to fulfil two of six core criteria, with at least one clinical attack being one of the three most common presentations (optic neuritis, transverse myelitis or an area postrema syndrome), along with additional MRI criteria.

Usually MRI findings reveal long segments (spanning at least 3 vertebral segments) of high signal on T2 weighted imaging within the spinal cord, which is the most specific MRI marker for NMO. Although brain MRI can be normal, it is not uncommon to see WMLs, which can appear non-specific or be asymptomatic, and up to 16% of patients can meet the Barkhof MS MRI criteria (Wingerchuk *et al.*, 2015). Brain lesions can involve the dorsal medulla (the most common site for infratentorial lesions), hypothalamus, periaqueductal grey and area postrema (Tackley *et al.*, 2014). Although 60% of patients with NMO can have asymptomatic lesions, lesions in the these specific regions can cause distinct symptomatology such as vomiting, hypersomnia and dysregulation of temperature (Poppe *et al.*, 2005; Nozaki *et al.*, 2009; Viegas *et al.*, 2009; Suzuki *et al.*, 2012). The morphology and distribution of WMLs can therefore sometimes differentiate between MS and NMO, but not always. Mealy et al. studied the epidemiology of NMO using the number of patients across three centres in the US. Of 187 patients, 151/187 had MRI brain scans. Of these 12.6% had 'MS-like' lesions. Furthermore, 29.4% of this group had been misdiagnosed with MS before the correct diagnosis of NMO.

Pittock et al. reported that in a cohort of 60 patients from the Mayo clinic and external institutions, 36 (60%) had MRI brain abnormalities with 17% of these

patients having symptoms related to these brain lesions e.g. nausea, diplopia, nystagmus and trigeminal neuralgia (Pittock *et al.*, 2006). In the same study six (10%) of patients had lesions suggestive of MS, five of whom had antibodies to aquaporin-4 and four of whom matched the original Barkhof MRI criteria. Matthews et al. demonstrated that from a cohort of 41 patients with positive serology for aquaporin-4 antibodies, 26 patients had T2 hyperintense lesions and of these 7 (15.9%) met the Barkhof MRI criteria for MS (Matthews *et al.*, 2013). It was thought that this number may increase if spinal cord imaging with gadolinium was also used. Further studies have shown similar findings such as that by Huh et al. who showed that 13% of 67 NMO patients met Barkhof DIS criteria and 9% fulfilled the McDonald 2010 DIS MRI criteria (Huh *et al.*, 2014).

In a non-specialist clinic, the distinction between MS and NMO may not be made due to the very similar onset of symptoms and CNS areas affected. This coupled with WMLs on MRI may convince a non-specialist that the patient has MS rather than NMO which may subsequently lead to inappropriate and potentially harmful treatments (Palace *et al.*, 2010; Barnett *et al.*, 2012; Kitley *et al.*, 2014).

1.6.3 Neurosarcoidosis

Sarcoidosis is a chronic, inflammatory, granulomatous disease that can affect multiple organ systems with an incidence of between 3-10 per 100,000 for Caucasians increasing to 35-80 per 100,000 among African Americans (Pawate *et al.*, 2009). Symptoms can sometimes take a relapsing remitting course and sometimes present with neurological symptoms similar to MS, allowing for potential misdiagnosis and incorrect treatments. The lungs and mediastinal lymph nodes are the most commons sites for the pathological hallmark of the disease; non-caseating granulomas. Neurosarcoidosis occurs in approximately 5% of patients

with the systemic disease although some feel that this is an underestimate (Pawate *et al.*, 2009). Common clinical presentations include a cranial neuropathy (facial palsy or optic neuropathy), meningitis, hypothalamic or pituitary involvement or arachnoiditis and medullary lesions of the spinal cord (Lacomis., 2011).

Pawate et al. performed a case note review of patients referred to their MS centre to confirm or refute a diagnosis of MS and found that 54/164 patients had a diagnosis of definite, probable or possible neurosarcoidosis. Nine of these cases had biopsy proven disease, showing non-caseating granulomas and of these, eight initially presented with neurological symptoms. Nineteen patients of their cohort (35%) presented with optic neuritis, with 13/19 having bilateral optic neuritis and 6/19 having unilateral symptoms. The second most common presenting symptoms were attributed to a myelopathy (19%). Other neurological presenting symptoms included; facial nerve palsy (6/54), ataxia (2/54) and vertigo (1/54). Brain MRI was normal in 6/53 cases, but non-enhancing, brain parenchymal T2 lesions were the most common finding in 30% of cases, with a minority having grey matter lesions. Lesion location ranged from subcortical and periventricular to large, diffuse WM disease with or without meningeal enhancement.

A case series of 68 patients by Zajicek showed similar neurological presentations as the Pawate study (Zajicek *et al.*, 1999). Again this study showed the most common MRI brain abnormality to be WMLs. CSF was also abnormal in this case series with 81% having elevated protein with or without lymphocytic pleocytosis, 50% having OCBs and two thirds of this group having unmatched OCBs. Usually unmatched CSF OCBs in neurosarcoidosis are present to a lesser extent (approximately 27-37%) (Ibitoye *et al.*, 2017), nevertheless this has similarities with MS patients who have unmatched OCBs, normal or slightly raised protein and

absent or marginally raised lymphocyte counts (Palace, 2001). Multiple case series have also shown the prevalence of periventricular WMLs on MRI in patients with neurosarcoidosis (Miller *et al.*, 1988; Smith *et al.*, 1989).

1.6.4 Neuro-Behçet's disease

Neuro-Behçet's disease (NBD) is an uncommon, autoimmune inflammatory disorder complicating Behçet's disease in approximately 10% of cases. Nonetheless it important to consider in the differential diagnosis of MS in certain populations, as brain WMLs can be seen alongside the classical infratentorial (particularly brainstem) findings (Figure 4). Prevalence is variable but is particularly common in the Middle East, Far East Asia and the Mediterranean (Al-Araji and Kidd, 2009), with peak incidence between the ages of 20-40. Neurological complications present with either a spinal cord syndrome, a meningoencephalitis or brainstem syndrome with a variety of systemic symptoms. As in MS there is no single test to help eliminate mimics and MRI findings classically show a brainstem hyperintensity on T2 imaging with asymmetrical extension into the basal ganglia and thalamus (Al-Araji and Kidd, 2009). Some patients follow a relapsing-remitting course with others having progressive disability after an initial attack of symptoms (Kidd *et al*., 1999).

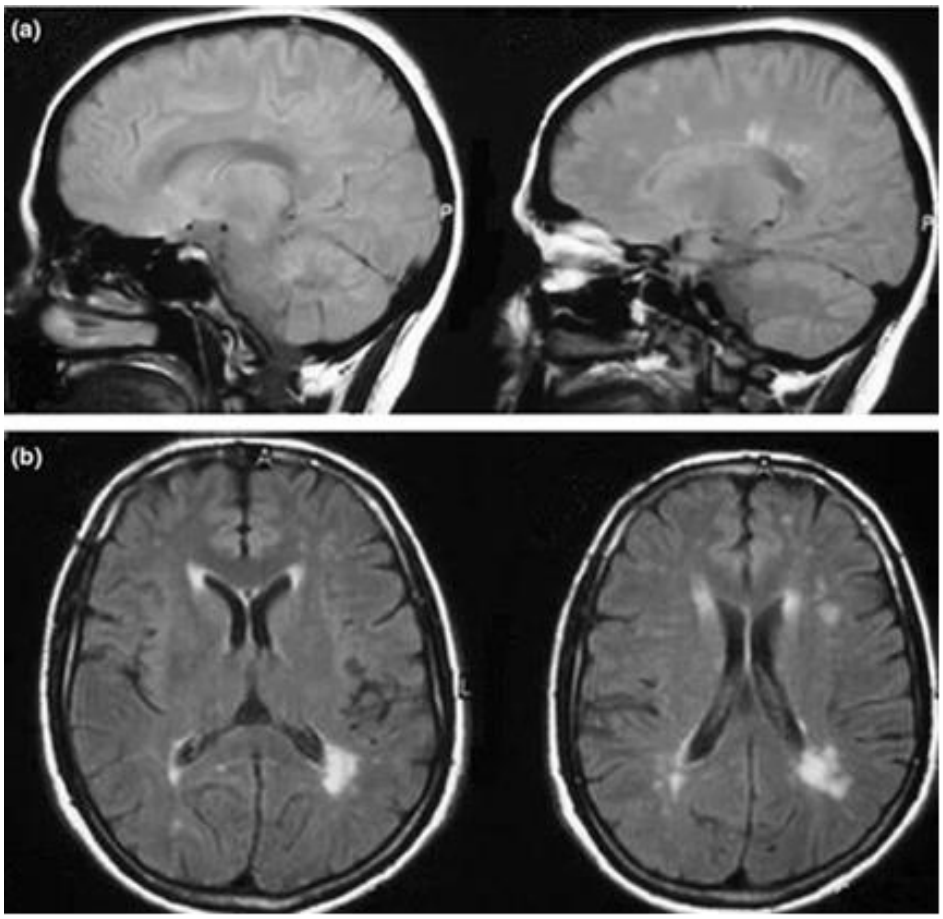

Figure 4. MS like lesions in Neuro-Behçet's disease.

Top row: Proton density and bottom row: axial FLAIR images showing periventricular and Dawson's finger like lesions resembling MS (Farahangiz *et al.*, 2012)

A case series by Kidd et al. studied 51 patients with Behçet's disease, of which 12 initially presented with neurological symptoms (Kidd *et al.,* 1999). Neurological syndromes included 25/51 with a meningoencephalitis, 7/51 with a spinal cord syndrome, 1/51 with an optic neuropathy and 2/51 with unilateral vestibulopathy. MRI imaging revealed 3 cases with brainstem as well as bilateral periventricular WMLs. Although the majority did not have periventricular lesions, those with hemisphere signs (hemiparesis or hemisensory symptoms) had WMLs in both hemispheres. The involvement of periventricular and subcortical areas has been shown in other studies (Lee *et al.*, 2001; Haghighi *et al.*, 2011; Farahangiz *et al.*,

2012), with the latter study having patients fulfilling McDonald criteria though they do not elaborate on this further.

1.6.5 Rheumatological disease

Specific rheumatological autoimmune diseases such as primary Sjögren's syndrome (Akasbi *et al*., 2012; Pelidou *et al*., 2007), Systemic lupus erythematosus (SLE) and Antiphospholipid syndrome (APS) (Cuadrado *et al*., 2000) can also mimic the MRI appearance of MS.

Pelidou et al. followed 132 patients referred to their hospital with a diagnosis of possible MS. After a mean follow up period of 14 months, 13% of this group had a confirmed alternate diagnosis, including Sjögren's syndrome, SLE and APS. (Pelidou *et al.*, 2007). A study by Akasbi et al. demonstrated that of 25 patients with Sjögren's syndrome, 3 had involvement of the corpus callosum and U fibres. WMLs were also seen infratentorially including the cerebellum and pons. Four patients from this study met the 1997 Barkhof criteria for DIS (Akasbi *et al.*, 2012).

APS is characterised by both arterial and venous thromboses, recurrent miscarriages, thrombocytopaenia and antiphospholipid antibodies. Treatment for this involves anticoagulation with resolution of symptoms and prevention of further thromboses; treatments which are completely different to that of MS. A report by Fernandez-Fernandez et al. describes two female patients who presented with neurological symptoms and whose MRI scans showed deep WM and periventricular lesions resembling that of MS, but who were diagnosed with APS (Fernández-Fernández *et al.*, 2006). Although the authors recognised the pitfalls of recall bias, a survey by Cuadrado et al. found that of 90 patients with antiphospholipid antibodies, 28% responded positively to the survey question; "Did

any of your doctors at any stage of your illness consider the diagnosis of MS?" (Cuadrado *et al.*, 2004). The same group retrospectively reviewed clinical notes of 27 patients referred to their lupus unit with suspicion of a connective tissue disease after having initially being diagnosed with definite or probable MS. Patients were referred if their neurological symptoms were not evolving like that of MS, if they had unusual MRI findings or antiphospholipid antibodies (Cuadrado *et al.*, 2000). Further diagnostic work up confirmed APS rather than MS. Individually the MRI scans of the APS group could not be distinguished from the scans of the MS control group, a finding repeated in other studies (Ijdo *et al.*, 1999). This latter study had patients who filled the criteria for definite or probable MS using Poser Criteria. This problem adds to the additional clinical similarities between the two conditions; APS can present with a relapsing neurological phenotype; both conditions usually affect patients between 20-40 years of age; both predominantly affect females, and some APS patients can have positive CSF OCBs.

SLE, like other rheumatological conditions may be managed with immunosuppression and so accurate, timely diagnosis is paramount. The female to male ratio is even higher than that of MS, and neurological symptoms can mimic those of MS including optic neuropathy. This was demonstrated by a follow up study of five patients who were misdiagnosed with MS, between the ages of 21-37 who presented with an optic neuropathy, diplopia or myelopathy. They had a relapsing-remitting course and the delay from diagnosis to the correct diagnosis of SLE varied from 1 – 12 years (Kurne *et al.*, 2008). These patients all had WMLs, some of which amalgamated around the ventricles. Retrospective review of the scans demonstrated occasional small cortical infarcts, which would be atypical for MS, along with development of antibodies to extractable nuclear antigens (ENA)

and anti-nuclear antibodies (ANA). Nevertheless, this small study shows the challenge at the beginning of a diagnostic pathway with disorders mimicking MS.

Rovaris et al. demonstrated the similarity of patients with SLE in terms of MRI brain imaging (Rovaris *et al.*, 2000). Blinded assessors reviewed MRI brains scans of patients with a variety of systemic inflammatory diseases, including fifteen patients with SLE and nine who had neurological symptoms (excluding migraine) as part of their SLE. Five of this group had multiple WMLs in a periventricular and subcortical distribution which, based on the scan alone could not be differentiated from MS. Again, SLE is diagnosed in predominantly women of child bearing age, and can be exacerbated by Interferon-β, one of the current first line medications used for RRMS (Ferreira *et al.*, 2005; Bonaci-Nikolic *et al.*, 2009). Hence accurate diagnosis is important in this setting especially since positive serological investigations seen in SLE, such as ANA and antiphospholipid antibodies can also be seen in MS (Ferreira *et al.*, 2005; Szmyrka-Kaczmarek *et al.*, 2012).

1.6.6 Acute Disseminated Encephalomyelitis

Acute Disseminated Encephalomyelitis (ADEM) is a rare disease in adults, being more prevalent in children with an incidence of 0.4 – 0.8/100,000 per year (Love, 2008). It has been described pathologically as showing sleeves of perivenous demyelinating lesions, containing small veins surrounded by macrophages. Lesions usually do not coalesce, in contrast to MS. ADEM takes the course of a monophasic illness (Young *et al.*, 2010). A polyphasic course is now thought to be more likely MS, NMO or an alternate chronic neurological disorder (Krupp *et al.*, 2013). The diagnosis of ADEM, amongst other features specifically includes encephalopathy. Brain MRI of patients with ADEM can still mimic those with MS, though there are

some features that may help distinguish the two conditions, including only the rare detection of OCBs in ADEM (Krupp *et al.*, 2013).

A study by Verhey et al. demonstrated that paediatric patients with ADEM are less likely to have periventricular and T1 hypointense lesions compared to those with MS. Additionally, ADEM was more likely to produce lesions in deep grey matter regions such as the thalamus and basal ganglia, but this feature was not as useful for differentiation as the presence of hypointense lesions. Of 284 paediatric patients followed up with an 'acquired demyelinating syndrome', 59 went on to develop MS after follow up. Of these, 49 had at least one periventricular lesion on their baseline MRI brain scan, which led to an increased likelihood of developing MS by a factor of 10 (sensitivity of 86%) (Verhey *et al.*, 2011). Periventricular lesions were not seen in 164/227 patients who did not develop MS, leading to a specificity of 72%. Having both periventricular lesions and at least one T1 hypointense lesion at baseline was even more suggestive of predicting the development of MS with a sensitivity of 84%, specificity of 93%, positive predictive value of 76% and negative predictive value of 96%. A pathological study by Young et al. goes against the hypothesis (described later in this chapter) that WML central veins would be a specific marker for MS (Young *et al*., 2010). Of 13 cases thought to have ADEM, all demonstrated perivenous demyelination, with 5 cases having multiple perivenous lesions coalescing together. Using the MRI WML central vein sign in the future therefore may require the neurologist to consider ADEM and MS if proven to represent perivenous demyelination.

1.6.7 Uncommon differentials of MS

Some conditions although rare, if diagnosed can lead to a change in management and sometimes prevent dire consequences. Fabry disease, is an X-linked inherited

disorder which affects lysosomal storage with deficiency of the enzyme alpha galactosidase A, causing a cerebral vasculopathy (Böttcher *et al*., 2013). It is frequently in the differential diagnosis in young patients following a stroke. Similar to MS it can first present in young patients with neurological symptoms without systemic manifestations. Böttcher et al. studied patients with genetically proven Fabry disease who had been previously misdiagnosed with MS (Böttcher *et al.*, 2013). These patients were correctly diagnosed on average 8 years after the misdiagnosis of MS. Of 187 patients, 5.9% had been given a diagnosis of MS, with a proportion receiving intravenous steroids, interferon or glatiramer acetate. MRI scans from these patients showed predominantly subcortical and periventricular WMLs which may have contributed to the initial misdiagnosis. (Figure 5). The authors suggested that with the latest revision of the McDonald criteria (2010), misdiagnoses based on MRI may become more common due to the DIS criteria being less rigid.

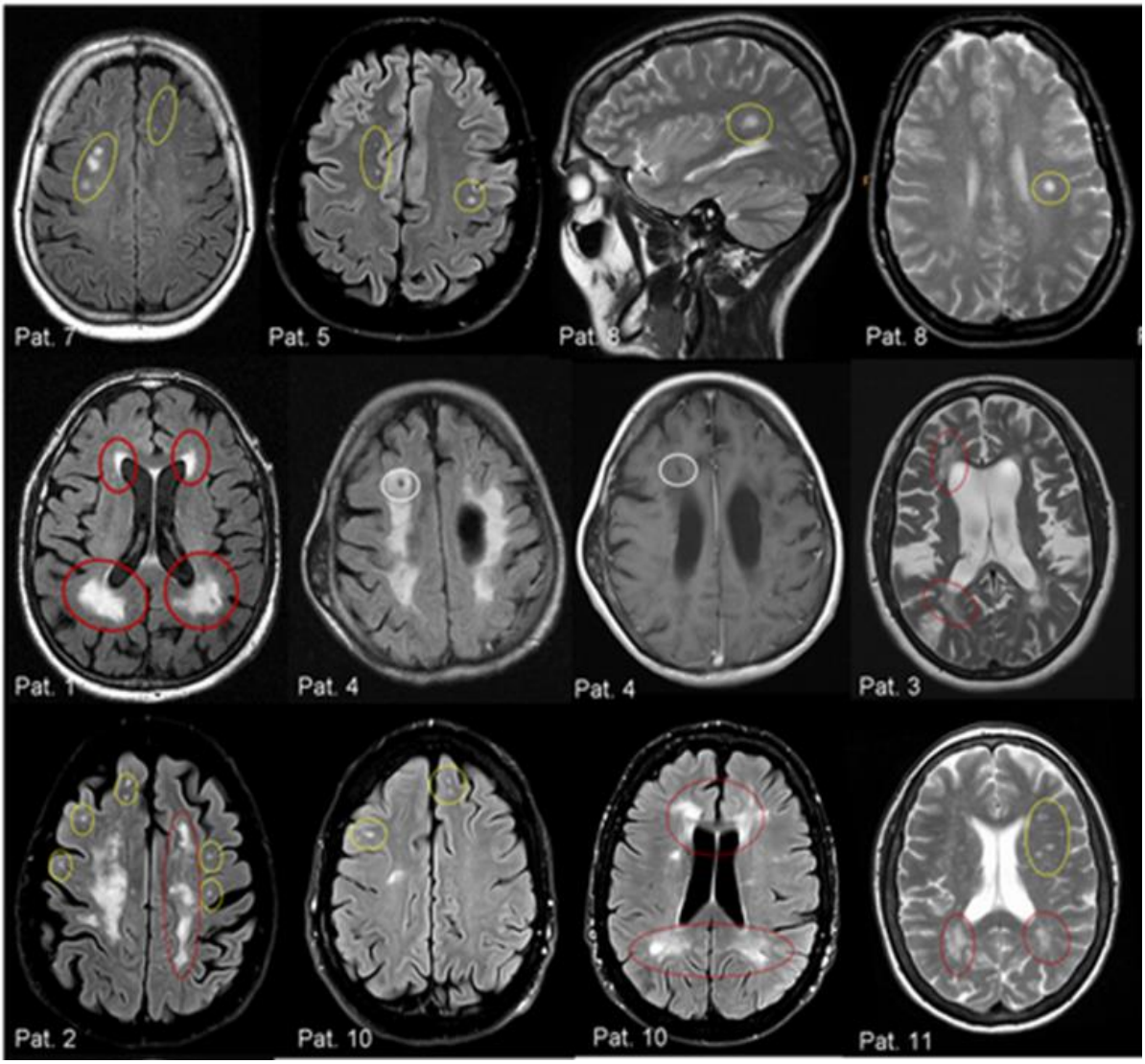

Figure 5. MRI showing WMLs secondary to Fabry disease in patients misdiagnosed with MS.

Top row: subcortical lesions circled by yellow circles. 2nd row: confluent WMLs particularly in a periventricular distribution (red circles) and T1 imaging showing black holes (white circles). 3rd row: periventricular lesions and subcortical lesions (Böttcher *et al.*, 2013).

Case reports of other rare diseases mimicking the symptoms and MRI appearance of MS have also been reported including Cerebral Autosomal Dominant Arteriopathy with Subcortical Infarcts and Leukoencephalopathy (CADASIL) (O'Riordan *et al.*, 2002; Pandey and Abubacker, 2006), Susac syndrome (Susac *et al.*, 2003) and a recent report of embolic phenomena secondary to an atrial myxoma (Quan *et al.*, 2015). Lyme disease, Human Immunodeficiency Virus (HIV) and

Syphilis are frequently quoted as common infective mimics of MS. Less common infections such as Cytomegalovirus (CMV), Hepatitis C, Whipple's disease, Neuroleptospirosis and Bartonella have been reported (Brinar and Habek, 2010; Rocha *et al.*, 2013).

Although in day-to-day clinical practice (at least in the UK) these diseases are uncommon, they are nevertheless important to keep in mind because they are treatable.

1.7 Asymptomatic patients and MRI suggesting demyelination; does it matter?

Darin Okuda and colleagues (2009) first used the term 'Radiologically Isolated Syndrome' (RIS) (Okuda *et al.*, 2009). This described the MRI brain or spinal cord scan of patients who had incidental WMLs fitting 3 out of 4 Barkhof criteria for DIS, but who were asymptomatic or who were scanned for another condition. The initial study included 44 patients with RIS, of which 30 were followed up. Ten patients developed MS or CIS. It has been suggested that there is a subclinical period before clinically evident MS, and RIS maybe the imaging evidence for this (Siva *et al.*, 2009; Siva, 2013).

However, this hypothesis is not as straightforward as initially thought. Two studies of patients with RIS have shown that those with spinal cord hyperintensities in addition to brain abnormalities are more likely to develop MS, than a patient with a normal spinal scan (Okuda *et al.*, 2011; Okuda *et al.*, 2014). An editorial by Dennis Bourdette questions the possible reason for this and suggests that perhaps not all RIS patients' brain lesions are demyelinating. RIS criteria depend on WMLs that match Barkhof DIS brain criteria which in itself were developed to predict the

onset of MS in patients with a typical CIS. As already noted they were not developed to differentiate MS from mimics and hence RIS patients with spinal cord lesions may be a subgroup that really does have asymptomatic MS, whereas those without spinal cord abnormalities may have another reason for their brain lesions (Bourdette and Yadav, 2011).

A recent retrospective, multicentre study by the RIS Consortium demonstrated that a proportion of these patients went on to develop a first clinical event within 5 years (Okuda *et al.*, 2014). RIS diagnosed before age 37, male gender or involvement of the cervical or thoracic cord increased the likelihood of MS, with a higher probability with multiple risk factors. The cumulative probability of a first clinical event was 34% at 5 years. In addition, 14 patients of 451 total cases developed progressive neurological symptoms with no improvement after the first clinical event, meeting the criteria for PPMS. Their study also suggested that at a younger age there may be an 'opportune age window' for symptom development. This would suggest careful monitoring of such RIS patients so as to not to miss the opportunity for accurate and timely diagnosis. Okuda concluded that it is important to correctly risk stratify RIS patients in order to reduce the amount of patients misclassified as having MS, avoid excessive tests and reduce psychological harm that may be produced by receiving a diagnosis (or misdiagnosis) of MS.

Sellner et al. suggested guidelines on how to monitor patients with RIS. This took into account a patient's preference for having regular follow-up with medical services and MRI scans, (but having to be reminded of a condition that they may not actually have), versus a 'waiting' approach where patients are asked to contact medical services if they have symptoms suggestive of a first clinical event. An MRI biomarker if shown to predict the development of MS could potentially help in this

regard, allowing stratification of patients at high and low risk of developing MS (Sellner *et al.*, 2010). In addition, in the 5 year study by Okuda et al. and previous studies, (Lebrun *et al.*, 2009; Okuda *et al.*, 2009; Siva *et al.*, 2009), all participants with RIS met criteria for DIS according to the Barkhof criteria. Therefore, we do not know the natural history of RIS patients with DIS criteria that do not match this or atypical WMLs. Searching for WML central veins in this 'atypical' cohort of patients might be useful in the future, but this has not been investigated so far.

1.8 Patient perceptions about the possible diagnosis of MS

Delivering the diagnosis of MS can be difficult from the view of the clinician even when one is certain of the diagnosis, and when tests and symptoms are all supportive. However, the disclosure of *possible* MS or informing a patient 'this may turn out to be MS in the future' can also be problematic.

Heesen et al. studied the views of patients and clinicians on diagnostic and treatment information given to patients via a retrospective questionnaire (Heesen *et al.*, 2003). Of the 434 patients who replied, 382 (92%) felt that every patient should be informed of the diagnosis as soon as the doctor has made it. If the diagnosis was suspected however, 69% felt that they should be told. The response of the clinicians to the disclosure of *possible* MS was less; 24% felt that they should inform a patient of the *possibility* of MS. In addition 60% of patients whose disease led to significant disability within 5 years (46/77), in retrospect would have preferred an earlier disclosure from their physician. The difference in opinion between clinicians and patients about disclosing the possibility of MS maybe due to the problems of misdiagnosis mentioned earlier by Solomon (2012) and Poser (1997). Also the

increasing chance of litigation may prevent doctors from discussing possibilities unless absolutely certain. The lack of a specific diagnostic test makes this difficult.

A Greek study also showed how patients preferred an earlier disclosure of the possible diagnosis (Papathanasopoulos *et al.*, 2005). Using a survey given to the members of the Greek MS society, they studied the attitudes of patients to the timing of the diagnosis and patient's reactions after being told. A significantly high proportion of patients who responded (598/657; 91%) thought that they should be told the diagnosis immediately, with just over a fifth of them declaring that they would continue to trust their doctor if the diagnosis was delayed intentionally. Although 59% had, as described in the paper 'very negative feelings' after disclosure, approximately a third of patients felt relief. This was because some patients felt afraid they had an alternative diagnosis such as Acquired Immunodeficiency Syndrome (AIDS) or more life threatening diseases like cancer. Others felt relief after the diagnosis of MS, after feeling guilty when being told they had 'psychosomatic symptoms'. The authors concluded that the rise in available DMTs was one reason for patients wanting earlier disclosure, along with general changes in attitudes towards more transparency between the patient and doctor.

Finally a small study, but nevertheless demonstrating the same trend as the others was conducted by Janssens et al (2004). Although again a retrospective survey, this showed that of 95 patients sampled, 24% preferred an earlier diagnosis and 70% were satisfied with the time taken for diagnosis. Satisfaction rates of the timing of diagnosis was dependent on the time taken for diagnostic work up. Patients who were satisfied had a median work up time of 1 month. This is in comparison to patients who wanted an earlier diagnosis (median diagnostic work up of nine months from first seeing a specialist). Patients wanting an earlier

diagnosis felt that the high level of uncertainty, lack of understanding from family and potentially missing out on DMTs were reasons for wanting to know early. Janssens and colleagues believed that in view of the high availability of medical information via the internet, patients can easily find out the possible differentials of their initial symptoms and hence patients with the possibility of MS should be informed as such (Janssens *et al.*, 2004).

1.9 Does an early diagnosis of MS change management?

There is much variation in the practice patterns amongst UK neurologists, let alone between different countries. There is no definite guidance on the use of specific DMTs to modify long term disability; a main endpoint that patients and physicians are trying to avoid. The question as to whether to use DMTs early in MS is a study in its own right, but a few studies which have had time to follow up their patients to assess long term outcome have highlighted the problems in this area. Recently the Association of British Neurologists revised the guidelines for prescribing DMTs for MS. They concluded that treatment of CIS (with interferons or glatiramer) could be considered for patients at high risk of converting to MS, for example with an abnormal MRI or positive OCBs (Scolding *et al.*, 2015).

The practice patterns of US Neurologists treating patients with CIS, RRMS and RIS was assessed by a series of web based surveys (Tornatore *et al.*, 2012). Although the number of respondents was small (75 neurologists) this study gave a flavour of prescribing patterns. Nearly 90% of respondents conveyed that they would start DMTs in a case of CIS and MRI showing non-enhancing WMLs. This increased to 97% if the hypothetical case showed one gadolinium enhancing corpus callosum lesion, three periventricular lesions and one cerebellar lesion, with the majority

(99%) choosing either interferons or glatiramer acetate. All respondents agreed that a DMT should be started for a hypothetical case of RRMS with 2 relapses in the last 4 years, with 5 non-enhancing brain WMLs. Again, if the relapse rate changed to 2 in 6 months, all respondents agreed on starting treatment, with 32% electing for Natalizumab and 39% choosing this drug if there was evidence of MRI T1 hypointense lesions or atrophy. Finally although no respondents would advise starting DMTs for a patient with RIS, 88% suggested they would perform follow up imaging in a patient with MRI WM changes.

An Austrian observational study found that the decision to start immediate DMTs was based on the number of WMLs on the baseline MRI scan. Specifically more than nine T2 lesions and a neurological syndrome suggestive of CIS prompted treatment (Fazekas *et al.*, 2010). Almost a third of patients (29%) were started on a DMT within 3 months of their CIS. Again this is not an insignificant number of patients and therefore the early, accurate diagnosis of MS is paramount before embarking on long term DMTs.

Natural history data from a longitudinal study by Brex et al. highlights the importance of early WML volume in long term disability (Brex *et al.*, 2002). After 14 years of follow-up the EDSS significantly correlated with the early MRI WML volumes. This was particularly noticeable during the first 5 years of the disease (change in MRI lesion volume over the initial 5 years was moderately correlated, r=0.61), indicating that although WMLs are not the only factor affecting disease progression, suppression of WML development early in the disease course is important. Again an early diagnosis will help to monitor and commence DMTs if needed.

A review by David Bates highlights some of the clinical studies that have shown some efficacy in diminishing the risk of developing MS after CIS with Interferon Beta (IFNβ) reducing the risk by 35-50% (Bates, 2011). The CHAMPS (Controlled High-Risk Subjects Avonex Multiple Sclerosis Prevention Study) demonstrated that Avonex (IFNβ-1a) reduced the risk of developing MS over 3 years and reduced the number of T2 MRI lesions and gadolinium enhancing lesions at 18 months. In the open labelled extension CHAMPIONS study (Controlled High Risk Avonex Multiple Sclerosis Prevention Study In Ongoing Neurological Surveillance), patients treated immediately with Avonex had less active disease than the delayed treatment group at 5 years. The ETOMS (Early Treatment of MS) study demonstrated similar results to CHAMPS with 34% and 45% of patients receiving IFNβ and placebo respectively developing MS after 2 years. BENEFIT (Betaferon in Newly Emerging Multiple Sclerosis for Initial Treatment study) demonstrated a risk reduction of 46% over 2 years of developing MS along with a reduction in T2 lesion volume over the same period with 5 year results continuing this trend with reduction of MS by 37%. Finally, the PreCISe study (Evaluate Early Glatiramer Acetate Treatment in Delaying Conversion to Clinically Definite Multiple Sclerosis of Subjects Presenting With Clinically Isolated Syndrome) evaluated the efficacy of Glatiramer acetate when used in patients with CIS, showing a 45% reduction in risk of developing MS at 2 years compared to placebo.

1.10 Non MRI biomarkers of MS

Before discussing MRI biomarkers of disease, it is important to consider potential non-MRI diagnostic biomarkers of MS. Numerous studies have been performed, details of which are beyond the scope of this thesis but some findings on CSF OCBs and light chains, serum KIR4.1 (inwardly rectifying potassium channel) antibodies,

CSF neurofilaments (Nf) and glial fibrillary acidic protein (GFAP) will be summarised.

1.10.1 CSF oligoclonal bands and kappa free light chains

Intrathecal IgG synthesis indicates the humoral immune response within the CNS in MS. Quantitative (IgG index) and qualitative (detection of OCBs) measurements of IgG exist to support the diagnosis of MS, although the use of CSF OCBs is now not strictly needed for diagnosis of RRMS, but is still part of supporting criteria for PPMS (Polman *et al.,* 2010). The IgG index is calculated by the ratio of CSF IgG to CSF albumin to the ratio of serum IgG to serum albumin. A high ratio above the value for the testing laboratory indicates intrathecal IgG synthesis (Rammohan, 2009). The qualitative detection of CSF OCBs involves isoelectric focusing with immunofixation, which compares the patient's CSF IgG pattern to their own serum IgG pattern (Freedman *et al.,* 2013). Five possible band patterns exist and laboratory staff qualitatively assess for the presence of one of these. In CIS or MS unmatched CSF OCBs indicate IgG synthesis and usually at least 2 bands are needed. Approximately 90% of patients with MS and 68% of patients with CIS have CSF OCBs, of which there is an increased risk of developing MS with an OR of 9.9 (Dobson *et al.,* 2013). A recent natural history study of patients with CIS demonstrated that the risk of developing MS was greater in patients with positive CSF OCBs and a higher number of MRI brain lesions (HR 5.1 for 1-3 lesions and HR 11.3 for more than 10 lesions) (Tintore *et al.,* 2015). With that said, OCBs are not only observed in MS and should be evaluated alongside the other CSF constituents that are routinely tested e.g CSF protein, cell count and glucose (Freedman et al., 2013) and only support the diagnosis with a clinical history compatible with MS. Sensitivity and specificities are quoted at approximately 88%

and 86% respectively (Presslauer et al., 2016). Other CNS inflammatory or infective diseases can also produce CSF OCBs (Bernitsas *et al.*, 2017), the specific details of each condition mimicking MS on CSF go beyond the scope of this thesis.

Because of the qualitative nature, rater dependency and difficulties in standardisation across laboratories, CSF kappa free light chains are increasingly being investigated as an alternative to OCBs for the diagnosis of MS (Senel *et al.*, 2014). Intact immunoglobulins consist of two heavy chains and two light chains, the light chains consisting of kappa or lambda subtypes. During the production of immunoglobulins, B lymphocytes produce an excess of kappa and lambda light chains, which can be detected themselves in serum, urine and CSF. CSF Kappa light chains are elevated in patients with MS, indicating intrathecal immunoglobulin synthesis by plasma cells (Senel et al., 2014). A recent study demonstrated that CSF kappa light chain detection had similar sensitivity (95%) and specificity (95%) for the diagnosis of MS compared to OCB detection, and superior diagnostic sensitivity in patients with CIS (82%) (Presslauer et al., 2016). Presslauer and colleagues also showed that only 3/60 in their cohort of other neurological diseases had CSF kappa light chains, and a proportion of CIS OCB negative patients had detectable light chains. However, kappa free light chains are also considered to be a general marker of plasma cell activity and raised levels can be seen, for example, in CNS infections. To date it has not replaced the regular measurement of CSF OCBs.

1.10.2 KIR4.1 antibodies

Autoantibodies directed against CNS antigens in the brain in MS have been hypothesized, much like the discovery of aquaporin-4 antibodies that allowed NMO to be distinguished, at least immunologically, from MS (Schneider, 2013). An

initial study by Srivastava demonstrated that antibodies to a protein present on oligodendrocytes and astrocytes (KIR4.1) were detected in the serum of 47% (186/397) of their cohort of MS patients, 1% in patients with other neurological diseases and none found in healthy controls (Srivastava *et al.*, 2012). However KIR4.1 is not specific to the brain and can be found in the retina, kidney and parietal cells of the gastric mucosa, leading to a hypothesis that the presence of antibodies could merely be an epiphenomena (Barkhof *et al.*, 1997). Furthermore, subsequent studies have not found such a high percentage of KIR4.1 antibodies, with a study in 2012 using similar enzyme-linked immunosorbent assay techniques reporting 7.5% of MS patients having the serum antibody (20/268) (Nerrant *et al.*, 2014). A further study has demonstrated even lower serum antibody levels (1%) with no loss of the KIR4.1 antigen in WMLs of 15 pathologically confirmed cases of MS (Brickshawana *et al.*, 2014). A more recent paper again showed a higher percentage of MS patients with the antibody (26%) but this was also present in patients with NMO, with no statistical difference between the two. It was therefore concluded that at present this cannot be used as a differentiator between MS and NMO, nor can it be associated with MS subtype, disease duration or EDSS (Brill *et al.*, 2015).

1.10.3 CSF neurofilaments

Neurofilaments are polypeptides present within the substance of the axon itself (with small amounts within the neuronal cell body and dendrites), released after axonal damage into the extracellular space and subsequently into the CSF (Clifford *et al.*, 2010; Housley *et al.*, 2015). They consist of heavy, medium and light (L) chains along with another protein termed alpha-internexin. NfL levels have been shown to be increased in the CSF of RRMS and progressive patients compared to healthy controls, and furthermore, increase during the first 1-2 months after a

clinical relapse (Lycke *et al.*, 1998). CSF levels of NfL are also increased early in the course of the disease, with CIS patients showing higher levels than controls (Disanto *et al.*, 2016). There is some indication that this could be used as a predictor of more severe disease, depending on early CSF NfL levels (Salzer *et al.*, 2010). However as one would have expected, CSF NfL are also present in other chronic neurological diseases causing axonal degeneration such as motor neuron disease (Menke *et al.*, 2015), multiple-system atrophy and progressive supranuclear palsy (Brettschneider *et al.*, 2006), frontotemporal and vascular dementia and Alzheimer's disease (Skillback *et al.*, 2014). Therefore, alongside the fact that a lumbar puncture would be needed (and at times repeatedly), this is unlikely to be used as a biomarker; but perhaps more realistically could be used as a marker of severity, disease progression or response to treatment (Clifford *et al.*, 2010).

1.10.4 Glial fibrillary acidic protein

GFAP is a protein which forms part of the cytoskeleton of astrocytes and is a marker of astrocyte damage (Housley *et al.*, 2015). Its presence has been demonstrated in patients with MS compared to healthy controls and has correlated with EDSS (Axelsson *et al.*, 2011). However, just as with CSF neurofilaments, GFAP is a non-specific marker of CNS damage and maybe more likely to indicate progressive disease (Axelsson *et al.*, 2011).

1.11 MRI image contrasts

1.11.1 Protons and spin

The hydrogen nucleus (^{1}H) is abundant in the body due its presence in water. Like any proton in the nucleus of an atom, it possesses an electrical charge and so generates a magnetic field, so in effect acting like a small magnet. The orientation

of the magnetic field caused by this proton is random, providing there is no external magnetic field affecting it. In the presence of an external magnetic field (termed B0 in MRI) the proton will align with that external field and also 'precess', following a trajectory of that of a cone. The net direction of the magnetic field produced by all the protons, aligns parallel to the external field and the sum of these is termed longitudinal magnetization. However the protons are not precessing together or 'in phase'. In order to detect signal from these precessing protons, they need to be precessing together. Applying a radiofrequency (RF) pulse will 'flip' the protons (usually perpendicular to the external field) causing the magnetic field to be perpendicular to the original field direction. This is termed transverse magnetization, following which the protons will be in phase, termed phase coherence. Transverse magnetization can be detected as it is a magnetic field that is moving and so will induce a voltage within a coil. The size of the voltage is linked to the amount of transverse magnetization and hence the intensity of the MR signal is equal to the amount of transverse magnetization (Lipton, 2008).

When the RF pulse is switched off, longitudinal magnetization starts to return, termed longitudinal relaxation (or spin-lattice relaxation). This is physically achieved by protons transferring energy to the external environment (lattice) as heat. T1 describes the time it takes to achieve 63% of longitudinal magnetization. Different tissues have different T1 times. At the same time, transverse magnetization diminishes, termed transverse relaxation (or spin-spin relaxation). This is achieved by protons transferring energy to adjacent protons, and the time it takes to lose 63% of transverse magnetization is termed T2. Therefore image contrast depends on both longitudinal and transverse relaxation times.

When the RF pulse is switched back on again (time to repeat or TR), transverse magnetization is achieved again. Different image contrasts can be achieved by altering the time interval (TR) between each RF pulse as well as the time to echo, explained next.

1.11.2 Spin echo and Time to echo

Spin echo is a technique that recovers lost transverse magnetization due to T2* effects (protons that were in phase start to dephase, which is caused by inhomogeneities in the local magnetic field and spin-spin interactions) and tries to recover phase coherence. This standard technique applies a 180º refocussing pulse after the initial 90º RF pulse. The 180º puts the dephasing protons back in phase. Recovery of the phase coherence produces an increase in signal. Much like an echo (a sound that increases in strength after a time delay), the dephasing protons that start to lose signal, increase in signal and coherence after the 180º pulse. The time at which the scanner or operator decides to *sample* the signal during the relaxation phase is termed time to echo (TE).

1.11.3 Localising the signal

In order to acquire an MR image, the location of the signal needs to be identified. This is achieved by further changes in the magnetic field, termed frequency and phase encoding gradients. Frequency encoding gradients are applied after the RF pulse is administered. This gradient varies in strength and therefore causes different precessing frequencies of the protons and so 'emitting' different signals. However all protons at a certain point will have the same precessing frequencies at a particular point in the gradient, and so this is not enough to localise the signal. To further accurately pinpoint the signal, a further gradient is subsequently applied (phase encoding gradient) and then turned off. This gradient causes the protons to

precess at different speeds according to the gradient strength. When it is switched off, the precession speeds of each proton are equal again (because of the same magnetic field) but importantly they are out of phase (as they were precessing at different speeds) and so their signals will be picked up at different times (Figure 6).

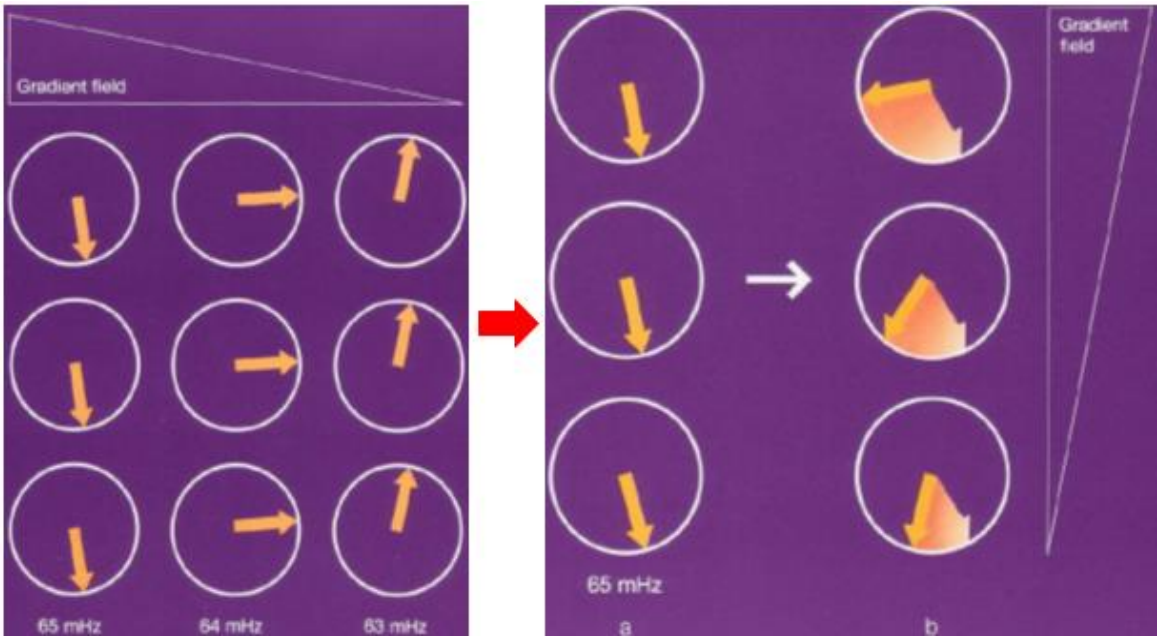

Figure 6. Frequency and phase encoding gradients.
Initially all protons are in phase. To locate the signal, first a magnetic field gradient is put across the protons (left). As this magnetic field is decreasing in strength (in this case left to right) the protons now precess at different speeds (frequency encoding gradient). Now all the protons in one column are precessing at the same speed. To accurately locate the signal, another magnetic field is placed across the protons (right) and switched off quickly (phase encoding gradient) and so the protons precess more quickly according to this new field. When this is switched off, they are exposed to the same field strength and so spinning at the same speed but they will be out of phase. This will enable the signal of different tissues to be accurately located (Schild, 1990).

1.11.4 Gradient Recalled Echo

Gradient recalled echo (GRE) imaging does not use a 180º refocussing pulse to re-phase dephasing protons. Instead, to refocus dephasing protons, a magnetic field gradient is applied after one RF pulse, causing even more dephasing (in addition to the internal and external inhomogeneities). Transverse magnetization disappears

more rapidly due to this. This field gradient is then switched off and switched back on again but this time in the opposite direction, causing the dephasing protons to re-phase again, leading to increased signal (similar to the 180º pulse). In contrast to spin echo the local magnetic field inhomogeneities are not corrected with gradient echo as a 180º pulse is not used (in fact the magnetic field gradient causes even more inhomogeneity). As such gradient echo images are more T2* weighted (Schild, 1990). GRE imaging is therefore quicker as a refocussing 180º pulse is not needed. Also the TE is shorter as dephasing is faster with GRE, thereby speeding up the overall acquisition time.

1.11.5 T1 and T2 imaging

T1 contrast occurs when protons are returning back to longitudinal magnetization after the RF pulse is switched off. Each tissue has different longitudinal relaxation times. To achieve T1 weighted imaging, a short TR is needed with a short TE. T2 contrast relies on different tissues having different transverse relaxation times, and is dependent on a long TE and long TR, and is mechanistically dependent on the loss of energy between adjacent protons in a tissue (spin-spin relaxation) and also the amount of protons in each tissue (proton density). The longer the TE the larger the difference in signal between tissues (Figures 7 and 8).

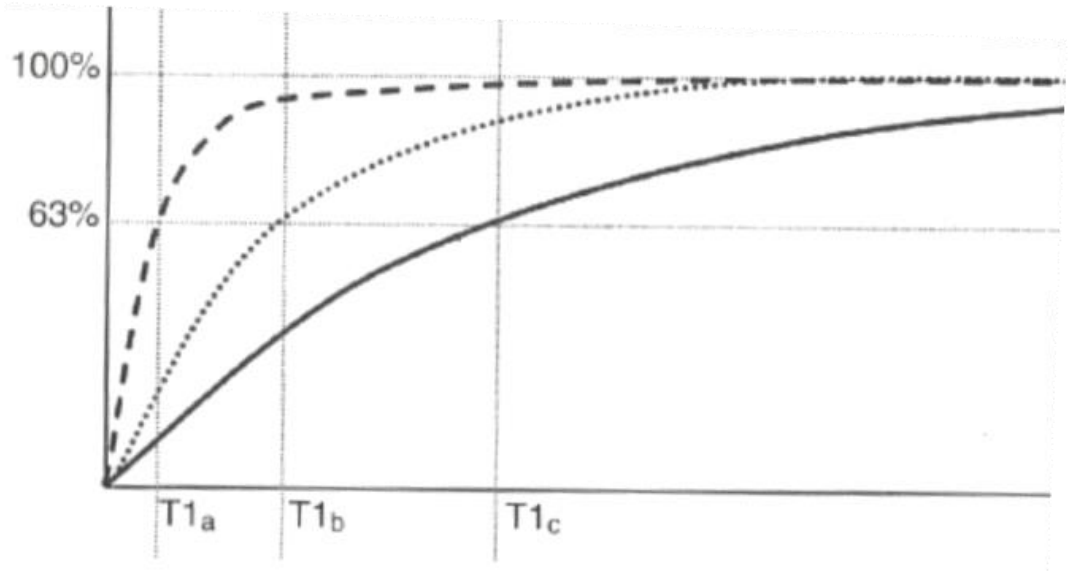

Figure 7. Longitudinal relaxation.

At time 0, a 90° RF pulse has been applied causing transverse magnetization. T1 represents the time taken for 63% of longitudinal magnetization to be achieved. Each different tissue has a different T1 time (dashed line=fat, dotted line=brain, solid line=CSF). X axis = Time, Y axis = longitudinal magnetization (Lipton, 2008).

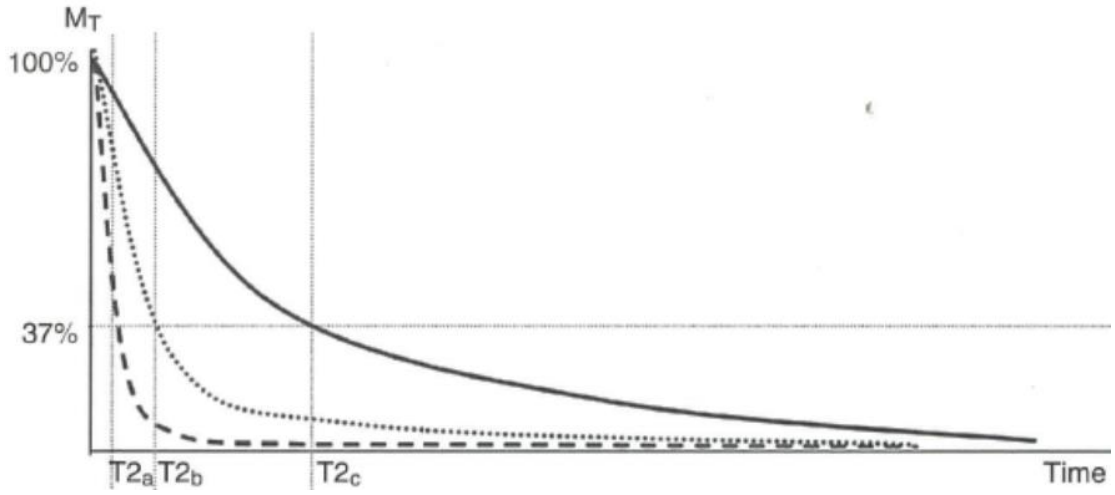

Figure 8. Transverse relaxation.

T2 represents the time taken for 63% of transverse magnetization to disappear and for 37% to remain and describes the rate of signal loss (dashed line=fat, dotted line=brain, solid line=CSF). X axis = Time, Y axis = transverse magnetization (Lipton, 2008).

1.11.6 T2* weighted imaging

T2*-weighted imaging forms the foundation of allowing the detection of central veins within MS lesions (described in more detail later), without needing intravenous contrast. T2*-weighted imaging depends on T2* relaxation, which itself is dependent on transverse magnetization after a RF pulse. At maximal transverse magnetization the protons are described as being 'in phase' (precessing together). Once the RF pulse is switched off the protons begin to 'de-phase' and start to re-align with the longitudinal magnetization. The rate at which the protons de-phase is, in part, related to the interactions between adjacent protons (which whilst precessing themselves cause a small local magnetic field) termed spin-spin relaxation, and extrinsic magnetic field inhomogeneities. The external field inhomogeneities are dependent on the tissue composition itself i.e. water, brain parenchyma and blood vessels. Due to the paramagnetic effect of deoxyhaemoglobin causing inhomogeneities within the local magnetic field, there is quick loss of the MR signal, termed the 'susceptibility effect'. Therefore T2* relaxation rate is dependent on the intrinsic *and* extrinsic magnetic field inhomogeneities. The rate at which protons de-phase with T2* is faster than T2, hence causing loss of signal more quickly at any given time point (Figure 9). T2* is a gradient echo sequence which does not use a refocussing 180 degree RF pulse and so makes it more likely to cause the susceptibility effect (Shams *et al*., 2015).

The amount of T2* weighting increases with time. The longer TE, the more dephasing that occurs and hence more signal loss. A low flip angle results in less T1 influence as does an increased TR. All these effects can make the image more T2*-weighted. Additionally an increased magnetic field strength will also improve the T2* effect as this will cause increased susceptibility leading to more dephasing

(Chavhan *et al*., 2009). From a practical standpoint using smaller voxels (usually less than 1mm) increases the acquisition time, and an increased chance of patient head movement leading to suboptimal images. This therefore limits the volume of the brain that can be viewed. Anisotropic voxels may improve the acquisition time but will result in more difficulty when searching for small anatomical structures, such as parenchymal veins (Sati *et al.*, 2014). Sati et al. based on work by Zwanenburg who used 7T MRI (Zwanenburg *et al*., 2011) improved the acquisition time of T2* by using a higher Echo Planar Imaging (EPI) factor (15 lines per excitation; i.e. per 90 degree pulse) whilst maintaining small voxels. This group used 0.5mm isotropic voxels and imaged the whole brain in just under 4 minutes. This is in contrast to the two studies by Tallantyre et al. who used an EPI factor of 3 (Tallantyre *et al*., 2011, 2008). EPI speeds up the phase encoding gradient that is used to pinpoint where the spin signal is originating from.

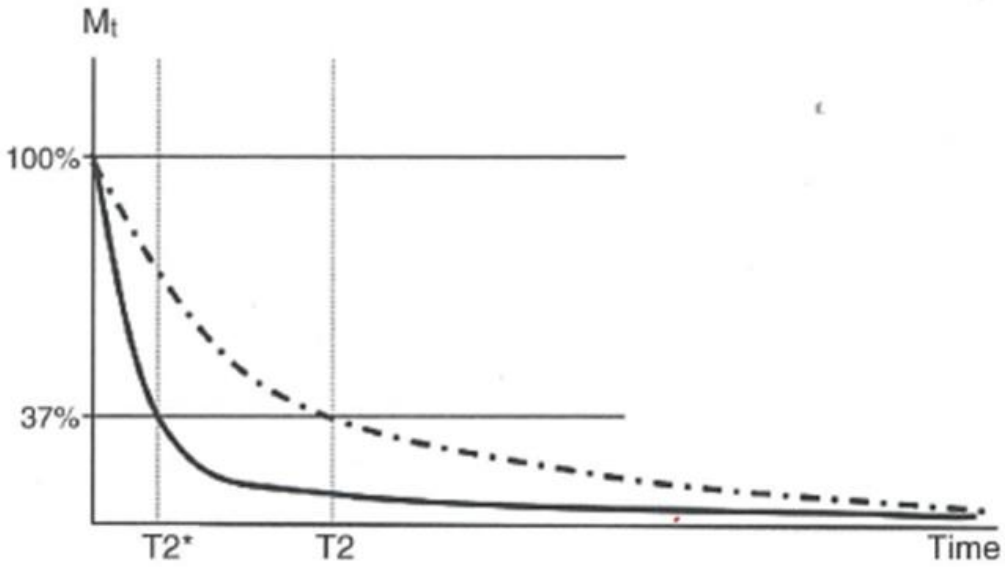

Figure 9. T2* curve.

Each line signifies two different relaxation curves for the same tissue. Dotted line=loss of transverse magnetization (T2 curve) and solid line=loss of transverse magnetization due to spin-spin interaction and extrinsic magnetic field inhomogeneities (T2*). X axis = Time, Y axis = transverse magnetization (Lipton, 2008).

1.11.7 Susceptibility weighted imaging

Susceptibility weighted imaging (SWI) is a method of providing contrast between tissue structures of different magnetic susceptibilities such as deoxyhaemoglobin, calcium and ferritin (Haacke *et al.*, 2009). In contrast to 'pure' T2*-weighted imaging, SWI is produced by multiplying phase images by the magnitude images. Alternatively SWI can be produced by multiplying minimum intensity projection images by the magnitude image. Minimum intensity projection images take the minimum intensity from each pixel across four slices (effectively producing an average intensity across these slices) to produce a slice with well-defined veins. However with this method WMLs may appear less defined, due to the fact that the minimum intensity of each voxel is used. Along with a long TE this increases the susceptibility effect, producing increased contrast between small veins and the brain parenchyma (Chavhan *et al*., 2009). SWI, like T2*, is dependent on the paramagnetic properties of deoxyhaemoglobin. In effect the venous blood is used as its own contrast agent, allowing differentiation between veins and arterioles (Gasparotti *et al.*, 2011), and so veins appearing as hypointense within hyperintense WMLs. Deoxygenated blood produces a smaller T2* signal than arterial blood, therefore increasing the TE will allow greater differentiation between veins, arteries and arterioles, which are not seen to such an extent (Chavhan *et al*., 2009). More clinical information on SWI is described in chapter 3.

1.12 Potential MRI markers of MS lesions

I will briefly describe potential MRI markers of MS which in combination with WML central veins could be used to aid diagnosis.

1.12.1 Hypointense rims

T2 hypointense rims have been identified in patients with MS and in different MS subtypes. The significance of such rims still remain to be clarified and various hypotheses exist, including iron deposition surrounding the WMLs and macrophage activity contributing to this appearance on MRI (Kilsdonk *et al.*, 2014b). Although little research has focussed on using this as an imaging biomarker in MS, numerous studies have incidentally shown that they are less frequently observed in MS lesions, compared to the central vein. This is demonstrated by recent work in Spain where T2 hypointense rims were detected in just 9% (24/257) of patients with a mixture of MS subtypes (Llufriu *et al.*, 2010). None were found in PPMS patients. The relative lack of this feature in other diseases such as Susac syndrome has been demonstrated in small studies (Hackmack *et al.*, 2012), which showed a hypointense rim in just 4% of lesions compared to 41% in MS. Similarly, Sinnecker et al (2012) showed the paucity of this feature in patients with NMO in comparison to MS. Again, NMO patients had hypointense rims in 2% of lesions (total lesions 140) with MS patients having 23%. The cohort of 10 NMO patients in the study by Kister et al (2013) showed no hypointense rims among a total of 92 lesions. Whether this could be used alongside the presence of central veins to improve the specificity of classifying a WML as inflammatory has not been established.

1.12.2 Subpial lesions

Cortical lesions have been detected throughout the brain including the cerebellum (Kutzelnigg *et al.*, 2005; Kutzelnigg *et al.*, 2007). They are categorised into three main groups: mixed (leukocortical) lesions which involve parts of the subcortical WM and cortex; intracortical lesions that do not reach the brain surface or WM; subpial lesions that extend from the pia mater into the cortex (Lucchinetti *et al.*, 2011). The latter is said to be specific for MS and accounts for the majority of the total cortical demyelinating volume (Bø *et al.*, 2003; Moll *et al.*, 2008; Mainero *et al.*, 2009). The exact cause of subpial lesions is not fully understood, although it is thought to occur secondary to inflammation of the meninges or subarachnoid space, with subsequent demyelination of the surface of the brain and underlying cortex (Lassmann, 2014). Moll et al (2008) demonstrated that subpial lesions in 4 MS patients after autopsy accounted for the largest percentage of the total number of cortical lesions. Furthermore, of the 442 cortical lesions identified in 13 patients with HIV associated Progressive Multifocal Leucoencephalopathy (PML), none were found to be in the subpial region. Control subjects which included five patients with X-linked Adrenoleukodystrophy and two with HIV associated encephalopathy did not have any cortical lesions. Histopathological examinations of 19 NMO patients did not show any cortical lesions, despite an abundance of aquaporin-4 water channels within the cortex (Popescu *et al.*, 2010). The lack of cortical lesions has also been observed in MRI studies using a technique called double inversion recovery at 1.5T. Of 30 patients with NMO, none demonstrated cortical lesions compared to 66.7% of MS patients (20/30), with both groups being of similar disease duration (Calabrese *et al.*, 2012). Furthermore it has been suggested that subpial lesions are more common in progressive forms of MS, with

additional evidence of mononuclear inflammatory infiltrates in the surrounding meninges (Kutzelnigg *et al.*, 2005). Although subpial lesions are common within the cortex, there are difficulties in observing them using MRI. Leukocortical lesions are the easiest to detect on MRI although subpial lesions have been detected using 7T fast low-angle shot (FLASH) T2* gradient echo images *in vivo* (Mainero *et al.*, 2009), and pathological studies using 9.4T (Schmierer *et al.*, 2010). Usually ultra-high field MRI e.g. 7T is needed with small voxel sizes in order to see these lesions. However partial volume effects secondary to subarachnoid CSF, and reduced contrast between cortical lesions and normal grey matter may still cause difficulty in interpreting the MRI. Therefore using subpial lesions to clarify a diagnosis of MS may be difficult to translate into clinical practice, due to the difficulty in identifying these lesions and the time consuming nature of trying to detect them with any certainty. Other limitations of using cortical lesions include less inflammatory pathology and blood-brain barrier leakage and a reduced density of myelin in the outermost cortical layers (Mainero *et al.*, 2009).

1.13 Studies detecting WML central veins on MRI

Many MRI studies have shown the perivenous nature of MS lesions after the initial study by Tan et al. who demonstrated this *in vivo* (Tan *et al.*, 2000) . Using 1.5T MRI, T2*-weighted GRE imaging, they studied 17 patients with MS and found 94/95 WMLs had a central vein traversing through the centre, with some WMLs having more than one vein. Although intravenous contrast was used to better visualise the veins, it demonstrated the radiological features of the perivenous nature of MS lesions (Figure 10).

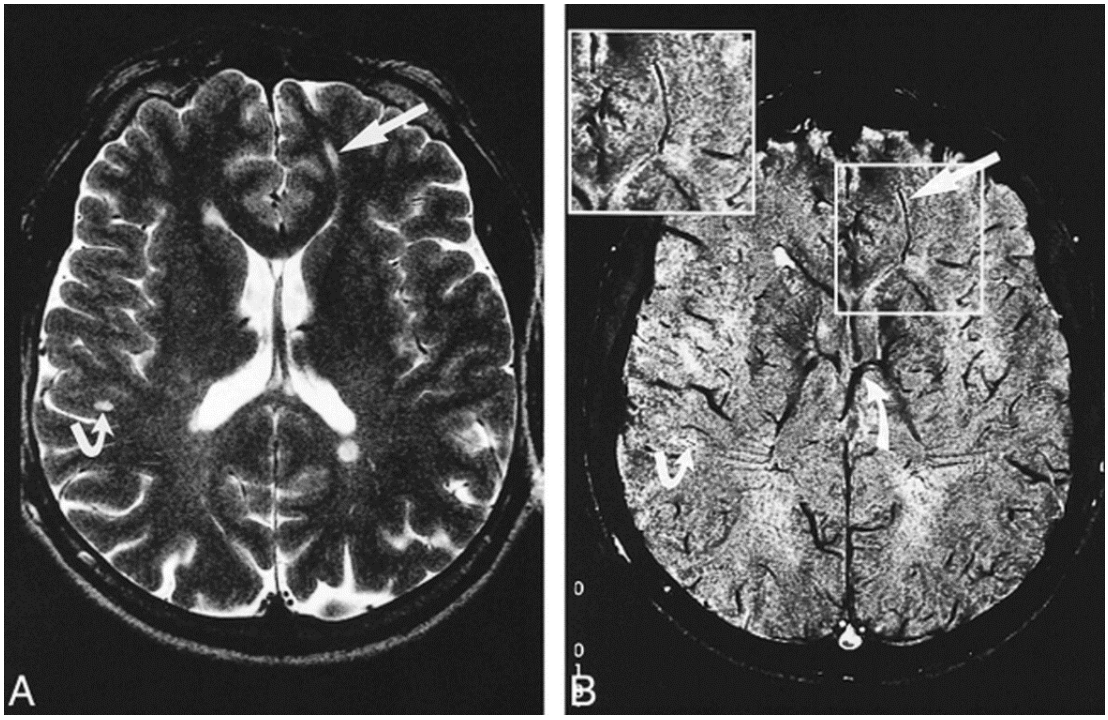

Figure 11. T2*-weighted imaging at 1.5T depicting a WML central vein.

(A) T2 image and (B) equivalent T2* with contrast showing periventricular, deep WML and a subcortical lesion (curved arrow) with central veins (Tan *et al.*, 2000).

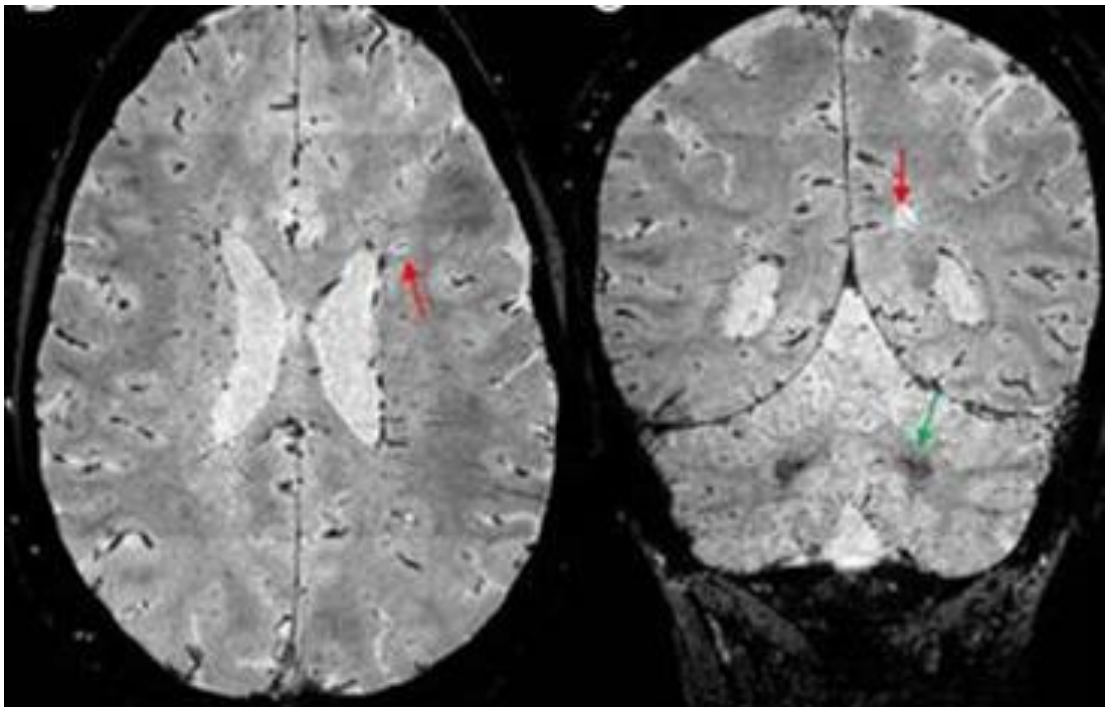

Figure 10. T2*-weighted imaging with high EPI factor at 3T.

Higher EPI factor has allowed quicker acquisition times, whilst using small voxels. Red arrows show WMLs with central veins, green arrows show deep grey matter nuclei (globus pallidus and dentate nucleus) (Sati et al., 2014).

Tallantyre et al studied the perivenular distribution of MS lesions using 7T MRI and T2*-weighted imaging. This proof of concept study found that in 8 patients who had a total of 89 WMLs, central veins could be seen in 82% of lesions (Tallantyre *et al.*, 2008). Veins were seen in 96% of periventricular lesions and 65% of peripheral lesions. The same group went on to compare the number of central veins in WMLs secondary to MS and those due to ischaemic small vessel disease (SVD) at 7T (Tallantyre *et al*., 2011). T2*-weighted imaging, with 0.5mm isotropic voxels and an EPI factor of 3 was used with an image acquisition time of 8.8 minutes. A rater (blinded to the diagnoses) was able to differentiate between patients with MS and asymptomatic WMLs based on the presence or absence of a WML central vein. A second observer was able to confirm or refute the presence of a central vein using individual lesions (so as to prevent the identification of lesions based on the location within the brain) with a high Cohen's kappa coefficient. The presence of a WML central vein was a common finding no matter the subtype of MS. Additionally they found that 4 of the non-MS group met the Fazekas criteria for MS (which is based on lesion location and size) (Fazekas *et al*., 1988). One limitation of this study was that the raters needed to count all WMLs in order to predict the diagnosis (again a potential limiting factor in clinical practice due to time constraints, and one that will need to be addressed). They could however predict the diagnosis on counting just 10 WML central veins in all but one patient.

A further longitudinal study by Mistry et al. followed 29 patients who had WMLs but who did not have a firm neurological diagnosis (Mistry *et al.*, 2013). A baseline 7T T2*-weighted scan using the same voxel size and EPI factor to that of Tallantyre et al (Tallantyre *et al*., 2011) was analysed by a blinded assessor. After a median

follow up period of 26 months, 22 patients had received a diagnosis. Of these, 13/22 were diagnosed with MS and all these patients had WML central veins visible in more than 40% of lesions on their baseline scan. Nine patients were thought to have ischaemic SVD who had less than 40% (range 9-33%) of their WMLs with central veins at baseline. It was suggested that this could be used as an imaging biomarker if confirmed on 3T MRI scanners. Sati et al. have since improved the acquisition time by increasing the EPI factor whilst maintaining small voxel size (Figure 11).

Preliminary work by Mistry et al. has shown that 6 or more WML central veins can confirm the diagnosis of MS, obviating the need to count all lesions. This was tested in a cohort of 20 subjects, and a rater blinded to the diagnosis confirmed all cases of MS or SVD using this threshold (Mistry *et al.*, 2016).

As described previously, patients with NMO can have WMLs that could potentially be mistaken for MS. Other groups therefore have used T2*-weighted imaging to study whether the central vein exists within these WMLs. Kister et al. (2013) studied 10 patients with NMO at 7T using T2*-weighted GRE imaging. They examined the supratentorial compartment alone due to poor signal to noise ratio in the infratentorial region. Of 92 WMLs (they could not identify any cortical lesions) 8 (9%) had a vein traversing the WML. They also commented that most of the WMLs were round in morphology on axial slices and 89/92 were less than 3 mm in diameter. These finding were echoed by Sinnecker et al. (2012) who also used 7T T2*-weighted imaging, to scan the supratentorial compartment of 10 patients with an NMO spectrum disorder (NMOSD) and 18 patients with MS. Again the majority of MS WMLs were located around a central vein (92%) compared to 35% in the NMOSD group. The blood vessels in the NMOSD group were in the periphery of

the WML rather than centrally located, and most were located in the deep WM. The location of the blood vessel within the WML could therefore be used to differentiate between the two conditions when there is doubt about WML or vein morphology.

A further study by Wuerfel and colleagues demonstrated the discrepancy in WML central veins in patients with Susac syndrome (Wuerfel *et al.*, 2012). Although the patient group was small in number, the principle remains the same. Using 7T T2*-weighted with a low flip angle, so called FLASH imaging, they demonstrated that 54% of WMLs in the Susac group had veins crossing the lesion, compared to 92% of WMLs in the MS group. Again, similar to the study by Sinnecker et al, the vein was usually in the peripheral aspect of the WML compared to the more central location seen in MS WMLs.

Solomon et al. have recently investigated if the central vein sign can be used to differentiate WMLs between patients with MS and migraine using a relatively new technique called FLAIR* (described in chapter 3) (Solomon *et al.*, 2016). The median number of WMLs with central veins was 84% in the MS group and 22% in patients with migraine. They also found that the probability of a scan being from an MS patient increased with the number of subcortical or deep WML central veins. I will explore the value of lesion location and the presence of central veins in chapter 6.

The majority of central vein studies have demonstrated that there is a significant difference between the number of WML central veins in patients with MS compared to their comparator group (Tallantyre *et al.*, 2008; Tallantyre *et al.*, 2011; Sinnecker *et al.*, 2012; Wuerfel *et al.*, 2012; Kau *et al.*, 2013; Kister *et al.*, 2013;

Mistry *et al.*, 2013; Kilsdonk *et al.*, 2014b; Mistry *et al.*, 2016; Solomon *et al.*, 2016). However, one study by Lummel and colleagues did not find this difference between their MS group and patients with SVD (Lummel *et al.*, 2011). Fifteen patients with MS and fifteen with WMLs secondary to SVD were scanned at 3T using Susceptibility weighted Angiography (SWAN). However they found no statistical difference in the number of WML central veins between the two groups. Possible reasons for this could be factors affecting spatial resolution, for example the slice thickness in this study was 2.6mm which is higher than some previous 3T studies using 1mm (Kau *et al.*, 2013; Mistry *et al.*, 2016). A larger slice thickness will reduce resolution and become more susceptible to partial volume effects, all of which may affect the visibility of small veins.

1.14 Summary and aims of this thesis

To date, the majority of studies have demonstrated the value of detecting WML central veins in small groups of patient with SVD and RRMS, and fewer studies with NMO, Susac syndrome and migraine. Most studies have used T2*-weighted imaging at 7T and more recently image fusion techniques (Sati *et al.*, 2012; Kilsdonk *et al.*, 2014a). Longitudinal, prospective studies have not been performed in large groups with other mimicking conditions (Miller *et al.*, 2008). In addition this has not been validated using different clinical 3T MRI scanners and some outstanding problems need to be investigated. This thesis aims to address some of them.

Firstly, each study to date has used one particular MRI scanner vendor to investigate MS patients and their comparator group. However in clinical practice each institution will have different scanners, and we do not yet know whether the same

results can be achieved if the same patient is scanned on different scanners using similar but not identical T2* sequences. Secondly, a variety of T2* based sequences have been used but the clinical use of these will depend on local expertise, and sequence variation may have some effect on the accuracy of any biomarker, which should be tested. Thirdly whether WML central veins can distinguish between RRMS and PPMS has not been investigated, something which would be useful to determine, as sometimes differentiating between these two subtypes clinically is difficult. In addition, it would be important to explore whether vascular risk factors have any influence on the number of WMLs with central veins. Finally determining the proportion of WMLs with central veins to make a diagnosis of MS needs further study. With these gaps in the current literature, the aims of this thesis are:

1. To determine if the 3T MRI scanner or T2* weighted sequence has any influence on the proportion of WMLs with central veins in patients with MS and SVD.
2. To compare T2* weighted sequences with fused images (described in chapter 3) to determine if there is a quantitative difference in the proportion of WML central veins in patients with MS.
3. To study if WML central veins are just as abundant in patients with PPMS as patients with RRMS, and if PPMS can be differentiated from SVD using WML central veins.
4. To explore whether vascular risk factors affect the proportion of WMLs with central veins in patients with MS.
5. To refine a potential diagnostic rule using WML central veins, which has the optimum sensitivity and specificity to diagnose MS.

Chapter 2. A comparison of T2* sequences across different 3T MRI scanners

2.1 Background

The significance of detecting a central vein within WMLs on MRI has increasingly been reported since the first *in vivo* study at 1.5T at the turn of the century (Tan *et al.*, 2000). Before the central vein sign is considered to be of diagnostic value in MS, its accuracy and ability to produce the same conclusions i.e. of MS or non-MS has to be demonstrated across different clinical scanners and T2* weighted sequences. The majority of studies to date have used 7T MRI to detect WML central veins (Tallantyre *et al.*, 2011; Hackmack *et al.*, 2012; Sinnecker *et al.*, 2012; Dixon *et al.*, 2013; Kister *et al.*, 2013; Kuchling *et al.*, 2014), although a few 3T studies have been published. The 3T studies have included SWI (Kau *et al.*, 2013), T2*-weighted imaging (Dixon *et al.*, 2013; Mistry *et al.*, 2016) and more recently a combination of fluid attenuated inversion recovery (FLAIR) and T2*, termed FLAIR*, described in chapter 3 (Sati *et al.*, 2012; Kilsdonk *et al.*, 2014b).

2.1.1 Causes of MR image variability

A further aspect of WML central veins that, to date, has not been investigated is the variation of the T2* sequence and scanner on the appearance of the central vein, and if this quantitatively influences the detection of WML or central vein numbers. It is well known that small changes in head position can drastically affect WML volume (Barkhof *et al.*, 1997; Rovaris *et al.*, 1998). Filippi et al. demonstrated that repositioning errors that occur in normal clinical practice can affect WML volume by 7%; close to the approximate 10% change in lesion load per year for untreated MS patients (Paty *et al.*, 1994; Filippi *et al.*, 1997). Alongside this, slice thickness

can affect WML clarity and volumes, with smaller slice thicknesses allowing detection of smaller lesions and delineating lesion margins more easily (Filippi *et al.*, 1995; Molyneux *et al.*, 1998). Molyneux et al found that reducing slice thickness from 5mm to 3mm using a 1.5T scanner, increased WML volume by a mean of 8.1%. Similar results were seen with Filippi and colleagues. This was thought to be secondary to a superior ability to identify small, low contrast lesions, which may have been difficult to see with volume averaging with the 5mm slices. They also found that what appeared to be confluent lesions at 3mm, were in fact multiple, smaller lesions with 1mm slices.

Partial volume effects, (when two or more tissue types in the same voxel cause averaging of signal and so cause difficulty in differentiating each component), also contribute to variability in lesion detection. This again is especially true for small, low contrast lesions (Bradley and Glenn, 1987). This is a potential problem for central vein detection in view of their small size and if larger slice thicknesses are being used with the T2* sequence.

WML volumes can also change with increasing field strength (Keiper *et al.*, 1998; Sicotte *et al.*, 2003). When comparing WML volumes of 15 MS patients scanned on a 1.5T scanner and subsequently a 4T scanner, Keiper et al. found a 45% increase in total WML numbers amongst all patients. Additionally what appeared to be hazy WM at 1.5T was in fact shown to be distinct, smaller WMLs at 4T. Sicotte and colleagues' results were of a similar theme after scanning MS patients at 1.5T and 3T. More gadolinium enhancing WMLs were identified at 3T (a total increase of 21%), and the volume of WMLs at 3T increased by a mean of 10% compared to the same patients at 1.5T. They also concluded that 3T imaging allowed easier

determination of WML boundaries especially with confluent lesions compared to 1.5T.

With these possible variables in mind, to advance the potential clinical applicability of the central vein sign, it is important to know if it is reliable, irrespective of the MRI scanner or T2* sequence used. I therefore chose to determine if different MR scanners using a similar T2* sequence allowed similar WML and central vein numbers.

2.1.2 Aims and hypothesis

The aim of this chapter was to assess if the presence or absence of the central vein sign in MS and ischaemic SVD lesions differed, if different T2* sequences were used at 3T. In clinical practice, different hospitals will have different MRI scanners and similar, but not identical T2* weighted protocols. Therefore similar, but not identical protocols on two different scanners were used to mimic translation of the central vein sign under more realistic clinical settings. We aimed to determine if this could significantly influence the number of WMLs, WML central vein numbers and proportion of WMLs with central veins within the MS or SVD groups. The hypothesis being, any differences in the proportion of WMLs with central veins on the same patient scanned with a different T2* sequence, could potentially affect diagnoses if this were to be translated to clinical practice. In addition, because in clinical practice assessing *all* WMLs for the presence of a central vein is time consuming especially for patients with large lesion loads, I wanted to test if a previously proposed rule of identifying 6 WMLs with central veins (Mistry *et al.*, 2016) could identify patients with MS irrespective of the scanner or T2* sequence.

2.2 Methods

2.2.1 Patient selection

Adult patients aged 18-75 who attended the MS or general neurology clinics at Nottingham University Hospitals NHS Trust, with a confirmed diagnosis of MS or SVD were recruited into the study. Patients were scanned between July 2013 and December 2014. I did not age or gender match for this exploratory study as the subjects' scans were compared to themselves (i.e. this was an intra-subject analysis, so different ages would not confound the results). Patients with MS were diagnosed by an experienced MS neurologist (according to Poser or McDonald 2005/2010 criteria) and all had typical MRI findings which was supported by a clinical report by a consultant neuroradiologist. The diagnosis of ischaemic SVD was based on expert clinical (lack of symptoms suggestive of demyelination or another white matter disease and identification of vascular risk factors) and radiological evaluation (consultant neuroradiologist report confirming the appearance of the scan was in keeping with SVD) with supportive laboratory findings (blood tests e.g. checking cholesterol, autoimmune screen and sometimes CSF). Written informed consent from all patients was obtained before inclusion in the study and the study was approved by the East Midlands - Nottingham Research Ethics Committee (05/Q2404/44) after a substantial amendment.

2.2.2 MRI protocol

MR imaging was performed using two 3T scanners, a MR750 (General Electric Healthcare (GE), Milwaukee, WI, USA) and an Achieva (Philips Healthcare, Best, The Netherlands) both using the manufacturers' respective 32 channel receive-only head coils. Protocols were set up on both scanners with the aim of being as similar

as possible, but with the pragmatic view of using the strengths of various options available on each scanner. The protocols consisted of;

1) 3D T2*-weighted GRE performed on each scanner, (MR750 specific: 0.43x0.43x1.5 mm voxels, 512x512x48 matrix, TE 25 ms, TR 38 ms, pixel bandwidth 110 Hz, duration 620 s; Achieva specific: parallel imaging factor 2, 0.55x0.55x1.05 mm voxels, 400x400x96 matrix, four interleaved 3D stacks with a small overlap, TE 25 ms, TR 150 ms, pixel bandwidth 160 Hz, duration 510 s). T2* GRE scans will be referred to as the 'standard T2*' sequences.

2) On the MR750 (GE specific), a T2*-weighted susceptibility-weighted angiography (SWAN) technique was acquired, 0.43x0.43x1.0 mm voxels, 400x400x94 matrix, TE 24 ms, TR 39 ms, pixel bandwidth 240 Hz, duration 430s.

3) On the Philips Achieva, a second 3D T2*-weighted GRE scan was acquired with a higher EPI factor of 15, similar to (Sati *et al.*, 2014) also using the 32 channel head coil, in the sagittal plane. The matrix was 448x448x336 with a non-interpolated voxel size of 0.55x0.55x0.55mm. Parallel imaging factors of 2 were used in both phase encoding directions. In addition, the water-only excitation flip angle was 10 degrees, effective TE 29 ms, TR 54 ms, two averages, duration 254 s. This will be referred to as 'T2* with high EPI'.

2.2.3 Image analysis

Images were saved in a DICOM (Digital Imaging and Communications in Medicine) format and then converted to Neuroimaging Informatics Technology Initiative (NIfTI) file format. In house image analysis software (NeuROI); (www.nottingham.ac.uk/research/groups/clinicalneurology/neuroi.aspx) was used to define and count WMLs using a semi-automated, seed growing technique.

Analysis of each T2* sequence was performed by trained rater (myself). The supratentorial brain was analysed on each T2* sequence, as only the supratentorial brain was covered by all acquisitions. WMLs were identified if seen on the axial plane and one other fixed plane to the acquisition plane (coronal or sagittal), and if larger than 3 voxels in diameter in the axial plane. Fixed, orthogonal planes were used as these mimic the views in clinical practice. A WML central vein was judged as present if it appeared in two orthogonal planes, surrounded by hyperintense signal, visually appearing in the central portion of the WML. I used T2* imaging to identify WMLs and central veins rather than using, for example, FLAIR and T2* to count each separately.

2.2.4 Data analysis

The proportion of WMLs with central veins was calculated as a percentage by one unblinded rater (myself), for each MS and SVD scan. In addition, three trained raters blinded to group and clinical status and not involved in the previous analysis (Margareta Clarke (MC), Amy Whitehead (AW) and Yasser Falah (YF)), counted a subset of 6 WMLs with central veins to assess agreement between the diagnostic classification based on WML central veins *alone*, and the known *clinical* diagnosis. Identifying a subset of WMLs with central veins was described recently (Mistry *et al.*, 2016) (Table 1).

Rule	Diagnosis
If T2* scan has more than 6 WMLs in total, and the rater identifies at least 6 with central veins	MS
If T2* scan has more than 6 WMLs in total, and the rater identifies less than 6 with central veins	non-MS
If T2* scan has less than 6 WMLs in total, and the rater identifies 50% or more with central veins	MS
If T2* scan has less than 6 WMLs in total, and the rater identifies less than 50% with central veins	non-MS

Table 1. Proposed diagnostic rule to make a diagnosis of MS or non-MS (Mistry *et al.*, 2016).

WMLs with central veins were identified on any slice and if there were more than one WML with a central vein on the same slice, these too could be counted towards the threshold of 6. Each rater was chosen according to their level of experience with clinical MR image analysis (Margareta Clarke; researcher in neuroscience with 1 year of experience, Amy Whitehead; 3rd year medical student with some prior experience and Yasser Falah; neurology registrar with 3 years of clinical neurology experience). I reviewed 25% of each raters' identified WML central veins to check for consistency.

2.2.5 Statistical Analysis

The Bland-Altman method for assessment of *agreement* was used to compare the proportion of WMLs with central veins between different scan sequences (Bland and Altman, 1999). This calculates the mean bias (mean difference) between the proportion of WMLs with central veins, the standard deviation of the differences and 95% limits of agreement (LoA), similar to a confidence interval (CI). Correlation coefficients have not been provided as these describe an *association* but not agreement between T2* sequences. Cohen's kappa (κ) was calculated to

measure each blinded raters' agreement between the central vein-based diagnostic classification of MS or SVD (after counting a subset of 6 WMLs with central veins) compared to the known clinical diagnosis. Kappa values <0.20 were considered a poor strength of agreement, between 0.21-0.40 fair, 0.41-0.60 moderate, 0.61-0.80 good and 0.81-1.0 very good (Altman, 1991). For differences between continuous data (e.g WML numbers in the same patient but scanned with different T2* sequences) that had a normal distribution, a paired t-test was used. Boxplots were used to check for outliers and extreme values (assume to have none unless specifically stated) and histograms were used to check for normality of data (assume to be normally distributed unless specifically stated) prior to running the t test. I did not use Bland-Altman plots for the individual components (central veins or WMLs) to test agreement as we need good agreement with the *proportion* of WMLs with central veins as this is one of the methods that could be used in clinical practice. A Mann-Whitney U test was used to compare differences in the proportion of WMLs with central veins between the MS and SVD groups. All patients were used for analyses unless stated. Statistical significance was set at $p<0.05$. Statistical analyses were performed using Statistical Package for the Social Sciences (IBM SPSS 22) and GraphPad Prism version 6.07.

2.3 Results

2.3.1 Demographics

This is summarised in Table 2. Ten patients with RRMS (4 female, 6 male) were recruited and 10 with SVD (6 female, 4 male). The mean age of the MS patients was 39.4 years (± 7.3) and 51.7 years (± 10.6) in the SVD group. The mean difference in age between groups was 12.3 years, p=0.007. Mean EDSS in the MS group was 3.8 (± 1.7). Median disease duration (from symptom onset to date of the

T2* scan) was 177 months (IQR 115.8 – 253.5). Median disease duration (from date of diagnosis to date of the T2* scan) was 138 months (IQR 66 -171). Of the 8 MS patients who had a lumbar puncture, 7 had positive CSF oligoclonal bands. The median number of days between the first and the second scan for the MS group was 24 days (IQR 12 – 35.5) and for the SVD group was 24 days (IQR 16.5 – 49).

Patient	Age (yrs)	Gender (M/F)	MS/SVD	Disease duration (mths)	EDSS	CSF OCBs	No. of days between scans
P01	38	M	RRMS	117	1.5	+	27
P02	47	M	RRMS	255	2.5	+	14
P03	44	F	RRMS	269	5	ND	37
P04	43	M	RRMS	174	6	-	14
P05	32	M	RRMS	128	4	ND	21
P08	36	F	RRMS	55	2	+	6
P11	41	M	RRMS	180	6	+	1
P12	32	M	RRMS	112	4.5	+	35
P16	29	F	RRMS	253	2	+	105
P20	52	F	RRMS	233	5	+	29
P09	56	F	SVD	N/A	N/A	N/A	49
P10	41	F	SVD	N/A	N/A	N/A	36
P13	55	F	SVD	N/A	N/A	N/A	15
P14	44	M	SVD	N/A	N/A	N/A	154
P15	48	M	SVD	N/A	N/A	N/A	27
P17	47	F	SVD	N/A	N/A	N/A	17
P23	75	M	SVD	N/A	N/A	N/A	49
P24	48	F	SVD	N/A	N/A	N/A	7
P25	62	M	SVD	N/A	N/A	N/A	21
P26	41	M	SVD	N/A	N/A	N/A	18

Table 2. Demographics of the MS and SVD patients groups.

Disease duration shown here = from symptom onset to time of T2* scan

As previously reported, within the MS group most WMLs had visible central veins. This was in contrast to patients with SVD who did not have central veins within the majority of their WMLs (Table 3; Figures 12 and 13).

T2* sequence	Proportion WMLs with central veins (median %)		p value†
	MS	SVD	
Standard T2* Philips	29.3	0	0.0001
IQR	19.4 – 34.8	0 – 3	
Standard T2* GE	35.5	0	0.0004
IQR	18.9 – 59.5	0	
T2* with high EPI Philips	69.6	6.1	0.0004
IQR	39.4 – 84.6	2 – 10.4	
SWAN GE	58.1	4.3	0.0002
IQR	40.6 – 66.7	0 – 11.1	

Table 3. Proportion of WMLs with central veins in the MS and SVD groups using each T2*-weighted sequence.

IQR = Interquartile range

†p values calculated using a Mann-Whitney U test

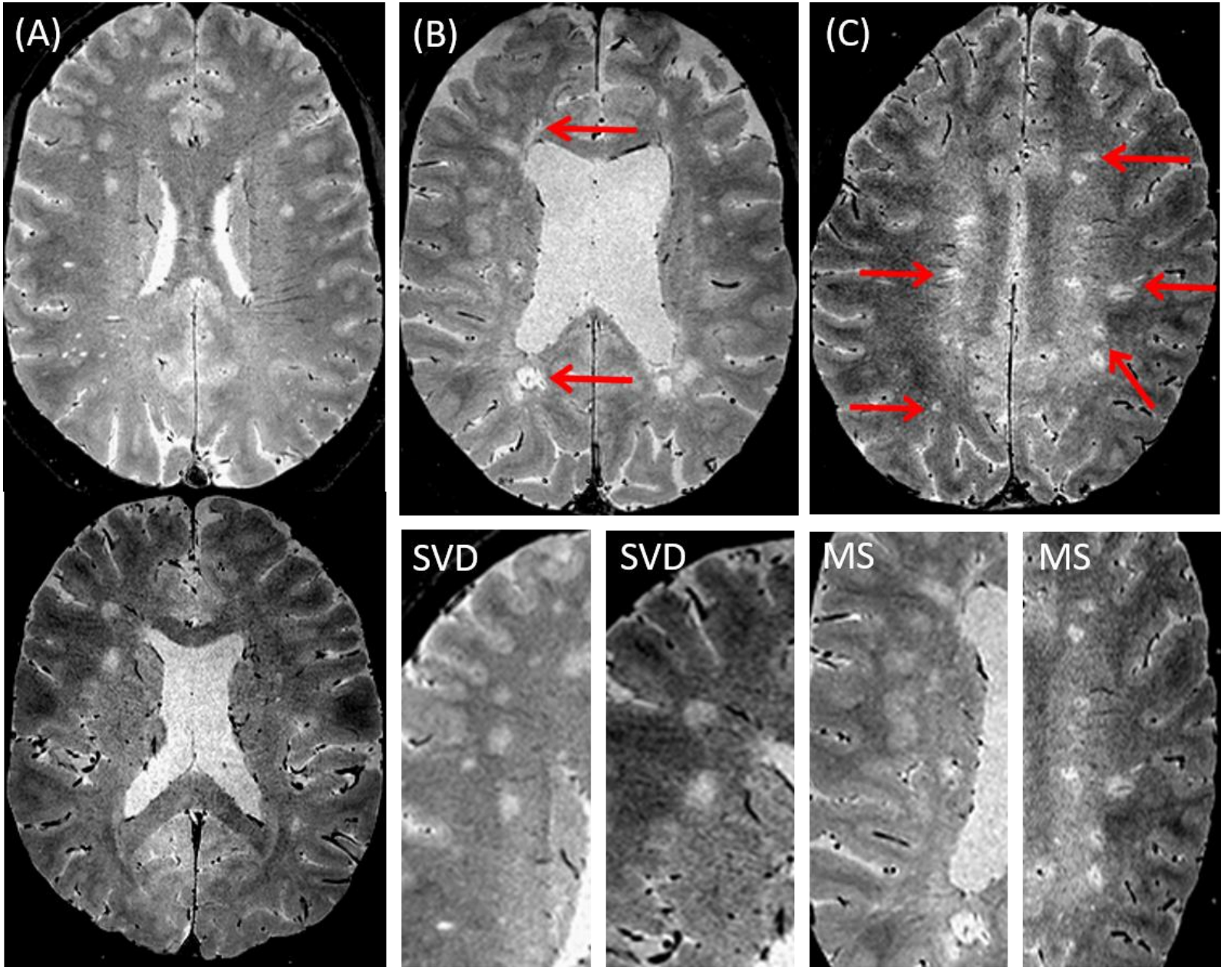

Figure 12. WMLs with and without central veins using T2* with high EPI.

(A) two SVD patients, each having deep WMLs with no visible central veins (magnified under SVD headings); (B) and (C) two different MS patients showing multifocal periventricular and deep WMLs with central veins indicated with arrows (magnified under MS headings).

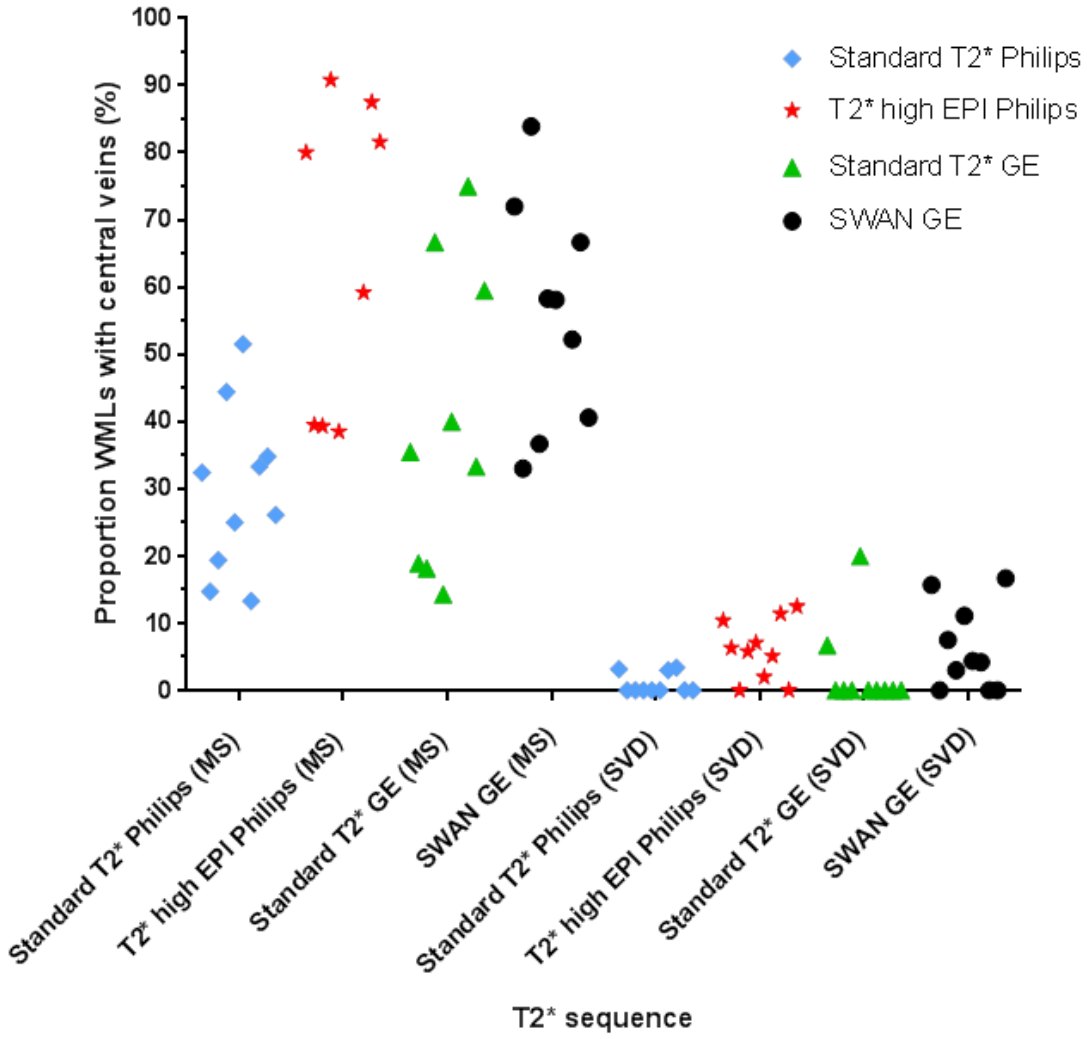

Figure 13. Dot plot chart demonstrating the proportion of WMLs with central veins in the MS and SVD groups when different T2* sequences are used.

The MS group has a higher proportion of WMLs with central veins compared to patients with SVD, irrespective of which MRI sequence is used.

2.3.2 WML numbers: comparison between T2* sequences – MS

Table 4 summarises how WML numbers differed in both groups when each T2* sequence was used. Figures 14 and 15 show the difference in the visibility of WMLs across T2* sequences. In the MS group the Philips 'standard T2*' identified more WMLs compared to the 'standard T2*' sequence on the GE (mean 45.3 and 15.4 WMLs respectively); which was statistically significant, p=0.01. Eight patients were used for the analysis as one patient did not have the 'standard T2*' on the GE scanner and one patient was removed as a boxplot showed that the difference in WML numbers for this patient produced an outlier. A paired t test with inclusion of the outlier (n=9) produced a mean difference of 37.6 which was statistically significant; p=0.008 (95% CI of the difference; 12.8 - 62.3). With the outlier excluded (n=8) the mean difference of WMLs between the two 'standard T2*' sequences was lower than before (29.9; p=0.01). Including the outlier does not affect the results in terms of the p value (both still statistically significant). I therefore excluded the outlier in the analysis in this case, resulting in a more conservative p value and difference in mean WML numbers between the two sequences.

'T2* with high EPI' allowed even greater WML identification (mean 66.1) compared to the 'standard T2*' (mean 53.8) on the same Philips scanner. The mean difference in WML numbers between these two scans was 12.4 which was statistically significant; p=0.002 (95% CI of the difference; 6.2 – 18.6). Eight patients were used for analysis as two did not have 'T2* with high EPI'. The mean WML numbers with the 'standard T2*' in this comparison is higher than the comparison between both 'standard T2*' scans above (53.8 vs 45.3 respectively).

This is because the patient with high WML numbers was included in calculating the mean (and they were not considered an outlier in this analysis).

Mean WMLs with SWAN was 51.2 and 17.8 with the 'standard T2*' scan on the GE scanner. The mean WML number difference between these two sequences was statistically significant (p=0.002). Nine patients were used for this comparison as one did not have the SWAN scan and the same patient did not have the 'standard T2*' scan.

2.3.3 WML numbers: comparison between T2* sequences – SVD

As with the MS patients, 'T2* high EPI' allowed the most number of WMLs to be identified (mean 36.3). The difference between this T2* sequence and the 'standard T2*' on the same scanner was 10.8 (95% CI of the differences; 5.6 – 16), which was statistically significant (p=0.001). SWAN imaging also allowed a high number of WMLs to be detected, with both 'standard T2*' sequences performing less well (Table 4).

WML numbers with T2*	MS Mean	95% CI of the difference Lower	Upper	Mean difference	p value	SVD Mean	95% CI of the difference Lower	Upper	Mean difference	p value
Standard T2* Philips	45.3	9.8	49.9	29.9	0.01	25.5	7	20.4	13.7	0.001
Standard T2* GE	15.4*					11.8				
Standard T2* Philips	53.8	6.2	18.6	12.4	0.002	25.5	5.6	16	10.8	0.001
T2* high EPI Philips	66.1**					36.3				
Standard T2* GE	17.8	16.3	50.6	33.4	0.002	11.8	5.7	31.3	18.5	0.01
SWAN GE	51.2***					30.3				

Central vein numbers with T2*	MS Mean	95% CI of the difference Lower	Upper	Mean difference	p value	SVD Mean	95% CI of the difference Lower	Upper	Mean difference	p value
Standard T2* Philips	15.3	0.5	17.9	9.2	0.04	0.3	-0.3	0.5	0.1	0.591
Standard T2* GE	6.1					0.2				
Standard T2* Philips	14.5	11.6	43.7	27.6	0.005	0.3	0.7	2.7	1.7	0.003
T2* high EPI Philips	42.1†					2				
Standard T2* GE	6.8	10.9	26.9	18.9	0.001	0.2	0.1	3.3	1.7	0.04
SWAN GE	25.7‡					1.9				

Table 4. Comparison of WML and central vein numbers between T2* sequences in MS and SVD cohorts.

8 patients used for comparison as 1 patient did not have T2 on the GE and 1 removed as an outlier. **8 patients used for comparison as 2 patients did not have T2* with high EPI. ***9 patients used for comparison as 1 patient did not have a SWAN scan. †8 patients used for comparison as 2 patients did not have the T2* with high EPI scan; ‡9 patients used for comparison as 1 patient did not have a SWAN scan. p values calculated using a paired t test.

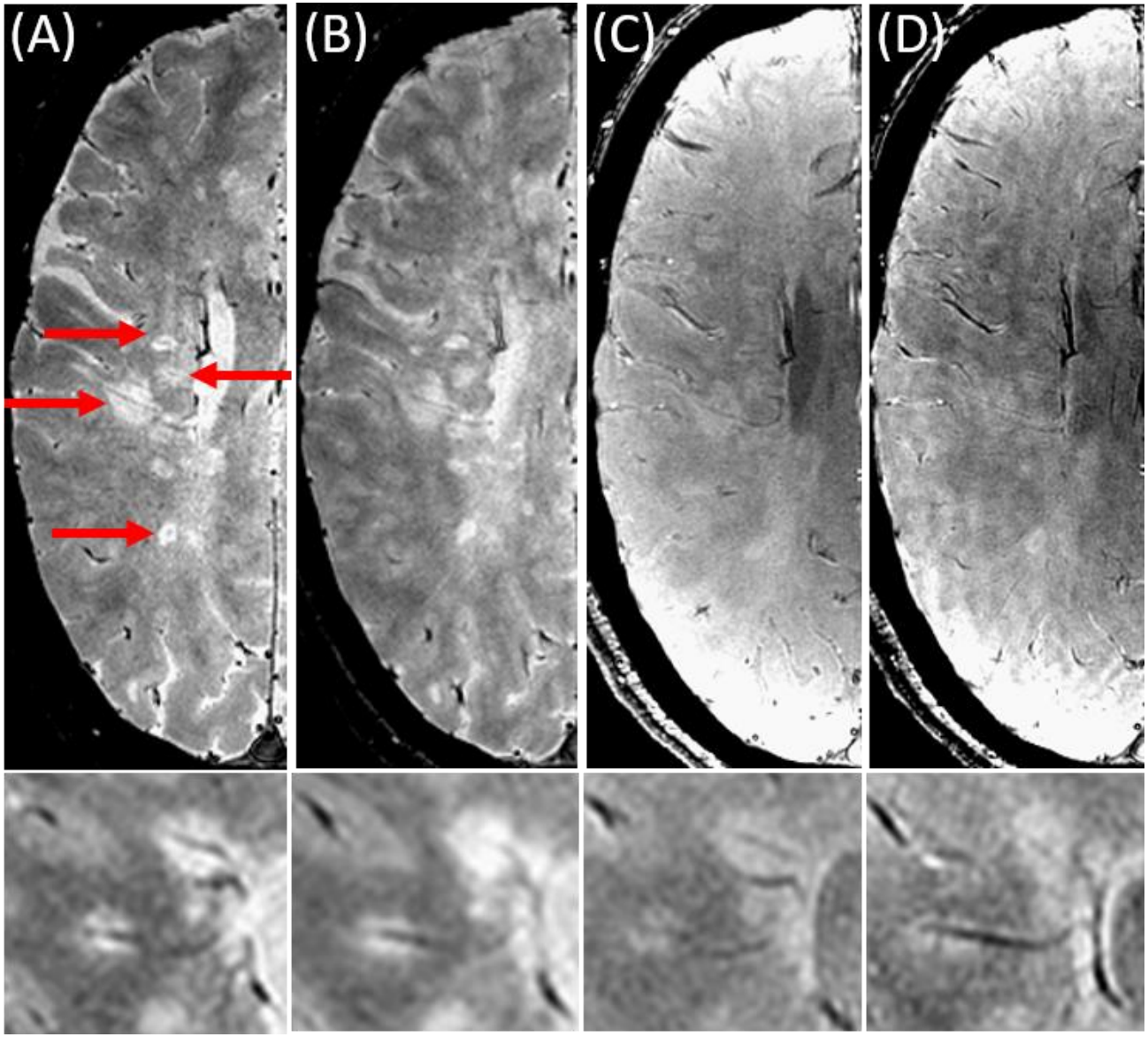

Figure 14. Two different MS patients scanned with all four T2* sequences.

The top and bottom rows are two different patients. Column (A) T2* with high EPI Philips; (B) standard T2* Philips; (C) SWAN GE; (D) standard T2* GE. Arrows indicate the ease of identifying WMLs with central veins when using T2* with high EPI, compared to similar T2* sequences. This illustrates why the differences in WMLs and hence proportion of WMLs with central veins can differ between scanners despite similar T2* weighted imaging. To identify WMLs using SWAN and T2* using the GE scanner, the image viewer contrast needs to be altered significantly, as shown by the bright edges around the images (C & D).

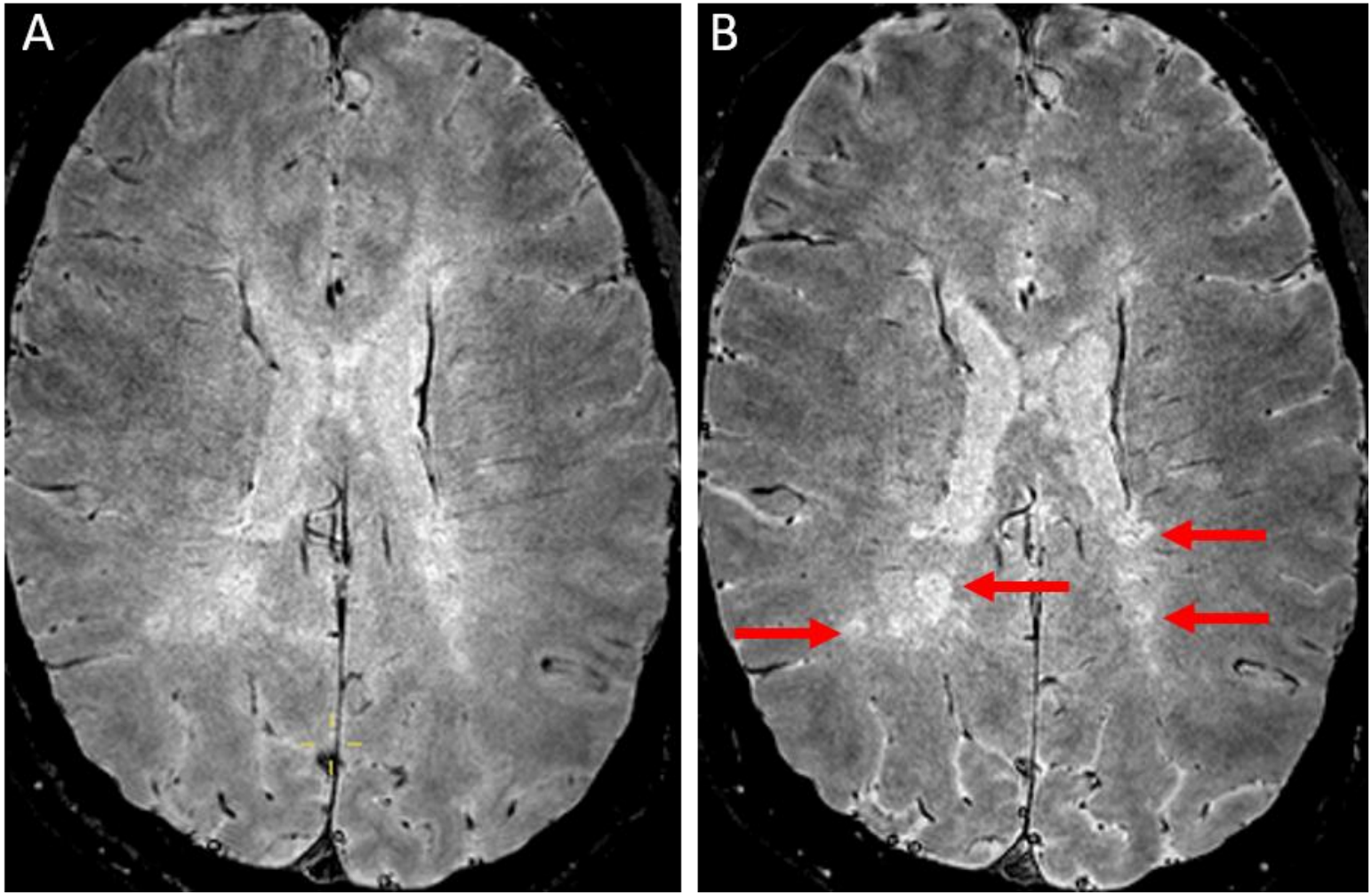

Figure 15. MS patient scanned using the Philips 3T scanner.

(A) standard T2* and (B) T2* with high EPI factor. Arrows in (B) show some areas which appear to be distinct WMLs but this is not so clear on the corresponding standard T2* image which could be mistaken for dirty appearing white matter instead.

2.3.4 WML central vein numbers: comparison between T2* sequences – MS

Results for WML central vein numbers are summarised in Table 4. Patients within the MS cohort had a variable number of WML central veins detected with each T2* sequence. 'T2* with high EPI' again allowed the most WML central veins to be identified in the MS group (mean 42.1), followed by SWAN imaging (mean 25.7) and both 'standard T2*' sequences.

Both 'standard T2*' sequences were compared across the Philips and GE scanners, producing mean WML central vein numbers of 15.3 and 6.1 respectively. The mean difference was statistically significant; p=0.04 (95% CI of the difference; 0.5 – 17.9).

'T2* with high EPI' was compared to the 'standard T2*' on the same scanner. Eight patients were used for this analysis as two did not have 'T2* with high EPI'. Mean WML central vein numbers were higher after using 'T2* with high EPI' compared to 'standard T2*' (42.1 and 14.5 respectively), with the mean difference of 27.6 being statistically significant; p=0.005 (95% CI of the difference; 11.6 – 43.7).

SWAN imaging also produced statistically significantly more WML central veins compared to the 'standard T2*' on the GE scanner (Table 4), although only nine patients were used for this comparison as one did not have SWAN because of technical issues with the scanner.

2.3.5 WML central vein numbers: comparison between T2* sequences – SVD

In contrast to the MS cohort, there was no significant difference in WML central vein numbers between the two 'standard T2*' sequences in the SVD cohort (Table 4). Ten patients were used for this comparison. Although a boxplot showed three extreme values (mean differences of 1) these were included in the analysis as although considered extreme, clinically this was not the case. A paired t test was attempted after the 3 extreme values were excluded to determine if this had any difference on the mean difference. However, since the mean difference was 0, the t test could not be run as there was no variability between the differences to test this hypothesis. I therefore included the extreme values in the calculation of the mean difference as it was so small (0.1) and was very close to the mean difference (if they were excluded).

Although both 'T2* with high EPI' and SWAN allowed more WML central veins to be identified compared to their corresponding 'standard T2*' sequences, from a clinical standpoint this was not significant. As can be seen in Table 4, all T2* weighted sequences allowed small mean numbers of WML central veins to be seen, with narrow confidence intervals.

2.3.6 Proportion of WMLs with central veins

MS group

Analysis of this data is summarised in Table 5 and Figure 16. The proportion of WMLs with central veins differed in the same MS patient when scanned with each T2* sequence. This is demonstrated by the wide LoA (which indicates ±1.96 SD of the mean) on the Bland-Altman plots. The largest mean bias (mean difference) of 36% being between the 'T2* with high EPI' and 'standard T2*' on the Philips scanner (indicating that the mean proportion of WML central veins with 'T2* with high EPI' was 36% greater compared to the 'standard T2*'.

The proportion of WMLs with central veins using the 'standard T2*' on both scanners also showed wide LoA on the Bland-Altman plots, indicating poor agreement across these two sequences. The difference between the two however was smaller, with the GE scanner estimating 8.9% more compared to the Philips 'standard T2*'.

SWAN allowed a higher proportion of WMLs with central veins (55.7%) compared to the 'standard T2*' (40.1%) on the equivalent scanner, with a mean bias of 16% in favour of the SWAN sequence and again wide LoA.

SVD group

Analysis of this data is summarised in Table 5 and Figure 17. The proportion of WMLs with central veins in the SVD group was statistically significantly much lower with all sequences compared to the MS group. The highest mean proportion being approximately 6% of WMLs with central veins when using 'T2* with high EPI' and SWAN, but lower proportions with each 'standard T2*' sequence. Bland-Altman plots demonstrate that LoA were narrower in the SVD group compared to MS, indicating more similar agreement between sequences. For example comparing

the two ‘standard T2*’ sequences showed a mean bias of 1.7% in favour of the GE scanner sequence, but SWAN produced a marginally higher mean bias of 3.6% compared to the ‘standard T2*’ on GE and ‘T2* with high EPI produced an even higher mean bias of 5.1% compared to ‘standard T2*’ on the same scanner. All comparisons however had wide LoA indicating potentially larger mean biases. However, the upper limits of agreement (ULA) are usually less than 15%, indicating that this would be the upper level mean difference in the SVD patients.

2.3.7 Rater agreement with clinical diagnoses

Results are summarised in Table 6. Rater agreements varied using different T2* sequences, but was particularly high in all raters when ‘T2* with high EPI’ (κ=0.78; 0.78; 0.89) and ‘standard T2*’ on the Philips scanner (κ=0.80; 0.60; 0.80) were used. Figure 14 illustrates why this might be the case and shows the variability in visibility of WMLs and central veins across sequences.

Group and T2* sequence	Proportion WMLs with central veins (mean %)				
	Philips	GE	Mean Diff. (%)	Lower LoA (%)	Upper LoA (%)
MS					
Standard T2*	29.5	40.1			
T2* with high EPI	64.5	N/A			
SWAN	N/A	55.7			
Standard T2* Philips vs T2* GE			8.9	-29	46
Standard T2* Philips vs T2* high EPI Philips			36	3.5	68
Standard T2* GE vs SWAN GE			16	-50	81
SVD					
Standard T2*	0.97	2.67			
T2* with high EPI	6.06	N/A			
SWAN	N/A	6.26			
Standard T2* Philips vs T2* GE			1.7	-11	15
Standard T2* Philips vs T2* high EPI Philips			5.1	-2.7	13
Standard T2* GE vs SWAN GE			3.6	-9.7	17

Table 5. Proportion of WMLs with central veins and comparison of T2* sequences within groups (MS and SVD)

LoA = Limits of agreement. LoA and mean difference calculated using Bland-Altman plots.

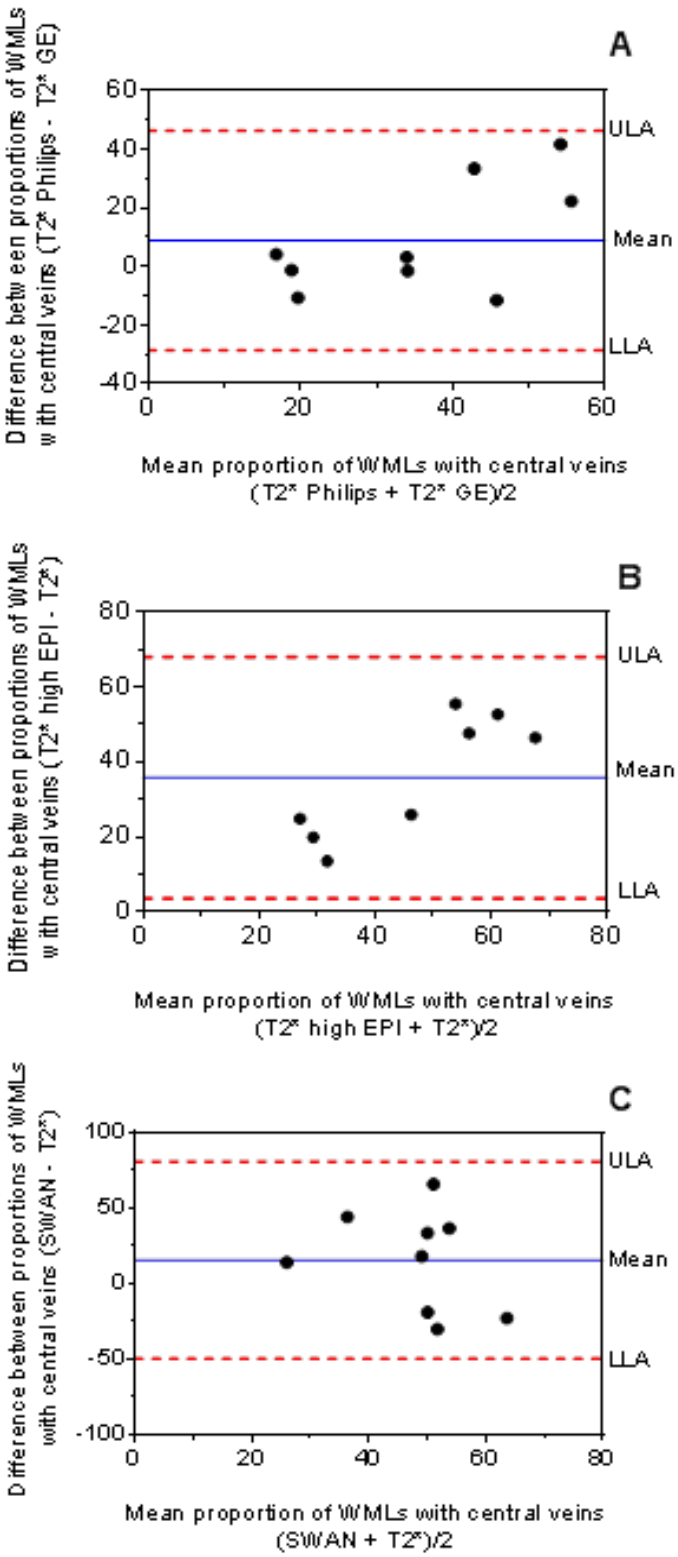

Figure 16. Bland-Altman plots showing the proportion of WMLs with central veins in the MS group.

This plots the difference between two values against the mean of two values. The bias, or mean difference of the proportion of WMLs with central veins between two sequences is shown with a solid line. ULA and LLA are shown as dotted lines. These indicate the range in which most differences in measurements by the two sequences will lie. The smaller the gap between these two extreme values the closer the two sequences are in identifying the same proportion of WMLs with central veins. (A) Comparison of the proportion of WMLs with central veins using standard T2* imaging on both scanners. (B) The same comparison using standard T2* and T2* with high EPI and (C) using standard T2* and SWAN.

ULA = upper limit of agreement; LLA = lower limit of agreement

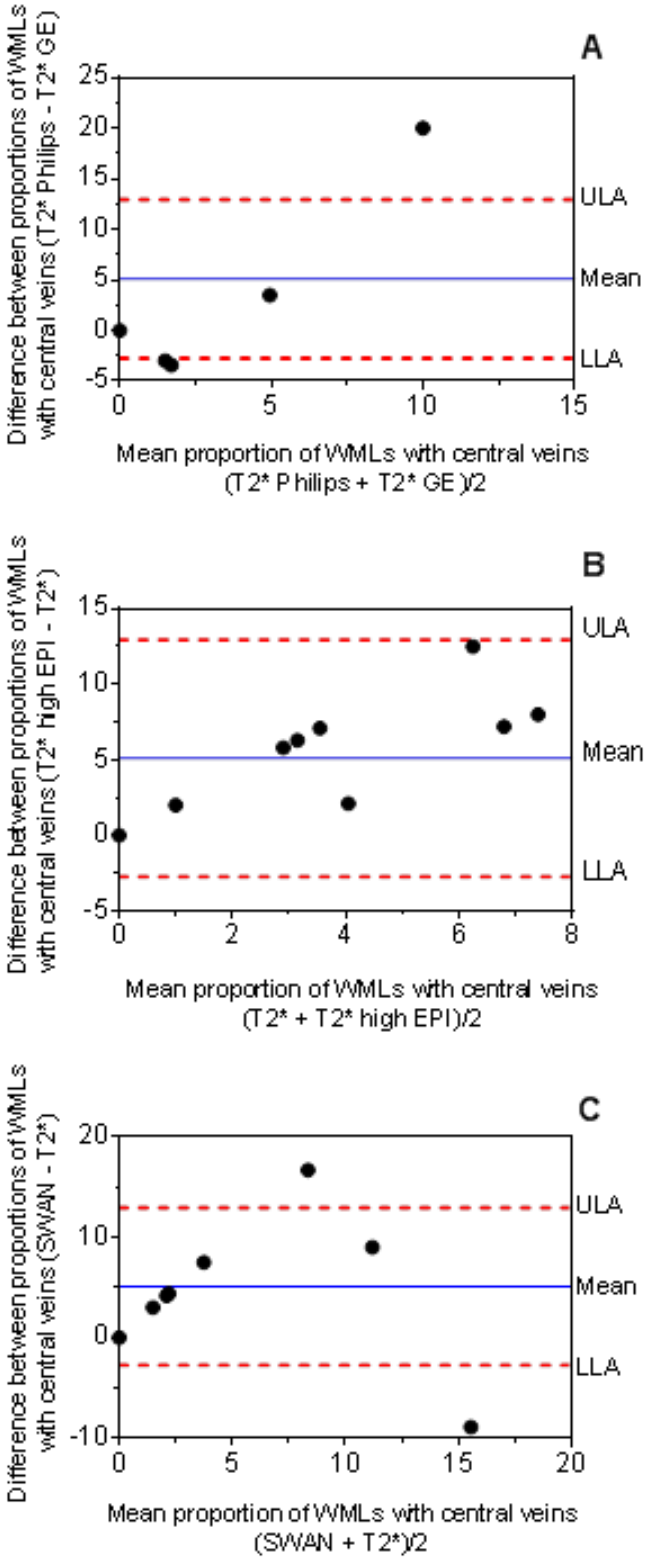

Figure 17. Bland-Altman plots showing the proportion of WMLs with central veins in the SVD group.

(A) Comparison of this proportion when using standard T2* imaging on both scanners. (B) The same comparison when using standard T2* and T2* with high EPI and (C) using standard T2* and SWAN.

ULA = upper limit of agreement; LLA = lower limit of agreement

T2* sequence	Rater AW			Rater MC			Rater YF		
	kappa coeff.	95% CI	p value	kappa coeff.	95% CI	p value	kappa coeff.	95% CI	p value
StandardT2* Philips	0.80	0.54 – 1	0.005	0.60	0.26 – 0.94	0.006	0.80	0.54 – 1	0.0003
Standard T2* GE	0.13	-0.21 – 0.47	0.47	0.58	0.22 – 0.94	0.009	0.37	-0.05 – 0.79	0.11
T2* with high EPI	0.78	0.48 – 1	0.001	0.78	0.49 – 1	0.001	0.89	0.68 – 1	0.0001
SWAN	0.37	-0.05 – 0.79	0.11	0.69	0.38 – 1	0.002	0.69	0.36 – 1	0.003

Table 6. Blinded rater agreements between the diagnostic classification based on WML central veins alone and the known clinical diagnosis.

CI = confidence interval; Kappa coeff = Cohen's kappa coefficient. Cohen's Kappa statistic was used for analysis

2.4 Discussion

I compared the proportion of WMLs that can be detected with central veins in patients with MS and ischaemic SVD at 3T, as this holds promise as a marker of MS especially in patients with diagnostic uncertainty (Dixon *et al.*, 2013; Quinn *et al.*, 2013).

My first observation was that the perivenous pathology of MS lesions can be observed irrespective of the 3T T2* sequence that we used. There was a clear difference between the proportions of WMLs with central veins in MS (highest when using 'T2* with high EPI'; median 69.6%), compared to SVD (approximately 6%). This large distinction between the MS and SVD groups reinforces findings of early studies (Tallantyre *et al.*, 2011; Hackmack *et al.*, 2012; Sinnecker *et al.*, 2012; Kau *et al.*, 2013; Kister *et al.*, 2013), and supports the idea that this feature could be used as an imaging biomarker, if validated in prospective studies.

The second finding demonstrated the variability in the *number* of WMLs and WML central veins within each group, depending on the T2* sequence. Variability of biomarker measurements is not uncommon when different MRI scanners and sequences are used. Filippi et al. showed differences in WML load when different scanners were used on the same patient (Filippi *et al.*, 1999). For example, fast-FLAIR imaging used on the same MS patients, on two different scanners produced mean lesion volumes of 15.5 and 18.1mls. Previous work by Gasperini and colleagues showed contrasting results and demonstrated smaller differences in whole brain volume measurements with different scanners (Gasperini *et al.*, 2001). This may be in part due to the easier segmentation of the whole brain and easier delineation of brain margins compared to CSF (although brain segmentation itself

comes with its own sources of error). In contrast, WML segmentation can cause under or over reporting due to difficulties in differentiating WMLs from dirty appearing white matter (DAWM), Virchow-Robin spaces, variable lesion visibility depending which sequence is used and misinterpretation of CSF for lesions, especially near the occipital ventricular horns

My third finding was the variability in the *proportion* of WMLs with central veins, within each group, demonstrated by the Bland-Altman plots. Despite wide LoA, when the proportions of WMLs with central veins were compared between the MS and SVD groups, there remained a clear, statistically significant difference, so allowing differentiation of MS and SVD based on the central vein sign alone. However identifying a threshold for diagnosis would need to take into consideration the subtle variations in T2* sequences across scanners.

A number of studies have compared the degree of variation in brain volume and lesion load in patients with MS, between different MRI scanner manufacturers at 1.5T (Barkhof *et al.*, 1997; Filippi *et al.*, 1998; Filippi *et al.*, 2016) and between different magnetic field strengths (Keiper *et al.*, 1998). To the best of my knowledge there has been no previous literature comparing the identification of WML central veins using different scanners and T2* sequences at 3T. Although there are limitations to this study (discussed later), the disparities in WML and central vein numbers are clinically important in view of the increasing recommendation of using 3T scanners for clinical practice (Canto *et al.*, 2015). Furthermore, these findings may have implications and be a barrier for future translation due to the inevitability of different institutions using different scanners and so using variations of the T2* weighted sequence.

The different T2* sequences produced different proportions of WMLs with central veins. However, the mean differences were more variable in the MS than the SVD group. I can hypothesize that this is because alongside lesions in the MS brain, DAWM can sometimes cause uncertainty about the presence or absence of a lesion. DAWM can be seen to some extent on T2*-weighted scans. If there was doubt that a hyperintensity may have been DAWM I did not count it. An example of this is shown in Figure 15. This may result in different WML numbers and hence proportions. This was less of a problem in scans with SVD, where the relative absence of DAWM may have facilitated WML identification.

In clinical practice, clinicians are unlikely to identify all WMLs due to time constraints (George *et al.,* 2016) and so more practical criteria such as counting a subset of WMLs with central veins may be a method of overcoming this problem. Hence I tested if agreement with the clinical diagnosis would alter depending on the T2* sequence used, when using previously published practical criteria. (Mistry *et al.*, 2016).

As a result of this, the fourth finding was that rater reproducibility did vary when comparing the identification of a subset of WML central veins alone to make a diagnosis and the established clinical diagnosis. This was in part dependent on the T2* sequence used. Good agreement was observed when all three raters used the 'standard T2*' on the Philips scanner to make a diagnosis using this method. Good – very good agreement was seen with all raters when using 'T2* with high EPI'. Both these findings could be due to the ease of identifying WMLs and hence central veins, using these two T2* sequences. Agreement when two of the raters (AW and YF) used the 'standard T2*' on the GE scanner was poor and fair when one rater (AW) used SWAN (κ=0.37) (though from a diagnostic point of view this would be

poor). Additionally, 95% confidence intervals were marginally below 0 for these kappa values, suggesting possibly no agreement with the clinical diagnosis of MS or SVD. This could be because of the difficulty in identifying WMLs and therefore central veins. One rater (MC) achieved better agreement with the 'standard T2*' and SWAN on the GE scanner.

Although the T2* sequence appears to affect the accuracy of making a diagnosis of MS or SVD using WML central veins, it seems that the experience of the rater needs to be taken into account too. Rater YF who has had the most clinical experience had high agreements with all T2* sequences, except the 'standard T2*' on the GE scanner. Rater MC had some neuroimaging analysis experience and scored more evenly across all sequences, with their lowest kappa coefficient being 0.58 with the 'standard T2*' on the GE scanner. Rater AW who although did have training, had the least experience, and had more variable coefficients. Again 'standard T2*' on the GE scanner produced their lowest results.

Although the size of the studied cohorts are small in this chapter, it suggests that, overall, 'T2* with high EPI' is more effective when searching for WML central veins compared to other sequences. Possible reasons for this include: 1) 'T2* with high EPI' has a longer TE compared to the 'standard T2*' sequences (29 versus 25ms). This would allow more dephasing, hence more T2* decay and so greater loss of signal from veins, therefore potentially allowing more contrast between WMLs and the black central veins; 2) the acquisition time for 'T2* with high EPI' was quicker (approximately 4 minutes) compared to 'standard T2*', so minimising artefact caused by head movement and more appropriate for patients who have difficulty lying still for prolonged periods of time; 3) it allowed easier identification of WMLs compared to the 'standard T2*' scan, which can have a knock on effect

on the number of central veins (WMLs need to be identified first before searching for veins). The anisotropic voxels in the 'standard T2*' sequences (0.43x0.43x1.5mm on the GE and 0.55x0.55x1.05mm on the Philips) may have increased partial volume effects, so reducing demarcation of WMLs and also hindered small central veins from being defined, compared to the isotropic voxels (0.55x0.55x0.55mm) used with the 'T2* with high EPI' sequence. The trade-off however is a slightly lower signal to noise ratio with smaller voxels. This has not appeared to have affected the image quality in the 'T2* with high EPI' images. Additionally a low flip angle (10º in the 'T2* with high EPI', 14º in the 'standard T2*' on the Philips scanner), reduces the influence of T1 weighting and increases T2* weighting (Nitz and Reimer, 1999). This may help central vein visibility and to some extent WML intensity. A final key reason in discrepancies between image quality is the use of a higher EPI factor compared to the 'standard T2*' scans. The higher EPI leads to a greater signal-to-noise ratio, because effectively EPI detects the signal over a longer duration than the GRE sequences, which takes a 'snapshot' of the signal coming from T2* decay (Zwanenburg *et al.*, 2011). Despite these differences, when identifying a subset of 6 WMLs with central veins, there was good agreement amongst all blinded raters using 'T2* with high EPI', 'standard T2*' on the Philips scanner and SWAN on the GE scanner.

The good inter rater agreement with some of the T2* sequences demonstrates that identifying a subset of WMLs with central veins could be used to make accurate diagnoses of MS or non-MS. To establish positive and negative predictive values however, prospective studies need to be undertaken.

2.4.1 Limitations

Firstly, patient numbers from both MS and SVD groups were small and a power calculation was not performed as this was exploratory in nature. However because of this, a type I statistical error is possible. Secondly, due to patient and scanner availability, trying to co-ordinate both scans within a short period of time of each other proved difficult. However, the median interval between scans for each group was 24 days thereby making it unlikely that in these relatively inactive patients, any change detected in the number of WMLs was due to new WML development. One patient did have an approximate 6 month gap between both scans, however he had SVD and so I would not expect any drastic changes in WML load in this timeframe. Thirdly, I have not compared these findings with other scanner vendors which may have further variations on the T2* sequence. Fourthly, I did not correct for vascular risk factors in the MS group, as previous studies have shown that ischaemic lesions have no or very few central veins. Although not all MS WMLs have central veins, I concluded that any ischaemic lesions in the MS group would still not affect the central vein count significantly. However, vascular risk factors should be accounted for in future studies. A further weakness is that one unblinded rater (myself) identified all WMLs and central veins for each group. Ideally this should be repeated with other raters to determine if the proportion of WMLs with central veins is similar and if the discrepancy between MS and SVD remains. However, as there was such a stark discrepancy between the two groups, I would hypothesize that this difference remains, regardless of rater.

2.4.2 Summary

In summary, my intention for this chapter was to mimic real life clinical practice, where variations of the T2* sequence would be used. It has continued to

demonstrate that patients with MS have a higher proportion of WMLs with central veins compared to those with ischaemic SVD. Scanner and T2* sequence variability may need to be taken into account when defining a threshold for the proportion or number of WMLs with central veins for the diagnosis; but I accept study numbers need to be larger to definitively confirm this. Furthermore, these preliminary results suggest that not all WMLs need to be assessed, but a practical radiological assessment can be performed by selecting a subset of WMLs with central veins with good inter rater reproducibility, especially using 'T2* with high EPI'. As a consequence of this study I have decided to use the 'T2* with high EPI' sequence for subsequent studies in this thesis.

Chapter 3. A comparison of 3T T2*, SWI and FLAIR-SWI in detecting WML central veins

3.1 Background

Various T2* weighted sequences have been used to depict WML central veins and this has already been described in chapter one.

T2* weighted GRE does not have a refocussing 180° RF pulse and so leads to the susceptibility effect, caused by inhomogeneity of the MR signal due to the iron content of deoxyhaemoglobin. Conventionally, T2* imaging has been a 2D acquisition, for example when investigating for cerebral microbleeds (Vernooij *et al.*, 2008), with a few research groups using 7T 2D T2* weighted sequences for central veins (Hackmack *et al.*, 2012; Sinnecker *et al.*, 2012; Kuchling *et al.*, 2014). Three dimensional acquisitions have also been used (Tallantyre *et al.*, 2011; Dixon *et al.*, 2013; Solomon *et al.*, 2016), giving the advantage of thinner slices, and with the addition of a high EPI factor, high acquisition speeds can be achieved (Gaitán *et al.*, 2014).

SWI is said to enhance this susceptibility effect even further thereby enhancing signal loss in blood vessels even more. It involves a post-acquisition step in addition to the T2* weighted acquisition, which involves combining a mask produced from its phase map with the magnitude image (Shams *et al.*, 2015). It is increasingly being applied in clinical practice to investigate brain disorders such as arteriovenous malformations, cerebral amyloid angiopathy and for the detection of iron deposition in neurodegenerative conditions (Robinson and Bhuta, 2011; Bosemani *et al.*, 2014). Variations of this are provided by different MRI vendors

such as SWAN and venous blood oxygen level dependent (VenoBOLD) (Hodel *et al.*, 2012), and it is part of Siemens' MRI scanners (with the post-acquisition processing performed automatically on the scanner) (Tong *et al.*, 2008). All this makes susceptibility weighting easily available in the clinical setting.

3.1.1 Post acquisition combination of MRI sequences

A few studies to date have used post processing image fusion which provides the benefit of using visually hyperintense WMLs from FLAIR, and superimposing dark veins from the SWI phase maps or T2* images (Grabner *et al.*, 2011; Sati *et al.*, 2012; Absinta *et al.*, 2013; Kilsdonk *et al.*, 2014b). Two new sequences have been developed: FLAIR-SWI and FLAIR*. A combination of 3T FLAIR images with 7T SWI phase maps to produce FLAIR-SWI, was proposed by Grabner and colleagues (2011). In this study ten patients were scanned twice; each on a 3T and 7T scanner. Of 299 WMLs detected, 75 (25%) had venous blood vessels traversing the lesion; a smaller proportion compared to other studies. They also showed that SWI scans alone allowed a much smaller detection of WMLs and hence central veins. A limitation to this study and for clinical translation however was the need for two scans, on two scanners using two different field strengths, although this has also been tested at purely 7T (Muller *et al.*, 2014).

Sati et al. introduced the term FLAIR* which allowed greater WML delineation along with vein visibility after fusing T2* and FLAIR at 3T (Sati *et al.*, 2012). Their pilot study used an intravenous contrast agent during the T2* acquisition to increase the visibility of veins, as susceptibility effects in the smaller veins are lost with lower magnetic field strengths. This sequence needed to be processed after image acquisition, and in view of the need for intravenous contrast, may be one of the

limitations in clinical practice. FLAIR* was used in a further study at 7T (Kilsdonk *et al*., 2014b) without intravenous contrast, which allowed greater differentiation of MS from vascular WMLs. Again this will be limited in clinical practice due to the current use of 7T scanners for research purposes only. Fused FLAIR-SWI imaging has been developed based solely on 3T data in view of the growing applications of SWI in the clinical setting (Tong *et al.*, 2008; Haacke *et al.*, 2009).

Gaitán et al combined 3T Proton density-weighted (PD) and T2 weighted imaging, termed 'PT2' to better visualise infratentorial lesions. Both these images were acquired during the same scan and so already co-registered. They found that infratentorial lesions were easier to identify than T2 weighted imaging alone, and had fewer artefacts and noise (Gaitan *et al.*, 2015).

Post-acquisition fusion of MR images may prove useful as users get 'best of both worlds', for example the ability to enhance the visibility of WMLs with FLAIR imaging, along with the ease of identifying central veins with T2* weighted imaging. However MR image fusion and post-acquisition processing comes with practical limitations for clinical practice. As two images are needed there is more likelihood of motion and inhomogeneity artefacts causing signal intensity changes due to local internal (i.e. tissue variations causing inhomogeneities) and external field inhomogeneities. Subtle variations in susceptibility across the region being scanned will also lead to this (McRobbie *et al.*, 2006). There is a potential need for intravenous contrast agent although it can be made without this. Skilled operators are needed for image processing as it is unlikely that clinicians will be able to perform this. Image fusion cannot be achieved without first spatially aligning the two images, termed co-registration (Rojas *et al.*, 2007), followed by correction for inhomogeneities.

The optimal sequence for use in routine clinical practice to detect the central vein using 3T MRI has not been established. Furthermore, whether fused images are quantitatively superior to the 'raw' T2* or SWI sequences has not been assessed and this is what this chapter focuses on.

3.1.2 Aims and hypothesis

I wanted to assess if the use of raw T2* (magnitude image) resulted in any quantifiable difference in WML central vein visibility compared to SWI (combined magnitude and phase image) and FLAIR-SWI. The hypothesis being that T2* and SWI would be inferior to FLAIR-SWI in the visibility of WMLs with central veins.

The primary aim was to assess any difference in the number of WMLs, WMLs with central veins and proportion of WMLs with central veins detected on the raw T2* scans, SWI and FLAIR-SWI images.

The secondary aim was to determine if the performance of a potential diagnostic rule (Mistry *et al.*, 2016) in differentiating MS from SVD is comparable using the raw T2* images or FLAIR-SWI-2 imaging.

3.2 Methods

3.2.1 Patient selection

For my primary aim, adult patients aged 18-75 who attended a general neurology or MS clinic at the Nottingham University Hospitals NHS Trust between July 2013 and February 2016 were asked to participate in the study. All patients had a confirmed diagnosis of MS (made by a consultant neurologist with a subspecialty interest in MS) with typical MRI findings. Poser and McDonald criteria 2001-2010 were used to support the MS diagnosis.

For my secondary aim, I included the scans of the MS patients above and the scans of MS and SVD patients from an ongoing study not described in this thesis (Single Test to Arrive at MS diagnosis study; STAR-MS). Ischaemic SVD was diagnosed if the patient did not have symptoms or objective signs of demyelination, supported by a consultant neuroradiologist's report of an MRI brain scan in keeping with SVD, blood tests excluding other causes for WMLs, and if necessary CSF testing ruling out the presence of oligoclonal bands. Written informed consent from all patients was obtained before inclusion in the study and the study was approved by the local research ethics committee.

3.2.2 MRI protocol

MR imaging was performed using a 3T Achieva, Philips Healthcare scanner with a 32 channel receive-only head coil. The protocols included:

1) 3D T2*-weighted GRE, TE 25 ms, TR 150 ms, parallel imaging factor 2, 0.55x0.55x1.05 mm voxels, 400x400x96 matrix, four interleaved 3D stacks with a small overlap, pixel bandwidth 160 Hz, duration 510 s. As in chapter 2, this will be referred to as the 'standard T2*'.

2) A second 3D T2*-weighted GRE scan was acquired with a higher EPI factor of 15, similar to Sati and colleagues (Sati *et al.*, 2014) also using the 32 channel head coil, in the sagittal plane. The matrix was 448x448x336 with a non-interpolated voxel size of 0.54x0.54x0.55mm. Parallel imaging factors of 2 were used in both phase encoding directions. In addition the water-only excitation flip angle was 10 degrees, effective TE 29 ms, TR 54 ms, two averages, duration 254 s.

3) 3D FLAIR acquired in the sagittal plane. Turbo spin echo readout, voxel size of 1x1x1 mm, 256x256x180 matrix, parallel imaging factor 2, TE 290 ms, TR 4800 ms, TI 1650 ms, pixel bandwidth 1220 Hz, duration 370 s.

3.2.3 SWI processing

Images for post-acquisition processing can be seen in appendix A. SWI processing was performed by Dr Olivier Mougin (Post-doctoral researcher in MRI physics) on a standard desktop computer as described in a previous study (Chavhan *et al.*, 2009). The raw data generated directly from the scanner are the magnitude and phase images. Before interpretation, the phase data needs to have inhomogeneities removed (caused by different susceptibilities of the brain tissue) using filters. In the filtered phase image, veins are bright and other brain tissue is dark. Any dark voxel (brain tissue) is assigned number '1' and anything bright (vein) is assigned 1 minus (whatever intensity the vein is). This phase image is then multiplied by itself 4 times (producing the phase mask). Any voxel that is 1 stays as 1, but any voxel that is below 1 becomes even higher in signal e.g. a voxel assigned 0.9 becomes even lower (0.9x0.9x0.9x0.9=0.66). Therefore the difference between the 1 and 0.66 increases and so the contrast between the vein and normal tissue increases. This data is then transformed into a phase mask where the veins appear dark and tissue appears brighter. This phase mask is then multiplied by the magnitude image to create SWI. No minimum intensity projection and no average was performed so as to preserve the clarity of the WMLs themselves.

3.2.4 FLAIR-SWI processing

FLAIR-SWI processing was performed by Dr Olivier Mougin. The T2* images and the FLAIR images were co-registered together using a software programme

called FLIRT from FSL (Jenkinson *et al.*, 2002). After transformation of the FLAIR images onto the T2* space, the FLAIR-SWI images were produced by multiplying FLAIR and SWI images together.

3.2.5 Image analysis

Sequences used for the analysis included: T2* with anisotropic voxels (standard T2*), T2* with high EPI and isotropic voxels (T2* hEPI), SWI with anisotropic voxels (standard SWI), SWI with high EPI and isotropic voxels (SWI hEPI), fusion of FLAIR and standard SWI (FLAIR-SWI-1) and fusion of FLAIR and SWI hEPI (FLAIR-SWI-2).

Images were saved in a DICOM format and then converted to NIfTI format. NeuROI image analysis software as described in chapter 2 was used to count WMLs using a manual technique. WMLs were identified if they could be seen on the axial plane and one other plane, as well as being more than 3 voxels in diameter in the axial plane with demarcated borders. If there was any doubt about whether the lesion was within the cortex, it was excluded. If the WM hyperintensity appeared to be DAWM (defined for this study as diffuse high signal in the WM, with no definite borders) it was excluded. WM hyperintensities present around the frontal and occiptal horns were included if they satisfied the above criteria for a WML. Hyperintensities that appeared to be a thin line over the lateral ventricular borders, between the frontal and occipital horns were not counted unless the hyperintensity was perpendicular to the border and was clearly a well defined WML.

A WML central vein was judged as present if it appeared as a black hypointense line (if running along the long axis of the lesion) or a hypointense dot within the

centre of a WML. This had to be present on the axial plane and on either the coronal or sagittal planes.

For the primary aim, WMLs, WML central veins and the proportion of WMLs with central veins were identified in the scans of 20 MS patients by myself. The scans analysed included; T2* with anisotropic voxels (standard T2*), T2* with high EPI and isotropic voxels (T2* hEPI), SWI with anisotropic voxels (standard SWI), SWI with high EPI and isotropic voxels (SWI hEPI), fusion of FLAIR and standard SWI (FLAIR-SWI-1) and fusion of FLAIR and SWI hEPI (FLAIR-SWI-2).

For the secondary aim, two blinded raters (Margareta Clarke (MC)) who had already been trained after analysing data for chapter 2, and (Matthew South (MS), 3rd year medical student) who had been trained by myself for an alternate but similar themed project were used. These two raters had further training to ensure that the rater reproducibility was as high as possible for correctly identifying the presence or absence of a WML and presence of an alternative anatomical structure e.g. perivascular space, GM border, CSF. This was achieved by having an unblinded rater (Dr Yasser Falah) choose a random sample of WMLs (with or without central veins), GM, CSF or perivascular spaces from MS and SVD patients. Twenty images were cropped so that the brain location could not bias the identification of the target structure. These 20 images were then analysed by the two blinded raters to test their agreement with the unblinded rater.

Once the blinded raters were confident in identifying WMLs, they then identified a subset of 6 WMLs with central veins (described in chapter 2) to make a diagnosis of MS or SVD using only the T2* hEPI and FLAIR-SWI-2 scans for a total of 39 scan pairs. The results of their diagnoses were compared to the established

diagnoses for each of these two sequences, to determine if one sequence allowed a more accurate diagnoses than the other. This was repeated by each rater after an average interval of seven days.

3.2.6 Statistical analysis

For statistical differences in demographic data e.g. age, independent t-tests were used. WML numbers, central vein numbers and the proportion of WMLs with central veins were checked for outliers using boxplots. Histograms were used to check for normality of data. Means ± two standard deviations in parentheses or medians and interquartiles (IQR) ranges in parentheses were provided for normally distributed and non-normal data. For normally distributed data, a one way repeated meaures analysis of variance (ANOVA) was performed for pairwise comparisons of the proportions of WMLs with central veins measured with each sequence. A Bonferroni adjustment for multiple comparisons was used for post hoc testing. For data that was not normally distributed, e.g. WML and central vein numbers, a non-parametric test (Friedman) was used. For the comparison of T2* hEPI and FLAIR-SWI for the differentiation of MS from SVD, Cohen's kappa (κ) coefficient (95% CI in parentheses) was used for each blinded rater to assess agreement of the diagnosis based on the central vein sign alone, compared to the established diagnosis. Sensitivity, specificity, positive and negative predictive values and likelihood ratios were also calculated for each rater (tests more commonly used in the clinical setting). Statistical significance was set at $p<0.05$. Statistical analyses were performed using Statistical Package for the Social Sciences (IBM SPSS 22) or an online statistical programme (MedCalc; www.medcalc.org/index.php).

3.3 Results

3.3.1 Demographics

This is summarised in Table 7. For the primary aim 20 MS patients were used (11 female, 9 male) with a mean age of 41.6 years (±12.8) and mean EDSS of 3 (±1.8). For the secondary aim, 39 patients were analysed (23 with MS; 13 female and 10 male) and (16 with SVD; 8 female and 8 male). The mean age of the RRMS group was 41.1 years (±12.3) and 50.9 years (±9.6) in the SVD group. The mean difference in age between the two groups was 9.7 years (95% CI of the difference 2.2 – 17.2) which was statistically significant (p=0.012). Mean EDSS was 2.7 (±1.7) within the MS group. Median disease duration for the 23 MS patients (from symptom onset to the date of the T2* scan) was 112 months (38 – 180) and median disease duration (from date of diagnosis to the date of the T2* scan) was 36 months (2 - 144). Two patients of the SVD group were from an alternative study (STAR-MS study), but were used for this analysis as they were found to have SVD (STAR MS patients A and B). The 20 MS patients from the primary aim were used and three others from the STAR MS study were also used for this analysis as they were found to have MS (STAR MS patients C, D and E).

Patient	Age (yrs)	Gender (M/F)	MS/SVD	Disease duration(mths)	EDSS	CSF OCBs
P03	44	F	RRMS	269	5	ND
P04	43	M	RRMS	174	6	-
P05	32	M	RRMS	128	4	ND
P08	36	F	RRMS	55	2	+
P11	41	M	RRMS	180	6	+
P12	32	M	RRMS	112	4.5	+
P16	29	F	RRMS	253	2	+
P20	52	F	RRMS	233	5	+
P32	44	M	RRMS	3	2	-
P35	64	F	RRMS	118	2.5	ND
P36	36	F	RRMS	129	1	unknown
P37	49	F	RRMS	374	3	unknown
P38	48	F	RRMS	68	4	ND
P39	23	M	RRMS	21	1	ND
P40	55	F	RRMS	181	1	ND
P41	27	M	RRMS	41	2.5	+
P42	18	F	RRMS	45	0	+
P43	56	M	RRMS	25	2	ND
P44	63	M	RRMS	38	1	+
P45	39	F	RRMS	133	3	ND
C (STAR MS)	44	F	RRMS	67	1	ND
D (STAR MS)	26	F	RRMS	22	1	ND
E (STAR MS)	45	M	RRMS	26	3	ND
P09	56	F	SVD	NA	NA	ND
P10	41	F	SVD	NA	NA	-
P13	55	F	SVD	NA	NA	ND
P14	44	M	SVD	NA	NA	ND
P15	48	M	SVD	NA	NA	ND
P17	47	F	SVD	NA	NA	ND
P21	58	M	SVD	NA	NA	-
P23	75	M	SVD	NA	NA	ND
P24	48	F	SVD	NA	NA	-
P25	62	M	SVD	NA	NA	ND
P26	41	M	SVD	NA	NA	ND
P27	48	M	SVD	NA	NA	ND
P28	38	F	SVD	NA	NA	ND
P31	41	F	SVD	NA	NA	ND
A (STAR MS)	56	M	SVD	NA	NA	ND
B (STAR MS)	56	F	SVD	NA	NA	ND

Table 7. Demographics of the MS and SVD patients.

This includes three patients with MS and two with SVD from another study (STAR MS study), whose scans we used for this analysis.

Disease duration shown here = from symptom onset to time of T2* scan. ND = not done

3.3.2 WML numbers: comparison between sequences

Twenty MS patients were used for this analysis (3 MS scans were not included as their FLAIR-SWI scans were not available at the time of analysis). Median WML numbers and IQR are summarised in Table 8. FLAIR-SWI-2 (a fusion of T2* hEPI and FLAIR) allowed the most WMLs to be identified (median 47), followed by FLAIR-SWI-1 (39.5) and then T2* hEPI (33.5). WML numbers were not normally distributed and a boxplot revealed 3 outliers, with 1 outlier being an extreme value using the SWI hEPI sequence. Therefore a Friedman test for pairwise comparisons corrected with a Bonferroni adjustment was applied to 20 patients with full data. Pairwise comparisons showed no significant difference between FLAIR-SWI-2 (median WMLs 47) and T2* hEPI (median WMLs 33.5) ($p=0.168$). FLAIR-SWI-2 allowed detection of more WMLs than the standard T2* ($p<0.0005$), standard SWI ($p<0.0005$) and SWI hEPI ($p<0.0005$). Similarly T2* hEPI allowed a significantly higher number of WMLs to be detected compared to standard SWI ($p<0.0005$), SWI hEPI ($p=0.009$) and a trend towards significance when compared with standard T2* ($p=0.06$).

3.3.3 WML central vein numbers: comparison between sequences

The same 20 MS patients were analysed and median central vein numbers and IQR are summarised in Table 8. WML central vein numbers were not normally distributed so a Friedman test for pairwise comparisons was used for 20 patients with all data. Pairwise comparisons showed statistically significantly more WML central veins detected with T2* hEPI compared to the standard T2* ($p<0.0005$), standard SWI ($p<0.0005$), FLAIR-SWI-1 ($p<0.0005$) and SWI hEPI ($p=0.004$). There was no statistical difference in central vein numbers between T2* hEPI and

FLAIR-SWI-2 (p=1.0). However FLAIR-SWI-2 detected more central veins compared to the following sequences; standard T2* (p<0.0005), standard SWI (p<0.0005), FLAIR-SWI-1 (p<0.0005) and SWI hEPI (p=0.04).

T2* weighted sequence	**Median WML no. (IQR)**	**Median WML central vein no. (IQR)**	**Mean proportion of WMLs with central veins (± 2SD)**
Standard T2*	30 (14.5 – 47.5)	8.5 (3.75 - 18.5)	34.9% (±18.0%)
T2* hEPI	33.5 (20.3 – 54.8)	23 (9.3 - 44.5)	66.9% (±19.2%)
Standard SWI	26 (13 - 38)	11.5 (3 - 18)	38.5% (±19.2%)
SWI hEPI	25.5 (16 – 39.8)	15 (3.5 - 32.3)	56.8% (±25.5%)
FLAIR-SWI-1	39.5 (27 – 62.3)	10 (6.25 - 19.5)	26.9% (±12.5%)
FLAIR-SWI-2	47 (30 – 70.8)	22 (11.3 - 36)	43.4% (±15.9%)

Table 8. Median WML, WML central vein numbers and mean proportion of WMLs with central veins after using each sequence for 20 MS patients.

SD = standard deviation; IQR = interquartile range

3.3.4 Proportion of WML with central veins: comparison between sequences

The same 20 patients with MS were analysed. This data is summarised in Table 8 with ANOVA data summarised in Table 9. The proportions of WMLs with central veins were normally distributed across each sequence. There were 3 outliers but these were included in the ANOVA analysis after repeating the ANOVA with the outliers removed. Addition of the outliers resulted in two new statistically significant results but a minimal change in the mean difference between the two sequences; FLAIR-SWI-2 (mean 43.4%) and standard T2* (mean 34.9%), mean difference of 8.49% (compared to 8.48% with the outliers removed), and standard SWI (38.5%) and FLAIR-SWI-1 (26.9%), mean difference of 11.59% (compared to 11.32% with the outlier removed). These small decreases in the mean differences were not clinically significant and so the outliers remained in the analysis. Pairwise comparisons showed that a larger proportion of WMLs with central veins was seen with T2* hEPI compared to other sequences, results which were statistically significant. T2* hEPI allowed detection of a higher proportion of WMLs with central veins compared to SWI hEPI, but the difference was smaller (mean difference 10.1% (95% CI -4.7 – 24.9), p=0.5). Similar significant results were seen with SWI hEPI allowing higher proportions of WMLs with central veins compared to all other sequences except T2* hEPI. FLAIR-SWI-2 allowed detection of a higher proportion of WMLs with central veins compared to standard T2* and FLAIR-SWI-1 which were statistically significant. Figures 18 and 19 show why the overall proportions of WMLs with central veins differ between T2* hEPI and FLAIR-SWI-2, and between T2* hEPI and SWI hEPI (albeit non significantly for the latter).

T2* weighted sequence		Mean Difference between T2* scans	p value	95% CI for Difference† Lower Bound	Upper Bound
Standard T2* &	T2* hEPI	-31.9	<0.0005	-43.6	-20.3
	FLAIR-SWI-1	8.1	0.289	-2.5	18.6
	FLAIR-SWI-2	-8.5	0.039	-16.7	-0.3
	standard SWI	-3.5	1.000	-17.6	10.6
	SWI hEPI	-21.8	0.001	-36.3	-7.3
T2* hEPI &	standard T2*	31.9	<0.0005	20.3	43.6
	FLAIR-SWI-1	40.0	<0.0005	27.6	52.4
	FLAIR-SWI-2	23.4	<0.0005	12.9	34.0
	standard SWI	28.4	<0.0005	14.7	42.1
	SWI hEPI	10.1	0.500	-4.7	24.9
FLAIR-SWI-1 &	standard T2*	-8.1	0.289	-18.6	2.5
	T2* hEPI	-40.0	<0.0005	-52.4	-27.6
	FLAIR-SWI-2	-16.5	<0.0005	-24.9	-8.2
	standard SWI	-11.6	0.040	-22.8	-0.3
	SWI hEPI	-29.9	<0.0005	-45.5	-14.2

Table 9. Pairwise comparisons of the mean proportions of WMLs with central veins after using each sequence for 20 MS patients.

This table is continued on the next page. One way repeated ANOVA was used for pairwise comparisons with a Bonferroni correction. Highlighted sections show statistically significant results

T2* weighted sequence		Mean Difference between T2* scans	p value	95% CI for Difference† Lower Bound	Upper Bound
FLAIR-SWI-2 &	standard T2*	8.5	0.039	0.3	16.7
	T2* hEPI	-23.4	<0.0005	-34.0	-12.9
	FLAIR-SWI-1	16.5	<0.0005	8.2	24.9
	standard SWI	5.0	1.000	-7.3	17.2
	SWI hEPI	-13.3	0.010	-24.3	-2.4
Standard SWI &	standard T2*	3.5	1.000	-10.6	17.6
	T2* hEPI	-28.4	<0.0005	-42.1	-14.7
	FLAIR-SWI-1	11.6	0.040	0.3	22.8
	FLAIR-SWI-2	-5.0	1.000	-17.2	7.3
	SWI hEPI	-18.3	0.041	-36.1	-0.5
SWI hEPI &	standard T2*	21.8	0.001	7.3	36.3
	T2* hEPI	-10.1	0.500	-24.9	4.7
	FLAIR-SWI-1	29.9	<0.0005	14.2	45.5
	FLAIR-SWI-2	13.3	0.010	2.4	24.3
	standard SWI	18.3	0.041	0.5	36.1

Table 9 continued.

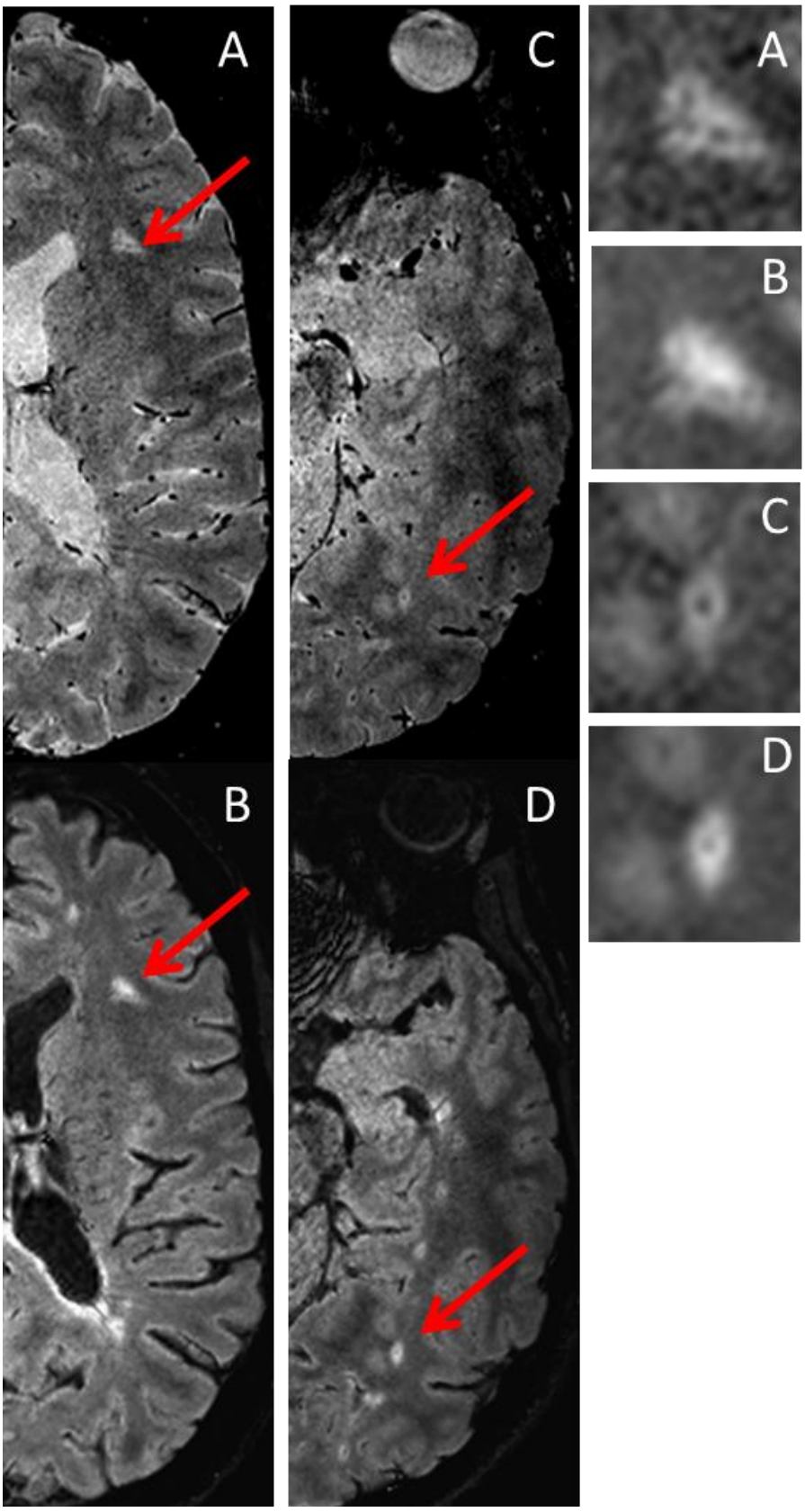

Figure 18. A comparison of T2* hEPI and FLAIR-SWI-2.

(A) and (C) are axial T2* hEPI images showing WMLs with central veins (arrows). The equivalent FLAIR-SWI-2 scans are shown in (B) and (D). The enlarged images show that for some WMLs, the central vein is easier to identify on the T2* hEPI image**.**

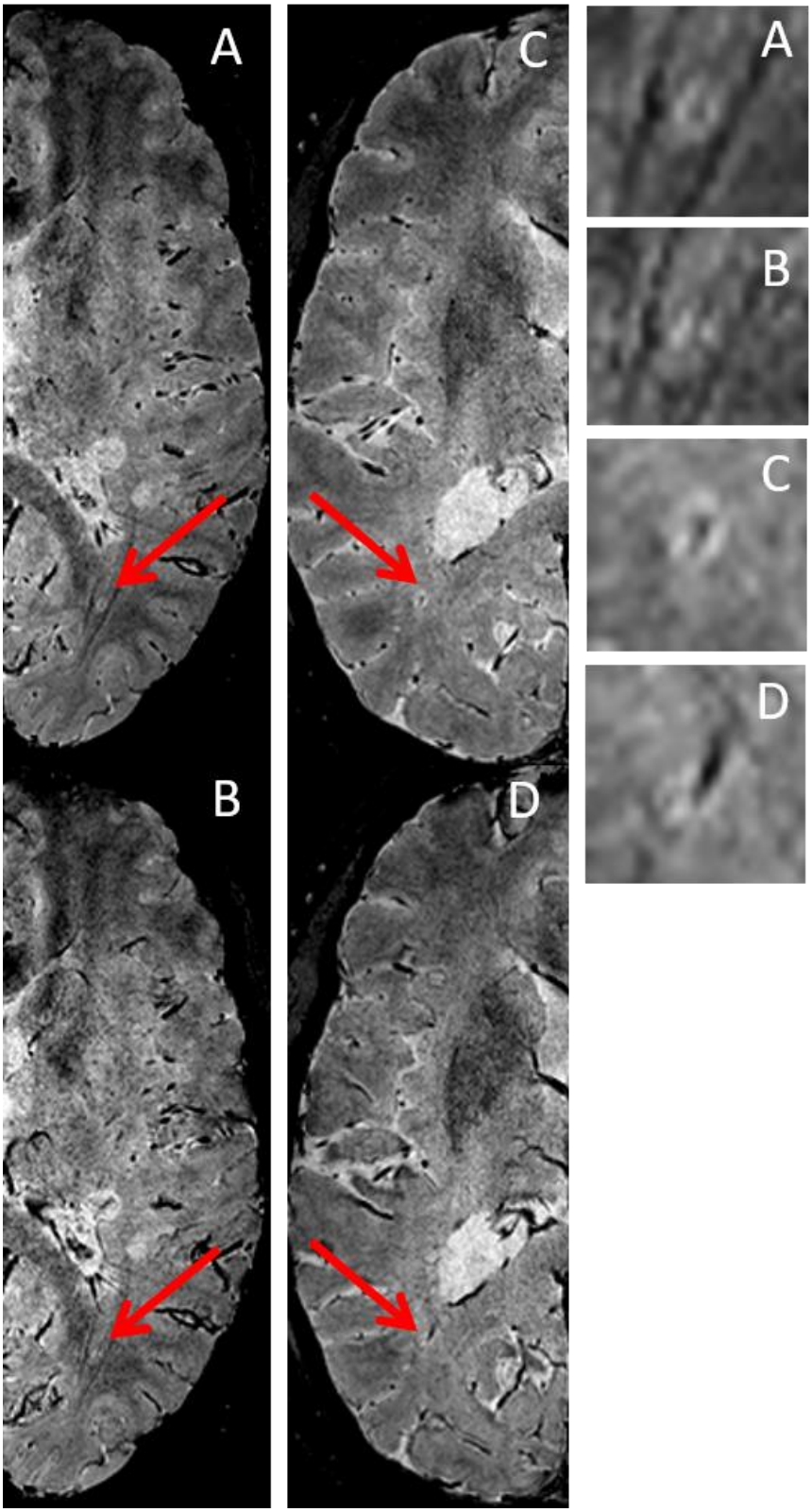

Figure 19. A comparison of T2* hEPI and SWI hEPI.

(A) and (C) are axial T2* hEPI images showing small WMLs with central veins (arrows). The equivalent SWI hEPI scans are shown in (B) and (D), with enlarged images demonstrating that for small WMLs, these could be missed on T2* hEPI, but possibly more likely to be missed (by the rater) or not be demarcated at all by the SWI hEPI sequence in the first place.

3.3.5 Blinded rater diagnoses using the central vein sign alone

Good inter-rater reproducibility was demonstrated after the practice session between the two blinded raters (MC and MS) and the unblinded rater; κ= 0.90 (95% CI 0.71 – 1), p<0.0005 and κ= 0.70 (95% CI 0.39 – 1), p=0.002 respectively.

Table 10 summarises Cohen's kappa agreements when each rater used a subset of 6 WMLs with central veins to make a diagnosis using T2* hEPI and FLAIR-SWI-2. The first rater (MC) produced a good Cohen's kappa agreement when using T2* hEPI; κ= 0.79 (95% CI 0.59 – 0.99) and when repeated a week later; κ=0.84 (95% CI 0.67 – 1.0). FLAIR-SWI-2 allowed an equally high agreement as T2* hEPI on the first attempt and was approximately the same when repeated one week later. The second rater (MS) produced a good agreement with the actual established diagnosis when using T2* hEPI; κ= 0.65 (95% CI 0.43 - 0.87) which again improved when repeated; κ= 0.73 (95% CI 0.51 - 0.95). When this rater used FLAIR-SWI-2 on their first attempt the agreement was marginally lower than the T2* hEPI values, but again improved on the second attempt. All κ coefficients were statistically significant (p<0.0005).

Sensitivities and specificities of the central vein sign with each rater and T2* hEPI and FLAIR-SWI-2 sequence are summarised in Table 11. Sensitivity was 91.3% when rater 1 used T2* hEPI, but lower with rater 2 (range 69.6 – 91.3%). Specificity was also high for both raters. FLAIR-SWI-2 produced similarly high sensitivities and specificities.

PPV, NPV and likelihood ratios were also calculated for this cohort of 39 patients, but keeping in mind that the prevalence of this sample will be higher than the

general population (23/39 patients had MS), therefore these values are not necessarily generalisable to the population.

Rater	Cohen's κ coeff	95% CI	p value	Intra-rater agreements (95% CI)
Rater 1 (MC)				
FLAIR-SWI- 2 (1st attempt)	0.79	0.59 - 0.99	< 0.0005	0.95 (0.85 - 1)
FLAIR-SWI- 2 (2nd attempt)	0.73	0.51 - 0.95	< 0.0005	
T2* hEPI (1st attempt)	0.79	0.59 - 0.99	< 0.0005	0.95 (0.85 - 1)
T2* hEPI (2nd attempt)	0.84	0.67 - 1.0	< 0.0005	
Rater 2 (MS)				
FLAIR-SWI- 2 (1st attempt)	0.61	0.39 - 0.83	< 0.0005	0.65 (0.43 - 0.87)
FLAIR-SWI- 2 (2nd attempt)	0.84	0.67 - 1.0	< 0.0005	
T2* hEPI (1st attempt)	0.65	0.43 - 0.87	< 0.0005	0.61 (0.39 - 0.83)
T2* hEPI (2nd attempt)	0.73	0.51 - 0.95	< 0.0005	

Table 10. Agreement of the diagnosis using the central vein sign alone with the established diagnosis when two raters used T2* hEPI and FLAIR-SWI-2.

Intra-rater agreements are also shown.

CI = confidence interval. Cohen's kappa coefficient was used to test agreement.

Rater	Sensitivity (95% CI)	Specificity (95% CI)	PPV (95% CI)	NPV (95% CI)	Likelihood ratio (95% CI)	
					Positive	Negative
Rater 1 (MC)						
FLAIR-SWI-2 (1st attempt)	91.3% (72 - 98.9)	87.5% (61.7 - 98.5)	91.3% (72 - 98.9)	87.5% (61.7 - 98.5)	7.3 (2 - 26.9)	0.1 (0.03 - 0.4)
FLAIR-SWI-2 (2nd attempt)	91.3% (72 - 98.9)	81.3% (54.4 - 96)	87.5% (67.6 - 97.3)	86.7% (59.5 - 98.3)	4.9 (1.7 - 13.6)	0.1 (0.03 - 0.4)
T2* hEPI (1st attempt)	91.3% (72 - 98.9)	87.5% (61.7 - 98.5)	91.3% (72 - 98.9)	87.5% (61.7 - 98.5)	7.3 (2 - 26.9)	0.1 (0.03 - 0.4)
T2* hEPI (2nd attempt)	91.3% (72 - 98.9)	93.8% (69.8 - 99.8)	95.5% (77.2 - 99.9)	88.2% (63.6 - 98.5)	14.6 (2.2 - 97.9)	0.1 (0.02 - 0.4)
Rater 2 (MS)						
FLAIR-SWI-2 (1st attempt)	65.2% (42.7 - 83.6)	100% (79.4 - 100)	100% (78.2 - 100)	66.7% (44.6 - 84.4)	NA	0.4 (0.2 - 0.61)
FLAIR-SWI-2 (2nd attempt)	91.3% (72 - 98.9)	93.8% (69.8 - 99.8)	95.5% (77.2 - 99.9)	88.2% (63.6 - 98.5)	14.6 (2.2 - 97.9)	0.1 (0.02 - 0.4)
T2* hEPI (1st attempt)	69.6% (47.1 - 86.8)	100% (79.4 - 100)	100% (79.4 - 100)	69.6% (47.1 - 86.8)	NA	0.3 (0.16 - 0.56)
T2* hEPI (2nd attempt)	91.3% (72 - 98.9)	81.3% (54.4 - 96)	87.5% (67.6 - 97.3)	86.7% (59.5 - 98.3)	4.9 (1.7 - 13.6)	0.1 (0.03 - 0.4)

Table 11. Sensitivities, specificities, predictive values and likelihood ratios of the central vein sign when two raters used T2* hEPI and FLAIR-SWI-2 to make a diagnosis of MS or SVD.

CI = confidence interval; PPV = positive predictive value; NPV = negative predictive value

3.4 Discussion

3.4.1 WML numbers

Median WML numbers were highest when using both FLAIR-SWI variations, especially with FLAIR-SWI-2. FLAIR-SWI-2 showed a statistically significant difference in WML numbers when compared to standard T2*, standard SWI and SWI hEPI. Similarly T2* hEPI allowed significantly more WMLs to be identified compared to standard SWI and SWI hEPI, with a trend towards statistical significance when compared to standard T2*. Although T2* hEPI allowed more WML detection than its equivalent SWI hEPI (median 33.5 and 25.5 respectively), their IQRs overlapped and so the population median values could be closer. Nevertheless my results go against the current literature with previous studies showing that SWI in general allows better lesion and vein detection (Soman *et al.*, 2013). There was no statistical difference in WMLs between T2* hEPI and FLAIR-SWI-2. However I cannot conclude that these two sequences are equal in detecting WMLs as the study was not powered and has a small sample size, so there is a possibility of making a type II error (obtaining a non-significant difference when an actual difference exists). Non-inferiority testing has not been performed but should be done for a future study (Ahn *et al.*, 2013).

Despite FLAIR-SWI-2 allowing more WMLs to be detected, diagnostically it was less useful as it detected fewer central veins in those lesions and as a result, a lower proportion of WMLs with central veins (see below).

3.4.2 WML central vein numbers

WML central vein numbers with T2* hEPI and FLAIR-SWI-2 showed statistically significant differences between standard T2*, FLAIR-SWI-1, standard SWI and SWI hEPI. This difference could also be clinically relevant, as these would not want to be missed, if the central vein count was being used to confirm or refute an MS diagnosis, especially in patients with low lesion numbers. The ability of T2* hEPI to detect more central veins could be due to its smaller voxel size of 0.54 x 0.54 x 0.55mm versus 0.55 x 0.55 x 1.05mm with the standard T2* and standard SWI. As described in chapter 2 smaller voxels and slice thickness will allow greater visibility of small veins and reduce partial volume effects (Gaitán *et al.*, 2014). Another reason could be the increased TE with T2* hEPI (29ms) allowing greater susceptibilty and so more likely to reveal veins. Overall T2* hEPI was also superior to both SWI sequences in detecting central veins. This goes against what may have been assumed, as SWI combines the magnitude image (which contains purely the T2* effect from internal and external inhomogeneities) and phase images, so in theory allowing greater visibility of veins. However T2* hEPI allowed better visualisation of WMLs. The central vein sign is *dependent* on identifying a WML first, and then identifying a vein within that WML.

T2* hEPI allowed a larger number of WML central veins to be detected compared to FLAIR-SWI-2 with overlapping IQRs (T2* hEPI median central veins = 23; FLAIR-SWI-2 median central veins = 22). The difference was not statistically significant and although I cannot claim that T2* hEPI is definitely equivalent to FLAIR-SWI-2, their IQRs overlap suggesting some possible similarity, but this needs to be re-tested.

3.4.3 Proportion of WMLs with central veins

In clinical practice it is the *proportion* of WMLs with central veins that will confirm the diagnosis of MS. ANOVA analysis revealed that T2* hEPI allowed the highest mean proportion of WMLs with central veins of 66.9%, followed by SWI hEPI (56.8%) and FLAIR-SWI-2 (43.4%). T2* hEPI allowed statistically significantly greater proportions of WMLs with central veins compared to all other sequences except SWI hEPI. The mean difference of 10.1% in favour of T2* compared to SWI hEPI maybe secondary to better visualisation of veins and WMLs with T2*. As FLAIR-SWI-2 detected more WMLs one would have expected, therefore, to see a higher proportion of WMLs with central veins with this sequence, but this was not the case. A possible reason could be that the use of SWI for creating FLAIR-SWI is not optimal for revealing central veins. Possible reasons include: SWI having some artefact; no gadolinium contrast was used and; some noise which could be affecting the visibility of small veins. Regardless therefore of whether the WMLs were being detected with FLAIR-SWI-2, if the veins could not be identified clearly, the clinically important *proportion* of WMLs with central veins will be lower.

3.4.4 Reasons for a difference in WML and central vein visibility

Veins appear dark on T2*-weighted images and this is re-enforced in SWI post-processing by applying a phase mask to further darken the pixels containing negative phase – typically also the veins. However the contrast of WMLs in T2* images and SWI is relatively low which may hinder their identification relative to FLAIR scans. However, veins are not visible on FLAIR scans. The perceived advantage of using a calculated FLAIR-SWI image is that WMLs are more

conspicuous on the FLAIR images, and the veins are added in as dark pixels by application of a co-registered phase mask as in SWI post-processing. However, this results in a potential confounding issue with FLAIR-SWI; on SWI, veins appear dark both from the T2* weighting *and* from the application of the phase mask. Particularly for small veins exhibiting partial volume effects, the phase mask in that pixel may not be negative overall, and so will not be 'darkened' sufficiently by application of the phase mask. Hence, that particular WML may not exhibit a central vein on FLAIR-SWI. The same lesion could still indicate a central vein on T2* and SWI – not from the phase mask but from the underlying T2*-weighting. This could result in a higher proportion of WMLs being measured with central veins on T2* and SWI, compared to FLAIR-SWI. Interestingly the initial study describing FLAIR-SWI (Grabner *et al.*, 2011) showed a smaller proportion of MS WMLs with central veins (25%), compared to most other studies to date.

Because of the potential difficulties in translating FLAIR-SWI into clinical practice, other more widely available imaging sequences like T2* or SWI may be more likely to be adopted. The potential barriers to translation were noted in section 3.1.2. Incidentally I noticed that FLAIR-SWI particularly allows infratentorial lesions to be seen more easily, and qualitatively in this instance seemed to be superior to T2* hEPI and SWI which have more noise infratentorially (see Appendix B for image). Furthermore, raters are less likely to mistake perivascular spaces on FLAIR-SWI (perivascular spaces appear the same intensity as CSF and WMLs on T2* and SWI).

T2* hEPI also allowed more WMLs and central veins to be detected compared to the equivalent SWI hEPI. There appears to be more noise in the SWI image (Borrelli *et al.*, 2015). Although the visibility of veins has been shown to improve with SWI (Chavhan *et al.*, 2009), minor artefacts in the phase data may contribute

to a lower signal to noise ratio. This in turn may result in WMLs being more difficult to see, especially small lesions (Figure 18) and so affecting the central vein count with SWI. Additionally with SWI, the orientation of the vein in relation to the direction of the magnetic field (B0) can alter the visibility of the vein (Haacke *et al.*, 2005).

3.4.5 Blinded rater diagnoses using the central vein sign alone

Two blinded raters produced good to very good agreements with the actual diagnoses when using the central vein sign using T2* and FLAIR-SWI-2. Each raters' κ coefficient when using T2* hEPI was good on their first attempt (κ= 0.79 and 0.65) and improved on their second attempt (κ= 0.84 and 0.73). FLAIR-SWI-2 produced similar results. This suggests that when these two sequences are used with a practical radiological rule, they allow the rater to make an accurate diagnosis of MS or SVD, whichever sequence is used. Overall the sensitivities of both raters was 91.3% (except for rater 2 during their first attempt when using the scans). Specificity in the most part ranged from 81 - 93%. Although some caution is needed with these results, this is further evidence that the use of WML central veins, and this particular rule of identifying a subset of WMLs with central veins can accurately identify cases of MS. However this was in a small cohort with patients who had MS or SVD and has yet to be tested with other MS mimics.

3.4.6 Limitations

My patient numbers for the primary aim were small and the study was not powered. Therefore any non-statistically significant differences in WML or central vein numbers (e.g. difference in proportions between T2* hEPI and SWI hEPI) may not

be representative of the population with a powered study. Despite this I have demonstrated significant differences in WML numbers between T2* hEPI and standard SWI and SWI hEPI. I used non-contrast FLAIR-SWI scans as a comparator. This may have reduced the ability to see central veins more clearly. Testing if gadolinium contrast enhanced FLAIR-SWI would allow better vein visibility has not been tried, but may limit its translational ability, particularly if non-contrast T2* hEPI can be performed with accurate results. Furthermore, the current debate on potential accumulation of gadolinium based contrast agents in the brain may also stem the use of contrast enhanced FLAIR-SWI (Kanda *et al.*, 2014; Radbruch *et al.*, 2015). Only I analysed all 120 T2* weighted scans (20 MS patients each having 6 scans) and so it would be important to check reproducibility of these results, perhaps with a neuroradiologist as a rater. On the same lines, the two blinded raters who made a diagnosis of MS or SVD had some experience and training in WML and central vein identification, but it would be important to see the outcome when experienced radiologists perform the same tests. Despite their limited experience however, they both produced high kappa coefficients and good agreements with the actual diagnoses. Finally, although PPV, NPV and likelihood ratios were high when identifying a subset of WMLs with central veins, the prevalence of MS in my sample was high (23/39 patients). It was higher than the general population of approximately 203 MS cases per 100,000 (Mackenzie *et al.*, 2014) or 1 per 492. Therefore the predictive values and likelihood ratios need to be calculated in a sample more representative of the population prevalence.

3.4.7 Summary

T2* hEPI and SWI hEPI allowed a higher proportion of WMLs with central veins in MS patients compared to FLAIR-SWI-2. Although FLAIR-SWI-2 can detect WMLs and central veins, translating its routine use into clinical practice maybe difficult. However using it for a specific need, for example, for looking at infratentorial lesions may prove useful. In contrast T2* hEPI does not need post-acquisition processing, so could be used immediately on existing scanners. Furthermore, using the central vein sign allowed raters to correctly diagnose MS or SVD with similarly high agreements with T2* hEPI and FLAIR-SWI-2.

Chapter 4. WML central veins in primary progressive MS at 3T

4.1 Background

4.1.1 Primary progressive MS phenotype and pathology

Approximately 15% of patients develop a progressive clinical course from the onset (PPMS) (Antel *et al.*, 2012), with a mean age of onset of 40 years compared to 30 years in RRMS (Stevenson *et al.*, 1999; Confavreux and Vukusic, 2006a). In contrast to RRMS, there is not such a striking gender difference between females and males with PPMS (1.1-1.3:1) compared to the 3:1 female: male bias in RRMS (Cottrell *et al.*, 1999). Furthermore the presenting symptoms of PPMS are different, with the majority of patients (approximately 85%) presenting with a spinal cord syndrome, about 10-15% first noting symptoms suggestive of cerebellar involvement, and a smaller number presenting with cognitive and brainstem symptoms (Cottrell *et al.*, 1999). This is in contrast to optic neuritis and brainstem syndromes as the presenting symptoms in RRMS (Confavreux and Vukusic, 2006a). Apart from minor fluctuations in symptoms, the disease course is relentlessly progressive compared to RRMS. Although the mean age of onset of PPMS is later than RRMS, it has been demonstrated that there is no difference in the age when disease progression begins. Natural history studies have shown that the time to reach constant disability in PPMS is similar to that of SPMS and is age dependent, with prior total relapse numbers and the phenotype of the initial disease having no influence on the final outcome of sustained disability (Confavreux and Vukusic, 2006a; Kremenchutzky *et al.*, 2006). It has been shown that the ages by which certain EDSS milestones are reached e.g. EDSS 4, 6, 7, differ by 2-3 years between RRMS, SPMS and PPMS (Confavreux and Vukusic, 2006a) indicating

that inflammatory activity secondary to relapses has partial influence on neurodegeneration; the pathological mode of action of accrued disability. The exception to this is frequent relapses in the first 2 years of disease onset, predicting higher probability and a shorter time interval to developing progressive MS (Scalfari *et al.,* 2010). Additionally brain atrophy and in particular GM atrophy more than WM atrophy has some influence on the risk of reaching certain EDSS milestones and long term disability in progressive MS (Fisniku *et al.,* 2008; Vidal-Jordana *et al.,* 2017).

Pathologically, actively demyelinating plaques become progressively more rare with longer disease duration (Mahad *et al.,* 2015), although there is a subset of chronic plaques that have slow, ongoing myelin and axonal degeneration at the edge of the lesion. On the whole, chronic lesions tend to shrink with time and with degeneration of axons contribute to brain atrophy, which with time leads to sustained clinical disability. PPMS patients predominately have less inflammation pathologically, but more oligodendrocyte and axonal degeneration (Lucchinetti and Bruck, 2004). However it has been shown that some progressive patients with chronic lesions show premyelinating oligodendrocyte processes that extend towards (and then become orientated parallel to) demyelinated axons, but do not actually remyelinate them (Chang *et al.,* 2002). In addition cortical demyelination has been demonstrated to be more abundant in PPMS and SPMS than in RRMS, especially evident in the subpial layers (Kutzelnigg *et al.,* 2005). Kutzelnigg et al. also found significantly more diffuse inflammatory activity (diffuse infiltration of T lymphocytes and microglial activation) in the NAWM of patients with progressive disease. Previous studies have also shown that many chronic lesions

continue to have venules within the lesion surrounded by mononuclear inflammatory cells (Revesz *et al.*, 1994).

4.1.2 Diagnosis of PPMS

As already described in chapter one, the diagnosis of PPMS can be more challenging than RRMS. Furthermore the confirmation of PPMS can be even more problematic due to the often later age of presentation (which may raise a suspicion of cervical spondylosis) and less inflammatory activity seen on MRI, with some patients having a normal brain MRI, therefore making spinal cord MRI more invaluable (Cottrell *et al.*, 1999; Miller and Leary, 2007). Also important to note is that WML topography and lesion appearance with MRI cannot differentiate PPMS from RRMS. The differential diagnosis is similar to that used when considering RRMS (Fisniku *et al.*, 2008).

Current McDonald 2010 diagnostic criteria (Polman *et al.*, 2011) for PPMS suggest one year of disease progression (either retrospectively or prospectively) along with 2 out of 3 of the following: evidence of DIS in the brain (1 or more T2 lesions in at least one characteristic area for MS); evidence of DIS in the spinal cord (2 or more T2 lesions in the cord) or; positive CSF oligoclonal bands. Again, lesions that are thought to be causing a spinal cord or brainstem syndrome, are not counted towards the DIS numbers. An updated descriptive classification has recently been proposed by the International Advisory Committee on Clinical Trials of MS (Lublin *et al.*, 2014). This further refines the subtypes of MS according to the perceived level of disease activity (as evidenced by clinical relapses and MR brain imaging) and presence of progression (supported by clinical objective signs or symptomatic progression). As an example, a diagnosis of PPMS can further be refined as: active

and with progression; active but without progression; not active but with progression and; not active and without progression. However the pathway to making the initial diagnosis remains as per the guidance of the McDonald 2010 criteria.

4.1.3 WML central veins in PPMS

To date studies evaluating the use of central veins in aiding the diagnosis of MS have included few PPMS patients (Tallantyre *et al.*, 2011; Sati *et al.*, 2012; Kilsdonk *et al.*, 2014b; Kuchling *et al.*, 2014), with the most number of patients being nine in two studies, both of which used 7T MRI (Tallantyre *et al.*, 2011; Kuchling *et al.*, 2014). Kuchling and colleagues' exploratory work used T2* FLASH on nine PPMS and nine RRMS patients, and in line with previous studies showed that the majority of WML had central veins (79% in PPMS and 69% in RRMS). There was no statistical difference between the two groups. Tallantyre et al. had nine PPMS patients amongst their cohort of 28 MS patients who were scanned using T2* GRE. They showed that 80% of MS lesions had a central vein compared to 19% of patients with ischaemic SVD, and central veins were equally common in all MS subtypes. One pilot study to date has used FLAIR* at 3T which included two PPMS patients (Sati *et al.*, 2012). Central veins were again seen but this was qualitatively assessed to describe the new scan technique. Therefore 3T MRI studies evaluating the use of WML central veins in PPMS are lacking and more data on this may be useful for this difficult to diagnose subgroup. To this end, this chapter focuses on the comparison of WML central veins in PPMS, RRMS and ischaemic SVD patients to evaluate if it continues to be useful as a diagnostic

marker, especially against patients with ischaemic SVD; a frequent imaging differential of MS, particularly in the older age group.

4.1.4 Aims and hypothesis

Aims for this chapter include: 1) to determine if there is any difference in the proportion of WMLs with central veins between RRMS and PPMS patients and; 2) confirming if the proportion of WML central veins can differentiate between PPMS and ischaemic SVD. My hypothesis is that there is no difference in the proportion of WMLs with central veins in PPMS and RRMS due to very similar pathology, and that WML central veins can differentiate between PPMS and SVD based on previous data from RRMS studies and from PPMS studies at 7T.

4.2 Methods

4.2.1 Patient selection

All patients were adults over the age of 18 who attended the MS clinics at Nottingham University Hospitals NHS Trust with a confirmed diagnosis of PPMS. Patients were scanned between April 2015 and February 2016, with the exception of 1 patient who was scanned in May 2016 for another study (STAR MS study), but data from this patient was able to be used for this chapter. All diagnoses had been confirmed by an MS neurologist and all had typical MRI findings. A proportion of patients had CSF analysis which supported the diagnosis (see Results).

4.2.2 MRI protocol

MR imaging was performed on an 3T Achieva (Philips Healthcare, Best, The Netherlands) using a 32 channel receive-only head coil. The T2* sequence and parameters used were the same as that described in chapter 2 (T2* with high EPI) as described by Sati and colleagues (Sati *et al*., 2014).

4.2.3 MRI Image analysis

Each scan was cut into 8^{ths} using the FSL toolbox (Dr Alain Pitiot) so as to achieve as much blinding as possible. The aim being to avoid identification of MS or SVD by preventing the entire brain volume from being seen at the same time.

Two raters (Dr Yasser Falah) and myself were blinded to patient and disease. I reviewed all scans of 71 patients, whilst Yasser Falah reviewed 36 scans (approximately 50%), with each scan having been divided into 8 blocks. WMLs were identified in addition to those which had central veins. The second rater (Dr Yasser Falah) was used to derive an estimate of inter-rater agreement on the proportion of WMLs with central veins for each patient. After all scans were reviewed, I re-reviewed a further 18 scans (25%) approximately two months later in order to determine intra-rater agreement. The diagnosis of MS or SVD using the central vein sign alone and the actual diagnosis was also compared. For this analysis previously published criteria of using a cut-off of >40% of WMLs with central veins as indicative of MS was used (Tallantyre *et al.*, 2011). Lesion location for every lesion on each scan was classified by myself as: 1) periventricular (PV) if one border of the WML was in contact with the ventricular surface; 2) juxtacortical (JC) if one border of the WML was in contact with cortical grey matter; 3) deep white matter (DWM) if the WML did not meet either of the above two criteria; 4)

infratentorial (IT) if the WML was located within the cerebellum or brainstem up to the foramen magnum. This classification is similar to previous studies in the literature (Barkhof *et al.*, 2003; Korteweg *et al.*, 2006).

4.2.4 Statistical analysis

For data that was normally distributed (assessed by histograms) means were calculated, with two standard deviations in parentheses. Median values were calculated with interquartile ranges in parentheses for non-normal data. For statistical differences in demographic data with normal distributions e.g. age, independent t-tests were used. For data not normally distributed e.g. disease duration, a Mann-Whitney U test was used. A one-way analysis of variance (ANOVA) with a correction for multiple comparisons was used to compare the proportion of WMLs with central veins between PPMS, RRMS and SVD patients. For dependent variables that were not normally distributed, or variables with outliers or extreme values e.g. WML numbers, proportions of WMLs with central veins by brain region, then a Kruskal-Wallis test was used for multiple comparisons. The variances in groups should be assumed to be normal unless otherwise stated (an assumption of the ANOVA). An intraclass correlation coefficient (ICC) two way random model was used to determine inter- and intra-rater absolute agreement of identifying the proportion of WMLs with central veins between two raters (myself and Yasser Falah). As these proportions were continous data, an ICC was used. Subsequently, the agreement between the two raters when using the central vein sign alone and the *actual* diagnosis of MS or SVD was determined with a Cohen's kappa coefficient (as MS or SVD were categorical data). Where possible for normally distributed data, the means and standard deviations

were used to calculate standardised effect sizes using Cohen's *d.* This measures how large a difference there is between groups e.g. the difference between the proportion of WMLs with central veins between PPMS and SVD patients.

4.3 Results

4.3.1 Demographics

Demographics for the RRMS and SVD groups are summarised in chapter 3, Table 7. Demographics for the PPMS group are summarised in Table 12. Thirty two patients with PPMS (14 females and 18 males), 23 with RRMS (13 female and 10 male) and 16 with SVD (8 female and 8 male) were used for this analysis. The mean age of the RRMS group was 41.1 years (±12.3); 50.9 years (±9.6) in the SVD group and 55.4 years (±9.5) in the PPMS group. The mean difference in age between the PPMS and SVD groups was 4.4 years (95% CI of the difference -1.4 – 10.3) which was not statistically significant (p=0.14). The mean difference in age between the PPMS and RRMS group was 14.2 years (95% CI of the difference 8.3 – 20.2) which was statistically significant (p<0.0005). Mean EDSS was 2.7 (±1.7) within the RRMS group and 5.6 (±1.3) in the PPMS group. Median disease duration (from symptom onset to the date of the T2* scan) in the RRMS group was 112 months (38 – 180) and in the PPMS group was 99 months (60.3 – 167). This difference was not statistically significant (p=0.79). Median disease duration (from date of diagnosis to the date of the T2* scan) in the RRMS cohort was 36 months (2 – 144) and 43.5 months (25 - 63) in the PPMS group, a difference which was not statistically different (p=0.93).

Patient	Age (yrs)	Gender (M/F)	MS subtype	Disease duration (mths)†	EDSS	CSF OCBs
P01	46	F	PPMS	51	6.5	ND
P02	62	M	PPMS	63	6	+
P03	44	M	PPMS	63	4	ND
P05	67	M	PPMS	168	6	+
P06	47	M	PPMS	70	6	+
P07	42	M	PPMS	97	6.5	ND
P09	45	M	PPMS	101	6.5	+
P10	56	M	PPMS	77	5.5	-
P11	62	M	PPMS	197	6.5	-
P12	49	M	PPMS	46	6	+
P14	63	F	PPMS	42	4.5	ND
P15	50	F	PPMS	173	6.5	ND
P16	54	M	PPMS	109	6	+
P17	62	M	PPMS	60	6	ND
P18	61	M	PPMS	121	3.5	+
P19	55	M	PPMS	56	7	-
P20	35	F	PPMS	116	4	+
P21	49	M	PPMS	37	6	ND
P22	73	F	PPMS	128	6.5	-
P23	58	M	PPMS	452	5.5	ND
P24	69	F	PPMS	272	7	unknown
P25	60	F	PPMS	164	5.5	+
P26	57	M	PPMS	34	2	ND
P27	50	F	PPMS	21	5.5	+
P28	37	M	PPMS	68	5	+
P29	59	F	PPMS	178	4	+
P30	64	M	PPMS	61	2	+
P31	61	F	PPMS	168	6.5	-
P32	58	F	PPMS	144	6.5	+
P33	72	F	PPMS	109	6.5	+
P34	48	F	PPMS	64	6	+
P35	57	F	PPMS	229	6.5	+

Table 12. Demographics of the PPMS patients.
†Disease duration = time from symptom onset to time of T2* scan. ND = not done

4.3.2 WML numbers; comparison between PPMS, RRMS and SVD

Results are summarised in Table 13. WML numbers for all three groups were not normally distributed after visual inspection of histograms. A Kruskal-Wallis test was used to determine if there were differences in the median WML numbers between all three groups. Median values were compared. Median WMLs in the PPMS group = 17 (8 – 44.5), RRMS group = 39 (13 - 57) and SVD group = 35 (17 – 44.8). Pairwise comparisons with a Bonferroni correction for multiple comparisons showed no statistically significant differences between the PPMS and RRMS WML numbers (p=0.07), PPMS and SVD WML numbers (p=0.21) or RRMS and SVD WML numbers (p=1.0).

The proportion of WMLs that constituted PV, DWM and JC lesions were compared between each group. The distribution of WML numbers per region were not normal and so a Kruskal-Wallis test was used. Median PV, DWM and JC WMLs for each group are summarised in Table 13. Pairwise comparisons were performed with a Bonferroni correction for multiple comparisons. The median number of WMLs that were in a PV distribution were statistically different between all three groups; PPMS and RRMS (p=0.04), PPMS and SVD (p=0.003) and RRMS and SVD (p=0.0005). There were statistically significantly more DWM lesions in the SVD group compared to the PPMS group (p=0.001), but there was no statistical difference in DWM lesion numbers between PPMS and RRMS groups (p=0.28) or between RRMS and SVD groups (p=0.19). Comparison of JC WMLs showed a statistically significant difference between RRMS and SVD groups (p=0.0005), but no difference between PPMS and SVD groups (p=0.07) or PPMS and RRMS groups (p=0.11).

Disease		WML numbers (median)	IQR	Total WMLs
PPMS	PV	5	3.3 - 8.8	290
	DWM	7	3 - 29	486
	JC	1.5	0 - 4	96
RRMS	PV	13	5 - 28	409
	DWM	18	7 - 27	522
	JC	4	1 - 8	148
SVD	PV	1	0 - 3.8	32
	DWM	31	16.8 - 44.5	549
	JC	0	0 - 1.8	12

Table 13. WML numbers per group and per brain region.

PV = periventricular; DWM = deep white matter; JC = juxtacortical; IQR = interquartile range

4.3.3 Proportion of WMLs with central veins; comparison between PPMS, RRMS and SVD

Results are summarised in Table 14. A one-way ANOVA was used to compare the proportions of WMLs with central veins between all three groups. Boxplots were used to test for outliers. There was one outlier in the RRMS group (WMLs with central veins of 25%). The ANOVA was used with and without the outlier to determine if it had any effect on the p value. Removal of the outlier did not significantly change the mean differences (and hence the p values) between groups and so the outlier was kept in for the analysis. Pairwise comparisons of each group was made, with each group having a normal distribution of values for the dependent variable (proportion of WMLs with central veins) after visually inspecting histograms. The mean proportion of WMLs with central veins in the PPMS group = 68.4% (±23.1%), RRMS group = 74.3% (±17.1%) and SVD group = 4.7%

(±4.3%) (Figure 20). The assumption of homogeneity of variances was not met, therefore a Games–Howell post hoc test was applied to compare the proportions of WMLs with central veins. There was a statistically significant difference between PPMS and SVD and RRMS and SVD groups ($p<0.0005$). The difference between the MS subtypes themselves was not statistically significant. Effect sizes show that the difference in the proportion of WMLs with central veins is large between the two MS groups and SVD group.

The proportion of WMLs with central veins in each of the PV, DWM and JC regions was also compared. These distributions were not normal so a Kruskal-Wallis test was used with multiple comparisons. Median proportions of WMLs with central veins per brain region, as well as mean ranks are summarised in Table 14. Distributions of the proportion of WMLs with central veins across groups was not similar as assessed by boxplots. Therefore, the median proportions of WMLs with central veins could not be compared directly. Instead mean ranks were compared. This revealed statistically significant differences in the proportion of WMLs with central veins in the PV and DWM regions between PPMS and SVD groups ($p=0.0005$) and RRMS and SVD groups ($p=0.0005$). The proportion of WMLs with central veins in the JC region was also statistically significantly different between PPMS and SVD groups ($p=0.001$) and between RRMS and SVD groups ($p=0.0005$). There were no central veins in any of the JC lesions in the SVD group.

Although overall RRMS patients had marginally higher proportions of WMLs with central veins in the PV, DWM and JC regions compared to PPMS patients, this did not reach statistical significance

Proportions of WMLs with central veins were also compared between males and females within each group. Within the PPMS group there was no significant difference in the mean proportions of WMLs with central veins between males and females; 73.8% in males and 61.4% in females (mean difference 12.4%, 95% CI -4 – 28.9%, p=0.13). There was no gender difference in the RRMS group either; 75.1% in males and 73.7% in females (mean difference 1.4%, 95% CI -13.9 – 16.6%, p=0.85). The RRMS group had one outlier in the female cohort, but removal of this did not affect the p value and so it was kept in the analysis. Furthermore, the proportion of WMLs with central veins did not differ significantly across both MS groups when gender was taken into account; mean difference between RRMS and PPMS females, 12.3%, 95% CI -5.7 – 30.3%, p=0.17; mean difference between RRMS and PPMS males, 1.2%, 95% CI -13.7 – 16.1%, p=0.87.

Disease		Proportion of WMLs with central veins (median, %)	IQR (%)	Proportion of WMLs with central veins (mean ranks)
PPMS	PV	80	65.7 - 100	39.9
	DWM	62.5	27.5 - 88.1	41.2
	JC	42.9	0 - 100	37.8
RRMS	PV	90	80 - 100	45.3
	DWM	68.2	51 - 85.7	46.2
	JC	66.7	28.6 - 100	47
SVD	PV	0	-	14.8
	DWM	2.8	0 - 6.3	10.9
	JC*	0	-	16.5

Disease		Mean Difference (%)	p value	95% Confidence Interval for Difference Lower Bound (%)	Upper Bound (%)	Effect size (Cohen's d)
PPMS	RRMS	-5.9	0.52	-19.0	7.1	
	SVD	63.7	0.0005	53.4	74.0	3.8
RRMS	PPMS	5.9	0.52	-7.1	19.0	0.3
	SVD	69.6	0.0005	60.4	78.8	5.6

Table 14. Proportion of WMLs with central veins in all groups per brain region (top table) and difference in mean proportion of WMLs with central veins between groups (bottom table).

PV = periventricular; DWM = deep white matter; JC = juxtacortical; IQR = interquartile range. *No JC lesions had a central vein in the SVD group, and so an IQR cannot be quoted.

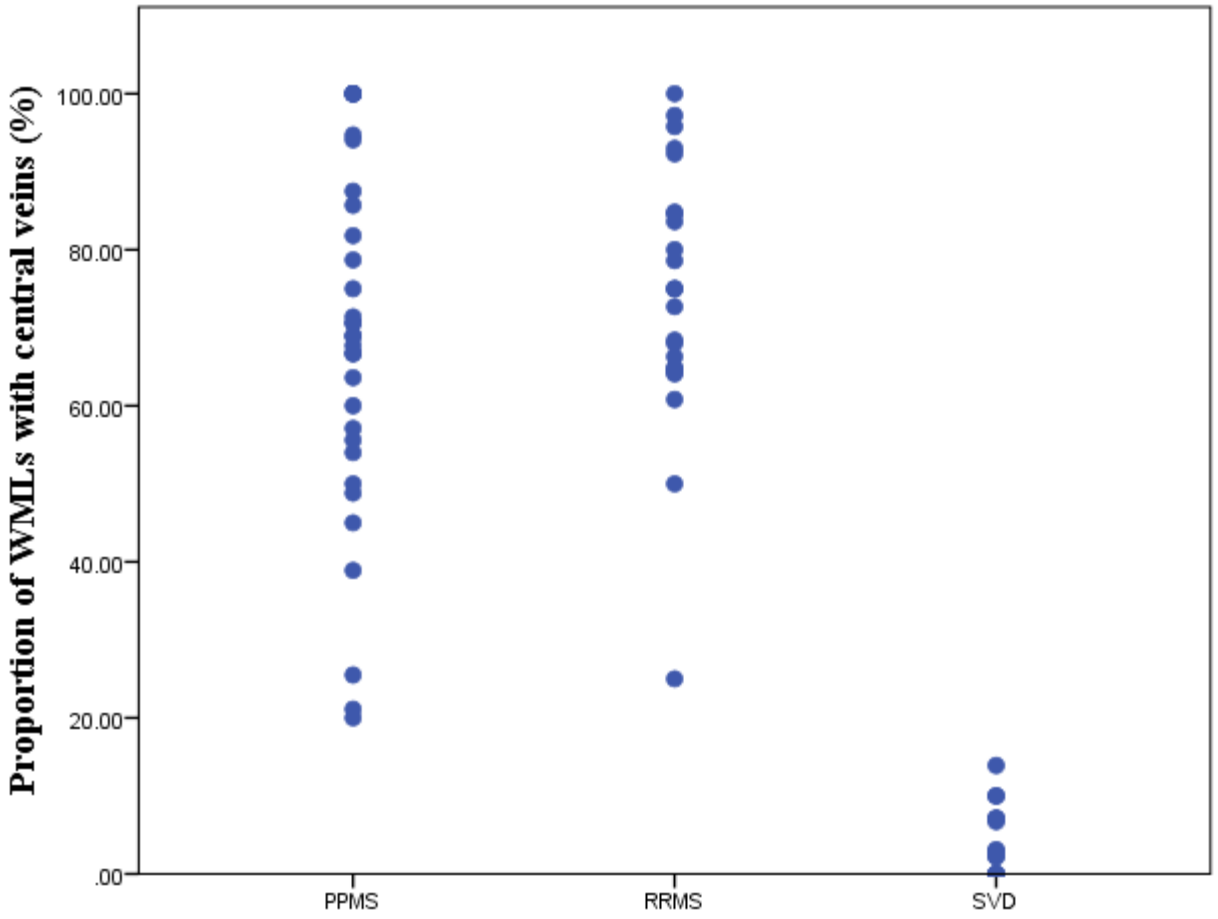

Figure 20. Proportion of WMLs with central veins in PPMS, RRMS and SVD patients.

There is a clear difference between both MS groups and the SVD cohort.

4.3.4 Rater agreements

ICC was 0.86 (95% CI 0.56 – 0.94), p<0.0005 for the two raters indicating good inter-rater agreement when the proportion of WMLs with central veins was calculated. As a consequence the level of agreement with regards to diagnosis (i.e. does each rater agree on the same diagnosis of MS or SVD) produced a Cohen's κ= 0.54 (95% CI 0.15 – 0.93), p=0.001. My intra-rater agreement was high (ICC 0.90 (95% CI 0.73 – 0.96)), p<0.0005 and the level of agreement with the diagnosis, between both attempts was κ= 0.73 (95% CI 0.38 – 1), p=0.001.

The level of agreement between the raters and the *actual* diagnosis (based on more than 40% of WMLs with central veins equalling MS), was good – very good. After assessing 36 patients (50% of the total) Cohen's kappa for Yasser Falah was κ= 0.84 (95% CI 0.54 – 1) and myself κ= 0.82 (95% CI 0.67 – 0.97) after I assessed all 71 scans. All results were statistically significant, p<0.0005.

4.4 Discussion

4.4.1 WML central veins in primary progressive MS

The first observation in this chapter is that WML central veins are present in patients with PPMS using the T2* sequence. Both MS cohorts had high proportions with a mean of 68.4% in the PPMS group and 74.3% in the RRMS patients. This is a clinically relevant finding and one which has not been shown previously at 3T. This has been shown in smaller cohorts in previous studies at 7T (Tallantyre *et al.*, 2011; Kuchling *et al.*, 2014). My findings are slightly different to the Kuchling study in that they found higher proportions in the PPMS group, which I did not demonstrate. However, the difference in proportions between the two groups did not reach statistical significance, in line with the 7T study by Kuchling et al. It is known that

progressive MS patients have similar pathology to RRMS with demyelination forming around venules (Revesz *et al.*, 1994). This can be detected on T2* weighted sequences. WML central veins could still be used to distinguish either subtype of MS from SVD (discussed later) but based on this data, cannot be used to differentiate between the two MS subtypes themselves. Further analysis of the proportion of WMLs with central veins according to brain lesion location was also performed. RRMS patients on average had more central veins in PV, DWM and JC WMLs, but the differences compared to PPMS were not statistically significant.

PPMS patients showed a marked difference in the proportion of WML central veins compared to SVD (68.4% and 4.7% respectively). The standard deviation of the PPMS group (±23.1%) at their lowest, would still indicate a large difference. Following on from this therefore, no matter where the WML was distributed, it was more likely to have a central vein in a PPMS patient than SVD.

The number of WMLs in the RRMS group was higher than in PPMS patients. This would be in keeping with previous work showing lower lesion numbers in PPMS patients compared to RRMS and SPMS patients (Thompson *et al*., 1990, Stevenson *et al*., 1999). Some suggest that lower lesion numbers in the brain in PPMS maybe secondary to lesions becoming larger over time, compared to RRMS patients who have more inflammatory activity and so accumulate more in number (Ingle *et al*., 2003). The proportions of PV, DWM and JC lesions were also similar between the RRMS and PPMS groups, but difficult to compare to previous 7T studies due to different magnetic field strengths and definition of lesion locations (Kuchling *et al*., 2014, Kilsdonk *et al*., 2014b). However the similar distributions of lesions in these areas amongst both groups fits the literature about similar lesion morphology and distributions between the two groups on MRI (Thompson *et al*., 1990). As expected

DWM lesions in the SVD group was higher (p=0.001), in keeping with the literature on the distribution of lesions in SVD (Breteler *et al*., 1994, Debette and Markus, 2010, Kilsdonk *et al*., 2014b). The high prevalence of DWM lesions in SVD was clearly demonstrated by Wen and colleagues who showed that 461 of 477 subjects with vascular risk factors (96.6%) had DWM lesions, but also that a majority of lesions were in a PV distribution (Wen and Sachdev, 2004). As SVD patients typically have high WML numbers in the DWM which can sometimes extend towards the ventricles, distinguishing this from MS can be difficult. Detecting a WML central vein in either the DWM or PV regions would be highly suggestive of MS rather than SVD (2.8% of DWM lesions in SVD patients had a central vein, in comparison to 62.5% in PPMS patients).

All MS patients were recruited from an outpatient clinical setting and reflected the usual clinical phenotype seen in specialist MS clinics. The WML numbers were lower in the PPMS group compared to RRMS (Thompson *et al*., 1990, Stevenson *et al*., 1999). The mean age of the PPMS patients at the time of scanning was higher (55.4 years) compared to the RRMS group (41.1 years). There were 3 more females in the RRMS group compared to males, but 4 more males in the PPMS group, demonstrating the known increased prevalence of PPMS in males (Cottrell *et al*., 1999).

WML central veins can be seen irrespective of gender, relapsing or primary progressive disease, age or disease duration. Four PPMS patients over the age of 65 had proportions of WMLs with central veins ranging from 21.1% - 100%. The patient with the longest disease duration from symptom onset in the PPMS cohort had the disease for 452 months, but 100% of WMLs had central veins. Similarly the PPMS patient with the longest disease duration from the date of diagnosis was

272 months and had 94.1% of WMLs with central veins. The high proportion of WMLs with central veins in the PPMS patients demonstrates that the central vein sign can also be detected regardless of lesion chronicity.

4.4.2 Rater reproducibility

Inter-rater reproducibility was high between myself and Yasser Falah. This was done to determine if each rater identified a similar proportion of WMLs with central veins per subject. However the 95% CI ranged from 0.56 – 0.94, so possibly repeating the test with other raters could have lower agreements. This is important, as a potential method for using the central vein sign for diagnosis is determining the proportion of WMLs with central veins and finding the optimum threshold or "cut-off" to make the diagnosis. Agreement between raters (in practice different radiologists) needs to be high. Counting all WMLs therefore may lead to more error – I think there is more likelihood of mistaking non-specific lesions, CSF, perivascular spaces and cortex as true demyelinating lesions. Whereas identifying a subset of WMLs and then establishing what proportion of those have central veins is more likely to be accurate, as I would envisage raters would identify the most clear/obvious lesions and so reducing the error that would come with smaller and subtle lesions. The level of agreement on whether the two raters diagnosed the same disease (based on the proportion of WMLs with central veins) was therefore only moderate (κ=0.54) with wide confidence intervals. Intra-rater reproducibility was marginally higher with a ICC of 0.90, indicating that the proportion of WMLs with central veins is similar if the same rater repeated the measurements. Agreement in the diagnosis between the first and second attempts was also good with a moderately high Cohen's kappa coefficient.

The level of agreement between each rater and the known, established diagnosis produced high kappa coefficients (above 0.8). However of the 71 patients that I reviewed, 5 were misdiagnosed (when using a threshold of >40% WMLs with central veins). Using this rule, all were classified as SVD, when in fact 4 had PPMS and 1 had RRMS. Three of these patients were diagnosed correctly by the second rater (the remaining two had not been analysed by the second rater). Reviewing these patients' clinical letters showed that the clinical diagnoses of MS was correct. PPMS patients presented with progressive pyramidal symptoms with an MRI brain or spinal scan suggestive of demyelinating lesions, two had absent oligoclonal bands and the remainder did not have CSF testing. The RRMS patient had an intermittent history of leg weakness and trigeminal neuralgia, with PV lesions and positive CSF oligoclonal bands. These five scans were re-reviewed and there was no movement artefact. The misdiagnoses could have been due to missing small WMLs, some of which had central veins, but also because not all WMLs have central veins. This may have had a larger impact on scans with a low WML load (two scans had a total of 5 and 12 WMLs).

4.4.3 Limitations

Some limitations of this study should be noted. Firstly, there was a statistically significant difference in age between the PPMS and RRMS group, with a mean difference of 14.2 years. This difference may account for the smaller proportion of WMLs with central veins in the PPMS group, possibly because with older age comes increased incidence of non-specific lesions or ischaemic WMLs (Breteler *et al*., 1994), therefore lowering the proportion of demyelinating lesions with central veins (discussed in chapter 5). Despite this possibility, the difference in the

proportion of WMLs with central veins between both MS groups was not statistically significant, with the actual mean percentage and standard deviations still indicating high proportions of WMLs with central veins.

Secondly, infratentorial lesions were not included in the analysis. I could detect very few (3 in PPMS, 2 in RRMS and 3 in SVD groups). This could have been because of limitations of T2* in detecting lesions in this area (more noise and sometimes it is difficult to delineate lesions from the CSF in between the folia of the cerebellum, which is also hyperintense). Brainstem lesions are qualitatively easier to detect than the cerebellum, but this needs further study. FLAIR-SWI or FLAIR* maybe a better option for infratentorial lesions as described in chapter 3. Because of the low numbers of infratentorial lesions, any differences in lesions or central veins would be based on insignificant numbers and so I excluded these. Despite this however, the proportion of WMLs with central veins in the supratentorial brain was high for both MS groups, and so exclusion of infratentorial lesions may not dramatically affect the overall proportion of WMLs with central veins or the ability to differentiate MS from SVD.

Thirdly, I allocated WMLs as PV, DWM and JC according to previously published criteria. Other studies will define lesion location differently (Caucheteux *et al*., 2015) and if repeated may have different proportions.

Finally, although each brain scan was divided into 8 blocks, this was not fully blinded. Although SVD patients can have PV and JC lesions, the fact that lesion location could be determined, may have introduced bias when deciding if a vein was present or not, especially in equivocal cases. To improve this for the future, one method would be to identify WMLs on FLAIR and then determine if these

lesions have veins. However, this still does not completely remove bias as lesion location would then be seen on FLAIR scans, and as such, raters may have already made a judgment on the diagnosis of MS or non-MS.

4.4.4 Summary

WML central veins are present in PPMS patients in as high proportions as those found in RRMS. These can be identified at 3T using non-contrast T2* weighted imaging. Although a small proportion of ischaemic SVD lesions have central veins, the *difference* in proportions between PPMS and SVD patients is significant, irrespective of PV, DWM or JC location and may be helpful in the clinical setting when there is difficulty in differentiating the two conditions, clinically or radiologically.

Chapter 5. Vascular risk factors and their influence on WML central veins in MS

5.1 Background

5.1.1 Brain WMLs and vascular risk factors

The prevalence of brain WMLs increases with age (Wardlaw *et al.*, 2013). One MRI study demonstrated that the number of PV and subcortical WMLs increased with age and was more common in women, especially in the frontal lobes (de Leeuw *et al.*, 2001). For both sexes, cardiovascular risk factors also increase with age (Rich-Edwards *et al.*, 1995; Jousilahti *et al.*, 1999). Some of these risk factors have been associated with a higher number of brain WMLs and total lesion volume. Patients with diabetes mellitus have a statistically significantly higher number and volumes of WMLs when scanned at 1.5T, compared to non-diabetic patients (Lucatelli *et al.*, 2015). These results have been reproduced in patients with type 2 diabetes and arterial disease; such patients having higher rates of brain atrophy and more WM hyperintensities than patients with arterial disease without diabetes (Tiehuis *et al.*, 2008). Numerous studies have also shown that smoking tobacco leads to small vessel disease (OR 2.81, CI 1.59-3.63) which can be detected on MRI (Staals *et al.*, 2014), and continued smoking can cause progression of WM hyperintensities (Power *et al.*, 2015). Furthermore, Gons et al. demonstrated that smoking is associated with disruption of NAWM as evidenced by an increase in mean diffusivity using diffusion tensor imaging (DTI). They also showed that current and previous smokers had higher WML volumes compared to patients who had never smoked (Gons *et al.*, 2011). Similarly hypertension is well known to contribute to WMLs (Murray *et al.*, 2005). Breteler and colleagues found that systolic blood pressure was associated with more WMLs in patients aged between

65-74 years (Breteler *et al.*, 1994). The duration of hypertension can also affect WML prevalence. Patients aged between 60-70 years, who were hypertensive for more than 20 years, had a relative risk of subcortical and PV WMLs (detected on 1.5T PD and T2 imaging) of 24.3 and 15.8 respectively (de Leeuw *et al.*, 2002). Additionally patients who have had treatment for their hypertension had a lower relative risk compared to those who were poorly controlled (3.3 and 8.4 respectively). Obesity and hyperlipidaemia and the prevalence of WMLs have also been evaluated but both with mixed results. One study investigating WMLs on CT in elderly patients at ages 85 or 88 found higher lesion loads in those who had a high body mass index (BMI) at age 70. This was even higher for obese women (Gustafson *et al.*, 2004). Similar results were seen in MRI studies, with higher BMIs associated with higher WML numbers in type 2 diabetic patients compared to patients with normal BMIs (Anan *et al.*, 2009). In a large prospective follow up study, total cholesterol levels once adjusted for sex and age were associated with WMLs in subjects aged between 65-74 (Breteler *et al.*, 1994). Interestingly, patients with the rare condition of familial hypercholesterolaemia, who have extremely high levels of total cholesterol, coronary and carotid artery disease, do not have a significant difference in the number of WMLs on FLAIR imaging at 1.5 or 3T MRI compared to healthy controls (Soljanlahti *et al.*, 2005; Schmitz *et al.*, 2007).

The majority of late onset MS patients (usually considered when diagnosed after the age of 50) have PPMS and tend to be male (Kis *et al.*, 2008). This later age at diagnosis is coupled with an increased risk of WMLs due to increasing age, male gender and an increased likelihood of cardiovascular risk factors. The PPMS

subgroup therefore maybe more of a challenge to differentiate from other neurological diseases, including small vessel ischaemia (Cottrell *et al.*, 1999).

5.1.2 Ischaemic SVD WMLs have fewer central veins

To date five studies using 3T and 7T MRI have compared the proportion of WMLs with central veins in MS, to patients with SVD (Lummel *et al.*, 2011; Tallantyre *et al.*, 2011; Mistry *et al.*, 2013; Kilsdonk *et al.*, 2014b; Mistry *et al.*, 2016). Four of the five studies (the exception being that by Lummel et al. in 2011) have shown statistically significant differences between the proportion of WMLs with central veins between the MS and SVD groups, ranging from 8 - 47% in SVD patients and 72 - 97% in the MS groups.

5.1.3 Aims and hypothesis

I wanted to determine if RRMS and PPMS patients with specific vascular risk factors have a lower proportion of WMLs with central veins. The hypothesis being that some of the WMLs will be caused by ischaemic SVD, which do not have central veins, so leading to a reduction in the proportion of WMLs with central veins. This may explain the fact that, in the majority of MS patients, some WMLs do not have central veins. Hence the presence of vascular risk factors in this group may need to be considered if WML central veins are to be used as a biomarker. As the evidence for WMLs in patients with vascular risk factors is already in the literature, I did not test if vascular risk factors in my cohort of 16 SVD patients affected WML numbers, as these numbers are small. Instead I tested if this finding could be found in MS patients only.

5.2 Methods

5.2.1 Patient selection, MRI protocol and image analysis

The same cohort of PPMS and RRMS patients from chapter 4 were used for this analysis. T2* with high EPI factor (parameters described in chapter 2) was used to determine the number of total WMLs, and subsequently, how many of these had central veins to calculate a proportion. The proportions of WMLs with central veins were already determined after the scans had been analysed by myself for chapter 4. The criteria for a WML or central vein remains the same as previously described. The analysis was performed with as much blinding as possible as each scan was cut into 8^{ths} as described in chapter 4.

5.2.2 Identification of vascular risk factors

The presence or absence of six different vascular risk factors and disease duration was determined for each patient. These included; age, hypertension, hypercholesterolaemia, diabetes mellitus (type 1 or 2), smoking status and BMI. Patients were asked if they had been given a diagnosis of hypertension or were being treated with anti-hypertensives specifically for hypertension. They were asked if they were taking a statin or had been advised to alter their diet for hypercholesterolaemia. The use of any medication for diabetes mellitus was noted and each patient was asked if they had been diagnosed with diabetes. If they did not know about any of these diagnoses their clinical letters were reviewed to check. They were also asked if they were a current, ex- or non-smoker in addition to their approximate weight and height. BMI was calculated by dividing weight (kilograms) by height (metres squared). Purely the presence or absence of the risk factor was noted and for example, if the patient was not on treatment for

hypertension, hypercholesterolaemia or diabetes or if they had not been informed by a health professional that they were being treated conservatively (e.g. diet control for diabetes), this was implied as not having the risk factor. In addition to the six vascular risk factors, disease duration was also used in the analysis. This was determined as the time from symptom onset till the date of the T2* scan, as well as from the date of MS diagnosis till the date of the T2* scan.

5.2.3 Statistical analysis

Means and two standard deviations in parentheses were used for normally distributed data. For non-normal data, medians and interquartile ranges in parentheses are used. Multiple linear regression was used to determine any associations with each vascular risk factor (independent variables) and the proportion of WMLs with central veins (dependent variable). For dependent variables that were not normally distributed, a negative binomial regression was used instead. Statistical significance was set at $p<0.05$. Statistical analyses were performed using IBM SPSS 22.

5.3 Results

5.3.1 Demographics

Thirty two patients with PPMS (14 females and 18 males) and 23 with RRMS (13 female and 10 male) were used for this analysis. Basic demographics for each group are described in chapters 3 and 4. The mean age of the group as a whole was 49.4 years (±12.8). Median disease duration for all patients, taken from symptom onset to the date of the T2* scan was 101 months (51 – 168) and from the date of diagnosis was 43 months (12 – 84).

5.3.2 Vascular risk factors and the proportion of WMLs with central veins

Results are summarised in Table 15. Multiple linear regression was originally planned to predict the proportion of WMLs with central veins based on age, disease duration, hypertension, hypercholesterolaemia, diabetes, smoking status and BMI. However of the 55 MS cases, only two had diabetes, six had hypertension and six had hypercholesterolaemia. When the regression was originally run, there was multicollinearity between hypertension and hypercholesterolaemia (Pearson's corrleation 0.81) and a tolerance value 0.195 (hypercholesterolaemia). In addition there was one case (P22, PPMS) that caused a relatively high Cook's value compared to the rest of the cohort. Therefore hypertension and hypercholesterolaemia were removed as covariates from the analysis because of multicollinearity and a small number of positive cases. Diabetes was removed because of only two positive cases. Therefore for the final analysis, multiple regression was used to predict the proportion of WMLs with central veins based on age, disease duration (from symptom onset and from date of diagnosis), smoking status and BMI on 55 patients. There was no evidence of multicollinearity between these covariates.

This produced an R^2 of 0.14 and adjusted R^2 of 0.06 (6%), p=0.17, when these covariates were used in the regression model. With all other dependent variables held constant, being a current or ex-smoker resulted in 9.6% less WMLs with central veins compared to being a never smoker, but this was not statistically significant (p=0.09). Regression coefficients for age, disease duration and BMI all showed small changes in the proportion of WMLs with central veins, but these were all statistically non significant.

Vascular risk factor	Regression coefficient (B)	95% CI for coefficient	p value
Disease duration (from symptom onset)	0.03	-0.07 - 0.1	0.57
Disease duration (from date of diagnosis)	0.02	-0.1 - 0.1	0.8
Age	-0.4	-0.9 - 0.05	0.08
BMI	0.5	-1.2 - 2.1	0.58
Smoking*	-9.6	-20.9 - 1.7	0.09

Table 15. Multiple regression to predict the effect of different vascular risk factors on the proportion of WMLs with central veins in MS patients.

*Coefficient for the smoking variable represents the difference in the proportion of WMLs with central veins between current/ex-smokers and never smokers.

5.3.3 Vascular risk factors and WML numbers

Results are summarised in Table 16. Negative binomial regression revealed no clinically significant changes in WML numbers in 55 MS patients when age, BMI or disease duration were used as covariates. Similarly, non-smokers compared to smokers showed no statistical or clinical difference in the WML numbers. Odds ratios for all continuous covariates ranged from 0.93 – 1, with confidence intervals for the odds ratios being marginally over 1, indicating no change in the odds after a change of one unit of a covariate.

Vascular risk factor	Regression coefficient (B)	95% CI for regression coefficient	p value	odds ratio (Exp(B))	95% CI for odds ratio
Disease duration (from symptom onset)	-0.005	-0.009 - 0	0.04	0.995	0.99 - 1
Disease duration (from date of diagnosis)	0.007	0 - 0.01	0.04	1.007	1 - 1.01
Age	-0.004	-0.03 - 0.02	0.74	0.996	0.97 - 1.02
BMI	-0.07	-0.15 - 0.02	0.11	0.936	0.86 - 1.02
Never smoker*	-0.22	-0.77 - 0.34	0.44	0.806	0.46 - 1.4

Table 16. Negative binomial regression to predict the effect of covariates on WML numbers in MS patients

*Coefficient for the smoking variable represents the difference in the number of WMLs between never smokers and current/ex-smokers

5.4 Discussion

The influence of vascular risk factors on the proportion of WMLs with central veins in MS patients has not been studied before. Previous studies show that numerous vascular risk factors impact lesion load and brain atrophy (Zivadinov *et al.*, 2009; Kappus *et al.*, 2016) and disability progression (Marrie *et al.*, 2010) in patients with MS. The number of WMLs and proportion of WMLs with central veins, do not appear to be heavily influenced by the presence of specific vascular risk factors used for the analysis in this chapter, except for a small influence of smoking on the proportion of WMLs with central veins. Smoking is consistently a positive contributor to WMLs in patients with MS (Zivadinov *et al.*, 2009) and non-MS (Dickie *et al.*, 2016). Multiple regression analysis showed that being a current or ex-smoker had some influence on the proportion of WMLs with central veins, having approximately 9.6% less than never smokers.

The other risk factors studied (age, disease duration and BMI) showed minor influences on the proportions of WMLs with central veins, which were not statistically significant. The regression coefficients were small for these variables and confidence intervals included zero. As such, any effect will not be clinically significant and would not change the clinical applicability of the central vein sign based on this sample. However, the limitations of this chapter need to be taken into account (discussed later).

From the standpoint of WML central veins as an imaging biomarker, the lack of vascular risk factors significantly influencing WML numbers and the proportion of WMLs with central veins is useful. This is because, as it stands, we could apply the central vein sign to any patient with suspected MS without having to take into

account the frequency or type of vascular risk factor. I would envisage the central vein sign being as simple as possible to be clinically useful, and independent of factors that would require altering the diagnostic threshold. However, as this analysis was performed on a small number of MS patients, some of whom had no risk factors, this should be repeated in larger groups.

A possible reason why my results are not in keeping with previous studies evaluating WMLs and vascular risk factors is that most other studies look for change in WML load as opposed to number (de Leeuw *et al.*, 2001; Zivadinov *et al.*, 2009; Kappus *et al.*, 2016). This will take into account existing, enlarging lesions, rather than individual new lesions. Another possible reason could be the specific T2* imaging that I used to identify WMLs. This does not delineate WMLs as distinctly as FLAIR or T2 imaging. WMLs close to the CSF or grey matter could be missed and infratentorial lesions are not well demarcated with T2*.

It is perhaps not surprising that vascular risk factors are not contributing significantly to these two measures. One possible reason is that the inflammatory nature of MS is so profound that the majority of WMLs are in fact inflammatory demyelination, and any small numbers of WMLs due to ischaemia are non-significant. Although, as described previously, there are studies that clearly show smoking as a contributor to WMLs in the normal population, others demonstrate small correlations with WMLs (Fukuda and Kitani, 1996). Fukuda et al. demonstrated that age and smoking duration had a small influence on periventricular WM hyperintensities, with regression coefficients of 0.374 and 0.128 respectively. A more recent study with a large cohort of patients with vascular risk factors demonstrated that the contribution of risk factors to the total WML variance ranged between 0.1 – 2% only, with smoking and hypertension

being the biggest predictors of the variance (Staals *et al.*, 2014). The contribution of various vascular risk factors as described may well be small, and at best, modest in such age groups (mean age 72 and 74 in both cohorts in the Wardlaw study and 78 - 79 in the Fukuda study) without MS. Therefore, the relatively small correlations and regression coefficients from my cohort of MS patients who are younger, and have a mixture of MS WMLs and possibly ischaemic WMLs, is perhaps not so surprising.

5.4.1 Limitations

Firstly, my sample size for this chapter was small, totalling 55 patients. Any statistically non-significant results may not be negative if more patients are analysed. Secondly, there would have been some error in data acquisition for the vascular risk factors. For example, we asked patients and/or checked their clinical letters for hypertension, hypercholesterolaemia etc. As we did not measure the actual values it is possible these patients may have had a subclinical risk factor. Additionally, I did not take into account all risk factors, such as previous stroke or myocardial infarction. However, I felt as this was exploratory in nature, studying a few risk factors would be the first step to determine if there was any influence on the proportion of WMLs with central veins. There may also have been error in the dependent variable (WML number and proportion of WMLs with central veins) as the identification, especially of small lesions and veins is subjective.

There were only six patients with hypertension, six with hypercholesterolaemia and two with diabetes. Furthermore, when running the regression, hypertension and hypercholesterolaemia demonstrated multicollinearity (indicating that the two variables correlated with each other). This makes it difficult to elucidate which

variable is contributing to the dependent variable. Hypertension and hypercholesterolaemia were therefore removed from the analysis, so further reducing the number of risk factors studied. The diabetes covariate was also removed as only two patients would have been used for the regression. An alternative approach to removing vascular risk factors which are small in number, maybe exploring the influence of having *any* vascular risk factor and grouping them together for the regression.

5.4.2 Summary

The vascular risk factors studied show no significant influence on the proportion of WMLs with central veins in patients with confirmed MS, with the exception of being a current or ex-smoker, which appears to lower the proportion of WMLs with central veins compared to never smokers. The central vein sign and the presence of vascular risk factors needs to be tested in the future in patients with suspected MS, along with additional vascular risk factors and larger patient cohorts.

Chapter 6. Refining the diagnostic rule with statistical modelling

6.1 Background

6.1.1 Misinterpretation of MRI in MS

The National Institutes of Health Biomarkers Definitions Working Group define a biomarker as "a characteristic that is objectively measured and evaluated as an indicator of normal biological processes, pathogenic processes, or pharmacologic responses to a therapeutic intervention" (Biomarkers Definitions Working, 2001). The MRI WML central vein sign has been increasingly investigated as a potential biomarker, but like with all biomarkers, misinterpretation of MRI can cause incorrect diagnoses. Over reliance on MRI, in part, leads to misinterpretation and misdiagnoses (Solomon and Weinshenker, 2013). In addition to this, misapplication of the McDonald criteria can also contribute to the error rate (Selchen *et al.*, 2012).

To date there has only been one prospective study at 7T, using the central vein sign in patients with diagnostic uncertainty (Mistry *et al.*, 2013). The diagnosis of MS or non-MS was then predicted based on the proportion of WMLs with central veins, using a threshold of more than 40% for the diagnosis of MS. Of 22 patients who had received a diagnosis after a median follow up time of 26 months, 13 had been predicted as having MS and 9 having SVD. All MS patients had more than 40% of WMLs with central veins, and all SVD patients had less than 40% of WMLs with central veins, resulting in a 100% positive predictive value.

In 2010, The International Panel on Diagnosis of MS produced revised diagnostic criteria (Polman *et al.*, 2011) predicting the likelihood of developing MS, after a

typical CIS, however alternate diagnoses need to be excluded first. The McDonald criteria however were designed, in part, incorporating clinical trial studies performed at tertiary centres with patients presenting with typical symptoms for CIS; they did not include patients with *possible* MS, and so should not be used if the presenting syndrome is not typical for demyelination. However at times such caveats are not remembered (Selchen *et al.*, 2012). A diagnostic 'rule' for using the central vein sign needs to be refined before it can be used in the clinical setting. A diagnostic rule based on identifying a proportion of WMLs and whether a subset of these have central veins, or the addition of the WML and its brain location as a variable needs to be determined.

WMLs in the brain in MS have a predilection for the periventricular, infratentorial, callosal and juxtacortical/subcortical areas (Ceccarelli *et al.*, 2008; Filli *et al.*, 2012). Periventricular lesions perpendicular to the ventricles or 'Dawson's fingers' are highly suggestive of MS (Dawson, 1916). In ischaemic SVD, a very common MRI mimic of MS in clinical practice, DWM and subcortical lesions are the most common areas for WMLs (Lambert *et al.*, 2016), although PV lesions can also frequently occur, often described as 'caps' or 'rims' (Kim *et al.*, 2008). WMLs in the DWM and JC areas are more likely to cause diagnostic confusion between MS and SVD (Kilsdonk *et al.*, 2014b). The density of veins around the ventricular system is high, because of deep medullary veins draining into it (Friedman, 1997), and so the chance of SVD WMLs in the PV area having a central vein by chance is also high (Tallantyre *et al.*, 2011; Kilsdonk *et al.*, 2014b). Tallantyre et al. (2011) demonstrated this, showing that although MS lesions in these three locations were likely to have a central vein, a high proportion of non-MS and SVD PV lesions also had central veins, with WMLs in DWM and JC less commonly having central veins.

Similar findings in DWM and subcortical lesions have been reproduced at 3 and 7T using FLAIR* (Kilsdonk *et al.,* 2014b; Solomon *et al.,* 2016). The study by Kilsdonk et al. showed that the specificity of a DWM lesion being from an MS patient was 94% if the lesion had a central vein (sensitivity 81%), and 69% if DWM lesion numbers alone were taken into account. This study had to ensure that 64% of the DWM lesions had a central vein to achieve this specificity however. Solomon et al. showed an OR of 5.21 of an MRI being from an MS patient if the DWM or subcortical lesion had a central vein.

Therefore practical diagnostic criteria to specifically differentiate MS from SVD would envisage using DWM lesions at the very least, with the presence of central veins in these lesions representing MS. The absolute numbers and proportions needed are what I aim to determine in this chapter.

6.1.2 Aims and hypothesis

The primary aim of this chapter is to determine the optimal proportion of WMLs with central veins, so that a clinically applicable diagnostic threshold can be devised. This will be based on statistical modelling which will determine the typical distribution of WML numbers, proportion of WMLs with central veins and brain location of WMLs with central veins in a group of MS patients ('derivation cohort') that I have scanned previously. Simulated patients will then be replicated with these same distributions. A diagnostic rule will then be applied to these simulated patients and sensitivities and specificities for the diagnosis of MS will be calculated for each diagnostic rule. I hypothesized that 1) one of the biggest discriminators of MS from SVD could be purely identifying DWM lesions with central veins and 2)

identifying a certain proportion of WMLs with central veins, irrespective of location could also distinguish the two conditions.

6.2 Methods

6.2.1 Patient sample to determine typical distributions

Seventy one patients were used (32 PPMS, 23 RRMS, 16 SVD) to calculate the typical WML numbers, WML central vein numbers and proportion of WMLs with central veins. These patients will collectively be described as the 'derivation cohort'. These patients had already been recruited for previous studies in this thesis. These patients all had MS, confirmed by a neurologist with a subspecialist interest in MS, all diagnosed in a typical neuroscience centre running an MS service. The SVD patients were diagnosed as described in chapter 3.

6.2.2 MRI protocol

Each patient already had a 3T T2* scan with high EPI factor, as described in previous chapters using a Philips Healthcare MRI scanner.

6.2.3 Image analysis

The PPMS, RRMS and SVD scans which had already been divided into 8 blocks for chapter 4 were used. WMLs and central veins were identified using the same criteria as described in chapter 2 (for the definition of a WML) and chapter 4 (for definitions of PV, DWM and JC). I identified all WMLs and central veins, for all 71 patients, blinded to the subtype of MS or SVD. Once all WMLs, central veins and allocation of WMLs to different brain regions was finalised, I was unblinded.

6.2.4 Statistical analysis

Statistical modelling was used with the guidance of Dr Chris Tench. Although from the derivation cohort, I can determine a typical distribution of WML numbers, WML central vein numbers and proportion of WMLs with central veins of PPMS, RRMS and SVD patients, the numbers are small. The idea here therefore was to simulate a larger number of MS and SVD patients ('simulated cohort') based on the distributions of the derivation cohort who have been diagnosed at our centre. Data was plotted on histograms and fitted with a distribution curve for each disease subtype using the statistical software programme R, version 3.3.1 (https://www.r-project.org/). Typical anatomical distributions for each patient i.e. number of PV, DWM and JC lesions and proportion of these with central veins were also plotted for each subtype. The optimum distribution curve that fitted the derivation cohort was a gamma distribution (a distribution with values that are always positive and skewed – like the presence of WMLs or central veins) (Figure 21).

Simulated PPMS, RRMS and SVD patients were then replicated 10,000 times based on the distributions of WMLs and WMLs with central veins from the derivation cohort (Figure 21). Diagnostic rules (see section 6.2.5) were applied to these simulated patients which determined the number of correct diagnoses of MS (true positives) and number of incorrect diagnoses of MS (false positives). Sensitivities and specificities with 95% confidence intervals were calculated for each different rule. Sensitivity is defined as the probability of the test identifying the disease in those who have the disease; (True Positives / True Positives + False Negatives) x 100; specificity is defined as the probability of the test identifying those without the disease in those who truly do not have the disease; (True Negatives / True Negatives + False Positives) x 100 (Motulsky, 1995).

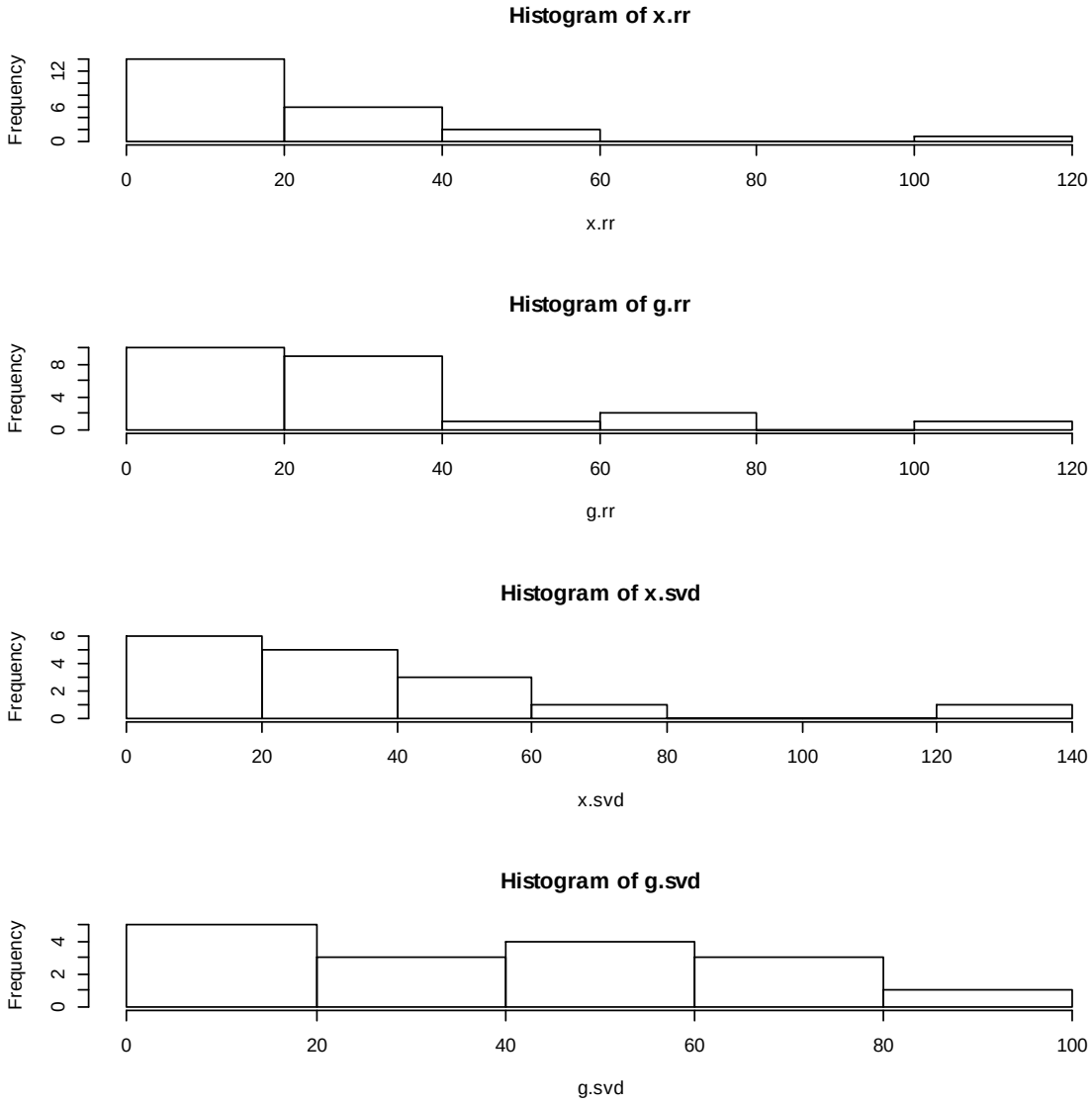

Figure 21. Example of gamma distributions fitted to the derivation cohort, with the same distributions then simulated for the replication cohort of patients.

This was done for both MS and SVD patients. Top histogram; DWM lesion distribution in the RRMS patients that I identified (derivation cohort), 2nd histogram; DWM lesion distribution in simulated RRMS patients, 3rd histogram; DWM lesion distribution in the SVD patients that I identified (derivation cohort), 4th histogram; DWM lesion distribution in simulated SVD patients.

6.2.5 Determining a practical clinical rule

For the purposes of this study the diagnostic rule was developed to include WML location in the supratentorial brain only, WML number and the proportion of these with central veins. For one diagnostic rule I therefore chose to use DWM lesions only, and determined how many of these e.g. 4, 6, 10, needed to be identified, and what proportion of those identified needed to have central veins to establish an MS diagnosis e.g. identify 6 WMLs and if 2 have centrals veins the diagnosis is MS. For the second diagnostic rule I tested if any WML irrespective of brain location could be used, and what proportion of these needed central veins to make a diagnosis of MS.

6.3 Results

6.3.1 Demographics

Basic demographics for each MS group are described in chapters 3 and 4.

6.3.2 Optimum threshold for diagnosing RRMS using DWM lesions

Distributions for WML numbers, central vein numbers and proportions of WMLs with central veins for the derivation groups are shown in Appendix C. Results for the simulated RRMS cohort and proportion of DWM lesions with central veins needed for a diagnosis of MS are summarised in Table 17. The number of simulated SVD patients misdiagnosed as RRMS are summarised in Table 18. As the number of DWM lesions needed to be identified increases e.g. from 4 to 6 to 8, the number of simulated patients that have that number of WMLs to identify reduces (the number of patients suitable for the test). The proportion of those correctly

diagnosed as RRMS also reduces as the number of central veins that are needed increases (sensitivity column).

Different thresholds for diagnosis can be used as a "cut-off" depending on how many DWM lesions a rater would initially identify. Identifying 4 DWM lesions and 2 central veins, would allow a sensitivity of 91.2% and specificity of 99.5%. Identifying 6 DWM lesions and 2 central veins would produce a sensitivity of 98.7% and specificity of 99%. However although this specificity is high, the raw numbers would still allow approximately 98/9699 patients to be incorrectly diagnosed as having RRMS. So, identifying 6 DWM lesions and 3 central veins although would lower the sensitivity to 92.9%, would increase specificity to 100% (potentially 2/9699 being incorrectly diagnosed as RRMS) and be applicable to 81% of patients. Increasing the number of DWM lesions identified to 8 and 10 suggests that 4 central veins would allow sensitivities of 94.4% and 98.8% respectively and specificities of 99.9% and 100% respectively (Figure 22) Although increasing the DWM lesions identified to 15 or 20 and still identifying 4 central veins would allow sensitivities and specificities above 99%, the fact that more DWM lesions need to be identified, results in less patients being suitable for the test (approximately 55% with 15 lesions and 42-43% with 20 lesions).

Total DWM lesions identified	No. WML central veins	No. pts suitable for test (RRMS)†	No. correctly diagnosed as RRMS‡	Proportion correctly diagnosed as RRMS (%) (sensitivity)
4	1	8868	8781	99
4	2	8847	8107	91.6
4	3	8847	5819	65.7
4	4	8864	2152	24.2
6	1	8212	8208	99.9
6	2	8158	8060	98.7
6	3	8164	7586	92.9
6	4	8161	6136	75.1
6	5	8196	3422	41.7
6	6	8167	970	11.8
8	1	7604	7604	100
8	2	7509	7499	99.8
8	3	7531	7439	98.7
8	4	7575	7153	94.4
8	5	7524	6085	80.8
8	6	7556	4162	55
8	7	7596	1907	25.1
8	8	7465	419	5.6

Table 17. Continued on next page.

Total DWM lesions identified	No. WML central veins	No. pts suitable for test (RRMS)†	No. correctly diagnosed as RRMS‡	Proportion correctly diagnosed as RRMS (%) (sensitivity)
10	1	7012	7012	100
10	2	6940	6939	99.9
10	3	6862	6851	99.8
10	4	6934	6855	98.8
10	5	6941	6574	94.7
10	6	6880	5806	84.3
10	7	6963	4608	66.1
10	8	6938	2650	38.1
10	9	6946	1045	15
10	10	6891	183	2.6

Table 17 (continued). Sensitivity of identifying a certain number of DWM lesions with central veins in simulated RRMS patients.

Each row shows the number of RRMS patients who would be correctly diagnosed depending on the proportion of DWM lesions with central veins.

Shaded rows show the optimum proportions of DWM lesions with central veins giving the best sensitivities.

† = number of simulated patients suitable for the test out of a total of 10,000.

‡ = no. of correctly diagnosed as RRMS = 'True positive' cases.

Total DWM lesions identified	No. WML central veins	No. pts suitable for test (SVD)†	No. incorrectly diagnosed as RRMS‡	Specificity* (%)
4	1	9847	1091	88.9
4	2	9852	51	99.5
4	3	9862	1	100
4	4	9860	0	100
6	1	9699	1585	83.7
6	2	9699	98	99
6	3	9699	2	100
6	4	9708	0	100
6	5	9696	0	100
6	6	9688	0	100
8	1	9461	2088	77.9
8	2	9487	216	97.7
8	3	9465	13	99.9
8	4	9473	1	99.9
8	5	9456	0	100
8	6	9438	0	100
8	7	9445	0	100
8	8	9461	0	100

Table 18. Continued on next page.

Total DWM lesions identified	No. WML central veins	No. pts suitable for test (SVD)†	No. incorrectly diagnosed as RRMS‡	Specificity* (%)
10	1	9111	2347	74.2
10	2	9188	310	96.6
10	3	9084	25	99.7
10	4	9122	1	100
10	5	9123	0	100
10	6	9106	0	100
10	7	9123	0	100
10	8	9164	0	100
10	9	9107	0	100
10	10	9135	0	100

Table 18 (continued). Specificity of identifying a certain number of DWM lesions with central veins in simulated SVD patients.

Each row shows the number of patients with SVD who would be misdiagnosed as having RRMS depending on the proportion of DWM lesions with central veins. Shaded rows show the optimum specificity.

† = number of simulated patients suitable for the test out of a total of 10,000.

‡ = no. of incorrectly diagnosed as RRMS = 'False positive' cases

*calculation: (Total number of patients suitable for test - number of patients incorrectly diagnosed as RRMS / total number of patients suitable for test) x 100

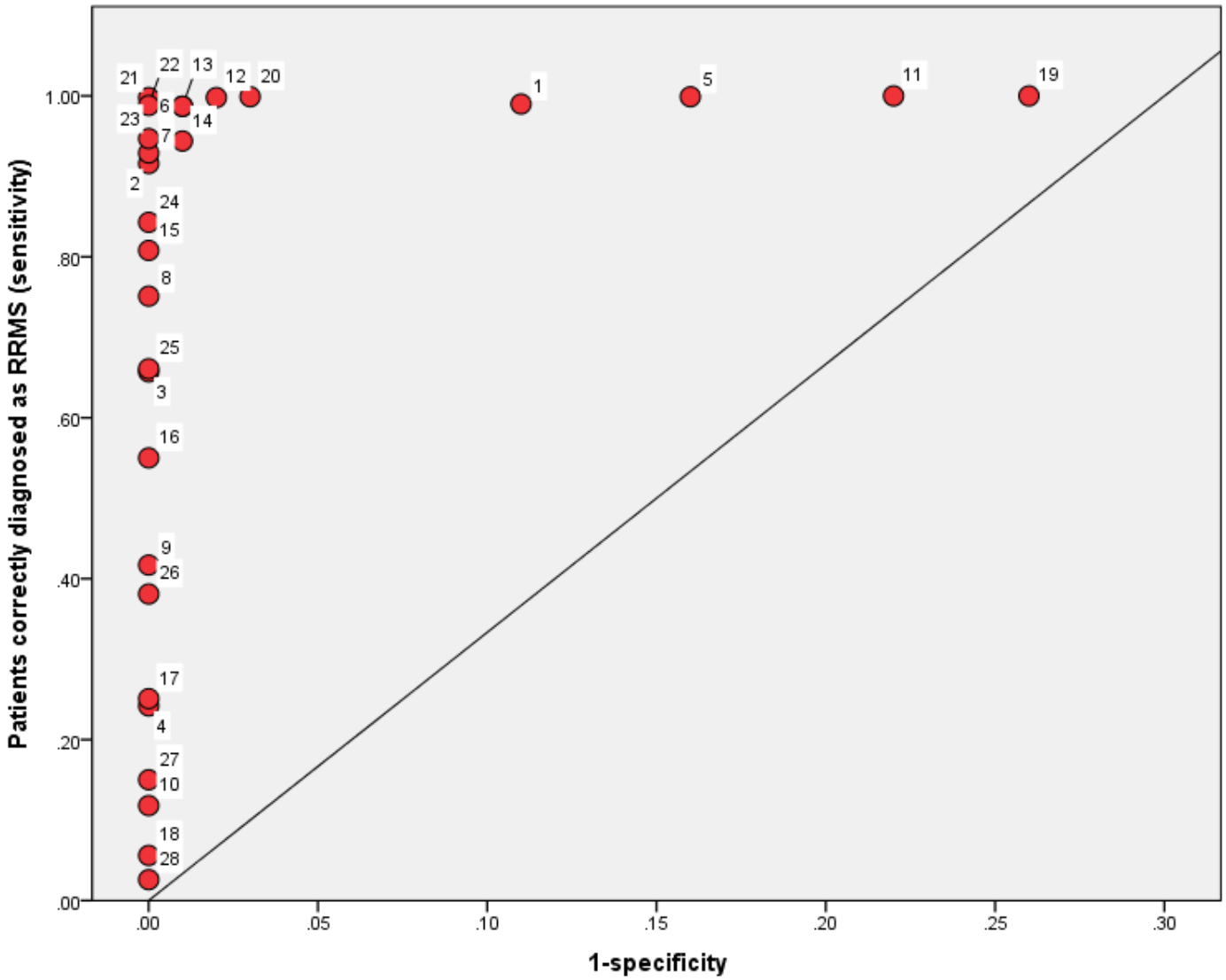

Figure 22. ROC curve depicting sensitivity against 1-specificity for the central vein sign when using the proportion of DWM lesions with central veins for RRMS patients.

Each dot represents a certain diagnostic rule, with data points closest to the top left of the graph representing the best sensitivity and specificity.

The following data points correspond to some of the best rules with highest sensitivity and specificity; data point 2 = 4/2; data point 7 = 6/3; data point 13 = 8/3; data point 21 = 10/3 (The first number = DWM lesion number, second number = number of central veins).

6.3.3 Optimum threshold for diagnosing PPMS using DWM lesions

Results for this analysis are summarised in Tables 19 and 20 and Figure 23. Identifying 4 DWM lesions in the PPMS replication group allows approximately 76% of patients to be suitable for the test. Although if one central vein was identified this would produce a sensitivity of 97.3%, the specificity of this rule would only be 88.4%. Increasing the number of central veins needed to 2, reduces the sensitivity to 81.9% but improves specificity to 99.4%. Further increases in central vein numbers to 3 or 4 dramatically reduces the sensitivity of this rule to below 50%.

Using 6 DWM lesions and identifying 2 central veins allows a sensitivity of 96.1% and specificity of 98.8% but the raw numbers of potential misdiagnoses being 112 SVD patients. Detecting 3 central veins as expected reduces the sensitivity to 81.1% but reduces the raw numbers of SVD patients incorrectly diagnosed as PPMS to 6 (specificity of 99.9%). This rule using 6 DWM lesions however only allows 67% of patients to be suitable for the test. As described in Table 19, further increasing the number of DWM lesions needed for the test to 8 and 10 only allows 53-59% of patients to be suitable for having the test. However high sensitivities and specificities above 95% can be achieved with as few as 3 central veins.

Total DWM lesions identified	No. WML central veins	No. pts suitable for test (PPMS)†	No. correctly diagnosed as PPMS‡	Proportion correctly diagnosed as PPMS (%) (sensitivity)
4	1	7601	7396	97.3
4	2	7629	6249	81.9
4	3	7651	3635	47.5
4	4	7618	977	12.8
6	1	6713	6687	99.6
6	2	6806	6545	96.1
6	3	6716	5451	81.1
6	4	6719	3711	55.2
6	5	6662	1582	23.7
6	6	6755	308	4.5
8	1	5943	5939	99.9
8	2	5892	5849	99.2
8	3	5949	5660	95.1
8	4	5925	4866	82.1
8	5	5879	3461	58.8
8	6	5878	1904	32.3
8	7	5881	622	10.5
8	8	5938	85	1.4

Table 19. Continued on next page.

Total DWM lesions identified	No. WML central veins	No. pts suitable for test (PPMS)†	No. correctly diagnosed as PPMS‡	Proportion correctly diagnosed as PPMS (%) (sensitivity)
10	1	5285	5285	100
10	2	5240	5232	99.8
10	3	5299	5230	98.6
10	4	5182	4885	94.2
10	5	5286	4427	83.7
10	6	5293	3354	63.3
10	7	5380	2086	38.7
10	8	5300	870	16.4
10	9	5339	255	4.7
10	10	5333	39	0.7

Table 19 (continued). Sensitivity of identifying a certain number of DWM lesions with central veins in simulated PPMS patients.

Each row shows the number of PPMS patients who would be correctly diagnosed depending on the proportion of DWM lesions with central veins. Shaded rows show the optimum proportions of DWM lesions with central veins giving the best sensitivities.

† = number of simulated patients suitable for the test out of a total of 10,000.

‡ = no. of correctly diagnosed as PPMS = 'True positive' cases.

Total DWM lesions identified	No. WML central veins	No. pts suitable for test (SVD)†	No. incorrectly diagnosed as PPMS‡	Specificity* (%)
4	1	9876	1142	88.4
4	2	9856	58	99.4
4	3	9870	0	100
4	4	9886	0	100
6	1	9715	1663	82.8
6	2	9686	112	98.8
6	3	9686	6	99.9
6	4	9683	0	100
6	5	9680	0	100
6	6	9664	0	100
8	1	9443	2033	78.4
8	2	9407	206	97.8
8	3	9473	9	99.9
8	4	9433	0	100
8	5	9407	0	100
8	6	9468	0	100
8	7	9431	0	100
8	8	9422	0	100

Table 20. Continued on next page.

Total DWM lesions identified	No. WML central veins	No. pts suitable for test (SVD)†	No. incorrectly diagnosed as PPMS‡	Specificity* (%)
10	1	9185	2398	73.8
10	2	9114	335	96.3
10	3	9122	32	99.6
10	4	9144	2	99.9
10	5	9138	0	100
10	6	9203	0	100
10	7	9141	0	100
10	8	9106	0	100
10	9	9115	0	100
10	10	9139	0	100

Table 20 (continued). Specificity of identifying a certain number of DWM lesions with central veins in simulated SVD patients.

Each row shows the number of patients with SVD who would be misdiagnosed as having PPMS depending on the proportion of DWM lesions with central veins. Shaded rows show the optimum specificity.

† = number of simulated patients suitable for the test out of a total of 10,000.

‡ = no. of incorrectly diagnosed as PPMS = 'False positive' cases

*calculation: (Total number of patients suitable for test - number of patients incorrectly diagnosed as PPMS / total number of patients suitable for test) x 100

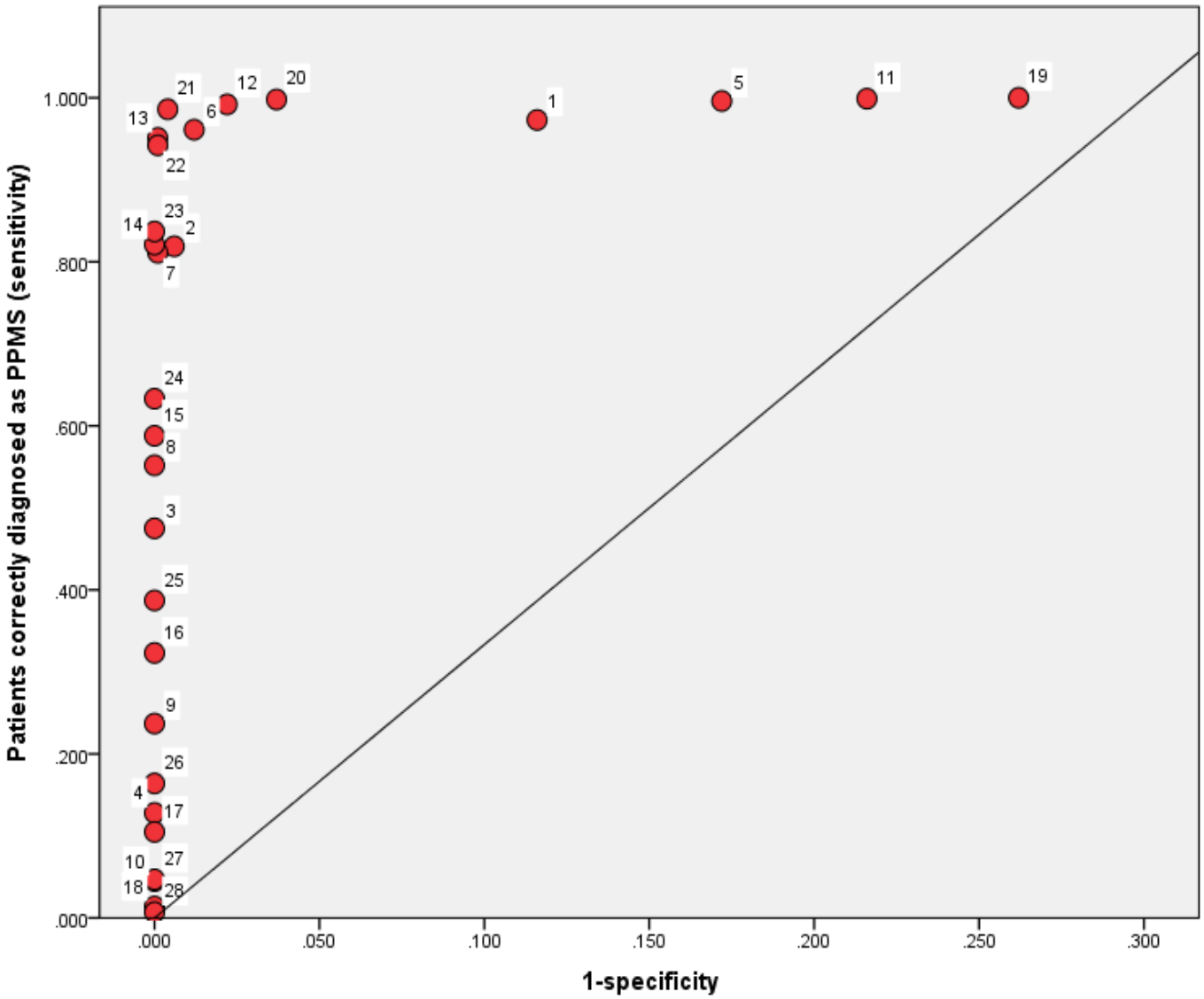

Figure 23. ROC curve depicting sensitivity against 1-specificity for the central vein sign when using the proportion of DWM lesions with central veins for PPMS patients.

Data points closest to the top left of the graph represent the best sensitivity and specificity.

The following data points correspond to some of the best rules with highest sensitivity and specificity; data point 2 = 4/2; data point 7 = 6/3; data point 13 = 8/3; data point 21 = 10/3 (The first number = DWM lesion number, second number = number of central veins).

6.3.4 Optimum threshold for diagnosing RRMS or PPMS using any WML central vein

Results for the RRMS group are summarised in Appendix D, Tables 1 and 2. The same analysis was performed as previously but this time without taking into consideration lesion location. Finding 6 WMLs and 3 having central veins produced a sensitivity of 95.7% and specificity of 99.9%, with 94% of RRMS and 97% of SVD patients being suitable for the test. Increasing the number of veins any further e.g. to 4, reduced the sensitivity to 82.2%. For higher WML numbers, the number of central veins for best sensitivity and specificity ranged from 4 (with 8 and 10 WMLs) to 5 or 6 (with 15 and 20 WMLs).

Results for the PPMS group are summarised in Appendix D, Tables 3 and 4. The same criteria of 6 WMLs with 3 central veins gave the most practical and accurate threshold for the diagnosis of PPMS (sensitivity 88.1% and specificity 99.9%). This allowed approximately 81% of PPMS to be suitable for the test. Higher lesion counts, like in RRMS patients needed marginally more central veins to be identified to reach high sensitivity and specificity.

6.4 Discussion

The diagnostic threshold that I tried to refine was based on identifying a subset of WMLs with central veins. Current radiological practice for supporting the diagnosis of MS using MRI should report if WMLs are in a typical distribution for MS (Traboulsee *et al.*, 2016). There is no requirement to identify or comment on all WMLs. The same method of not identifying *all* WMLs with central veins to make a diagnosis can also be made. The threshold for deciding how many WMLs to identify depended partially on how many are likely to be counted in practice i.e.

asking a radiologist to count ten or less is more likely to be achieved than identifying, for example, thirty. Deciding the WML number was also dependent on the likelihood that MS or SVD scans will have a certain amount of WMLs in the first place. For example, as the results indicate, approximately 81% of the replication RRMS patients had 6 or more DWM lesion but about 69% had 10 or more, and 55% had 15 or more lesions. This is based on the derivation cohort DWM lesion numbers from the RRMS group. Therefore to make the diagnostic threshold as applicable as possible to as many RRMS patients as possible, it appears a "cut-off" of 6 DWM lesions and identifying 3 with central veins would produce the best sensitivity, specificity and be suitable for the majority of RRMS (81%) and SVD (96%) patients. It seems that if more DWM lesions needed to be identified such as 8, 10, 15 or 20, having 4 of these with central veins allows a sensitivity of above 94% (94% for 8 WMLs and 100% for 20 WMLs), but as the number of patients with this many lesions gradually decreases, the test is less useful for the wider MS population. Therefore 6 DWM lesions seems to be the most practical, and applicable to more RRMS patients.

The same rule of identifying 6 DWM lesions and finding 3 with central veins could also be used for PPMS patients. A sensitivity of 81.1% and specificity of 99.9% could be achieved. However as the number of DWM lesions in the PPMS population, and indeed in my derivation cohort was lower than RRMS patients, this rule would only be suitable for approximately 67% of PPMS patients but 96% of SVD patients. As with the RRMS replication patients, higher numbers of DWM lesions could be identified (10, 15 and 20) with just 4 central veins giving high sensitivity and specificity (above 94%) for PPMS. Unlike in the RRMS group, in

the PPMS patients 8 DWM lesions would still require 3 central veins to maintain its sensitivity above 90%.

Identifying 6 DWM lesions with 3 of these having central veins seems to be the most practical rule therefore for the diagnosis of RRMS and PPMS, with good sensitivity and specificity. This is however, specifically when compared to patients with SVD. As described in section 6.1.1, WMLs in the PV and DWM regions are common in other diseases mimicking MS and particularly common in ischaemic SVD. Bot et al. used MRI to investigate WMLs in MS patients, those with inflammatory disorders such as SLE, Sjögren's syndrome, sarcoidosis (patients had at least one episode of neurological symptoms indicating CNS involvement) or patients with cerebrovascular disease (defined as patients who have had a minor stroke or TIA with at least two vascular risk factors) (Bot *et al.*, 2002). PV lesions were seen in all MS patients, 31% of patients with inflammatory disorders and 71% in patients with cerebrovascular disease. DWM lesions were frequent in subjects with cerebrovascular disease and inflammatory disorders (82% and 42% respectively). Previous studies have shown that PV lesions at the anterior horn of the lateral ventricles and DWM lesions in the frontal and parietal lobes are also common in migraine (Rossato *et al.*, 2010; Casini *et al.*, 2013). Absinta et al. found that 32% of their migraine cohort had one or more PV lesions and 53% had at least one JC lesion (Absinta *et al.*, 2012). My findings showing that DWM lesions with central veins alone could diagnose MS, support a recent study comparing the number of central veins in patients with MS and migraine (Solomon *et al.*, 2016). Solomon et al. found that although the probability of diagnosing MS or migraine was not possible based on the number of subcortical or DWM lesions alone, the presence of a central vein changed this. Every time a subcortical or DWM lesion

had a central vein, the likelihood of the MRI scan being from an MS patient increased by fivefold. Results from this chapter therefore support these results when just using DWM lesions with central veins to differentiate MS from SVD. However limiting the diagnostic rule to just this location may prevent applicability of the rule to other potential diseases, and may cause uncertainty when clinicians may have to decide which lesion is periventricular, deep or juxtacortical. Therefore I tried to determine if removing lesion location had any impact on the sensitivity and specificity of the rule.

Identifying *any* WML with central veins, rather than just DWM lesions would allow greater usage of the diagnostic rule. For RRMS patients, I found that identifying 6 WMLs with 3 central veins, from any supratentorial location in the brain allows a sensitivity of 95.7% and specificity of 99.9%. This takes into account PV, DWM or JC lesions and allows more RRMS patients to be suitable for the test (94% of RRMS patients, compared to 81% when only allowing for DWM lesions). This rule could be more useful because of the many differential diagnoses that can produce not only DWM lesions but also PV and JC lesions (Chen *et al.*, 2016).

For PPMS patients the sensitivity is marginally higher when identifying any WML with central veins (88.1%) than when identifying only DWM lesions (81.1%), and the specificity remains high at 99.9%. More patients would also be suitable for the test (81%) when counting any WML.

The diagnostic rule should have a high specificity with as high as possible sensitivity. Specificity needs to be high to avoid misdiagnosing patients that may have SVD, with MS. Whether using DWM lesion central veins alone or any WMLs with central veins, a small drop in sensitivity to accommodate higher specificities

is needed. Although specificities are still high when identifying less than 3 central veins, the raw numbers of patients that would be misdiagnosed would be high. For example, identifying 2 central veins in any 6 WMLs in SVD patients would produce a specificity of 97.9%, but in raw numbers this would equate to 202 patients being misdiagnosed with RRMS, compared to 6 misdiagnoses with 3 central veins. Therefore, although an early diagnosis is desirable, the accuracy of the diagnosis is most important (Miller, 2016). Changes to the MRI DIS criteria for the McDonald 2010 criteria (Polman *et al.*, 2011) led to more "user friendly", practical criteria (Selchen *et al.*, 2012). The DIS sensitivity improved to 85.9%, but specificity reduced a little to 59.4% compared to McDonald 2005 criteria (Swanton *et al.*, 2007). The patients used for this chapter already had confirmed MS, compared to the Swanton study which evaluated CIS patients, so my results are not directly comparable. However, they do give an estimation of the sensitivities and specificities that could be achieved in a CIS cohort. The Barcelona inception cohort showed that of 951 patients who had a baseline MRI scan, 28.8% had 1-9 T2 lesions and 39.7% had more than 10 lesions (Tintore *et al.*, 2015). Therefore identifying a small number of WMLs with central veins may be suitable for a substantial number of CIS patients.

6.4.1 Limitations

A few limitations should be noted. Firstly the derivation cohort distributions were based on patients who already had confirmed RRMS, PPMS or ischaemic SVD. Although there is an ongoing prospective study evaluating the central vein sign in atypical and uncertain cases of MS, I did not have enough numbers to devise a derivation distribution for these type of patients. Once the prospective study has

stopped recruiting, it would be important to determine if applying the central vein sign rules, still produce high sensitivities and specificities. If however this rule was to be used in clinical practice, it would have to be derived from patients without a confirmed diagnosis (diagnostically uncertain cases) rather than those with an already confirmed diagnosis.

I could not run an analysis for PV or JC lesions with central veins because of smaller lesion numbers. Although RRMS and PPMS patients had moderately high numbers of PV and JC lesions, SVD patients did not. The total number of PV and JC lesions in the SVD patients were 32 and 12 respectively. Therefore a gamma distribution would not accurately fit this data, so deriving a replication cohort of patients and subsequent diagnostic thresholds based on such small numbers would have been inaccurate.

6.4.2 Summary

Identifying a proportion of WMLs with central veins to make a diagnosis of MS or non-MS would be more practical for clinicians. Detecting as few as 6 WMLs on a 3T T2* MRI scan, with 3 of these having central veins, appears to provide high sensitivities and specificities, regardless of lesion location. Application of these rules to a prospective cohort of patients with diagnostic uncertainty should be performed next to determine if they are still as accurate.

Chapter 7. Conclusions

7.1 WML central veins as an MRI biomarker of MS

The use of the WML central vein sign as an imaging biomarker for MS has yet to be firmly established in clinical practice. With the rapidly growing list of disease modifying treatments for RRMS and a positive clinical trial in PPMS (Montalban *et al.*, 2017), accurate and timely diagnosis is increasingly important. Serum and CSF biomarkers to date are lacking, but advances in MRI now allow the pathological characteristics of the MS lesion to be seen, including central veins and hypointense rims. So far, the central vein sign has been shown in small studies to be a promising differentiator of MS from lesions secondary to ischaemic SVD, and possibly from NMO. Many studies have been performed using ultra-high field MR scanners, and so one purpose of this thesis was to determine if this potential biomarker could be brought to clinical MRI scanners. Determining what T2* weighted sequences are accurate in detecting WML central veins, the clinical and practical barriers in implementing the use of various T2* weighted sequences, and the problems that may affect the use of the central vein sign as a diagnostic test, were the overarching aims of this thesis.

The initial study investigating the use of different 3T scanners and similar T2* weighted sequences showed that the scanner and sequence lead to different proportions of WMLs with central veins. An *a priori* hypothesis was that the difference in the proportions of WMLs with central veins between those with MS and ischaemic SVD would be large. This was shown to be true, but mean proportions varied significantly in the same MS patients when similar (but not identical) T2* sequences were used. Using a proportional method as a diagnostic

threshold for MS could be affected by variations in the T2* scan. Any future multicentre studies using T2* should, therefore, take this factor into account.

With this in mind, another factor that needs to be understood before clinical translation, was the ability of fused images to be used in identifying WML central veins. FLAIR-SWI and FLAIR* being relatively recent additions to the list of sequences to detect WML central veins, have not been tested quantitatively against more established techniques. A comparison of 3T T2*, SWI and FLAIR-SWI demonstrated the superior ability of T2* in particular, to delineate WML central veins compared to FLAIR-SWI. Although a small number of MS patients were used, this will hopefully show that 'basic' T2* imaging or SWI can be used in modern scanners and that there is not always a need to fuse images. Encouraging radiology units to use a 'new' sequence, would be more likely if it was simple to set up, easy to use and quick.

Perhaps a more realistic use of the central vein sign would be in the differentiation of ischaemic SVD from MS, whilst other MS mimics are more likely to be distinguished with alternate, distinct MRI findings and clinical red flags (Miller *et al.*, 2008). PPMS patients are more likely to have vascular risk factors and ischaemic SVD patients can frequently mimic MS on MRI (Sanchez Aliaga, 2014). WML central veins were seen in almost as high a proportion in our PPMS cohort compared to RRMS patients, and there remained a significant difference in these proportions from the SVD group. Vascular risk factors themselves do not appear to alter the proportion of WMLs with central veins, although smoking may have some influence. This will need to be repeated with much larger numbers and other risk factors.

The accuracy of identifying only a subset of WMLs with central veins to diagnose MS has only been tested in the last decade (Tallantyre *et al.*, 2011; Mistry *et al.*, 2016; Solomon *et al.*, 2016). For the central vein sign to be more practical this needs to be taken forward and validated prospectively. The preliminary work in the last chapter focuses on how identifying 6 WMLs with 3 central veins is sensitive, specific and suitable for many MS and SVD patients, but whether this can be applied to patients who may have symptoms or scans resembling MS, remains to be clarified.

7.2 Future studies and how WML central veins could be incorporated into future diagnostic pathways

Only a multicentre, prospective study will confirm or refute WML central veins as an accurate biomarker in diagnosing MS in cases of uncertainty. A single centre, prospective study at 3T is underway at Nottingham, which will enable power calculations for the number of patients needed in a multicentre study. This is the most likely way to recruit patients with other MS mimics, as anecdotally SVD dominates the referrals for MRI mimics of MS. It would also be useful to further test whether my hypothesis that a 0.55mm isotropic T2* sequence with high EPI factor is as good in identifying WMLs and central veins as compared to other sequences. Further studies looking at specific cohorts of diseases that mimic MS, e.g. ADEM and neurosarcoidosis, should be investigated for WML central veins. For example, ADEM is pathologically a perivenular disease that would be expected to have veins within the lesions, but confirming that these are central veins on MRI like those in MS needs more work. Furthermore, and something which I have not studied, is optimising T2* imaging for infratentorial analysis. The use of FLAIR-SWI or FLAIR* may come in useful here. Following on from this would be an

attempt to develop an MRI protocol to image central veins in lesions within the spinal cord. This would add another tool to aid diagnosis, especially in patients with low lesion loads or predominantly spinal cord disease. This has not been achieved to date, due to problems with inhomogeneities caused by the close proximity of structures such as vertebral bones, artefacts caused by subtle movements such as respiration and the small cord area that needs to be imaged. Finally, a consensus from neuroradiology colleagues on whether they feel such a biomarker would be helpful is essential; informal discussions have suggested that they would.

Whether the central vein sign could be used after the first episode of symptoms suggestive of demyelination, as a predictor of conversion to confirmed MS, much like the presence of CSF oligoclonal bands, remains to be proven. Therefore, precisely where in the diagnostic pathway the central vein sign could be used needs further study. The basic building blocks for the diagnosis of MS; DIS and DIT remain pivotal for the diagnosis, but potentially could be supplemented with the addition of the MRI character of the lesion. Specificity of T2 DIS criteria has always been lower than sensitivity. It appears that the specificity of the central vein sign in confirmed cases of PPMS and RRMS is high, but it remains to be definitively confirmed whether this characteristic of demyelinating lesions can be useful in patients who *may* have MS. Furthermore, whether it should be used for all patients who are being considered as having MS, or just patients with diagnostic uncertainty needs to be established.

References

Absinta M, Rocca MA, Colombo B, Copetti M, De Feo D, Falini A, *et al.* Patients with migraine do not have MRI-visible cortical lesions. J Neurol 2012; 259(12): 2695-8.

Absinta M, Sati P, Gaitán MI, Maggi P, Cortese ICM, Filippi M, *et al.* 7T Phase imaging of acute MS lesions: A new window into the inflammatory process. Ann Neurol 2013; 74(5).

Adams C. Perivascular iron deposition and other vascular damage in multiple sclerosis. J Neurol Neurosurg Psychiatry 1988; 51: 260-5.

Ahn S, Park SH, Lee KH. How to demonstrate similarity by using noninferiority and equivalence statistical testing in radiology research. Radiology 2013; 267(2): 328-38.

Akasbi M, Berenguer J, Saiz A, Brito-Zerón P, Pérez-De-Lis M, Bové A, *et al.* White matter abnormalities in primary Sjögren syndrome. QJM 2012; 105(5): 433-43.

Al-Araji A, Kidd DP. Neuro-Behçet's disease: epidemiology, clinical characteristics, and management. Lancet Neurol 2009; 8(2): 192-204.

Allen IV, McKeown SR. A histological, histochemical and biochemical study of the macroscopically normal white matter in multiple sclerosis. J Neurol Sci 1979; 41(1): 81-91.

Altman DG. Practical Statistics for Medical Research. London: Chapman and Hall; 1991.

Anan F, Masaki T, Eto T, Iwao T, Shimomura T, Umeno Y, *et al.* Visceral fat accumulation is a significant risk factor for white matter lesions in Japanese type 2 diabetic patients. Eur J Clin Invest 2009; 39(5): 368-74.

Antel J, Antel S, Caramanos Z, Arnold DL, Kuhlmann T. Primary progressive multiple sclerosis: part of the MS disease spectrum or separate disease entity? Acta Neuropathol 2012; 123(5): 627-38.

Ascherio A, Munger KL. Environmental risk factors for multiple sclerosis. Part I: the role of infection. Ann Neurol 2007; 61(4): 288-99.

Axelsson M, Malmestrom C, Nilsson S, Haghighi S, Rosengren L, Lycke J. Glial fibrillary acidic protein: a potential biomarker for progression in multiple sclerosis. J Neurol 2011; 258(5): 882-8.

Banwell B, Krupp L, Kennedy J, Tellier R, Tenembaum S, Ness J, *et al.* Clinical features and viral serologies in children with multiple sclerosis: a multinational observational study. Lancet Neurol 2007; 6(9): 773-81.

Barkhof F, Filippi M, Miller DH, Scheltens P, Campi A, Polman CH, *et al.* Comparison of MRI criteria at first presentation to predict conversion to clinically definite multiple sclerosis. Brain 1997; 120(11): 2059-69.

Barkhof F, Rocca M, Francis G, Van Waesberghe JH, Uitdehaag BM, Hommes OR, *et al.* Validation of diagnostic magnetic resonance imaging criteria for multiple sclerosis and response to interferon beta1a. Ann Neurol 2003; 53(6): 718-24.

Barnett MH, Prineas JW, Buckland ME, Parratt JDE, Pollard JD. Massive astrocyte destruction in neuromyelitis optica despite natalizumab therapy. Mult Scler 2012; 18(1): 108-12.

Bates D. Treatment effects of immunomodulatory therapies at different stages of multiple sclerosis in short-term trials. Neurology 2011; 76(Supplement 1): S14-S25.

Bernitsas E, Khan O, Razmjou S, Tselis A, Bao F, Caon C, *et al.* Cerebrospinal fluid humoral immunity in the differential diagnosis of multiple sclerosis. PLoS One 2017; 12(7): e0181431.

Biomarkers Definitions Working G. Biomarkers and surrogate endpoints: preferred definitions and conceptual framework. Clin Pharmacol Ther 2001; 69(3): 89-95.

Bland JM, Altman DG. Measuring agreement in method comparison studies. Statistical Methods in Medical Research 1999; 8(2): 135-60.

Bø L, Vedeler CA, Nyland HI, Trapp BD, Mørk SJ. Subpial demyelination in the cerebral cortex of multiple sclerosis patients. J Neuropathol Exp Neurol 2003; 62(7): 723-32.

Bonaci-Nikolic B, Jeremic I, Andrejevic S, Sefik-Bukilica M, Stojsavljevic N, Drulovic J. Anti–double stranded DNA and lupus syndrome induced by interferon-β therapy in a patient with multiple sclerosis. Lupus 2009; 18(1): 78-80.

Borrelli P, Palma G, Tedeschi E, Cocozza S, Comerci M, Alfano B, *et al.* Improving Signal-to-Noise Ratio in Susceptibility Weighted Imaging: A Novel Multicomponent Non-Local Approach. PLoS One 2015; 10(6): e0126835.

Bosemani T, Poretti A, Huisman TA. Susceptibility-weighted imaging in pediatric neuroimaging. J Magn Reson Imaging 2014; 40(3): 530-44.

Bot JC, Barkhof F, Lycklama a Nijeholt G, van Schaardenburg D, Voskuyl AE, Ader HJ, *et al.* Differentiation of multiple sclerosis from other inflammatory disorders and cerebrovascular disease: value of spinal MR imaging. Radiology 2002; 223(1): 46-56.

Böttcher T, Rolfs A, Tanislav C, Bitsch A, Köhler W, Gaedeke J, *et al.* Fabry Disease – Underestimated in the Differential Diagnosis of Multiple Sclerosis? PLoS One 2013; 8(8): e71894.

Bourdette D, Yadav V. The radiologically isolated syndrome revisited When is it presymptomatic multiple sclerosis? Neurology 2011; 76(8): 680-1.

Bradley WG, Glenn BJ. The effect of variation in slice thickness and interslice gap on MR lesion detection. AJNR Am J Neuroradiol 1987; 8(6): 1057-62.

Breteler MMB, Swieten JCv, Bots ML, Grobbee DE, Claus JJ, Hout JHWvd, *et al.* Cerebral white matter lesions, vascular risk factors, and cognitive function in a population-based study The Rotterdam Study. Neurology 1994; 44(7): 1246-52.

Brettschneider J, Petzold A, Sussmuth SD, Landwehrmeyer GB, Ludolph AC, Kassubek J, *et al.* Neurofilament heavy-chain NfH(SMI35) in cerebrospinal fluid supports the differential diagnosis of Parkinsonian syndromes. Mov Disord 2006; 21(12): 2224-7.

Brex PA, Ciccarelli O, O'Riordan JI, Sailer M, Thompson AJ, Miller DH. A longitudinal study of abnormalities on MRI and disability from multiple sclerosis. N Engl J Med 2002; 346(3): 158-64.

Brickshawana A, Hinson SR, Romero MF, Lucchinetti CF, Guo Y, Buttmann M, *et al.* Investigation of the KIR4.1 potassium channel as a putative antigen in patients with multiple sclerosis: a comparative study. Lancet Neurol 2014; 13(8): 795-806.

Brill L, Goldberg L, Karni A, Petrou P, Abramsky O, Ovadia H, *et al.* Increased anti-KIR4.1 antibodies in multiple sclerosis: could it be a marker of disease relapse? Mult Scler 2015; 21(5): 572-9.

Brinar VV, Habek M. Rare infections mimicking MS. Clin Neurol Neurosurg 2010; 112(7): 625-8.

Brownell B, Hughes JT. The distribution of plaques in the cerebrum in multiple sclerosis. J Neurol Neurosurg Psychiatry 1962; 25(4): 315-20.

Calabrese M, Poretto V, Favaretto A, Alessio S, Bernardi V, Romualdi C, *et al.* Cortical lesion load associates with progression of disability in multiple sclerosis. Brain 2012; 135(10): 2952-61.

Canto E, Tintore M, Villar LM, Costa C, Nurtdinov R, Alvarez-Cermeno JC, *et al.* Chitinase 3-like 1: prognostic biomarker in clinically isolated syndromes. Brain 2015; 138(Pt 4): 918-31.

Carmosino MJ, Brousseau KM, Arciniegas DB, Corboy JR. Initial evaluations for multiple sclerosis in a university multiple sclerosis center: Outcomes and role of magnetic resonance imaging in referral. Arch Neurol 2005; 62(4): 585-90.

Casini G, Yurashevich M, Vanga R, Dash S, Dhib-Jalbut S, Gerhardstein B, *et al.* Are Periventricular Lesions Specific for Multiple Sclerosis? J Neurol Neurophysiol 2013; 4(2): 150.

Caucheteux N, Maarouf A, Genevray M, Leray E, Deschamps R, Chaunu M *et al.* Criteria improving multiple sclerosis diagnosis at the first MRI. J Neurol 2015; 262(4):979-87.

Ceccarelli A, Rocca MA, Pagani E, Colombo B, Martinelli V, Comi G, *et al.* A voxel-based morphometry study of grey matter loss in MS patients with different clinical phenotypes. Neuroimage 2008; 42(1): 315-22.

Chang A, Tourtellotte WW, Rudick R, Trapp BD. Premyelinating Oligodendrocytes in Chronic Lesions of Multiple Sclerosis. N Engl J Med 2002; 346(3): 165-73.

Chavhan GB, Babyn PS, Thomas B, Shroff MM, Haacke EM. Principles, Techniques, and Applications of T2*-based MR Imaging and Its Special Applications. Radiographics 2009; 29(5): 1433-49.

Chen JJ, Carletti F, Young V, Mckean D, Quaghebeur G. MRI differential diagnosis of suspected multiple sclerosis. Clin Radiol 2016; 71(9): 815-27.

Ciccarelli O, Werring DJ, Wheeler–Kingshott CaM, Barker GJ, Parker GJM, Thompson AJ, *et al.* Investigation of MS normal-appearing brain using diffusion tensor MRI with clinical correlations. Neurology 2001; 56(7): 926-33.

Clifford DB, DeLuca A, Simpson DM, Arendt G, Giovannoni G, Nath A. Natalizumab-associated progressive multifocal leukoencephalopathy in patients with multiple sclerosis: lessons from 28 cases. Lancet Neurol 2010; 9(4): 438-46.

Cohen JA, Barkhof F, Comi G, Hartung H-P, Khatri BO, Montalban X, *et al.* Oral Fingolimod or Intramuscular Interferon for Relapsing Multiple Sclerosis. New Engl J Med 2010; 362(5): 402-15.

Compston A, Confavreux C, Lassmann H, McDonald I, Miller D, Noseworthy J, *et al.* McAlpine's Multiple Sclerosis. 4th Ed. ed: Elsevier; 2005.

Confavreux C, Vukusic S. Age at disability milestones in multiple sclerosis. Brain 2006a; 129(3): 595-605.

Confavreux C, Vukusic S. Natural history of multiple sclerosis: a unifying concept. Brain 2006b; 129(3): 606-16.

Cottrell DA, Kremenchutzky M, Rice GPA, Koopman WJ, Hader W, Baskerville J, *et al.* The natural history of multiple sclerosis:a geographically based study 5. The clinical features and natural history of primary progressive multiple sclerosis. Brain 1999; 122(4): 625-39.

Cuadrado MJ, Khamashta MA, Ballesteros A, Godfrey T, Simon MJ, Hughes GR. Can neurologic manifestations of Hughes (antiphospholipid) syndrome be distinguished from multiple sclerosis? Analysis of 27 patients and review of the literature. Medicine (Baltimore) 2000; 79(1): 57-68.

Cuadrado MJ, Wakefield K, Sanna G, Khamashta MA, Hughes GR. Multiple sclerosis and the antiphospholipid (Hughes) syndrome: a common differential diagnosis? Clin Exp Rheumatol 2004; 22(5): 652-3.

Dawson JW. XVIII.—The Histology of Disseminated Sclerosis. Earth and Environmental Science Transactions of the Royal Society of Edinburgh 1916; 50(03): 517-740.

Debette S and Markus HS. The clinical importance of white matter hyperintensities on brain magnetic resonance imaging: systematic review and meta-analysis. BMJ 2010; 341:c3666.

De Jager PL, Simon KC, Munger KL, Rioux JD, Hafler DA, Ascherio A. Integrating risk factors: HLA-DRB1*1501 and Epstein-Barr virus in multiple sclerosis. Neurology 2008; 70(13 Pt 2): 1113-8.

de Leeuw FE, de Groot JC, Achten E, Oudkerk M, Ramos LM, Heijboer R, *et al.* Prevalence of cerebral white matter lesions in elderly people: a population based magnetic resonance imaging study. The Rotterdam Scan Study. J Neurol Neurosurg Psychiatry 2001; 70(1): 9-14.

de Leeuw FE, de Groot JC, Oudkerk M, Witteman JC, Hofman A, van Gijn J, *et al.* Hypertension and cerebral white matter lesions in a prospective cohort study. Brain 2002; 125(Pt 4): 765-72.

de Seze J, Delalande S, Michelin E, Gauvrit JY, Mackowiak MA, Ferriby D, *et al.* Brain MRI in late-onset multiple sclerosis. Eur J Neurol 2005; 12(4): 241-4.

Dickie DA, Ritchie SJ, Cox SR, Sakka E, Royle NA, Aribisala BS, *et al.* Vascular risk factors and progression of white matter hyperintensities in the Lothian Birth Cohort 1936. Neurobiol Aging 2016; 42: 116-23.

Disanto G, Adiutori R, Dobson R, Martinelli V, Dalla Costa G, Runia T, *et al.* Serum neurofilament light chain levels are increased in patients with a clinically isolated syndrome. J Neurol Neurosurg Psychiatry 2016; 87(2): 126-9.

Disanto G, Pakpoor J, Morahan JM, Hall C, Meier UC, Giovannoni G, *et al.* Epstein-Barr virus, latitude and multiple sclerosis. Mult Scler 2013; 19(3): 362-5.

Dixon JE, Simpson A, Mistry N, Evangelou N, Morris PG. Optimisation of MRI for the detection of small veins in multiple sclerosis at 3 T and 7 T. Eur J Radiol 2013; 82(5): 719-27.

Dobson R, Giovannoni G, Ramagopalan S. The month of birth effect in multiple sclerosis: systematic review, meta-analysis and effect of latitude. J Neurol Neurosurg Psychiatry 2013; 84(4): 427-32.

Dobson R, Ramagopalan S, Davis A, Giovannoni G. Cerebrospinal fluid oligoclonal bands in multiple sclerosis and clinically isolated syndromes: a meta-analysis of prevalence, prognosis and effect of latitude. J Neurol Neurosurg Psychiatry 2013; 84: 909-914.

Dow RS, Berglund G. Vascular pattern of lesions of multiple sclerosis. Archives of Neurology & Psychiatry 1942; 47(1): 1-18.

Elian M, Dean G. Multiple sclerosis among the United Kingdom-born children of immigrants from the West Indies. J Neurol Neurosurg Psychiatry 1987; 50(3): 327-32.

Elian M, Nightingale S, Dean G. Multiple sclerosis among United Kingdom-born children of immigrants from the Indian subcontinent, Africa and the West Indies. J Neurol Neurosurg Psychiatry 1990; 53(10): 906-11.

Evangelou N, Esiri MM, Smith S, Palace J, Matthews PM. Quantitative pathological evidence for axonal loss in normal appearing white matter in multiple sclerosis. Ann Neurol 2000; 47(3): 391-5.

Evans AC, Frank JA, Antel J, Miller DH. The Role of MRI in clinical trials of multiple sclerosis: Comparison of image processing techniques. Ann Neurol 1997; 41(1): 125-32.

Farahangiz S, Sarhadi S, Safari A, Borhani-Haghighi A. Magnetic resonance imaging findings and outcome of neuro-Behçet's disease: the predictive factors. International Journal of Rheumatic Diseases 2012; 15(6): e142-e9.

Fazekas F, Baumhackl U, Berger T, Deisenhammer F, Fuchs S, Kristoferitsch W, *et al.* Decision-making for and impact of early immunomodulatory treatment: the Austrian Clinically Isolated Syndrome Study (ACISS). Eur J Neurol 2010; 17(6): 852-60.

Fazekas F, Offenbacher H, Fuchs S, Schmidt R, Niederkorn K, Horner S *et al.* Criteria for an increased specificity of MRI interpretation in elderly subjects with suspected multiple sclerosis. Neurology 1988; 38(12): 1822-1822.

Fernández-Fernández FJ, Rivera-Gallego A, de la Fuente-Aguado J, Pérez-Fernández S, Muñoz-Fernández D. Antiphospholipid syndrome mimicking multiple sclerosis in two patients. European Journal of Internal Medicine 2006; 17(7): 500-2.

Ferreira S, D'Cruz DP, Hughes GRV. Multiple sclerosis, neuropsychiatric lupus and antiphospholipid syndrome: where do we stand? Rheumatology 2005; 44(4): 434-42.

Filippi M, Horsfield MA, Campi A, Mammi S, Pereira C, Comi G. Resolution-dependent estimates of lesion volumes in magnetic resonance imaging studies of the brain in multiple sclerosis. Ann Neurol 1995; 38(5): 749-54.

Filippi M, Marcianò N, Capra R, Rocca MA, Prandini F, Gasparotti R, *et al.* The effect of imprecise repositioning on lesion volume measurements in patients with multiple sclerosis. Neurology 1997; 49(1): 274-6.

Filippi M, Rocca MA, Ciccarelli O, De Stefano N, Evangelou N, Kappos L, *et al.* MRI criteria for the diagnosis of multiple sclerosis: MAGNIMS consensus guidelines. Lancet Neurol 2016; 15(3):292-303.

Filippi M, Rocca MA, Gasperini C, Sormani MP, Bastianello S, Horsfield MA, *et al.* Interscanner Variation in Brain MR Lesion Load Measurements in Multiple

Sclerosis Using Conventional Spin-Echo, Rapid Relaxation-Enhanced, and Fast-FLAIR Sequences. AJNR Am J Neuroradiol 1999; 20(1): 133-7.

Filippi M, Yousry TA, Rocca MA, Pereira C, Alkadhi H, Comi G. The effect of cross-talk on MRI lesion numbers and volumes in multiple sclerosis using conventional and turbo spin-echo. Mult Scler 1998; 4(6): 471-4.

Filli L, Hofstetter L, Kuster P, Traud S, Mueller-Lenke N, Naegelin Y, *et al.* Spatiotemporal distribution of white matter lesions in relapsing-remitting and secondary progressive multiple sclerosis. Mult Scler 2012; 18(11): 1577-84.

Fisniku LK, Chard DT, Jackson JS, Anderson VM, Altmann DR, Miszkiel KA, *et al.* Gray Matter Atrophy Is Related to Long-Term Disability in Multiple Sclerosis. Ann Neurol 2008; 64: 247-254.

Fisniku LK, Brex PA, Altmann DR, Miszkiel KA, Benton CE, Lanyon R, *et al.* Disability and T2 MRI lesions: a 20-year follow-up of patients with relapse onset of multiple sclerosis. Brain 2008; 131(3): 808-17.

Flanagan EP, Weinshenker BG. Neuromyelitis Optica Spectrum Disorders. Current Neurology and Neuroscience Reports 2014; 14(9): 1-12.

Fog T. On the vessel-plaque relationships in the brain in multiple sclerosis. Acta Neurol Scand 1964; 40(S10): 9-15.

Freedman MS, Thompson EJ, Deisenhammer F, Giovannoni G, Grimsley G, Keir, G, *et al.* Recommended Standard of Cerebrospinal Fluid Analysis in the Diagnosis of Multiple Sclerosis. A Consensus Statement. Arch Neurol 2005; 62: 865-870.

Friedman DP. Abnormalities of the deep medullary white matter veins: MR imaging findings. AJR Am J Roentgenol 1997; 168(4): 1103-8.

Fukuda H, Kitani M. Cigarette smoking is correlated with the periventricular hyperintensity grade of brain magnetic resonance imaging. Stroke 1996; 27(4): 645-9.

Gaitan MI, Yanes P, Sati P, Romero C, Reich DS, Correale J. Optimal detection of infratentorial lesions with a combined dual-echo MRI sequence: "PT2". Mult Scler 2015; 22(10):1367-70.

Gaitán MI, Maggi P, Wohler J, Leibovitch E, Sati P, Calandri IL, *et al.* Perivenular brain lesions in a primate multiple sclerosis model at 7-tesla magnetic resonance imaging. Mult Scler 2014; 20(1): 64-71.

Gasparotti R, Pinelli L, Liserre R. New MR sequences in daily practice: susceptibility weighted imaging. A pictorial essay. Insights into Imaging 2011; 2(3): 335-47.

Gasperini C, Rovaris M, Sormani MP, Bastianello S, Pozzilli C, Comi G, *et al.* Intra-observer, inter-observer and inter-scanner variations in brain MRI volume measurements in. Mult Scler 2001; 7(1): 27-31.

George IC, Sati P, Absinta M, Cortese IC, Sweeney EM, Shea CD, *et al.* Clinical 3-tesla FLAIR* MRI improves diagnostic accuracy in multiple sclerosis. Mult Scler 2016; 22(12):1578-1586.

Goldacre MJ, Wotton CJ, Seagroatt V, Yeates D. Multiple sclerosis after infectious mononucleosis: record linkage study. J Epidemiol Community Health 2004; 58(12): 1032-5.

Gons RA, van Norden AG, de Laat KF, van Oudheusden LJ, van Uden IW, Zwiers MP, *et al.* Cigarette smoking is associated with reduced microstructural integrity of cerebral white matter. Brain 2011; 134(Pt 7): 2116-24.

Grabner G, Dal-Bianco A, Schernthaner M, Vass K, Lassmann H, Trattnig S. Analysis of multiple sclerosis lesions using a fusion of 3.0 T FLAIR and 7.0 T SWI phase: FLAIR SWI. J Magn Reson Imaging 2011; 33(3): 543-9.

Gustafson D, Lissner L, Bengtsson C, Bjorkelund C, Skoog I. A 24-year follow-up of body mass index and cerebral atrophy. Neurology 2004; 63(10): 1876-81.

Haacke EM, Cheng NYC, House MJ, Liu Q, Neelavalli J, Ogg RJ, *et al.* Imaging iron stores in the brain using magnetic resonance imaging. Magn Reson Imaging 2005; 23(1): 1-25.

Haacke EM, Mittal S, Wu Z, Neelavalli J, Cheng YCN. Susceptibility-Weighted Imaging: Technical Aspects and Clinical Applications, Part 1. AJNR Am J Neuroradiol 2009; 30(1): 19-30.

Hackmack K, Weygandt M, Wuerfel J, Pfueller CF, Bellmann-Strobl J, Paul F, *et al.* Can we overcome the 'clinico-radiological paradox' in multiple sclerosis? J Neurol 2012; 259(10): 2151-60.

Haghighi AB, Sarhadi S, Farahangiz S. MRI findings of neuro-Behçet's disease. Clin Rheumatol 2011; 30(6): 765-70.

Handel AE, Williamson AJ, Disanto G, Handunnetthi L, Giovannoni G, Ramagopalan SV. An updated meta-analysis of risk of multiple sclerosis following infectious mononucleosis. PLoS One 2010; 5(9).

Hayes CE. Vitamin D: a natural inhibitor of multiple sclerosis. Proc Nutr Soc 2000; 59(4): 531-5.

Hedstrom AK, Hillert J, Olsson T, Alfredsson L. Smoking and multiple sclerosis susceptibility. Eur J Epidemiol 2013; 28(11): 867-74.

Hedstrom AK, Olsson T, Alfredsson L. Smoking is a major preventable risk factor for multiple sclerosis. Mult Scler 2016; 22(8): 1021-6.

Heesen C, Kolbeck J, Gold SM, Schulz H, Schulz KH. Delivering the diagnosis of MS – results of a survey among patients and neurologists. Acta Neurologica Scand 2003; 107(5): 363-8.

Hernan MA, Jick SS, Logroscino G, Olek MJ, Ascherio A, Jick H. Cigarette smoking and the progression of multiple sclerosis. Brain 2005; 128(Pt 6): 1461-5.

Hodel J, Rodallec M, Gerber S, Blanc R, Maraval A, Caron S, *et al.* Susceptibility weighted magnetic resonance sequences "SWAN, SWI and VenoBOLD": technical aspects and clinical applications. J Neuroradiol 2012; 39(2): 71-86.

Housley WJ, Pitt D, Hafler DA. Biomarkers in multiple sclerosis. Clin Immunol 2015; 161(1):51-8.

Huh S-Y, Min J-H, Kim W, Kim S-H, Kim HJ, Kim B-J, *et al.* The usefulness of brain MRI at onset in the differentiation of multiple sclerosis and seropositive neuromyelitis optica spectrum disorders. Mult Scler 2014; 20(6): 695-704.

Ibitoye RT, Wilkins A, Scolding NJ. Neurosarcoidosis: a clinical approach to diagnosis and management. J Neurol 2017; 264(5): 1023-1028.

Ijdo JW, Conti-Kelly AM, Greco P, Abedi M, Amos M, Provenzale JM, *et al.* Anti-phospholipid antibodies in patients with multiple sclerosis and MS-like illnesses: MS or APS? Lupus 1999; 8(2): 109-15.

Ingle GT, Stevenson VL, Miller DH, Thompson AJ. Primary progressive multiple sclerosis: a 5-year clinical and MR study. Brain 2003; 126(Pt 11): 2528-36.

Janssens ACJW, de Boer JB, Kalkers NF, Passchier J, van Doorn PA, Hintzen RQ. Patients with multiple sclerosis prefer early diagnosis. Eur J Neurol 2004; 11(5): 335-7.

Jarius S, Wildemann B, Paul F. Neuromyelitis optica: clinical features, immunopathogenesis and treatment. Clin Exp Immunol 2014; 176(2): 149-64.

Jenkinson M, Bannister P, Brady M, Smith S. Improved optimization for the robust and accurate linear registration and motion correction of brain images. Neuroimage 2002; 17(2): 825-41.

Josey L, Curley M, Jafari Mousavi F, Taylor BV, Lucas R, Coulthard A. Imaging and diagnostic criteria for Multiple Sclerosis: Are we there yet? Journal of Medical Imaging and Radiation Oncology 2012; 56(6): 588-93.

Jousilahti P, Vartiainen E, Tuomilehto J, Puska P. Sex, age, cardiovascular risk factors, and coronary heart disease: a prospective follow-up study of 14 786 middle-aged men and women in Finland. Circulation 1999; 99(9): 1165-72.

Kanda T, Ishii K, Kawaguchi H, Kitajima K, Takenaka D. High signal intensity in the dentate nucleus and globus pallidus on unenhanced T1-weighted MR images: relationship with increasing cumulative dose of a gadolinium-based contrast material. Radiology 2014; 270(3): 834-41.

Kappus N, Weinstock-Guttman B, Hagemeier J, Kennedy C, Melia R, Carl E, *et al.* Cardiovascular risk factors are associated with increased lesion burden and brain atrophy in multiple sclerosis. J Neurol Neurosurg Psychiatry 2016; 87(2): 181-7.

Kau T, Taschwer M, Deutschmann H, Schönfelder M, Weber JR, Hausegger KA. The “central vein sign”: is there a place for susceptibility weighted imaging in possible multiple sclerosis? Eur Radiol 2013; 23(7): 1956-62.

Keiper MD, Grossman RI, Hirsch JA, Bolinger L, Ott IL, Mannon LJ, *et al.* MR identification of white matter abnormalities in multiple sclerosis: a comparison between 1.5 T and 4 T. AJNR Am J Neuroradiol 1998; 19(8): 1489-93.

Kelly SB, Chaila E, Kinsella K, Duggan M, Walsh C, Tubridy N, *et al.* Using atypical symptoms and red flags to identify non-demyelinating disease. J Neurol Neurosurg Psychiatry 2012; 83(1): 44-8.

Kidd D, Steuer A, Denman AM, Rudge P. Neurological complications in Behçet's syndrome. Brain 1999; 122(11): 2183-94.

Kilsdonk ID, Lopez-Soriano A, Kuijer JPA, Graaf WLd, Castelijns JA, Polman CH, *et al.* Morphological features of MS lesions on FLAIR* at 7 T and their relation to patient characteristics. J Neurol 2014a; 261(7): 1356-64.

Kilsdonk ID, Wattjes MP, Lopez-Soriano A, Kuijer JPA, Jong MCd, Graaf WLd, *et al.* Improved differentiation between MS and vascular brain lesions using FLAIR* at 7 Tesla. Eur Radiol 2014b; 24(4): 841-9.

Kim KW, MacFall JR, Payne ME. Classification of white matter lesions on magnetic resonance imaging in elderly persons. Biol Psychiatry 2008; 64(4): 273-80.

Kis B, Rumberg B, Berlit P. Clinical characteristics of patients with late-onset multiple sclerosis. J Neurol 2008; 255(5): 697-702.

Kister I, Herbert J, Zhou Y, Ge Y. Ultrahigh-Field MR (7 T) Imaging of Brain Lesions in Neuromyelitis Optica. Mult Scler Int 2013; 398259.

Kitley J, Evangelou N, Küker W, Jacob A, Leite MI, Palace J. Catastrophic brain relapse in seronegative NMO after a single dose of natalizumab. J Neurol Sci 2014; 339(1–2): 223-5.

Koch-Henriksen N, Sorensen PS. The changing demographic pattern of multiple sclerosis epidemiology. Lancet Neurol 2010; 9(5): 520-32.

Korteweg T, Tintore M, Uitdehaag B, Rovira A, Frederiksen J, Miller D, *et al.* MRI criteria for dissemination in space in patients with clinically isolated syndromes: a multicentre follow-up study. Lancet Neurol 2006; 5(3): 221-7.

Kremenchutzky M, Rice GP, Baskerville J, Wingerchuk DM, Ebers GC. The natural history of multiple sclerosis: a geographically based study 9: observations on the progressive phase of the disease. Brain 2006; 129(Pt 3): 584-94.

Kruit MC, Launer LJ, Ferrari MD, van Buchem MA. Brain Stem and Cerebellar Hyperintense Lesions in Migraine. Stroke 2006; 37(4): 1109-12.

Kruit MC, van Buchem MA, Hofman PM, et al. Migraine as a risk factor for subclinical brain lesions. JAMA 2004; 291(4): 427-34.

Krupp LB, Tardieu M, Amato MP, Banwell B, Chitnis T, Dale RC, *et al.* International Pediatric Multiple Sclerosis Study Group criteria for pediatric multiple sclerosis and immune-mediated central nervous system demyelinating disorders: revisions to the 2007 definitions. Mult Scler 2013; 19(10): 1261-7.

Kuchling J, Ramien C, Bozin I, Dörr J, Harms L, Rosche B, *et al.* Identical lesion morphology in primary progressive and relapsing–remitting MS –an ultrahigh field MRI study. Mult Scler 2014; 20(14): 1866-71.

Kuhlmann T, Ludwin S, Prat A, Antel J, Brück W, Lassmann H. An updated histological classification system for multiple sclerosis lesions. Acta Neuropathol 2017; 133(1): 13-24.

Kurne A, Isikay IC, Karlioguz K, Kalyoncu U, Aydin OF, Calguneri M, *et al.* A clinically isolated syndrome: A challenging entity. J Neurol 2008; 255(11): 1625-35.

Kurtzke JF. A reassessment of the distribution of multiple sclerosis. Acta Neurol Scand 1975; 51(2): 110-36.

Kutzelnigg A, Faber-Rod JC, Bauer J, Lucchinetti CF, Sorensen PS, Laursen H, *et al.* Widespread demyelination in the cerebellar cortex in multiple sclerosis. Brain Pathol 2007; 17(1): 38-44.

Kutzelnigg A, Lucchinetti CF, Stadelmann C, Brück W, Rauschka H, Bergmann M, *et al.* Cortical demyelination and diffuse white matter injury in multiple sclerosis. Brain 2005; 128(Pt 11): 2705-12.

Lacomis D. Neurosarcoidosis. Curr Neuropharmacol 2011; 9(3): 429-436.

Lambert C, Benjamin P, Zeestraten E, Lawrence AJ, Barrick TR, Markus HS. Longitudinal patterns of leukoaraiosis and brain atrophy in symptomatic small vessel disease. Brain 2016; 139(Pt 4): 1136-51.

Lassmann H. Multiple sclerosis: lessons from molecular neuropathology. Exp Neurol 2014; 262 Pt A: 2-7.

Lebrun C, Bensa C, Debouverie M, Wiertlevski S, Brassat D, de Seze J et al. Association between clinical conversion to multiple sclerosis in radiologically isolated syndrome and magnetic resonance imaging, cerebrospinal fluid, and visual evoked potential: Follow-up of 70 patients. Arch Neurol 2009; 66(7): 841-6.

Lee SH, Yoon PH, Park SJ, Kim DI. MRI Findings in Neuro-Behçet's Disease. Clin Radiol 2001; 56(6): 485-94.

Levin N, Mor M, Ben-Hur T. Patterns of misdiagnosis of multiple sclerosis. Isr Med Assoc J 2003; 5(7): 489-90.

Lipton M. Totally Accessible MRI. A Users Guide to Principles, Technology, and Applications. New York: Springer; 2008.

Liu S, Kullnat J, Bourdette D, Simon J, Kraemer DF, Murchison C, *et al.* Prevalence of brain magnetic resonance imaging meeting Barkhof and McDonald criteria for dissemination in space among headache patients. Mult Scler 2013; 19(8): 1101-5.

Llufriu S, Pujol T, Blanco Y, Hankiewicz K, Squarcia M, Berenguer J, *et al.* T2 hypointense rims and ring-enhancing lesions in MS. Mult Scler 2010; 16(11): 1317-25.

Love S, Louis, DN, Ellison, DW, editor. Greenfield's Neuropathology. 8th ed. London: Hodder Arnold; 2008.

Lublin FD, Reingold SC, Cohen JA, Cutter GR, Sørensen PS, Thompson AJ, *et al.* Defining the clinical course of multiple sclerosis: the 2013 revisions. Neurology 2014; 83(3): 278-86.

Lucatelli P, Montisci R, Sanfilippo R, Sacconi B, Suri JS, Catalano C, *et al.* Is there an association between leukoaraiosis volume and diabetes? J Neuroradiol 2015.

Lucchinetti C, Bruck W. The pathology of primary progressive multiple sclerosis. Mult Scler 2004; 10 Suppl 1: S23-30.

Lucchinetti C, Brück W, Parisi J, Scheithauer B, Rodriguez M, Lassmann H. Heterogeneity of multiple sclerosis lesions: Implications for the pathogenesis of demyelination. Ann Neurol 2000; 47(6): 707-17.

Lucchinetti CF, Guo Y, Popescu BFG, Fujihara K, Itoyama Y, Misu T. The Pathology of an Autoimmune Astrocytopathy: Lessons Learned from Neuromyelitis Optica. Brain Pathol 2014; 24(1): 83-97.

Lucchinetti CF, Popescu BF, Bunyan RF, Moll NM, Roemer SF, Lassmann H, *et al.* Inflammatory cortical demyelination in early multiple sclerosis. N Engl J Med 2011; 365(23): 2188-97.

Lummel N, Boeckh-Behrens T, Schoepf V, Burke M, Brückmann H, Linn J. Presence of a central vein within white matter lesions on susceptibility weighted imaging: a specific finding for multiple sclerosis? Neuroradiology 2011; 53(5): 311-7.

Lycke JN, Karlsson JE, Andersen O, Rosengren LE. Neurofilament protein in cerebrospinal fluid: a potential marker of activity in multiple sclerosis. J Neurol Neurosurg Psychiatry 1998; 64(3): 402-4.

Mackenzie IS, Morant SV, Bloomfield GA, MacDonald TM, O'Riordan J. Incidence and prevalence of multiple sclerosis in the UK 1990-2010: a descriptive study in the General Practice Research Database. J Neurol Neurosurg Psychiatry 2014; 85(1): 76-84.

Mahad DH, Trapp BD, Lassmann H. Pathological mechanisms in progressive multiple sclerosis. Lancet Neurol 2015; 14(2): 183-93.

Mainero C, Benner T, Radding A, van der Kouwe A, Jensen R, Rosen BR, *et al.* In vivo imaging of cortical pathology in multiple sclerosis using ultra-high field MRI. Neurology 2009; 73(12): 941-8.

Marrie RA. Environmental risk factors in multiple sclerosis aetiology. Lancet Neurol 2004; 3(12): 709-18.

Marrie RA, Rudick R, Horwitz R, Cutter G, Tyry T, Campagnolo D, *et al.* Vascular comorbidity is associated with more rapid disability progression in multiple sclerosis. Neurology 2010; 74(13): 1041-7.

Martinelli V, Dalla Costa G, Colombo B, Dalla Libera D, Rubinacci A, Filippi M *et al.* Vitamin D levels and risk of multiple sclerosis in patients with clinically isolated syndromes. Mult Scler 2014; 20(2): 147-55.

Martinelli V, Rodegher M, Moiola L, Comi G. Late onset multiple sclerosis: clinical characteristics, prognostic factors and differential diagnosis. Neurological Sciences 2004; 25(4): s350-s5.

Matthews L, Marasco R, Jenkinson M, Kuker W, Luppe S, Leite MI, *et al.* Distinction of seropositive NMO spectrum disorder and MS brain lesion distribution. Neurology 2013; 80(14): 1330-7.

McDonald WI, Compston A, Edan G, Goodkin D, Hartung H-P, Lublin FD, *et al.* Recommended diagnostic criteria for multiple sclerosis: Guidelines from the international panel on the diagnosis of multiple sclerosis. Ann Neurol 2001; 50(1): 121-7.

McRobbie D, Moore E, Graves M, Prince M. MRI. From picture to proton. USA: Cambridge University Press; 2006.

Menke RA, Gray E, Lu CH, Kuhle J, Talbot K, Malaspina A, *et al.* CSF neurofilament light chain reflects corticospinal tract degeneration in ALS. Ann Clin Transl Neurol 2015; 2(7): 748-55.

Miller AE, Pelletier, D. Multiple Sclerosis. Rapid diagnosis or right diagnosis? Neurology 2016; 16;87(7):652-3.

Miller DH, Kendall BE, Johnson SBG, MacManus DG, Logsdail SJ, Ormerod IEC, *et al.* Magnetic resonance imaging in central nervous system sarcoidosis. Neurology 1988; 38(3): 378-83.

Miller DH, Leary SM. Primary-progressive multiple sclerosis. Lancet Neurol 2007; 6(10): 903-12.

Miller DH, Weinshenker BG, Filippi M, Banwell BL, Cohen JA, Freedman MS, *et al.* Differential diagnosis of suspected multiple sclerosis: a consensus approach. Mult Scler 2008; 14(9): 1157-74.

Milo R, Miller A. Revised diagnostic criteria of multiple sclerosis. Autoimmunity Reviews 2014; 13(4–5): 518-24.

Mistry N, Abdel-Fahim R, Samaraweera A, Mougin O, Tallantyre E, Tench C, *et al.* Imaging central veins in brain lesions with 3-T T2*-weighted magnetic resonance imaging differentiates multiple sclerosis from microangiopathic brain lesions. Mult Scler 2016; 22(10): 1289-96.

Mistry N, Dixon J, Tallantyre E, Tench C, Abdel-Fahim R, Jaspan T et al. Central veins in brain lesions visualized with high-field magnetic resonance imaging: A pathologically specific diagnostic biomarker for inflammatory demyelination in the brain. JAMA Neurology 2013; 70(5): 623-8.

Moll NM, Rietsch AM, Ransohoff AJ, Cossoy MB, Huang D, Eichler FS, *et al.* Cortical demyelination in PML and MS: Similarities and differences. Neurology 2008; 70(5): 336-43.

Molyneux PD, Tubridy N, Parker GJ, Barker GJ, MacManus DG, Tofts PS, *et al.* The effect of section thickness on MR lesion detection and quantification in multiple sclerosis. AJNR Am J Neuroradiol 1998; 19(9): 1715-20.

Montalban X, Hauser SL, Kappos L, Arnold DL, Bar-Or A, Comi G, *et al.* Ocrelizumab versus Placebo in Primary Progressive Multiple Sclerosis. N Engl J Med 2017; 19;376(3):209-220.

Morrissey SP, Miller DH, Hermaszewski R, Rudge P, MacManus DG, Kendall B, *et al.* Magnetic Resonance Imaging of the Central Nervous System in Behçets Disease. Eur Neurol 1993; 33(4): 287-93.

Motulsky H. Intuitive Biostatistics. New York: Oxford University Press, Inc; 1995.

Muller K, Kuchling J, Dorr J, Harms L, Ruprecht K, Niendorf T, *et al.* Detailing intra-lesional venous lumen shrinking in multiple sclerosis investigated by sFLAIR MRI at 7-T. J Neurol 2014; 261(10): 2032-6.

Murray AD, Staff RT, Shenkin SD, Deary IJ, Starr JM, Whalley LJ. Brain white matter hyperintensities: relative importance of vascular risk factors in nondemented elderly people. Radiology 2005; 237(1): 251-7.

Nerrant E, Salsac C, Charif M, Ayrignac X, Carra-Dalliere C, Castelnovo G, *et al.* Lack of confirmation of anti-inward rectifying potassium channel 4.1 antibodies as reliable markers of multiple sclerosis. Mult Scler 2014; 20(13): 1699-703.

Nielsen JM, Korteweg T, Barkhof F, Uitdehaag BMJ, Polman CH. Overdiagnosis of multiple sclerosis and magnetic resonance imaging criteria. Ann Neurol 2005; 58(5): 781-3.

Nielsen JM, Uitdehaag BMJ, Korteweg T, Barkhof F, Polman CH. Performance of the Swanton multiple sclerosis criteria for dissemination in space. Mult Scler 2010; 16(8): 985-7.

Nielsen TR, Rostgaard K, Askling J, Steffensen R, Oturai A, Jersild C, *et al.* Effects of infectious mononucleosis and HLA-DRB1*15 in multiple sclerosis. Mult Scler 2009; 15(4): 431-6.

Nitz WR, Reimer P. Contrast mechanisms in MR imaging. Eur Radiol 1999; 9(6): 1032-46.

Noseworthy J, Paty D, Wonnacott T, Feasby T, Ebers G. Multiple sclerosis after age 50. Neurology 1983; 33(12): 1537-44.

Nozaki H, Shimohata T, Kanbayashi T, Sagawa Y, Katada S-i, Satoh M, *et al.* A patient with anti-aquaporin 4 antibody who presented with recurrent hypersomnia, reduced orexin (hypocretin) level, and symmetrical hypothalamic lesions. Sleep Medicine 2009; 10(2): 253-5.

O'Gorman C, Lucas R, Taylor B. Environmental risk factors for multiple sclerosis: a review with a focus on molecular mechanisms. Int J Mol Sci 2012; 13(9): 11718-52.

O'Riordan JI, Thompson AJ, Kingsley DP, MacManus DG, Kendall BE, Rudge P, *et al.* The prognostic value of brain MRI in clinically isolated syndromes of the CNS. A 10-year follow-up. Brain 1998; 121 (Pt 3): 495-503.

O'Riordan S, Nor AM, Hutchinson M. CADASIL imitating multiple sclerosis: the importance of MRI markers. Mult Scler 2002; 8(5): 430-2.

Okuda DT, Mowry EM, Beheshtian A, Waubant E, Baranzini SE, Goodin DS, *et al.* Incidental MRI anomalies suggestive of multiple sclerosis The radiologically isolated syndrome. Neurology 2009; 72(9): 800-5.

Okuda DT, Mowry EM, Cree BaC, Crabtree EC, Goodin DS, Waubant E, *et al.* Asymptomatic spinal cord lesions predict disease progression in radiologically isolated syndrome. Neurology 2011; 76(8): 686-92.

Okuda DT, Siva A, Kantarci O, Inglese M, Katz I, Tutuncu M, *et al.* Radiologically Isolated Syndrome: 5-Year Risk for an Initial Clinical Event. PLoS One 2014; 9(3).

Orton SM, Wald L, Confavreux C, Vukusic S, Krohn JP, Ramagopalan SV, *et al.* Association of UV radiation with multiple sclerosis prevalence and sex ratio in France. Neurology 2011; 76(5): 425-31.

Palace J. Making the Diagnosis of Multiple Sclerosis. J Neurol, Neurosurg Psychiatry 2001; 71(suppl 2): ii3-ii8.

Palace J, Leite M, Nairne A, Vincent A. Interferon beta treatment in neuromyelitis optica: Increase in relapses and aquaporin 4 antibody titers. Arch Neurol 2010; 67(8): 1016-7.

Pandey T, Abubacker S. Cerebral Autosomal Dominant Arteriopathy with Subcortical Infarcts and Leukoencephalopathy: An Imaging Mimic of Multiple Sclerosis. Medical Principles and Practice 2006; 15(5): 391-5.

Papathanasopoulos PG, Nikolakopoulou A, Scolding NJ. Disclosing the diagnosis of multiple sclerosis. J Neurol 2005; 252(11): 1307-9.

Paty DW, Li DK, Oger JJ, Kastrukoff L, Koopmans R, Tanton E, *et al.* Magnetic resonance imaging in the evaluation of clinical trials in multiple sclerosis. Ann Neurol 1994; 36 Suppl: S95-6.

Pawate S, Moses H, Sriram S. Presentations and outcomes of neurosarcoidosis: a study of 54 cases. QJM 2009; 102(7): 449-60.

Pelidou S-H, Giannopoulos S, Tzavidi S, Tsifetaki N, Kitsos G, Stefanou D, *et al.* Neurological manifestations of connective tissue diseases mimicking multiple sclerosis. Rheumatology International 2007; 28(1): 15-20.

Pittock SJ, Lennon VA, Krecke K, Wingerchuk DM, Lucchinetti CF, Weinshenker BG. Brain abnormalities in neuromyelitis optica. Arch Neurol 2006; 63(3): 390-6.

Polman CH, Reingold SC, Banwell B, Clanet M, Cohen JA, Filippi M, *et al.* Diagnostic criteria for multiple sclerosis: 2010 Revisions to the McDonald criteria. Ann Neurol 2011; 69(2): 292-302.

Polman CH, Reingold SC, Edan G, Filippi M, Hartung H-P, Kappos L, *et al.* Diagnostic criteria for multiple sclerosis: 2005 revisions to the "McDonald Criteria". Ann Neurol 2005; 58(6): 840-6.

Popescu BF, Parisi JE, Cabrera-Gómez JA, Newell K, Mandler RN, Pittock SJ, *et al.* Absence of cortical demyelination in neuromyelitis optica. Neurology 2010; 75(23): 2103-9.

Poppe AY, Lapierre Y, Melançon D, Lowden D, Wardell L, Fullerton LM, *et al.* Neuromyelitis optica with hypothalamic involvement. Mult Scler 2005; 11(5): 617-21.

Poser CM. Misdiagnosis of multiple sclerosis and β-interferon. The Lancet 1997; 349(9069).

Poser CM, Paty DW, Scheinberg L, McDonald WI, Davis FA, Ebers GC, *et al.* New diagnostic criteria for multiple sclerosis: Guidelines for research protocols. Ann Neurol 1983; 13(3): 227-31.

Power MC, Deal JA, Sharrett AR, Jack CR, Jr., Knopman D, Mosley TH, *et al.* Smoking and white matter hyperintensity progression: the ARIC-MRI Study. Neurology 2015; 84(8): 841-8.

Presslauer S, Milosavljevic D, Huebl W, Aboulenein-Djamshidian F, Krugluger W, Deisenhammer F, *et al.* Validation of kappa free light chains as a diagnostic biomarker in multiple sclerosis and clinically isolated syndrome: A multicenter study. Mult Scler 2016; 22(4): 502-510.

Quan C, ZhangBao J, Luo S, Fang K, Xi J, Du Z, *et al.* Multiple deep white matter lesions mimic multiple sclerosis as an unusual complication of left atrial myxoma. Mult Scler 2015; 21(1):108-10.

Quinn MP, Kremenchutzky M, Menon RS. Venocentric lesions: an MRI marker of MS? Front Neurol 2013; Jul 22;4:98.

Radbruch A, Weberling LD, Kieslich PJ, Eidel O, Burth S, Kickingereder P, *et al.* Gadolinium retention in the dentate nucleus and globus pallidus is dependent on the class of contrast agent. Radiology 2015; 275(3): 783-91.

Rae-Grant AD, Wong C, Bernatowicz R, Fox RJ. Observations on the brain vasculature in multiple sclerosis: A historical perspective. Multiple Sclerosis and Related Disorders 2014; 3(2): 156-62.

Rammohan KW. Cerebrospinal fluid in multiple sclerosis. Ann Indian Acad Neurol 2009; 12(4): 246-253.

Revesz T, Kidd D, Thompson AJ, Barnard RO, McDonald WI. A comparison of the pathology of primary and secondary progressive multiple sclerosis. Brain 1994; 117 (Pt 4): 759-65.

Rich-Edwards JW, Manson JE, Hennekens CH, Buring JE. The primary prevention of coronary heart disease in women. N Engl J Med 1995; 332(26): 1758-66.

Robinson RJ, Bhuta S. Susceptibility-weighted imaging of the brain: current utility and potential applications. J Neuroimaging 2011; 21(4): e189-204.

Rocha AJd, Littig IA, Nunes RH, Tilbery CP. Central nervous system infectious diseases mimicking multiple sclerosis: recognizing distinguishable features using MRI. Arquivos de Neuro-Psiquiatria 2013; 71(9B): 738-46.

Rojas GM, Raff U, Quintana JC, Huete I, Hutchinson M. Image fusion in neuroradiology: three clinical examples including MRI of Parkinson disease. Comput Med Imaging Graph 2007; 31(1): 17-27.

Rossato G, Adami A, Thijs VN, Cerini R, Pozzi-Mucelli R, Mazzucco S, *et al.* Cerebral distribution of white matter lesions in migraine with aura patients. Cephalalgia 2010; 30(7): 855-9.

Rovaris M, Gawne-Cain ML, Sormani MP, Miller DH, Filippi M. The effect of repositioning on brain MRI lesion load assessment in multiple sclerosis: reliability of subjective quality criteria. J Neurol 1998; 245(5): 273-5.

Rovaris M, Viti B, Ciboddo G, Gerevini S, Capra R, Iannucci G, *et al.* Brain involvement in systemic immune mediated diseases: magnetic resonance and magnetisation transfer imaging study. J Neurol Neurosurg Psychiatry 2000; 68(2): 170-7.

Salzer J, Svenningsson A, Sundstrom P. Neurofilament light as a prognostic marker in multiple sclerosis. Mult Scler 2010; 16(3): 287-92.

Sanchez Aliaga E, Barkhof, F. Multiple Sclerosis and Related Disorders. In: Goodin DS, editor. Handbook of Clinical Neurology: Elsevier; 2014. p. 291 - 316.

Sati P, George IC, Shea CD, Gaitán MI, Reich DS. FLAIR*: A Combined MR Contrast Technique for Visualizing White Matter Lesions and Parenchymal Veins. Radiology 2012; 265(3): 926-32.

Sati P, Thomasson DM, Li N, Pham DL, Biassou NM, Reich DS, *et al.* Rapid, high-resolution, whole-brain, susceptibility-based MRI of multiple sclerosis. Mult Scler 2014; 20(11): 1464-70.

Scalfari A, Neuhaus A, Degenhardt A, Rice G, Muraro P, Daumer M, *et al.* The natural history of multiple sclerosis, a geographically based study 10: relapses and long-term disability. Brain 2010; 133(7); 1914-1929.

Schild H. MRI made easy. Berlin: Schering AG; 1990.

Schmierer K, Parkes HG, So PW, An SF, Brandner S, Ordidge RJ, *et al.* High field (9.4 Tesla) magnetic resonance imaging of cortical grey matter lesions in multiple sclerosis. Brain 2010; 133(Pt 3): 858-67.

Schmitz SA, O'Regan DP, Fitzpatrick J, Neuwirth C, Potter E, Tosi I, *et al.* MRI at 3 Tesla detects no evidence for ischemic brain damage in intensively treated patients with homozygous familial hypercholesterolemia. Neuroradiology 2007; 49(11): 927-31.

Schneider R. Autoantibodies to Potassium Channel KIR4.1 in Multiple Sclerosis. Front Neurol 2013; 4: 125.

Schumacher GA, Beebe G, Kibler RF, Kurland LT, Kurtzke JF, McDowell F, *et al.* Problems of Experimental Trials of Therapy in Multiple Sclerosis: Report by the Panel on the Evaluation of Experimental Trials of Therapy in Multiple Sclerosis. Ann N Y Acad Sci 1965; 122(1): 552-68.

Scolding N, Barnes D, Cader S, Chataway J, Chaudhuri A, Coles A, *et al.* Association of British Neurologists: revised (2015) guidelines for prescribing disease-modifying treatments in multiple sclerosis. Pract Neurol 2015; 15(4): 273-9.

Selchen D, Bhan V, Blevins G, Devonshire V, Duquette P, Grand'Maison F, *et al.* MS, MRI, and the 2010 McDonald criteria A Canadian expert commentary. Neurology 2012; 79(23 Supplement 2): S1-S15.

Sellner J, Schirmer L, Hemmer B, Mühlau M. The radiologically isolated syndrome: take action when the unexpected is uncovered? J Neurol 2010; 257(10): 1602-11.

Senel M, Tumani H, Lauda F, Presslauer S, Mojib-Yezdani R, Otto M, *et al.* Cerebrospinal Fluid Immunoglobulin Kappa Light Chain in Clinically Isolated Syndrome and Multiple Sclerosis. PLoS ONE 2014; 9(4):e88680.

Seneviratne U, Chong W, Billimoria PH. Brain white matter hyperintensities in migraine: Clinical and radiological correlates. Clin Neurol Neurosurg 2013; 115(7): 1040-3.

Shams S, Martola J, Cavallin L, Granberg T, Shams M, Aspelin P, *et al.* SWI or T2*: which MRI sequence to use in the detection of cerebral microbleeds? The Karolinska Imaging Dementia Study. AJNR Am J Neuroradiol 2015; 36(6): 1089-95.

Sicotte NL, Voskuhl RR, Bouvier S, Klutch R, Cohen MS, Mazziotta JC. Comparison of multiple sclerosis lesions at 1.5 and 3.0 Tesla. Invest Radiol 2003; 38(7): 423-7.

Simpson S, Blizzard L, Otahal P, Van der Mei I, Taylor B. Latitude is significantly associated with the prevalence of multiple sclerosis: a meta-analysis. J Neurol Neurosurg Psychiatry 2011; 82(10): 1132-41.

Sinnecker T, Dörr J, Pfueller CF, Harms L, Ruprecht K, Jarius S, *et al.* Distinct lesion morphology at 7-T MRI differentiates neuromyelitis optica from multiple sclerosis. Neurology 2012; 79(7): 708-14.

Siva A. Asymptomatic MS. Clin Neurol Neurosurg 2013; 115, Supplement 1: S1-S5.

Siva A, Saip S, Altintas A, Jacob A, Keegan BM, Kantarci OH. Multiple sclerosis risk in radiologically uncovered asymptomatic possible inflammatory-demyelinating disease. Mult Scler 2009; 15(8): 918-27.

Skillback T, Farahmand B, Bartlett JW, Rosen C, Mattsson N, Nagga K, *et al.* CSF neurofilament light differs in neurodegenerative diseases and predicts severity and survival. Neurology 2014; 83(21): 1945-53.

Smith AS, Meisler DM, Weinstein MA, Tomsak RL, Hanson MR, Rudick RA, *et al.* High-signal periventricular lesions in patients with sarcoidosis: neurosarcoidosis or multiple sclerosis? American Journal of Roentgenology 1989; 153(1): 147-52.

Smolders J, Menheere P, Kessels A, Damoiseaux J, Hupperts R. Association of vitamin D metabolite levels with relapse rate and disability in multiple sclerosis. Mult Scler 2008; 14(9): 1220-4.

Soljanlahti S, Autti T, Lauerma K, Raininko R, Keto P, Turtola H, *et al.* Familial hypercholesterolemia patients treated with statins at no increased risk for intracranial vascular lesions despite increased cholesterol burden and extracranial atherosclerosis. Stroke 2005; 36(7): 1572-4.

Solomon AJ, Klein EP, Bourdette D. "Undiagnosing" multiple sclerosis The challenge of misdiagnosis in MS. Neurology 2012; 78(24): 1986-91.

Solomon AJ, Schindler MK, Howard DB, Watts R, Sati P, Nickerson JP, *et al.* "Central vessel sign" on 3T FLAIR* MRI for the differentiation of multiple sclerosis from migraine. Ann Clin Transl Neurol 2016; 3(2): 82-7.

Solomon AJ, Weinshenker BG. Misdiagnosis of Multiple Sclerosis: Frequency, Causes, Effects, and Prevention. Current Neurology and Neuroscience Reports 2013; 13(12): 1-7.

Soman S, Holdsworth SJ, Barnes PD, Rosenberg J, Andre JB, Bammer R, *et al.* Improved T2* imaging without increase in scan time: SWI processing of 2D gradient echo. AJNR Am J Neuroradiol 2013; 34(11): 2092-7.

Srivastava R, Aslam M, Kalluri SR, Schirmer L, Buck D, Tackenberg B, *et al.* Potassium channel KIR4.1 as an immune target in multiple sclerosis. N Engl J Med 2012; 367(2): 115-23.

Staals J, Makin SD, Doubal FN, Dennis MS, Wardlaw JM. Stroke subtype, vascular risk factors, and total MRI brain small-vessel disease burden. Neurology 2014; 83(14): 1228-34.

Stevenson VL, Miller DH, Rovaris M, Barkhof F, Brochet B, Dousset V, *et al.* Primary and transitional progressive MS: a clinical and MRI cross-sectional study. Neurology 1999; 52(4): 839-45.

Susac JO, Murtagh FR, Egan RA, Berger JR, Bakshi R, Lincoff N, *et al.* MRI findings in Susac's syndrome. Neurology 2003; 61(12): 1783-7.

Suzuki K, Nakamura T, Hashimoto K, Miyamoto M, Komagamine T, Nagashima T *et al.* Hypothermia, hypotension, hypersomnia, and obesity associated with hypothalamic lesions in a patient positive for the anti–aquaporin 4 antibody: A case report and literature review. Arch Neurol 2012; 69(10): 1355-9.

Swanton JK, Rovira A, Tintore M, Altmann DR, Barkhof F, Filippi M, *et al.* MRI criteria for multiple sclerosis in patients presenting with clinically isolated syndromes: a multicentre retrospective study. Lancet Neurol 2007; 6(8): 677-86.

Szmyrka-Kaczmarek M, Pokryszko-Dragan A, Pawlik B, Gruszka E, Korman L, Podemski R, *et al.* Antinuclear and antiphospholipid antibodies in patients with multiple sclerosis. Lupus 2012; 21(4): 412-20.

Tackley G, Kuker W, Palace J. Magnetic resonance imaging in neuromyelitis optica. Mult Scler 2014; 20(9): 1153-64

Tallantyre EC, Brookes MJ, Dixon JE, Morgan PS, Evangelou N, Morris PG. Demonstrating the Perivascular Distribution of MS Lesions in Vivo with 7-Tesla MRI. Neurology 2008; 70(22): 2076-8.

Tallantyre EC, Dixon JE, Donaldson I, Owens T, Morgan PS, Morris PG, *et al.* Ultra-high-field imaging distinguishes MS lesions from asymptomatic white matter lesions. Neurology 2011; 76(6): 534-9.

Tan IL, van Schijndel RA, Pouwels PJW, van Walderveen MA, Reichenbach JR, Manoliu RA, *et al.* MR Venography of Multiple Sclerosis. AJNR Am J Neuroradiol 2000; 21(6): 1039-42.

Taylor BV, Pearson JF, Clarke G, Mason DF, Abernethy DA, Willoughby E. MS prevalence in New Zealand, an ethnically and latitudinally diverse country. Mult Scler 2010; 16(12): 1422-31.

Thompson AJ, Kermode AG, MacManus DG, Kendall BE, Kingsley DP, Moseley IF *et al.* Patterns of disease activity in multiple sclerosis: clinical and magnetic resonance imaging study. BMJ 1990; 300(6725): 631-4.

Tiehuis AM, van der Graaf Y, Visseren FL, Vincken KL, Biessels GJ, Appelman AP, *et al.* Diabetes increases atrophy and vascular lesions on brain MRI in patients with symptomatic arterial disease. Stroke 2008; 39(5): 1600-3.

Tintoré M, Rovira A, Rio J, Otero-Romero S, Arrambide G, Tur C, *et al.* Defining high, medium and low impact prognostic factors for developing multiple sclerosis. Brain 2015; 138(Pt 7): 1863-74.

Tintoré M, Rovira A, Martínez MJ, Rio J, Díaz-Villoslada P, Brieva L, *et al.* Isolated Demyelinating Syndromes: Comparison of Different MR Imaging Criteria to Predict Conversion to Clinically Definite Multiple Sclerosis. AJNR Am J Neuroradiol 2000; 21(4): 702-6.

Tong KA, Ashwal S, Obenaus A, Nickerson JP, Kido D, Haacke EM. Susceptibility-weighted MR imaging: a review of clinical applications in children. AJNR Am J Neuroradiol 2008; 29(1): 9-17.

Tornatore C, Phillips JT, Khan O, Miller AE, Barnes CJ. Practice patterns of US neurologists in patients with CIS, RRMS, or RIS. Neurology Clinical Practice 2012; 2(1): 48-57.

Traboulsee A, Simon JH, Stone L, Fisher E, Jones DE, Malhotra A, *et al.* Revised Recommendations of the Consortium of MS Centers Task Force for a Standardized MRI Protocol and Clinical Guidelines for the Diagnosis and Follow-Up of Multiple Sclerosis. AJNR Am J Neuroradiol 2016; 37(3): 394-401.

Verhey LH, Branson HM, Shroff MM, Callen DJA, Sled JG, Narayanan S, *et al.* MRI parameters for prediction of multiple sclerosis diagnosis in children with acute CNS demyelination: a prospective national cohort study. Lancet Neurol 2011; 10(12): 1065-73.

Vernooij MW, Ikram MA, Wielopolski PA, Krestin GP, Breteler MM, van der Lugt A. Cerebral microbleeds: accelerated 3D T2*-weighted GRE MR imaging versus conventional 2D T2*-weighted GRE MR imaging for detection. Radiology 2008; 248(1): 272-7.

Vidal-Jordana A, Sastre-Garriga J, Pareto D, Tur C, Arrambide G, Otero-Romero S, *et al.* Brain atrophy 15 years after CIS: Baseline and follow-up clinico-radiological correlations. Mult Scler 2017; Apr 1:1352458517707070. doi: 10.1177/1352458517707070. [Epub ahead of print]

Viegas S, Weir A, Esiri M, Kuker W, Waters P, Leite MI, *et al.* Symptomatic, radiological and pathological involvement of the hypothalamus in neuromyelitis optica. J Neurol Neurosurg Psychiatry 2009; 80(6): 679-82.

Wang L, Lai H, Thompson A, Miller D. Survey of the distribution of lesion size in multiple sclerosis: implication for the measurement of total lesion load. J Neurol Neurosurg Psychiatry 1997; 63(4): 452-5.

Wardlaw JM, Smith EE, Biessels GJ, Cordonnier C, Fazekas F, Frayne R, *et al.* Neuroimaging standards for research into small vessel disease and its contribution to ageing and neurodegeneration. Lancet Neurol 2013; 12(8): 822-38.

Wen W and Sachdev P. The topography of white matter hyperintensities on brain MRI in healthy 60- to 64-year-old individuals. Neuroimage 2004; 22(1): 144-54.

Wingerchuk DM, Banwell B, Bennett JL, Cabre P, Carroll W, Chitnis T, *et al.* International consensus diagnostic criteria for neuromyelitis optica spectrum disorders. Neurology 2015; 85(2): 177-89.

Wingerchuk DM, Lennon VA, Lucchinetti CF, Pittock SJ, Weinshenker BG. The spectrum of neuromyelitis optica. Lancet Neurol 2007; 6(9): 805-15.

Wuerfel J, Sinnecker T, Ringelstein EB, Jarius S, Schwindt W, Niendorf T, *et al.* Lesion morphology at 7 Tesla MRI differentiates Susac syndrome from multiple sclerosis. Mult Scler 2012; 18(11): 1592-9.

Young NP, Weinshenker BG, Parisi JE, Scheithauer B, Giannini C, Roemer SF, *et al.* Perivenous demyelination: association with clinically defined acute disseminated encephalomyelitis and comparison with pathologically confirmed multiple sclerosis. Brain 2010; 133(2): 333-48.

Zajicek JP, Scolding NJ, Foster O, Rovaris M, Evanson J, Moseley IF, *et al.* Central nervous system sarcoidosis—diagnosis and management. QJM 1999; 92(2): 103-17.

Zivadinov R, Weinstock-Guttman B, Hashmi K, Abdelrahman N, Stosic M, Dwyer M, *et al.* Smoking is associated with increased lesion volumes and brain atrophy in multiple sclerosis. Neurology 2009; 73(7): 504-10.

Zwanenburg JJM, Versluis MJ, Luijten PR, Petridou N. Fast high resolution whole brain T2* weighted imaging using echo planar imaging at 7 T. NeuroImage 2011; 56(4): 1902-7.

Appendix A

Magnitude

Phase

Raw data (magnitude and phase maps) generated directly from the MR scanner. The phase data needs to have inhomogeneities removed after acquisition.

Phase mask

Phase image with inhomogeneities removed

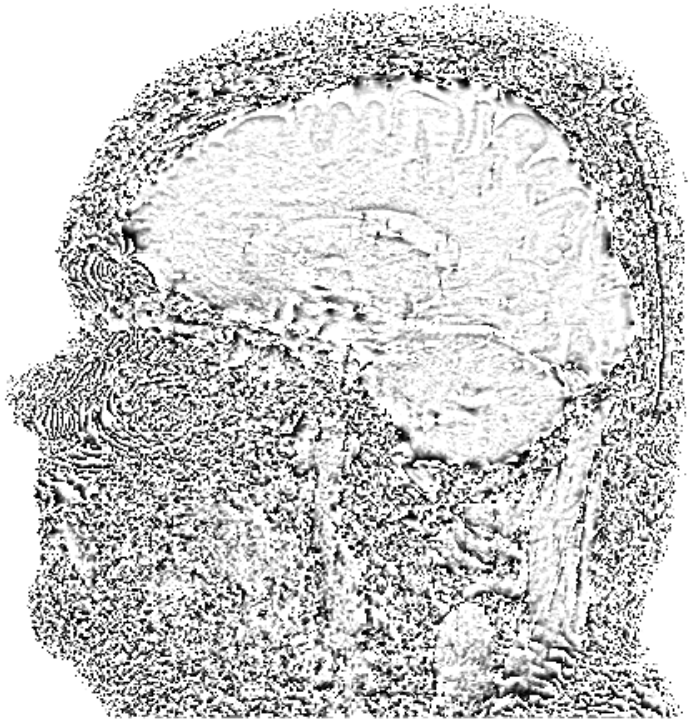

The filtered phase image is multiplied by itself 4 times (see text 3.2.3) to produce the phase mask, which causes greater contrast between veins and brain parenchyma.

SWI

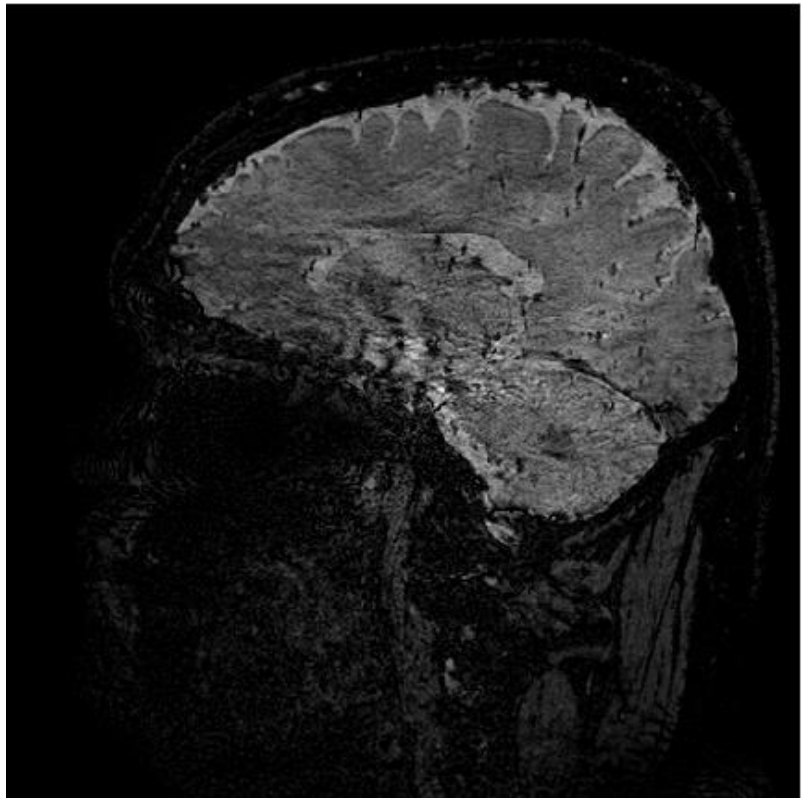

The phase mask is multiplied by the magnitude image to produce SWI.

Appendix B

Infratentorial WMLs with central veins using FLAIR-SWI-2

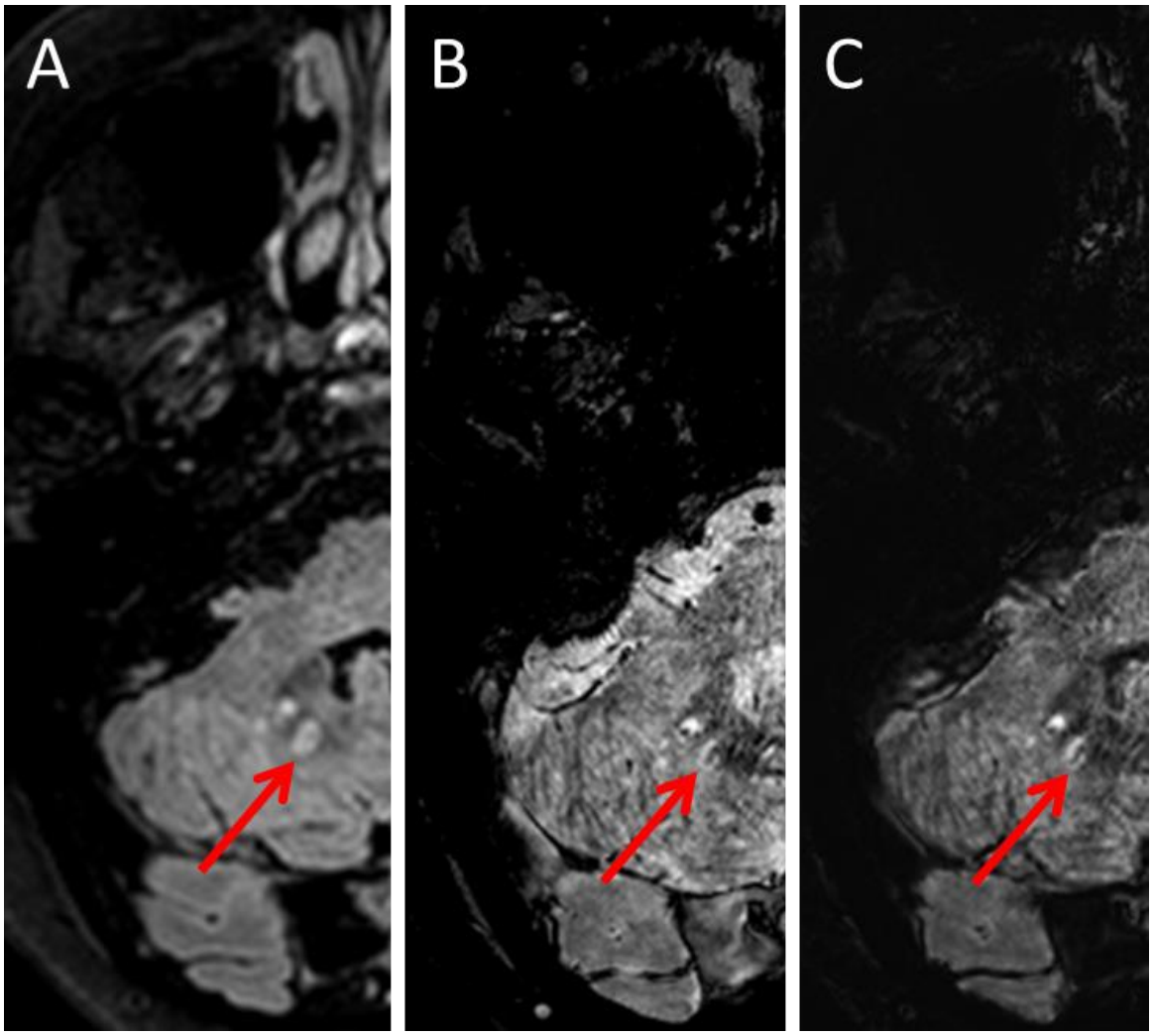

Figure B1. Infratentorial MS lesion in the cerebellum. (A) shows the lesion on FLAIR, (B) is a T2* hEPI image which shows the lesion reasonably well, (C) is a FLAIR-SWI-2 scan which clearly depicts a well demarcated lesion with a central vein.

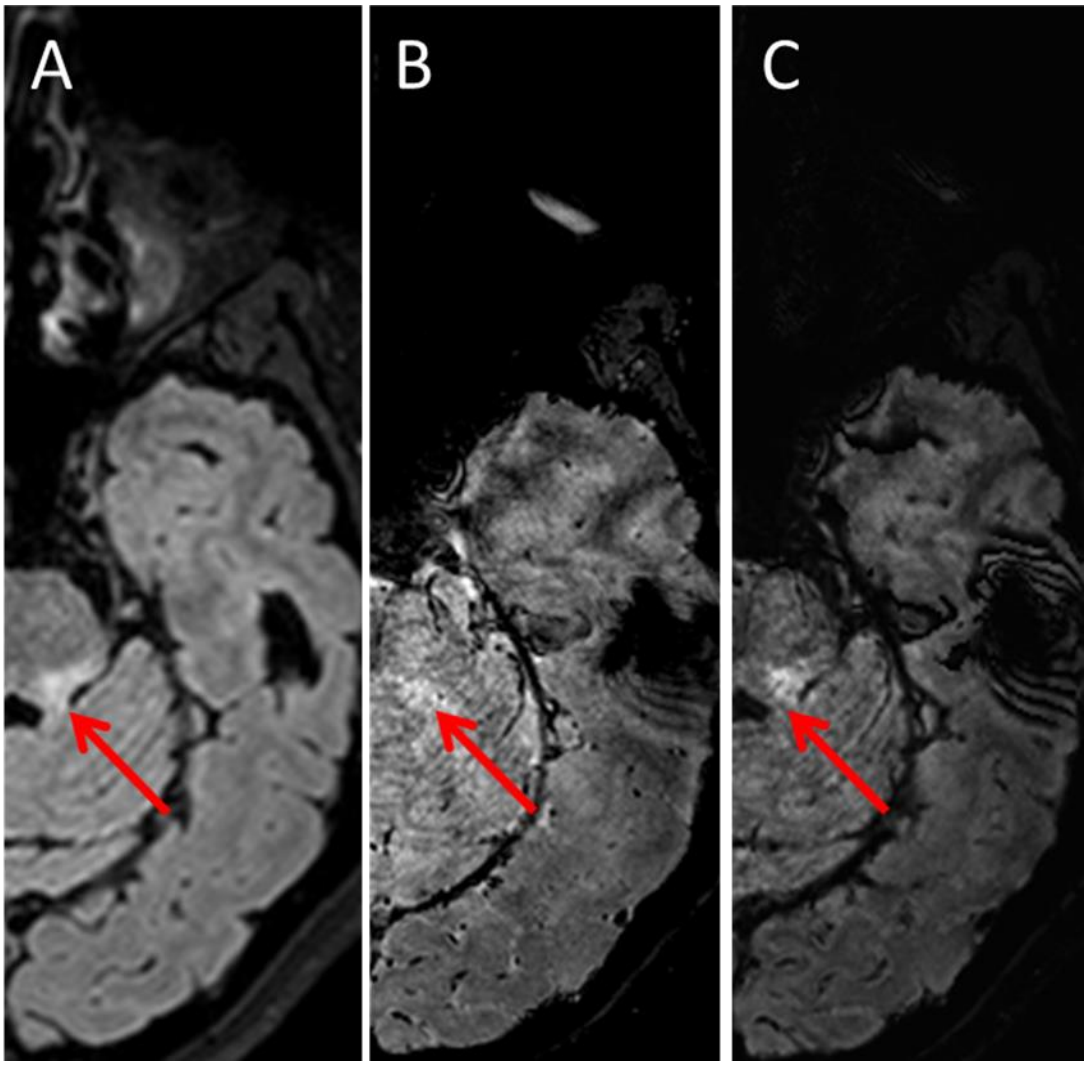

Figure B2. Infratentorial lesion in the superior cerebellar peduncle. (A) shows the hyperintense lesion on FLAIR, (B) is a T2* hEPI image showing a small vein but this is not as clear as in (C) a FLAIR-SWI-2 scan.

Appendix C

Distributions of WMLs and proportion of WMLs with central veins in PPMS and RRMS patients

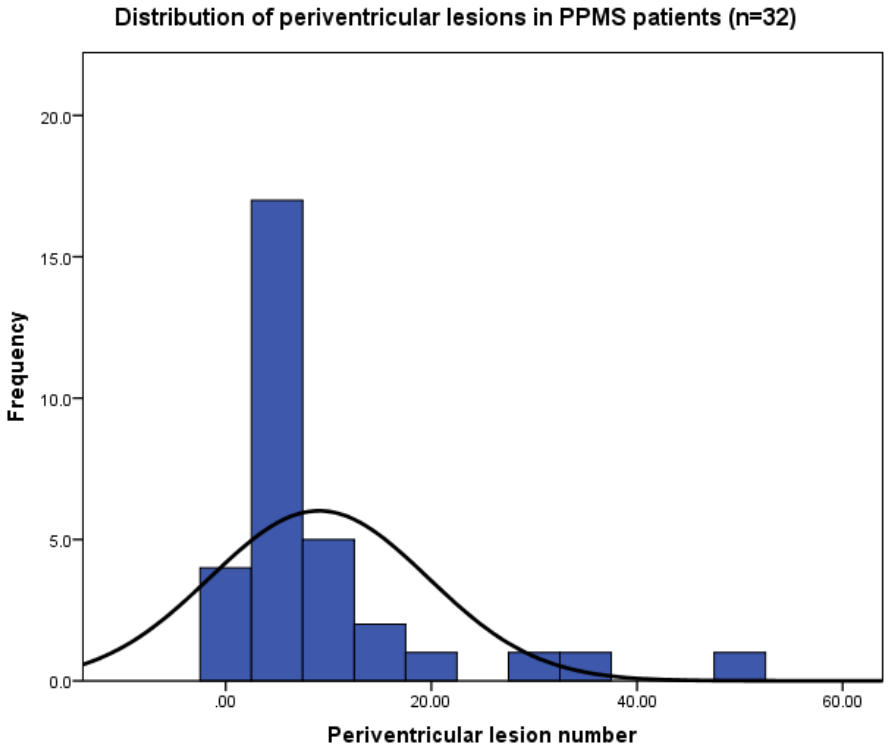

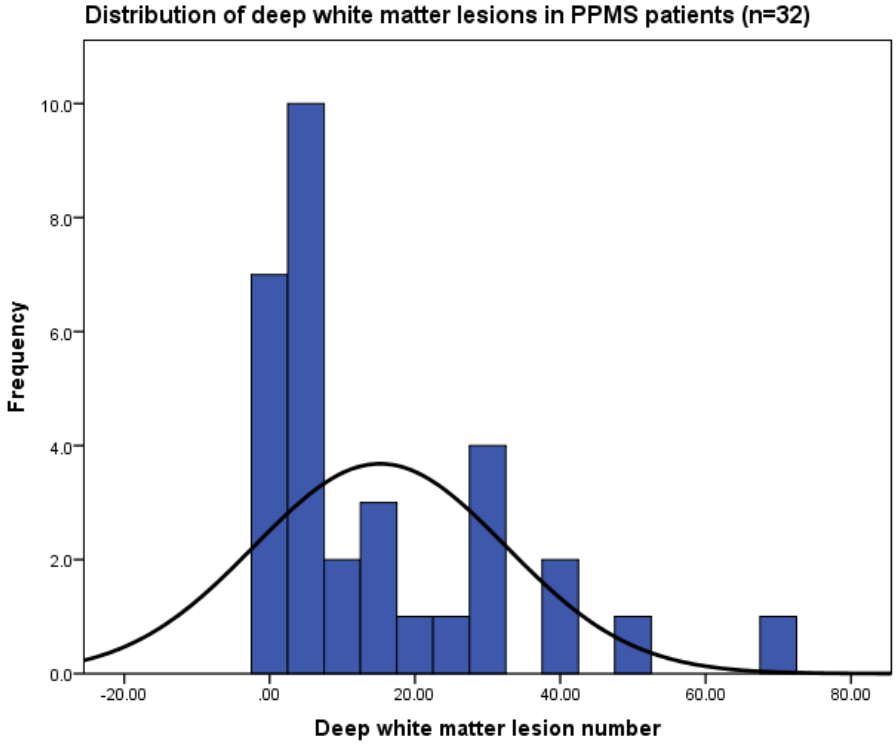

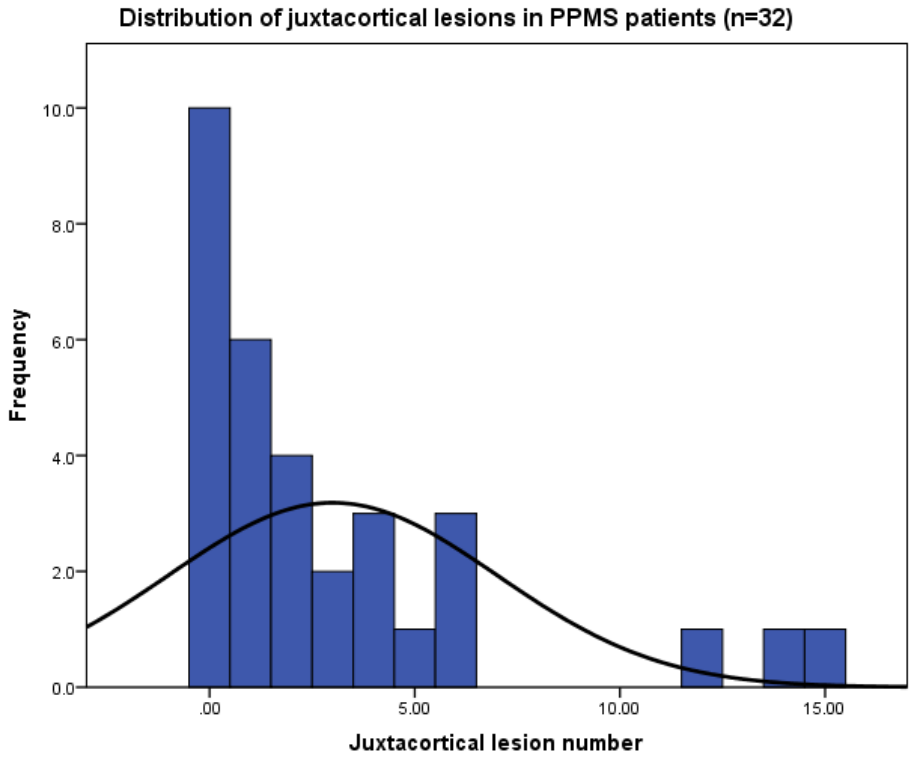
Distribution of juxtacortical lesions in PPMS patients (n=32)
Frequency
10.0
8.0
6.0
4.0
2.0
0.0
.00
5.00
10.00
15.00
Juxtacortical lesion number

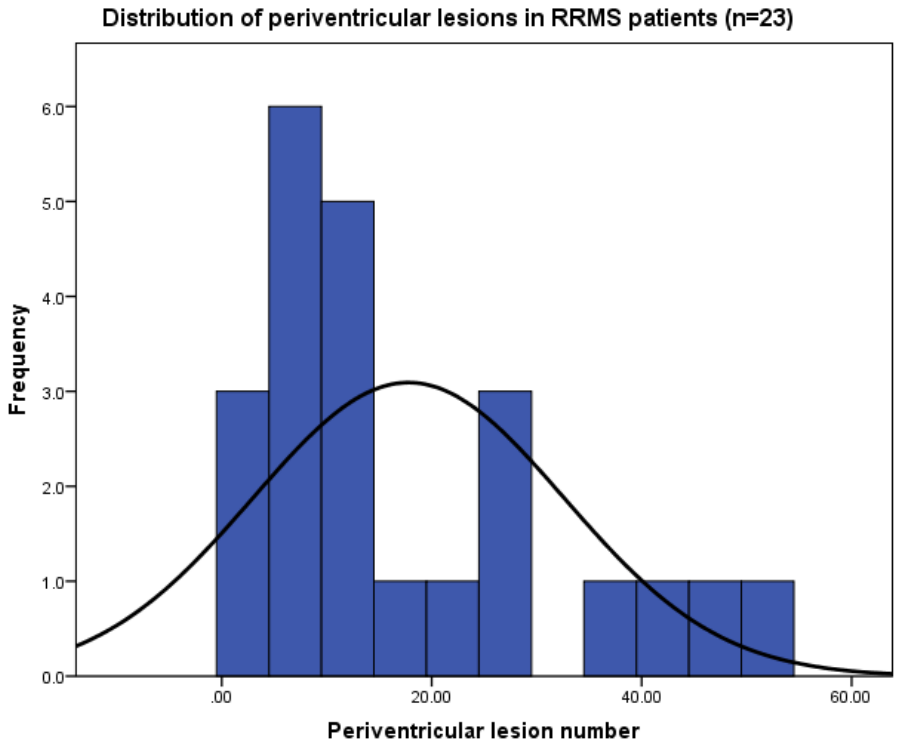
Distribution of periventricular lesions in RRMS patients (n=23)
Frequency
6.0
5.0
4.0
3.0
2.0
1.0
0.0
.00
20.00
40.00
60.00
Periventricular lesion number

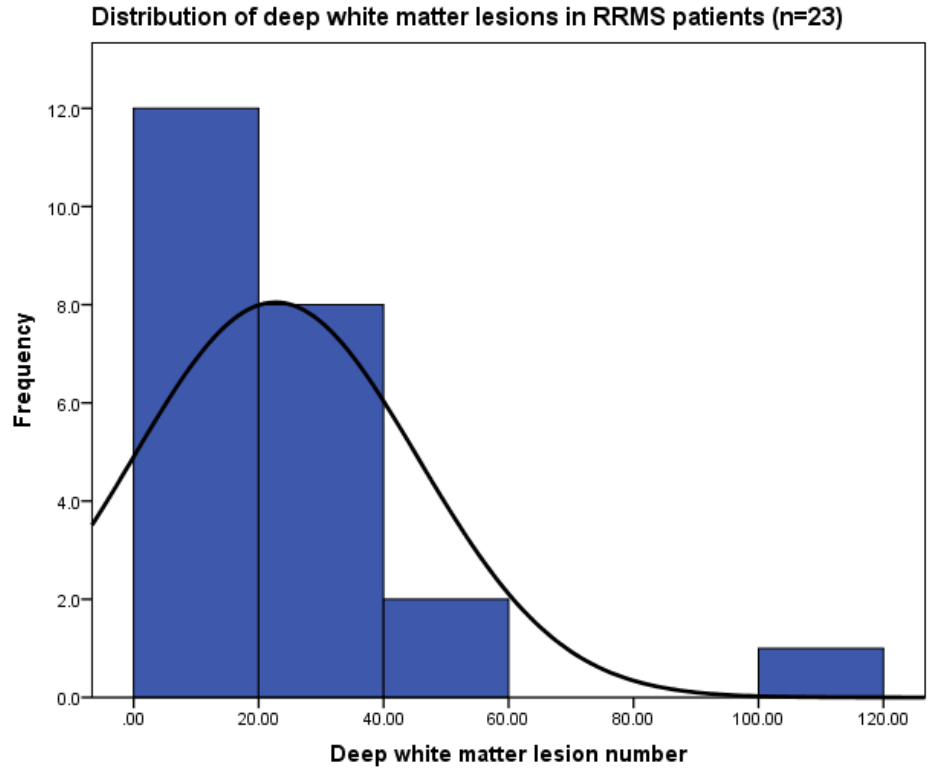
Distribution of deep white matter lesions in RRMS patients (n=23)
Frequency
12.0
10.0
8.0
6.0
4.0
2.0
0.0
.00
20.00
40.00
60.00
80.00
100.00
120.00
Deep white matter lesion number

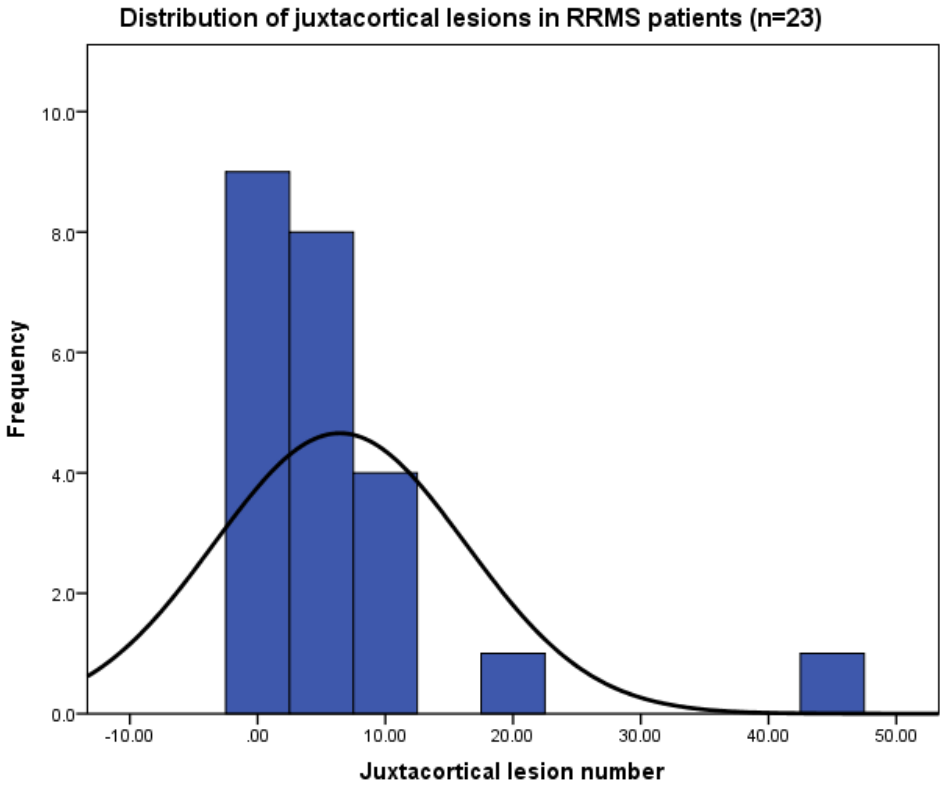
Distribution of juxtacortical lesions in RRMS patients (n=23)
Frequency
10.0
8.0
6.0
4.0
2.0
0.0
-10.00
.00
10.00
20.00
30.00
40.00
50.00
Juxtacortical lesion number

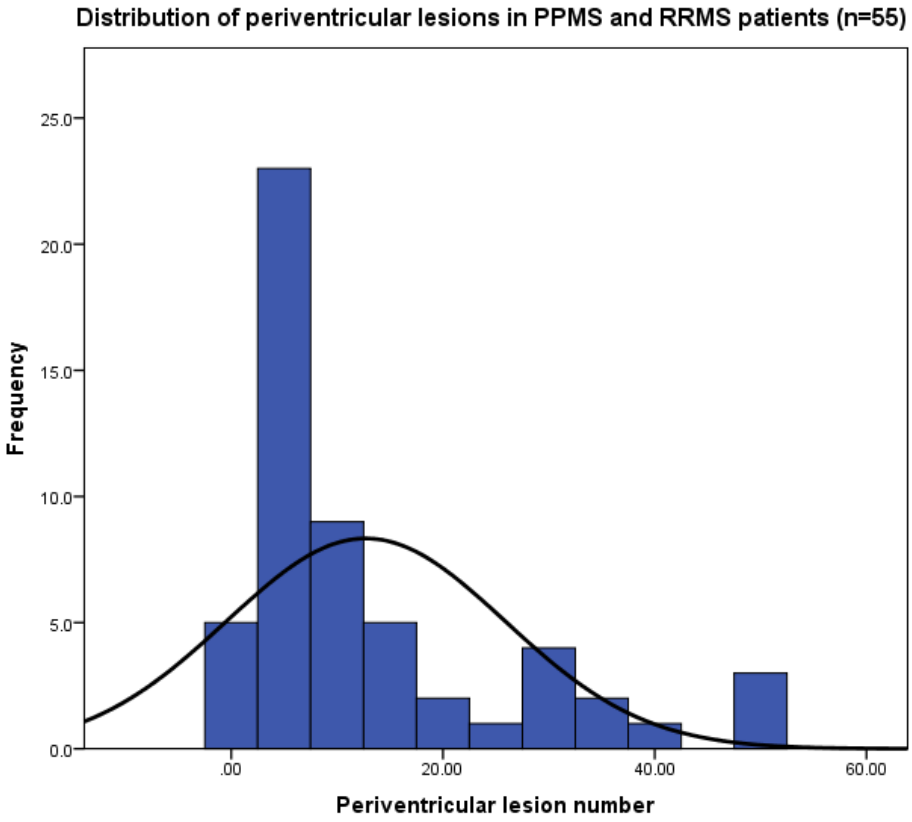
Distribution of periventricular lesions in PPMS and RRMS patients (n=55)
Frequency
25.0
20.0
15.0
10.0
5.0
0.0
.00
20.00
40.00
60.00
Periventricular lesion number

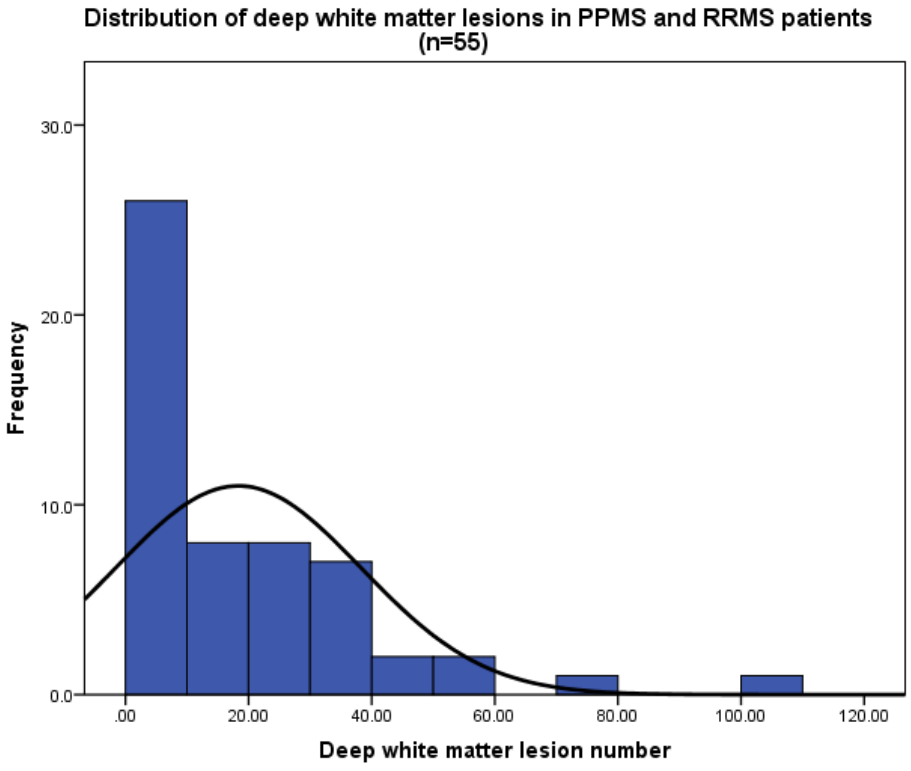
Distribution of deep white matter lesions in PPMS and RRMS patients (n=55)
Frequency
30.0
20.0
10.0
0.0
.00
20.00
40.00
60.00
80.00
100.00
120.00
Deep white matter lesion number

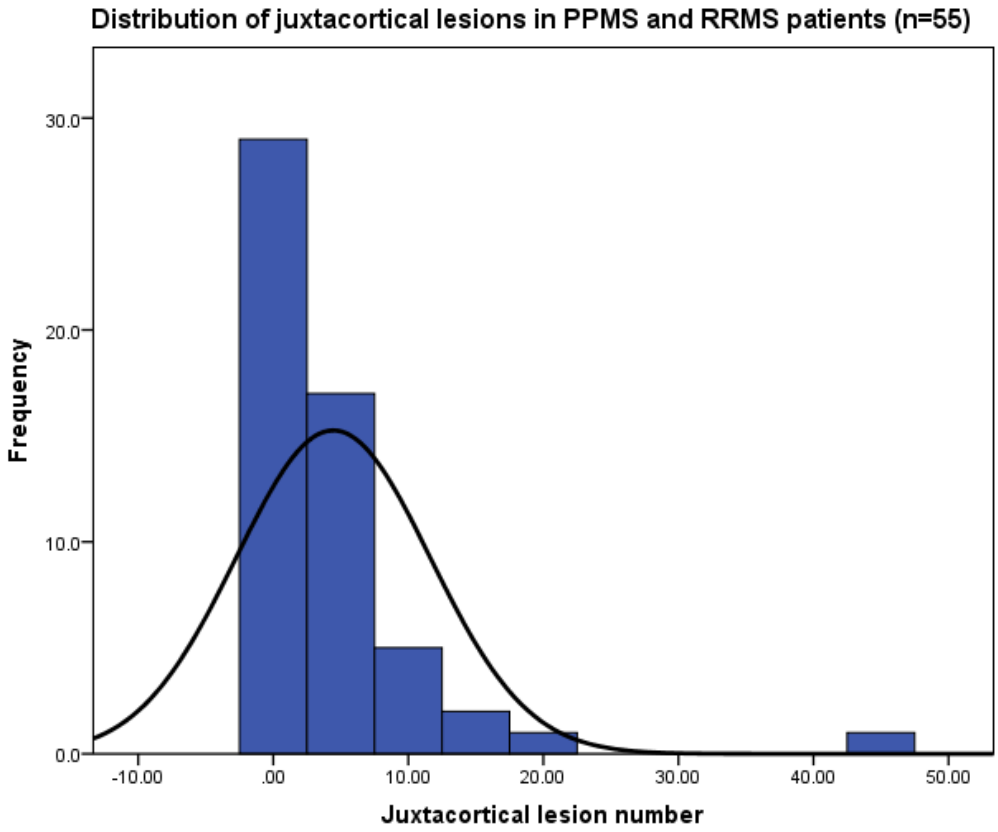
Distribution of juxtacortical lesions in PPMS and RRMS patients (n=55)
Frequency
30.0
20.0
10.0
0.0
-10.00
.00
10.00
20.00
30.00
40.00
50.00
Juxtacortical lesion number

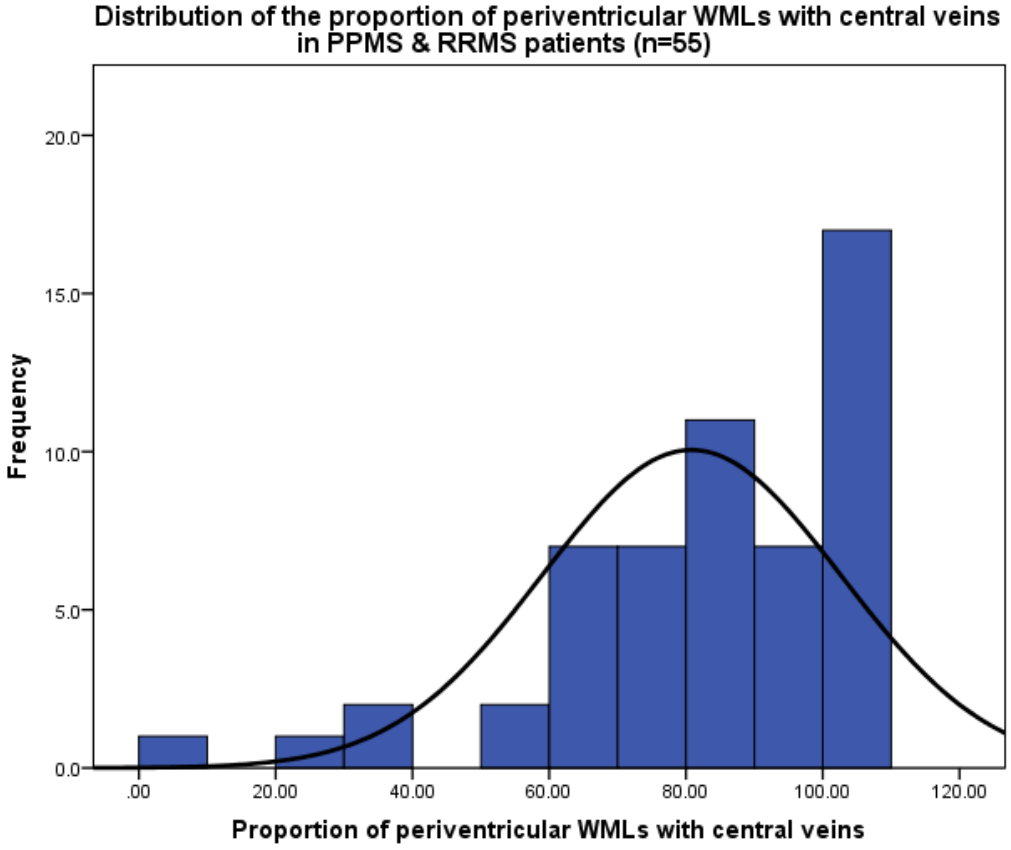
Distribution of the proportion of periventricular WMLs with central veins in PPMS & RRMS patients (n=55)
Frequency
20.0
15.0
10.0
5.0
0.0
.00
20.00
40.00
60.00
80.00
100.00
120.00
Proportion of periventricular WMLs with central veins

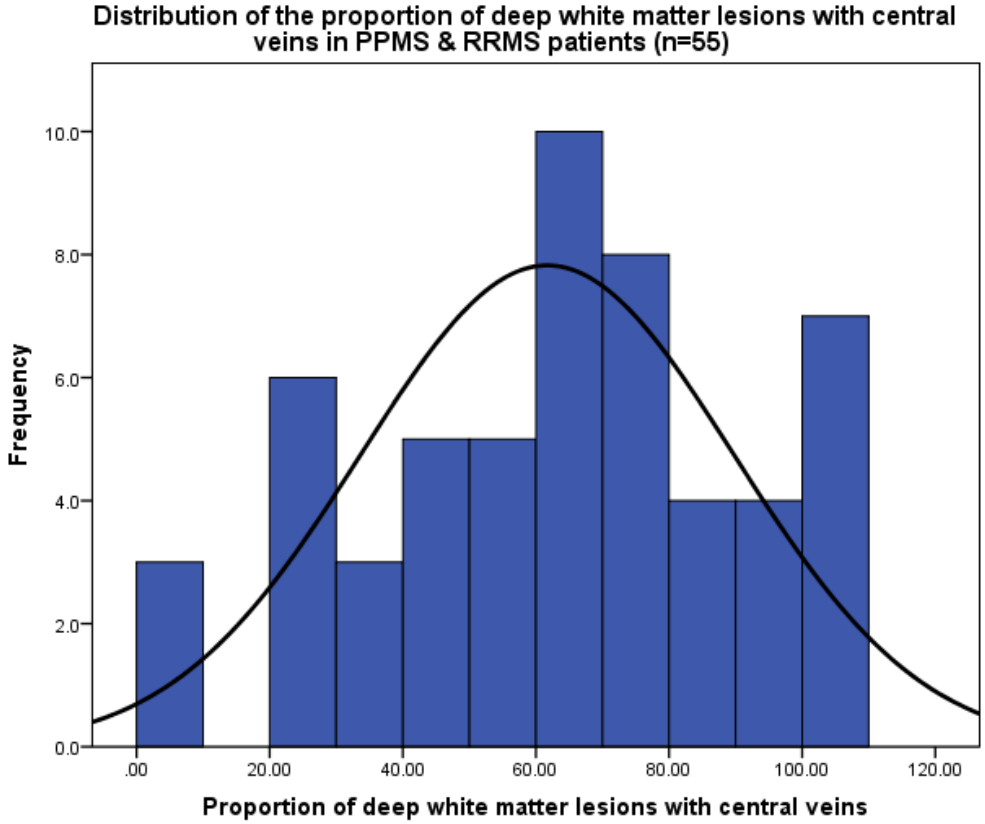
Distribution of the proportion of deep white matter lesions with central veins in PPMS & RRMS patients (n=55)
Frequency
10.0
8.0
6.0
4.0
2.0
0.0
.00
20.00
40.00
60.00
80.00
100.00
120.00
Proportion of deep white matter lesions with central veins

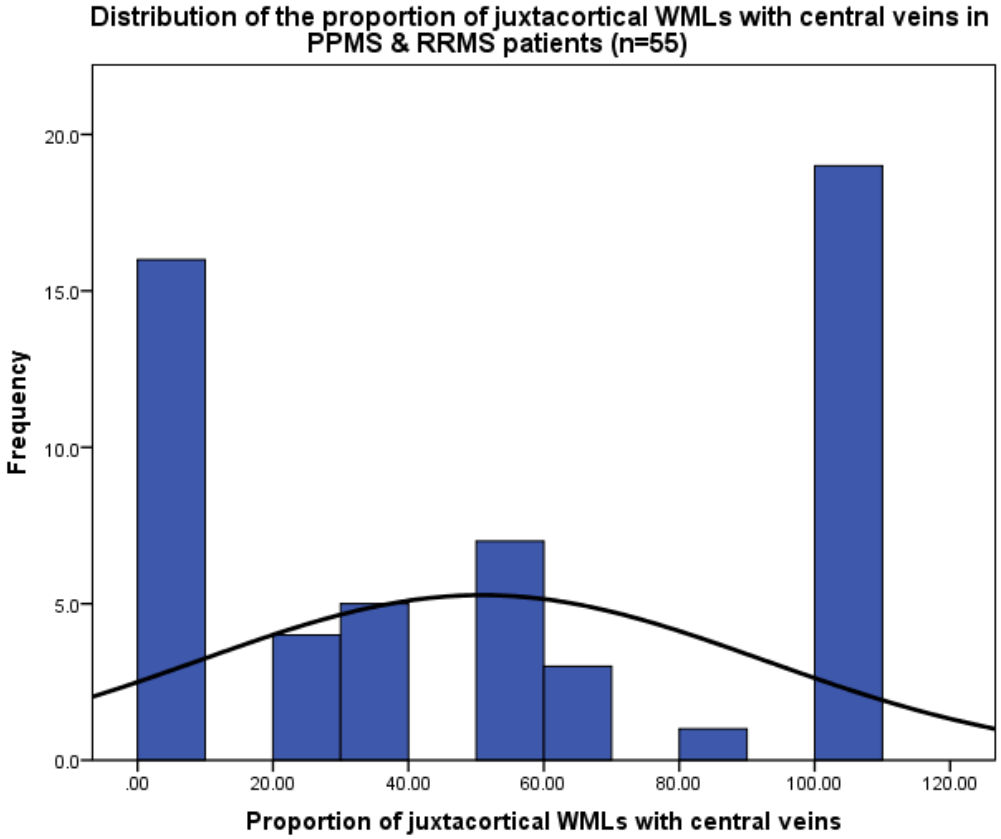
Distribution of the proportion of juxtacortical WMLs with central veins in PPMS & RRMS patients (n=55)
Frequency
20.0
15.0
10.0
5.0
0.0
.00
20.00
40.00
60.00
80.00
100.00
120.00
Proportion of juxtacortical WMLs with central veins

Total WMLs identified	No. WML central veins	No. pts suitable for test (RRMS)†	No. correctly diagnosed as RRMS‡	Proportion correctly diagnosed as RRMS (%) (sensitivity)
4	1	9647	9616	99.6
4	2	9720	9213	94.7
4	3	9718	7165	73.7
4	4	9694	3097	31.9
6	1	9945	9438	99.9
6	2	9469	9423	99.5
6	3	9463	9057	95.7
6	4	9422	7748	82.2
6	5	9443	5004	52.9
6	6	9470	1666	17.5
8	1	9221	9221	100
8	2	9178	9175	99.9
8	3	9189	9142	99.4
8	4	9168	8914	97.2
8	5	9128	8133	89
8	6	9187	6256	68
8	7	9176	3380	36.8
8	8	9158	920	10

Table 1. Continued on next page.

Total WMLs identified	No. WML central veins	No. pts suitable for test (RRMS)†	No. correctly diagnosed as RRMS‡	Proportion correctly diagnosed as RRMS (%) (sensitivity)
10	1	8944	8944	100
10	2	8888	8886	99.9
10	3	8893	8889	99.9
10	4	8856	8821	99.6
10	5	8857	8676	97.9
10	6	8920	8242	92.3
10	7	8921	6953	77.9
10	8	8827	4621	52.3
10	9	8874	2201	24.8
10	10	8899	502	5.6

Table 1. Sensitivity of identifying a certain number of WMLs with central veins in simulated RRMS patients.

Each row shows the number of RRMS patients who would be correctly diagnosed depending on the proportion WMLs with central veins. Shaded rows show the optimum proportions of WMLs with central veins giving the best sensitivities.

† = number of simulated patients suitable for the test out of a total of 10,000.

‡ = no. of correctly diagnosed as RRMS = 'True positive' cases.

Total WMLs identified	No. WML central veins	No. pts suitable for test (SVD)†	No. incorrectly diagnosed as RRMS‡	Specificity* (%)
4	1	9913	1470	85.1
4	2	9919	90	99
4	3	9941	1	99.9
4	4	9923	0	100
6	1	9837	2138	78.2
6	2	9776	202	97.9
6	3	9774	6	99.9
6	4	9801	0	100
6	5	9797	0	100
6	6	9789	0	100
8	1	9629	2650	72.4
8	2	9592	390	95.9
8	3	9619	30	99.6
8	4	9620	0	100
8	5	9603	0	100
8	6	9636	0	100
8	7	9609	0	100
8	8	9608	0	100

Table 2. Continued on next page.

Total WMLs identified	No. WML central veins	No. pts suitable for test (SVD)†	No. incorrectly diagnosed as RRMS‡	Specificity* (%)
10	1	9417	3114	66.9
10	2	9388	532	94.3
10	3	9407	64	99.3
10	4	9368	6	99.9
10	5	9392	0	100
10	6	9362	0	100
10	7	9421	0	100
10	8	9402	0	100
10	9	9392	0	100
10	10	9390	0	100

Table 2. Specificity of identifying a certain number of WMLs with central veins in simulated SVD patients.
Each row show the number of patients with SVD who would be misdiagnosed as having RRMS depending on the proportion of WMLs with central veins. Shaded rows show the optimum specificity.

† = number of simulated patients suitable for the test out of a total of 10,000.

‡ = no. of incorrectly diagnosed as RRMS = 'False positive' cases

* calculation: (Total number of patients suitable for test - number of patients incorrectly diagnosed as RRMS / total number of patients suitable for test) x 100

Total WMLs identified	No. WML central veins	No. pts suitable for test (PPMS)†	No. correctly diagnosed as PPMS‡	Proportion correctly diagnosed as PPMS (%) (sensitivity)
4	1	8679	8532	98.3
4	2	8695	7592	87.3
4	3	8703	4925	56.5
4	4	8732	1545	17.6
6	1	8093	8082	99.8
6	2	7986	7804	97.7
6	3	8195	7223	88.1
6	4	8030	5166	64.3
6	5	8151	2517	30.8
6	6	8129	569	6.9
8	1	7513	7512	99.9
8	2	7509	7482	99.6
8	3	7525	7354	97.7
8	4	7542	6727	89.1
8	5	7533	5307	70.4
8	6	7561	3224	42.6
8	7	7569	1322	17.4
8	8	7623	245	3.2

Table 3. Continued on next page.

Total WMLs identified	No. WML central veins	No. pts suitable for test (PPMS)†	No. correctly diagnosed as PPMS‡	Proportion correctly diagnosed as PPMS (%) (sensitivity)
10	1	7101	7101	100
10	2	6935	6934	99.9
10	3	7025	6989	99.4
10	4	7058	6891	97.6
10	5	6976	6309	90.4
10	6	7012	5274	75.2
10	7	6961	3592	51.6
10	8	7069	1901	26.8
10	9	7075	597	8.4
10	10	6985	85	1.2

Table 3. Sensitivity of identifying a certain number of WMLs with central veins in simulated PPMS patients.

Each row shows the number of PPMS patients who would be correctly diagnosed depending on the proportion of WMLs with central veins. Shaded rows show the optimum proportions of WMLs with central veins giving the best sensitivities.

† = number of simulated patients suitable for the test out of a total of 10,000.

‡ = no. of correctly diagnosed as PPMS = ‘True positive’ cases.

Total WMLs identified	No. WML central veins	No. pts suitable for test (SVD)†	No. incorrectly diagnosed as PPMS‡	Specificity* (%)
4	1	9908	1491	84.9
4	2	9925	85	99.1
4	3	9911	2	99.9
4	4	9921	0	100
6	1	9806	2064	78.9
6	2	9784	191	98
6	3	9765	4	99.9
6	4	9789	0	100
6	5	9787	0	100
6	6	9817	0	100
8	1	9646	2633	72.7
8	2	9574	332	96.5
8	3	9640	31	99.6
8	4	9616	0	100
8	5	9621	0	100
8	6	9645	0	100
8	7	9592	0	100
8	8	9603	0	100

Table 4. Continued on next page.

Total WMLs identified	No. WML central veins	No. pts suitable for test (SVD)†	No. incorrectly diagnosed as PPMS‡	Specificity* (%)
10	1	9414	3184	66.1
10	2	9391	557	94
10	3	9353	57	99.3
10	4	9367	4	99.9
10	5	9364	1	99.9
10	6	9364	0	100
10	7	9372	0	100
10	8	9325	0	100
10	9	9369	0	100
10	10	9417	0	100

Table 4. Specificity of identifying a certain number of WMLs with central veins in simulated SVD patients.

Each row show the number of patients with SVD who would be misdiagnosed as having PPMS depending on the proportion of WMLs with central veins. Shaded rows show the optimum specificity.

† = number of simulated patients suitable for the test out of a total of 10,000.

‡ = no. of incorrectly diagnosed as PPMS = 'False positive' cases

* calculation: (Total number of patients suitable for test - number of patients incorrectly diagnosed as PPMS / total number of patients suitable for test) x 100